KATHOLIEKE UNIVERSITEIT LEUVEN
FACULTEIT INGENIEURSWETENSCHAPPEN
DEPARTEMENT COMPUTERWETENSCHAPPEN
AFDELING NUMERIEKE ANALYSE EN
TOEGEPASTE WISKUNDE
Celestijnenlaan 200A – B-3001 Heverlee

POWELL–SABIN SPLINE BASED MULTILEVEL PRECONDITIONERS FOR ELLIPTIC PARTIAL DIFFERENTIAL EQUATIONS

Promotor:
Prof. Dr. A. Bultheel

Proefschrift voorgedragen tot
het behalen van het doctoraat
in de ingenieurswetenschappen

door

Jan MAES

Mei 2006

KATHOLIEKE UNIVERSITEIT LEUVEN
FACULTEIT INGENIEURSWETENSCHAPPEN
DEPARTEMENT COMPUTERWETENSCHAPPEN
AFDELING NUMERIEKE ANALYSE EN
TOEGEPASTE WISKUNDE
Celestijnenlaan 200A – B-3001 Heverlee

POWELL–SABIN SPLINE BASED MULTILEVEL PRECONDITIONERS FOR ELLIPTIC PARTIAL DIFFERENTIAL EQUATIONS

Jury:
Prof. Dr. ir. E. Aernoudt, voorzitter
Prof. Dr. A. Bultheel, promotor
Prof. Dr. ir. P. Dierckx,
Prof. Dr. ir. A. Kuijlaars,
Prof. Dr. A. Kunoth,
(Universität Bonn, Germany)
Prof. Dr. ir. S. Vandewalle

Proefschrift voorgedragen tot
het behalen van het doctoraat
in de ingenieurswetenschappen

door

Jan MAES

U.D.C. 519.63

Mei 2006

D/2006/7515/35

ISBN 90-5682-701-4

Powell–Sabin spline based multilevel preconditioners for elliptic partial differential equations

Jan Maes
Departement Computerwetenschappen, K.U.Leuven
Celestijnenlaan 200A, B-3001 Heverlee, België

Abstract

In this dissertation we are concerned with the development of multilevel preconditioners for linear systems that arise from Galerkin methods for fourth order elliptic equations on two-dimensional polygonal domains. The key ingredients are the construction of multiscale bases for C^1 conforming finite element spaces of Powell–Sabin type, and the characterization of certain Sobolev spaces by weighted norm equivalences related to the multiscale representation of functions. The latter immediately yields bounds on the growth rate of the condition numbers of the preconditioned systems. Multiscale bases that characterize a large range of Sobolev spaces are preferable, since the corresponding preconditioners are more robust. We explore different types of multiscale bases, such as a suboptimal standard hierarchical basis, an optimal hierarchical basis based on Lagrange interpolation, and several wavelet-type bases. On non-uniform triangulations we construct a biorthogonal wavelet basis that characterizes the Sobolev spaces $H^s(\Omega)$ with $s \in (0.802774, 2.5)$. On uniform triangulations we construct a semi-orthogonal wavelet basis that characterizes the Sobolev spaces $H^s(\Omega)$ with $|s| < 2.5$. Furthermore we develop an elegant way to extend the obtained results to similar constructions on the surface of the two-sphere.

Preface

Deze thesis is het resultaat van 4 jaar onderzoek dat ik steeds met veel plezier gedaan heb. Het is fantastisch om een job te hebben waarbij studeren, inzicht verwerven in nieuwe materie en experimenteren samenvloeien tot een mooi geheel. Het lijkt me dan ook een goed idee om hier enkele mensen te bedanken die mee bijgedragen hebben tot dit werk.

In de eerste plaats wil ik mijn promotor Prof. Adhemar Bultheel bedanken. Dankzij hem kwam ik in contact met dit onderzoeksgebied en stapte ik, als exacte wetenschapper, over naar het gebied van de toegepaste wetenschappen. Hij heeft mij steeds de nodige vrijheid gegeven in mijn onderzoek en steunde mij volledige bij de keuzes die ik maakte. Verder dank ik hem ook voor de tijd die hij steeds wist vrij te maken om over bepaalde onderwerpen te praten of voor het nalezen van geschreven teksten.

Ook wil ik mijn twee assessoren, Prof. Paul Dierckx en Prof. Stefan Vandewalle, bedanken voor hun waardevolle suggesties en opmerkingen bij het zorgvuldig nalezen van deze tekst. Hun opbouwende commentaar heeft sterk bijgedragen tot de leesbaarheid van dit werk.

A very important thank you goes to Prof. Angela Kunoth of Universität Bonn, not just for being part of my jury, but also for making my visit to Bonn a great experience. She is very knowledgeable about the subject of my research, brought me into contact with several interesting people, and she taught me what numerical analysis is all about. Furthermore our fruitful collaboration resulted in an interesting paper.

Verder wil ik natuurlijk ook Prof. Arno Kuijlaars bedanken, die naast mijn licentiaatsthesis nu ook mijn doctoraatsthesis wil beoordelen.

Ik mag natuurlijk mijn collega's niet vergeten. In het bijzonder wil ik Pats en Joris bedanken voor de uitermate leuke sfeer op bureau. Evelyne Vanraes en Jan Van lent wil ik bedanken voor de vele boeiende discussies en samenwerking.

Tenslotte wil ik mijn vrienden en familie bedanken voor hun steun en voor al de leuke momenten die we samen hadden. Zij hebben niet zozeer bijgedragen tot de resultaten in deze thesis, maar bij hen kon ik steeds terecht voor de andere dingen die het leven zo aangenaam maken. In het bijzonder wil ik Kelly bedanken voor de steun en toeverlaat die ze de voorbije jaren geweest is, en voor de vele jaren die nog komen moeten.

Jan
Mei 2006

Acknowledgement

The research reported in this thesis was supported by the Flemish Fund for Scientific Research (FWO Vlaanderen) projects MISS (G.0211.02) and SMID (G.0431.05), and by the Belgian Programme on Interuniversity Attraction Poles, initiated by the Belgian Federal Science Policy Office.

Nederlandse samenvatting

Powell–Sabin spline gebaseerde multischaal preconditioners voor elliptische partiële differentiaalvergelijkingen

Inhoudsopgave

1 Inleiding

De geconjugeerde gradiëntmethode is zeer efficiënt voor het oplossen van grote lineaire stelsels, waarbij de matrix van het stelsel overeenkomt met een Galerkin discretisatie van een elliptische partiële differentiaalvergelijking. Deze stelsels lineaire vergelijkingen moeten dan wel op gepaste wijze voorgeconditioneerd worden. Gedurende de voorbije 15 jaar is er actief gezocht naar verscheidene efficiënte preconditioners die qua complexiteit vergelijkbaar zijn met de optimale multigridmethode. In deze thesis willen we zulke optimale preconditioners ontwikkelen voor vierde orde elliptische partiële differentiaalvergelijkingen.

1.1 Elliptische partiële differentiaalvergelijkingen

Zij p_{2k} een veelterm van graad $2k$ op $\mathbb{R}^d$. Met $p_{2k}(D)$ bedoelen we de differentiaaloperator waarbij elke veranderlijke in p_{2k} vervangen wordt door de overeenstemmende partiële afgeleide. We zijn geïnteresseerd in het oplossen van randwaardeproblemen van de vorm

$$p_{2k}(D)u = f \quad \text{op} \quad \Omega, \qquad Bu = 0 \quad \text{op} \quad \partial\Omega,$$

waarbij B een operator is die de randvoorwaarden uitdrukt. De zwakke formulering van zulk randwaardeprobleem is steeds van de vorm

$$a(u, v) = \langle f, v \rangle \quad \text{voor alle } v \in H^k_B(\Omega),$$

waarbij $a(\cdot,\cdot)$ een bilineaire vorm is en waarbij $H^k_B(\Omega)$ een deelruimte van de Sobolev ruimte $H^k(\Omega)$ is die afhangt van de randvoorwaarden. De Sobolev ruimte $H^k(\Omega)$ is gedefinieerd als de ruimte van functies op Ω waarvoor alle zwakke partiële afgeleiden tot orde k in L_2 liggen. We veronderstellen dat de partiële differentiaaloperator elliptisch is:

$$a(v,v) \sim \|v\|^2_{H^k(\Omega)}, \quad v \in H^k_B(\Omega).$$

Met $a \sim b$ bedoelen we steeds dat $a \lesssim b$ en $a \gtrsim b$ gelden, waarbij $a \lesssim b$ betekent dat a kan afgeschat worden door een constant aantal keren b en $a \gtrsim b$ betekent $b \lesssim a$. De stelling van Lax–Milgram garandeert het bestaan van een unieke oplossing voor de zwakke formulering van een elliptische partiële differentiaalvergelijking.

Stel dat we beschikken over een nodale basis $\phi_l := \{\phi_{i,l} \mid i \in I_l\}$ die een deelruimte $S_l \subset H^k_B(\Omega)$ opspant. We zoeken een benaderende oplossing $u_l \in S_l$ van de zwakke formulering door het lineaire stelsel

$$A_{\phi_l} c = b_{\phi_l}, \qquad (A_{\phi_l})_{i,j} := a(\phi_{i,l}, \phi_{j,l}), \qquad (b_{\phi_l})_i := \langle f, \phi_{i,l}\rangle$$

op te lossen. De benaderende oplossing wordt dan gegeven door $u_l = \sum_j c_j \phi_{j,l}$. De matrix A_{ϕ_l} wordt de stijfheidsmatrix genoemd. De geconjugeerde gradiëntmethode is zeer efficiënt voor zulke lineaire stelsels op voorwaarde dat het conditiegetal van de stijfheidsmatrix klein blijft. Het is welbekend dat de equivalentie

$$k_1 \sum_{i\in I_l} |c_i|^2 \le \left\| \sum_{i\in I_l} c_i \phi_{i,l} \right\|^2_{H^k(\Omega)} \le k_2 \sum_{i\in I_l} |c_i|^2$$

impliceert dat

$$\kappa(A_{\phi_l}) \lesssim \frac{k_2}{k_1},$$

waarbij $\kappa(A_{\phi_l})$ het conditiegetal van de stijfheidsmatrix A_{ϕ_l} is. Idealiter willen we dat k_1 en k_2 constanten zijn, zodat $\kappa(A_{\phi_l}) = \mathcal{O}(1)$.

1.2 Voorconditionering

Voor een typische nodale basis is het conditiegetal $\kappa(A_{\phi_l})$ van de orde $h^{-4k/d}$ met h de stapgrootte van de discretisatie. Daarom is het noodzakelijk om een geschikte preconditioner te vinden voor het lineaire stelsel $A_{\phi_l} c = b_{\phi_l}$. Dit kan door een andere basis te gebruiken. Stel dat $\psi := \{\psi_j \mid j \in J\}$, $\#J = \#I_l$, een andere basis is voor S_l en dat L de transformatiematrix is tussen de twee basissen. Dan geldt er dat

$$A_\psi = L^T A_{\phi_l} L.$$

Als nu

$$\gamma \sum_{j\in J} |d_j|^2 \leq \left\| \sum_{j\in J} d_j \psi_j \right\|^2_{H^k(\Omega)} \leq \Gamma \sum_{j\in J} |d_j|^2$$

geldt, zodat het quotient Γ/γ klein is vergeleken met $h^{-4k/d}$, dan is LL^T een geschikte kandidaat preconditioner.

Ondertussen bestaan er verscheidene preconditioners die geïnterpreteerd kunnen worden als een verandering van basis, zoals de hiërarchische basis preconditioner en de nauw verwante BPX-preconditioner. Ook wavelet basissen kunnen gebruikt worden voor voorconditionering. Deze voorconditioneringstechnieken werden in eerste instantie geformuleerd voor tweede orde problemen op twee-dimensionale vlakke domeinen, zoals de vergelijking van Poisson.

1.3 Overzicht van de thesis

In deze thesis richten we ons vooral op de constructie van preconditioners voor vierde orde elliptische partiële differentiaalvergelijkingen. Als modelprobleem beschouwen we de biharmonische vergelijking met Dirichlet randvoorwaarden:

$$\Delta^2 u = f \text{ op } \Omega, \quad u = \frac{\partial u}{\partial n} = 0 \text{ op } \partial\Omega,$$

waarbij n de normaal is op $\partial\Omega$.

In Hoofdstuk 2 herhalen we de fundamentele theorie van Bernstein–Bézier veeltermen en voeren we de ruimte van Powell–Sabin splines in. We onderzoeken de stabiliteit van een klasse van B-spline basissen en tonen aan dat gladde functies en hun afgeleiden optimaal benaderd worden door de Hermite interpolerende PS spline.

Hoofdstuk 3 start met spline subdivisieschema's voor PS splines. Deze schema's laten toe om geneste PS spline ruimten te creëren en we bewijzen dat deze ruimten een multiresolutie analyse vormen voor de Banach ruimte $C^1(\overline{\Omega})$, waarbij $\overline{\Omega} = \Omega \cup \partial\Omega$. We onderzoeken de stabiliteit van de hiërarchische basis. Uit die stabiliteitsresultaten volgen twee toepassingen. Als eerste toepassing gebruiken we de hiërarchische basis voor de compressie van oppervlakken, en als tweede toepassingen leiden we de suboptimale hiërarchische basis preconditioner en de optimale BPX-preconditioner voor vierde orde elliptische partiële differentiaalvergelijkingen af. Numerieke experimenten staven de theoretische bevindingen.

In Hoofdstuk 4 construeren we een stabiele lokale Lagrange basis voor de ruimte van PS splines. Door spline subdivisie bekomen we een hiërarchische basis van Lagrange type. We tonen theoretisch aan dat deze basis als preconditioner robuuster is dan de standaard hiërarchische basis van Hermite type.

In Hoofdstuk 5 geven we een algemene constructiemethode voor wavelets op willekeurige domeinen, waarbij we gebruik maken van het lifting schema. Tevens tonen we hoe men de stabiliteit van deze wavelet basissen kan schatten. We besteden ook aandacht aan de constructie van wavelets op uniforme domeinen.

Hoofdstuk 6 behandelt elliptische partiële differentiaalvergelijkingen op een boloppervlak. We introduceren Powell–Sabin splines op de bol en hiermee construeren we een hiërarchische basis preconditioner en een BPX-preconditioner op de bol.

Tenslotte geven we een overzicht van de nieuwe bijdragen en enkele suggesties voor verder onderzoek in Hoofdstuk 7.

2 Powell–Sabin splines

Verscheidene C^1 continue eindige elementen ruimten zijn reeds onderzocht voor de numerieke oplossing van vierde orde elliptische partiële differentiaalvergelijkingen, zoals C^1 stuksgewijs kwadratische veeltermen op een Powell–Sabin 12-split, C^1 stuksgewijs kubieke veeltermen op Clough–Tocher driehoeken en op quadrangulaties, and C^1 stuksgewijs vijfde orde veeltermen van Argyris-type. In deze thesis beschouwen we C^1 stuksgewijs kwadratische veeltermen op een Powell–Sabin 6-split, omdat deze splines een redelijk eenvoudige structuur hebben en omdat ze een lage dimensie hebben in vergelijking met andere constructies.

2.1 Bernstein–Bézier veeltermen

Beschouw een driehoek $\tau(V_1, V_2, V_3)$ in het vlak met hoekpunten V_i met Cartesische coördinaten (x_i, y_i), $i = 1, 2, 3$. Elk punt v met Cartesische coördinaten (x, y) kan voorgesteld worden door middel van zijn barycentrische coördinaten ten opzichte van τ, die gedefinieerd zijn als de unieke oplossing van het stelsel

$$\begin{bmatrix} x_1 & x_2 & x_3 \\ y_1 & y_2 & y_3 \\ 1 & 1 & 1 \end{bmatrix} \begin{bmatrix} b_1(v) \\ b_2(v) \\ b_3(v) \end{bmatrix} = \begin{bmatrix} x \\ y \\ 1 \end{bmatrix}.$$

Zij $\mathcal{P}_d$ de ruimte van bivariate veeltermen van graad $\leq d$. Elke veelterm $p_d(v) \in \mathcal{P}_d$ heeft een unieke Bernstein–Bézier voorstelling

$$p_d(v) = \sum_{i+j+k=d} c_{ijk} B^d_{ijk}(v),$$

met

$$B^d_{ijk}(v) := \frac{d!}{i!j!k!} b_1^i(v) b_2^j(v) b_3^k(v)$$

de Bernstein veeltermen op de driehoek. De coëfficiënten c_{ijk} worden de Bézier ordinaten genoemd.

2.2 Powell–Sabin splines

Zij Δ een willekeurige driehoeksverdeling van een domein $\Omega \subset \mathbb{R}^2$ met polygonale rand $\partial\Omega$, bestaande uit punten V_i, $i = 1, \ldots, N$, en driehoeken T_j, $j = 1, \ldots, t$. De spline ruimte $S_d^r(\Delta)$ is gedefinieerd als

$$S_d^r(\Delta) := \{s \in C^r(\Omega) \mid s|_\tau \in \mathcal{P}_d \text{ for all } \tau \in \Delta\},$$

waarbij $d > r \geq 0$ gegeven natuurlijke getallen zijn. Wij zijn voornamelijk geïnteresseerd in $r = 1$ en $d = 2$. In het algemeen is de dimensie van de ruimte $S_2^1(\Delta)$ niet gekend. Daarom beperken we ons tot de Powell–Sabin 6-split Δ^{PS} van Δ. De ruimte $S_2^1(\Delta^{PS})$ wordt de ruimte van de Powell–Sabin splines genoemd.

De Powell–Sabin 6-split Δ^{PS} verdeelt elke driehoek T_j in zes kleinere driehoeken met een gemeenschappelijk hoekpunt als volgt (zie Figure 2.3):

1. Kies een punt Z_j in elke driehoek T_j, zodat als twee driehoeken T_i en T_j een gemeenschappelijke zijde hebben, de lijn die de punten Z_i en Z_j verbindt deze gemeenschappelijke zijde snijdt in het punt R_{ij} tussen de hoekpunten.
2. Verbindt elk punt Z_j met de hoekpunten van T_j.
3. Voor elke zijde van T_j
   - die tot de rand van Ω behoort, verbind Z_j met een willekeurig punt tussen de hoekpunten.
   - die gemeenschappelijk is met een driehoek T_i, verbind Z_j met R_{ij}.

Elk van de $6t$ driehoeken in Δ^{PS} wordt het domein van een kwadratische Bernstein–Bézier veelterm. Zij f een voldoende gladde functie op Ω. Powell en Sabin toonden aan dat het interpolatieprobleem

$$s(V_k) = f(V_k),\ D_x s(V_k) = D_x f(V_k),\ D_y s(V_k) = D_y f(V_k), \quad k = 1, \ldots, N,$$

een unieke oplossing $s(x, y) \in S_2^1(\Delta^{PS})$ heeft. De dimensie van $S_2^1(\Delta^{PS})$ is dus $3N$. We tonen aan dat

$$\|D_x^\alpha D_y^\beta (f - s)\|_{L_p(\Omega)} \lesssim |\Delta|^{3-\alpha-\beta}$$

voor alle $p > 1$, waarbij $|\Delta|$ het maximum is van de diameters van de driehoeken in Δ en waarbij $0 \leq \alpha + \beta \leq 2$. De functie f en haar afgeleiden worden dus optimaal benaderd door de Hermite interpolerende Powell–Sabin spline. Optimaal hier wil zeggen dat de optimale benaderingsorde $|\Delta|^{d+1}$ bereikt wordt, met d de graad van de splines.

2.3 De B-spline basis

In deze thesis gebruiken we voornamelijk een klasse van B-spline representaties

$$s(x,y) = \sum_{i=1}^{N}\sum_{j=1}^{3} c_{ij} B_{ij}(x,y) \quad , \quad (x,y) \in \Omega,$$

waarbij elke B-spline basis uit die klasse een eenheidspartitie op Ω vormt. Dat wil zeggen dat de B-splines niet negatief zijn en optellen tot één. Verder hebben de B-splines een lokale drager.

Stabiliteit is een belangrijke eigenschap voor een basis. Het is van groot belang in toepassingen dat een kleine storing op de coëfficiënten niet resulteert in een grote verandering van de functie zelf. We bewijzen dat

$$k_1 \|c\|_\infty \leq \left\| \sum_{i=1}^{N}\sum_{j=1}^{3} c_{ij} B_{ij} \right\|_{L_\infty(\Omega)} \leq k_2 \|c\|_\infty,$$

met

$$k_1 = \left(1 + \frac{192\sqrt{3}K}{\tan(\theta_{\Delta^{PS}}/2)}\right)^{-1}, \quad k_2 = 1.$$

Hierbij is K een factor die verbonden is met de keuze van de B-spline basis uit de klasse. Typisch is K kleiner dan één. Met $\theta_{\Delta^{PS}}$ bedoelen we de kleinste hoek in de driehoeksverdeling Δ^{PS}. We tonen ook aan dat

$$\left\| \sum_{i=1}^{N}\sum_{j=1}^{3} c_{ij} B_{ij} \right\|_{L_p(\Omega)} \sim \left(\sum_{i=1}^{N}\sum_{j=1}^{3} |c_{ij}|^p \operatorname{vol}(\operatorname{supp} B_{ij}) \right)^{1/p}$$

voor alle $0 < p < \infty$. Merk op dat $\|\cdot\|_{L_p}$ een quasi-norm is voor $p < 1$.

3 De hiërarchische basis

Het vertrekpunt in de constructie van een hiërarchische basis is steeds een rij van eindig dimensionale functieruimten die genest zijn:

$$S_0 \subset S_1 \subset S_2 \subset \cdots \subset S_n \subset \cdots .$$

Hoe hoger de waarde van n, hoe meer detail kan voorgesteld worden door functies in S_n. Elke functieruimte S_n heeft een eindige basis, en de verzameling functies

$$\bigcup_{l=0}^{n} \{\phi_{k,l}\}_{k \in I_l}$$

is een hiërarchische basis voor S_n als

$$\bigcup_{l=0}^{m} \{\phi_{k,l}\}_{k \in I_l}$$

een basis is voor S_m voor alle $m = 0, 1, \ldots, n$.

3.1 Powell–Sabin spline subdivisie

Het doel van PS spline subdivisie is om de B-spline representatie van een PS spline s op een driehoeksverdeling Δ_l te berekenen, waarbij s gegeven is op een initiële driehoeksverdeling Δ_0 en waarbij Δ_l verkregen is door Δ_0 te verfijnen. Als we een verfijningsstrategie vinden die ervoor zorgt dat

$$\Delta_0 \subset \Delta_1 \subset \Delta_2 \subset \cdots$$
$$\Delta_0^{PS} \subset \Delta_1^{PS} \subset \Delta_2^{PS} \subset \cdots$$

dan vinden we onmiddellijk PS spline ruimten $S_l := S_2^1(\Delta_l^{PS})$ die genest zijn. We kunnen dan een willekeurige $s \in S_0$ voorstellen als lineaire combinatie van basisfuncties in S_n.

In deze thesis beschouwen we drie verfijningsstrategieën. De meest gebruikte procedure om driehoeksroosters te verfijnen is dyadische subdivisie (Figure 3.1). Hierbij wordt een nieuw punt toegevoegd tussen elke twee oude punten en elke oorspronkelijke driehoek wordt gesplitst in vier nieuwe driehoeken. Dyadische subdivisie is echter enkel toepasbaar voor PS splines als de initiële driehoeksverdeling Δ_0 niet sterk onregelmatig is. Daarom beschouwen we ook triadische verfijning (Figure 3.2). Hier wordt een nieuw hoekpunt geplaatst in elke oude driehoek, en twee nieuwe hoekpunten worden geplaats op elke zijde in de oude driehoeksverfijning. De oorspronkelijke driehoeken worden gesplitst in negen nieuwe driehoeken. Een nadeel van triadische verfijning is dat het aantal driehoeken te snel stijgt per subdivisiestap, zodat in de praktijk maar enkele subdivisiestappen mogelijk zijn. Triadische subdivisie is echter wel steeds toepasbaar voor PS splines. Een derde mogelijkheid is $\sqrt{3}$-subdivisie (Figure 3.3). Hier wordt een punt toegevoegd in elke driehoek en de punten worden opnieuw getriangulariseerd. De oude zijden van de driehoeken worden niet behouden, maar worden vervangen door nieuwe zijden die het nieuwe punt verbinden met de oude hoekpunten en met de nieuwe punten in de aangrenzende oude driehoeken. Tweemaal $\sqrt{3}$-subdivisie toepassen geeft triadische subdivisie. Een nadeel van $\sqrt{3}$-subdivisie is dat er op de rand van het domein speciale constructies nodig zijn.

Een subdivisieschema resulteert in geneste spline ruimten. Daarom kan een basisfunctie op een ruw niveau steeds geschreven worden als een lineaire

combinatie van basisfuncties op het volgende fijnere niveau:

$$\boldsymbol{\phi}_l = \boldsymbol{\phi}_{l+1} A_l,$$

waarbij de rijvector $\boldsymbol{\phi}_l$ alle basisfuncties op niveau l bevat. We kunnen $\boldsymbol{\phi}_{l+1}$ splitsen in een deel $\boldsymbol{\phi}_{l+1}^o$ dat de basisfuncties bevat die overeenkomen met de hoekpunten in Δ_l en een deel $\boldsymbol{\phi}_{l+1}^n$ dat de basisfuncties bevat die overeenkomen met de hoekpunten in $\Delta_{l+1} \setminus \Delta_l$. We definiëren de hiërarchische basis voor S_m als de verzameling basisfuncties

$$\boldsymbol{\phi}_0 \cup \bigcup_{l=1}^{m} \boldsymbol{\phi}_l^n.$$

De resultaten in deze thesis zijn steeds geformuleerd voor geneste PS spline ruimten die verkregen zijn door triadische verfijning. De resultaten blijven geldig voor dyadische of $\sqrt{3}$ subdivisieschema's na enkele kleine aanpassingen.

3.2 Multiresolutie analyse

Een multiresolutie analyse bestaat uit

1. een Banach ruimte $\mathcal{B}$ met norm $\|\cdot\|_{\mathcal{B}}$,
2. een rij van geneste ruimten $S_0 \subset S_1 \subset \cdots \subset \mathcal{B}$ die dicht zijn in $\mathcal{B}$,
3. een verzameling operatoren $\mathcal{Q}_l : \mathcal{B} \to S_l$ met de eigenschappen

$$\begin{aligned} \mathcal{Q}_l \mathcal{Q}_l &= \mathcal{Q}_l, \\ \mathcal{Q}_l \mathcal{Q}_{l+1} &= \mathcal{Q}_l, \\ \mathcal{Q}_l(\mathcal{B}) &= S_l. \end{aligned}$$

We kunnen $\mathcal{B}$ schrijven als de directe som

$$\mathcal{B} = S_0 \oplus W_0 \oplus W_1 \oplus W_2 \oplus \cdots,$$

waarbij $S_{l+1} = S_l \oplus W_l$ en $W_l := \{s \in S_{l+1} | \mathcal{Q}_l s = 0\}$.

We tonen aan dat een multiresolutie analyse verkregen kan worden met $S_l := S_2^1(\Delta_l^{PS})$ en met $\mathcal{B} = C^1(\overline{\Omega})$. Als operatoren $\mathcal{Q}_l$ nemen we de Hermite interpolatoren $\mathcal{I}_l$: voor een willekeurige $f \in C^1(\overline{\Omega})$ is $\mathcal{I}_l f$ uniek gedefinieerd als de Powell–Sabin spline die de functie f en haar afgeleiden interpoleert in de hoekpunten van de driehoeksverfijning Δ_l. De ruimten W_l worden in dit geval opgespannen door de basisfuncties in de rijvector $\boldsymbol{\phi}_{l+1}^n$. Deze multiresolutie analyse wordt dus opgespannen door de hiërarchische basis.

3.3 Stabiliteit van de hiërarchische basis

Stel dat we beschikken over een multiresolutie analyse waarbij $\mathcal{B}$ kan ontbonden worden als

$$\mathcal{B} = S_0 \oplus W_0 \oplus W_1 \oplus W_2 \oplus \cdots ,$$

en dat we beschikken over een stabiele basis $\psi_l := \{\psi_{k,l} | k \in J_l\}$ voor elke W_l. Elke $f_n \in S_n$ kan geschreven worden in de nodale basis voorstelling als

$$f_n = \sum_{k \in I_n} c_{k,n} \phi_{k,n}$$

of in multischaal voorstelling als

$$f_n = \sum_{l=-1}^{n-1} \sum_{k \in J_l} d_{k,l} \psi_{k,l},$$

waarbij $\psi_{-1} := \{\phi_{k,0} | k \in I_0\}$, $J_{-1} := I_0$. Deze multischaal voorstelling is vooral nuttig als de norm van f in een L_p of Sobolev ruimte kan afgeleid worden door de grootte van de coëfficiënten $d_{k,l}$ te onderzoeken. Stel dat voor elke $n \geq 0$

$$C_1^{-1} \left\| (d_{k,l})_{l \in K_n, k \in J_l} \right\|_v \leq \left\| \sum_{l \in K_n} \sum_{k \in J_l} d_{k,l} \psi_{k,l} \right\|_{\mathcal{B}} \leq C_2 \left\| (d_{k,l})_{l \in K_n, k \in J_l} \right\|_v$$

met $\| \cdot \|_v$ een vector norm en $K_n := \{-1, \ldots, n-1\}$, dan zeggen we dat de multischaal basis sterk stabiel is als C_1, C_2 niet afhangen van n. Indien de constanten C_1, C_2 nog afhangen van n, maar niet van exponentiële orde, dan zeggen we dat de multischaal basis zwak stabiel is.

We tonen aan dat de hiërarchische basis van Powell–Sabin splines een zwak stabiele basis is voor de Banach ruimte $C^1(\overline{\Omega})$, maar dat ze een sterk stabiele basis is voor de fractionele Sobolev ruimten $H^s(\Omega)$ met $2 < s < \frac{5}{2}$. Als onmiddellijk gevolg kunnen we dan bewijzen dat het conditiegetal van de stijfheidsmatrix van een vierde orde elliptische partiële differentiaalvergelijking, gediscretiseerd met deze hiërarchische basis, van de orde $|\log h|^2$ is, met h de stapgrootte van de discretisatie. Deze discretisatie is equivalent aan de hiërarchische basis preconditioner.

3.4 Compressie van oppervlakken

Sterke stabiliteit duidt aan dat kleine coëfficiënten in de basisvoorstelling weggelaten kunnen worden. Dit vormt de basis van compressie. We beschrijven hier een compressie-algoritme dat gebaseerd is op niet-lineaire N-termen benadering, waarbij men een basis kiest en dan een gegeven functie

zo goed mogelijk benadert door een lineaire combinatie van N termen uit die basis te nemen.

We hebben reeds aangetoond dat de hiërarchische basis sterk stabiel is voor de Sobolev ruimten $H^s(\Omega)$ met $2 < s < 5/2$. Bijgevolg is de hiërarchische basis geschikt voor compressiedoeleinden. Stel dat we een PS spline benadering S van f zoeken zodat de benaderingsfout $\|f - S\|_{L_\infty(\Omega)}$ onder een gegeven drempelwaarde ϵ ligt. Dan zoeken we eerst een $K \in \mathbb{N}$ en een PS spline $s \in S_K$ zodat

$$\|f - s\|_{L_\infty(\Omega)} \leq \epsilon/2.$$

Hier is s een lineaire benadering van f. Vervolgens schrijven we s in de hiërarchische basisvoorstelling en laten we alle coëfficiënten weg die kleiner zijn dan de drempelwaarde $\epsilon/(2K + 2)$. De gecomprimeerde benadering S van f voldoet nu aan $\|f - S\|_{L_\infty(\Omega)} \leq \epsilon$.

Stel nu dat we een gecomprimeerde niet-lineaire benadering S en een lineaire benadering s hebben van f, waarbij beide benaderingen S en s uit N termen bestaan. Dan tonen we aan dat $\|f - S\|_{L_\infty} = \mathcal{O}(N^{-\sigma/2})$ als f beschikt over σ "afgeleiden" in $L_{2/\sigma}$ en dat $\|f - s\|_{L_\infty} = \mathcal{O}(N^{-\sigma/2})$ als f beschikt over σ "afgeleiden" in L_∞, wat een veel strengere voorwaarde is.

3.5 De BPX-preconditioner

De BPX-preconditioner is nauw verwant aan de hiërarchische basis preconditioner. We hebben reeds gezien dat de hiërarchische basis preconditioner equivalent is aan het discretiseren van een gegeven partiële differentiaalvergelijking met de hiërarchische basis. De BPX-preconditioner is equivalent aan het discretiseren van een differentiaalvergelijking door alle basisfuncties $B_{ij,l}$ op alle niveau's l te gebruiken. Bijgevolg maakt de BPX-preconditioner niet echt gebruik van een basis, maar van een frame. Aangezien het aantal basisfuncties in het BPX-frame veel groter is dan de eigenlijke dimensie van de ruimte opgespannen door deze basisfuncties zal het conventionele conditiegetal van de bijhorende stijfheidsmatrix oneindig zijn. Men kan echter aantonen dat niet het conventionele conditiegetal van belang is, maar wel het veralgemeende conditiegetal dat gedefinieerd is als de grootste eigenwaarde gedeeld door de kleinste eigenwaarde verschillend van nul. Dit veralgemeende conditiegetal is van constante orde voor de BPX-voorgeconditioneerde stijfheidsmatrix voor vierde orde elliptische partiële differentiaalvergelijkingen. Deze BPX-preconditioner is dus optimaal.

4 De hiërarchische basis van Lagrange type

In het vorige hoofdstuk construeerden we een multiresolutie analyse met behulp van Hermite interpolatoren. Die Hermite interpolatoren zijn enkel goed gedefinieerd voor voldoende gladde functies, meer bepaald functies in de Sobolev ruimten $H^s(\Omega)$ met $s > 2$. In dit hoofdstuk construeren we een multiresolutie analyse met behulp van Lagrange interpolatoren. Deze interpolatoren zijn reeds goed gedefinieerd voor functies in de Sobolev ruimten $H^s(\Omega)$ met $s > 1$. We kunnen dus minder gladde functies benaderen en dit opent perspectieven voor meerdere toepassingen. Wij zijn vooral geïnteresseerd in de constructie van een optimale preconditioner.

4.1 Een stabiele lokale Lagrange basis

Zij Ω een gebied in $\mathbb{R}^2$ met polygonale rand waarvoor er een driehoeksverfijning Δ_0 bestaat zodat

(a) $\Omega = \bigcup_{T\in\Delta_0} T$,

(b) de doorsnede van twee driehoeken in Δ_0 is ofwel leeg ofwel een gemeenschappelijk hoekpunt ofwel een gemeenschappelijke zijde,

(c) alle inwendige hoekpunten hebben waarde zes,

(d) alle driehoeken in Δ_0 kunnen wit of zwart gekleurd worden zodat elk inwendig hoekpunt in Δ_0 tot juist één zwarte driehoek behoort.

Zo een driehoeksverfijning kan geconstrueerd worden voor elk willekeurig domein Ω. Stel nu dat Δ_1 de triadische verfijning is van Δ_0. Dan is het eenvoudig om na te gaan dat Δ_1 nog steeds voldoet aan (a)–(d). Bijgevolg voldoet elke verfijning Δ_l aan (a)–(d). Definieer $\Delta_l^\bullet$ als de deelverzameling van Δ_l die bestaat uit de zwarte driehoeken en Δ_l° als $\Delta_l \setminus \Delta_l^\bullet$.

We willen een elliptische partiële differentiaalvergelijking met Dirichlet randvoorwaarden oplossen. Daarom zijn we vooral geïnteresseerd in de multischaal ruimten $S_l \subset S_2^1(\Delta_l^{PS})$ gegeven door

$$S_l := \left\{ s \in C^1(\overline{\Omega}) \mid s|_\tau \in \mathcal{P}_2 \ \forall \tau \in \Delta_l^{PS}, s = D_x s = D_y s = 0 \text{ op } \partial\Omega \right\}.$$

De ruimten S_l zijn genest. Voor elk inwendig hoekpunt $V_i \in \Delta_l$ bestaat er een driehoek $T_{V_i} \in \Delta_l^\bullet$ zodat V_i tot T_{V_i} behoort. Definieer $D_l(V_i)$ als de verzameling $\{V_i, V_{ij}, V_{ik}\}$, met V_{ij} en V_{ik} zo gekozen dat de driehoek $T(V_i, V_{ij}, V_{ik})$ behoort tot de triadische verfijning van driehoek $T_{V_i} \in \Delta_l^\bullet$. Definieer Ξ_l als de unie van alle verzamelingen $D_l(V_i)$,

$$\Xi_l := \bigcup_{V_i \in \Delta_l \setminus \partial\Omega} D_l(V_i).$$

We tonen aan dat voor een willekeurige functie $f \in C^0(\Omega)$ er een unieke spline $s \in S_l$ bestaat zodat $s(\xi) = f(\xi)$ voor alle $\xi \in \Xi_l$.

Bijgevolg kunnen we Lagrange basisfuncties $B_{\xi,l}$ met $\xi \in \Xi_l$ definiëren voor de ruimte S_l. Zij zijn de unieke oplossingen van het interpolatieprobleem

$$B_{\xi,l}(\zeta) = \delta_{\xi,\zeta}, \quad \forall \xi, \zeta \in \Xi_l,$$

met $\delta_{\xi,\zeta}$ de Kronecker delta. De Lagrange basisfuncties hebben een compacte drager en ze zijn stabiel:

$$\left\| \sum_{\xi \in \Xi_l} c_\xi B_{\xi,l} \right\|_{L_\infty(\Omega)} \sim \|\mathbf{c}\|_\infty$$

en

$$\left\| \sum_{\xi \in \Xi_l} c_\xi B_{\xi,l} \right\|_{L_p(\Omega)} \sim \left(\sum_{\xi \in \Xi_l} |c_\xi|^p \operatorname{vol}(\operatorname{supp} B_{\xi,l}) \right)^{1/p}.$$

4.2 Een hiërarchische basis van Lagrange type

We introduceren de Lagrange interpolant $\mathcal{L}_l : C^0(\Omega) \to S_l$ die gedefinieerd is als

$$\mathcal{L}_l f := \sum_{\xi \in \Xi_l} f(\xi) B_{\xi,l}.$$

Deze operator is geschikt voor het construeren van een multiresolutie analyse voor de Banach ruimte $C_0^0(\Omega)$, de ruimte van C^0 continue functies die verdwijnen op de rand $\partial\Omega$ van het domein Ω. De operator $\mathcal{L}_l$ is uniform begrensd in $C_0^0(\Omega)$ en de splineruimten S_l zijn dicht in $C_0^0(\Omega)$. We kunnen $C_0^0(\Omega)$ nu schrijven als de directe som

$$C_0^0(\Omega) = S_0 \oplus W_0 \oplus W_1 \oplus W_2 \oplus \cdots,$$

met $W_l := \{s \in S_{l+1} \mid \mathcal{L}_l s = 0\}$. De ruimten W_l worden opgespannen door de basisfuncties $\{B_{\xi,l+1} \mid \xi \in \Xi_{l+1} \setminus \Xi_l\}$.

We tonen tevens aan dat de hiërarchische basis

$$\bigcup_{l=0}^{\infty} \left\{ 3^{(1-s)l} B_{\xi,l} \mid \xi \in \Xi_l \setminus \Xi_{l-1} \right\}$$

een sterk stabiele basis is voor de Sobolev ruimten $H_0^s(\Omega)$ voor alle $s \in (1, \frac{5}{2})$. Door Lagrange interpolatie te gebruiken in plaats van Hermite interpolatie breiden we het stabiliteitsinterval dus uit van $2 < s < 5/2$ naar $1 < s < 5/2$. We kunnen nu praktisch onmiddellijk aantonen dat het conditiegetal van de

stijfheidsmatrix van een vierde orde elliptische partiële differentiaalvergelijking, gediscretiseerd met deze hiërarchische basis, van constante orde is. De Lagrange type hiërarchische basis preconditioner is optimaal.

5 Optimale wavelet preconditioners

In plaats van nodale basisfuncties te gebruiken in de discretisatie van elliptische partiële differentiaalvergelijkingen kunnen we ook wavelets gebruiken. We beschrijven meerdere methoden voor het creëren van wavelets die geschikt zijn voor de discretisatie van differentiaalvergelijkingen.

5.1 Multischaal decompositie en lifting

Stel dat Ω een begrensd domein in $\mathbb{R}^d$ is of $\mathbb{R}^d$ zelf, en dat we beschikken over een rij geneste splineruimten $S_0 \subset S_1 \subset \cdots \subset L_2(\Omega)$ waarbij elke S_l opgespannen wordt door de verzameling basisfuncties $\{\phi_{k,l} \mid k \in I_l\}$. De basisfuncties $\phi_{k,l}$ worden ook wel schaalfuncties genoemd. Zij $\boldsymbol{\phi}_l$ de rijvector van alle schaalfuncties $\phi_{k,l}$ met $k \in I_l$. Dan bestaat er een subdivisiematrix A_l zodat $\boldsymbol{\phi}_l = \boldsymbol{\phi}_{l+1} A_l$. De subdivisiematrix A_l heeft de vorm

$$A_l = \begin{bmatrix} O_l \\ N_l \end{bmatrix},$$

waarbij het deel O_l de coëfficiënten berekent van de basisfuncties $\phi_{k,l+1}$ die geassocieerd kunnen worden met oude punten en waarbij het deel N_l de coëfficiënten berekent van de basisfuncties $\phi_{k,l+1}$ die geassocieerd kunnen worden met de nieuwe punten. Op dezelfde manier delen we $\boldsymbol{\phi}_{l+1}$ op als $[\boldsymbol{\phi}^o_{l+1} \quad \boldsymbol{\phi}^n_{l+1}]$.

We willen S_{l+1} schrijven als $S_l \oplus W_l$ waarbij W_l opgespannen wordt door wavelets $\psi_{m,l}$. Dit wordt uitgedrukt in matrixvorm als

$$[\boldsymbol{\phi}_l \quad \boldsymbol{\psi}_l] = \boldsymbol{\phi}_{l+1}[A_l \quad B_l],$$

waarbij $\boldsymbol{\psi}_l = \boldsymbol{\phi}_{l+1} B_l$ de rijvector met wavelets is die W_l opspannen. De wavelets $\boldsymbol{\psi}_l$ zijn initieel gedefinieerd als $\boldsymbol{\phi}^n_{l+1}$ zodat

$$B_l = \begin{bmatrix} 0 \\ I \end{bmatrix}.$$

We vertrekken dus van de standaard hiërarchische basis. Het lifting schema laat nu toe om de wavelets te wijzigen op de volgende manier:

$$\boldsymbol{\psi}_l = \boldsymbol{\phi}^n_{l+1} - \boldsymbol{\phi}_l C_l$$

met C_l de lifting matrix. Er geldt nu dat

$$[\boldsymbol{\phi}_l \quad \boldsymbol{\psi}_l] = \boldsymbol{\phi}_{l+1}[A_l \quad B_l - A_l C_l].$$

De matrix C_l wordt zo gekozen zodat de wavelets bepaalde gewenste eigenschappen hebben. De semi-orthogonale constructie bijvoorbeeld orthogonaliseert de wavelets $\boldsymbol{\psi}_l$ ten opzichte van S_l. De lifting matrix C_l wordt nu gevonden als de oplossing van het lineaire stelsel $C_l = \langle \boldsymbol{\phi}_l, \boldsymbol{\phi}_l \rangle^{-1} \langle \boldsymbol{\phi}_l, \boldsymbol{\phi}_{l+1} \rangle$. Deze keuze geeft een stabiele multischaal basis, maar de wavelets zijn niet bruikbaar in de praktijk omdat ze een globale drager hebben.

Om ervoor te zorgen dat de wavelets een lokale drager hebben is het voldoende te eisen dat de lifting matrix C_l een bandmatrix is. Dit betekent in de praktijk dat een waveletfunctie in de liftingstap

$$\boldsymbol{\psi}_l = \boldsymbol{\phi}_{l+1}^n - \boldsymbol{\phi}_l C_l$$

niet door alle schaalfuncties in $\boldsymbol{\phi}_l$ aangepast wordt, maar slechts door enkelen.

Onze constructiemethode is als volgt. Voor elke waveletfunctie $\psi_{m,l}$ in $\boldsymbol{\psi}_l$ kiezen we op voorhand een beperkt aantal schaalfuncties die we mogen gebruiken in de liftingstap. De vrijheidsgraden worden dan zo gebruikt dat de wavelets één nulmoment hebben en dat ze zo orthogonaal mogelijk zijn ten opzichte van de gekozen schaalfuncties in de liftingstap. We kunnen aantonen dat de wavelets in $\boldsymbol{\psi}_l$ een stabiele basis vormen voor W_l.

Een belangrijk aspect van het lifting schema is het bestaan van een biorthogonale basis. Dit wil zeggen dat er duale schaalfuncties en duale wavelets bestaan die voldoen aan de relatie

$$[\widetilde{\boldsymbol{\phi}}_l \quad \widetilde{\boldsymbol{\psi}}_l] = \widetilde{\boldsymbol{\phi}}_{l+1}[\widetilde{A}_l^T \quad \widetilde{B}_l^T]$$

met filters $\widetilde{A}_l$, $\widetilde{B}_l$ zodat

$$\begin{aligned} &\langle \widetilde{\phi}_{k,l}, \phi_{k',l} \rangle = \delta_{k,k'}, \quad &&\langle \widetilde{\psi}_{m,l}, \psi_{m',l} \rangle = \delta_{m,m'}, \\ &\langle \widetilde{\phi}_{k,l}, \psi_{m,l} \rangle = 0, &&\langle \widetilde{\psi}_{m,l}, \phi_{k,l} \rangle = 0, \end{aligned}$$

geldig is voor alle k, k', m, m'.

5.2 Stabiliteit over alle resolutieniveaus

De wavelets $\boldsymbol{\psi}_l$ zijn een stabiele basis voor W_l maar dat impliceert niet dat de multischaal basis $\bigcup_{l=0}^{\infty} \boldsymbol{\psi}_l$ een sterk stabiele basis is. We willen alle Sobolev ruimten $H^s(\Omega)$ kennen waarvoor $\bigcup_{l=0}^{\infty} \boldsymbol{\psi}_l$ een stabiele basis vormt.

Men kan aantonen dat $\bigcup_{l=0}^{\infty} \boldsymbol{\psi}_l$ een sterk stabiele basis is voor $H^s(\Omega)$ voor alle s met $-s_{\widetilde{\phi}_{k,l}} < s < s_{\phi_{k,l}}$. Met s_f bedoelen we de Sobolev regulariteit van een functie f:

$$s_f := \sup \{ s : f \in H^s(\Omega) \}.$$

Het is dus voldoende om $s_{\widetilde{\phi}_{k,l}}$ en $s_{\phi_{k,l}}$ te berekenen. Aangezien $\phi_{k,l}$ meestal een goed gekende splinefunctie is, is het berekenen van $s_{\phi_{k,l}}$ niet zo moeilijk. Men maakt hiervoor gebruik van zogenaamde Jackson en Bernstein afschattingen. De duale functie $\widetilde{\phi}_{k,l}$ is echter meestal niet expliciet gekend. Vaak beschikt men enkel over een recursiebetrekking van de vorm $\widetilde{\boldsymbol{\phi}}_l = \widetilde{\boldsymbol{\phi}}_{l+1}\widetilde{A}_l^T$ en is het berekenen van $s_{\widetilde{\phi}_{k,l}}$ moeilijk. De enige mogelijke berekeningswijze momenteel maakt gebruik van Fouriertechnieken.

Het gebruik van Fouriertechnieken legt echter enkele ernstige beperkingen op de geneste splineruimten. Ze moeten namelijk invariant zijn ten opzichte van verschuivingen en dilaties. Realistische toepassingen houden hier natuurlijk geen rekening mee, daarom ook dat de constructiemethode van de vorige paragraaf geldig is op willekeurige domeinen. Voor onze stabiliteitsanalyse zullen we echter eisen dat de splineruimten invariant zijn voor verschuivingen en dilaties. We hopen dat de zo bekomen resultaten goede schattingen zijn voor de constructies op willekeurige domeinen.

5.3 Wavelet constructies

We construeren verscheidene wavelet basissen. Hiervoor maken we gebruik van het lifting schema en de stabiliteit wordt geanalyseerd met Fouriertechnieken. We vinden

- een lineaire wavelet basis op $\mathbb{R}$ die sterk stabiel is voor $H^s(\mathbb{R})$ met $-0.440765 < s < 1.5$,
- een lineaire wavelet basis op $\mathbb{R}^2$ die sterk stabiel is voor $H^s(\mathbb{R}^2)$ met $-0.328857 < s < 1.5$,
- een Powell–Sabin spline wavelet basis op $\mathbb{R}^2$ die sterk stabiel is voor $H^s(\mathbb{R}^2)$ met $0.802774 < s < 2.5$,
- een kubische spline wavelet basis op $\mathbb{R}$ die sterk stabiel is voor $H^s(\mathbb{R})$ met $-0.828823 < s < 2.5$,
- een lineaire wavelet basis op $\mathbb{R}^2$ die sterk stabiel is voor $H^s(\mathbb{R}^2)$ met $-0.440765 < s < 1.5$.

Tevens bespreken we ook een andere constructietechniek waarbij we semi-orthogonale Powell–Sabin spline wavelets creëren die sterk stabiel zijn voor $H^s(\mathbb{R}^2)$ met $-2.5 < s < 2.5$.

6 Elliptische partiële differentiaalvergelijkingen op de bol

Stel dat Ω een deelverzameling is van de eenheidsbol S in $\mathbb{R}^3$. We willen het modelprobleem

$$\Delta_S^2 u = f \quad \text{op} \quad \Omega, \qquad u = \frac{\partial u}{\partial \overline{n}} = 0 \quad \text{op} \quad \partial\Omega$$

oplossen, met Δ_S de Laplace–Beltrami operator op S, en $\overline{n}$ de normaal op $\partial\Omega$ rakend aan S. De Laplace–Beltrami operator is gedefinieerd als

$$\Delta_S = \nabla_S \cdot \nabla_S$$

met ∇_S de tangentiële gradiënt

$$\nabla_S u := \nabla u - (n \cdot \nabla u) n,$$

waarbij n de normaal is op het boloppervlak S.

Om dit modelprobleem te discretiseren gebruiken we eindige elementen op de bol. Meer bepaald zoeken we naar een geschikte stabiele basis waarvan de basisfuncties lokale dragers hebben.

6.1 Homogene en sferische spline ruimten

Een functie f gedefinieerd op $\mathbb{R}^3$ is homogeen van graad d als en slechts als $f(\alpha v) = \alpha^d f(v)$ voor alle reële getallen α en voor alle $v \in \mathbb{R}^3$. Met $\mathbb{H}_d$ bedoelen we de ruimte van trivariate veeltermen van graad d die homogeen zijn van graad d. Dit is een $\binom{d+2}{2}$ dimensionale deelruimte van de ruimte van trivariate veeltermen van graad d. Stel dat $\{v_1, v_2, v_3\}$ een verzameling onafhankelijke eenheidsvectoren zijn in $\mathbb{R}^3$, dan noemen we

$$\mathcal{T} := \{v \in \mathbb{R}^3 \mid v = b_1(v)v_1 + b_2(v)v_2 + b_3(v)v_3 \quad \text{met} \quad b_i(v) \geq 0\}$$

de trihedron gegenereerd door $\{v_1, v_2, v_3\}$ en elke $v \in \mathbb{R}^3$ kan geschreven worden als

$$v = b_1(v)v_1 + b_2(v)v_2 + b_3(v)v_3.$$

We noemen $b_1(v), b_2(v), b_3(v)$ de trihedrale coördinaten van v met betrekking tot $\mathcal{T}$. De homogene Bernstein basisveeltermen van graad d op $\mathcal{T}$ zijn de veeltermen

$$B_{ijk}^d(v) := \frac{d!}{i!j!k!} b_1(v)^i b_2(v)^j b_3(v)^k, \qquad i + j + k = d,$$

en zij vormen een basis voor $\mathbb{H}_d$. Een sferische driehoek is gedefinieerd als de beperking van een trihedron $\mathcal{T}$ tot de eenheidsbol S. De beperkingen

van de trihedrale coördinaten tot een sferische driehoek worden de sferische barycentrische coördinaten genoemd. Elke homogene veelterm p van graad d en zijn beperking tot een sferische driehoek τ heeft een Bernstein–Bézier voorstelling met betrekking tot τ

$$p(v) := \sum_{i+j+k=d} c_{ijk} B^d_{ijk}(v),$$

en de coëfficiënten c_{ijk} zijn de Bézier ordinaten.

Met $\mathbb{H}_d(\Omega)$ duiden we de beperking van $\mathbb{H}_d$ tot een deelverzameling Ω van de eenheidsbol S aan en we noemen dit de ruimte van sferische veeltermen van graad d. Zij Δ een conforme sferische driehoeksverfijning van $\Omega \subset S$. De ruimte van sferische splines van graad d en gladheid r op Δ wordt gegeven door

$$S^r_d(\Delta) := \{s \in C^r(S) \mid s|_\tau \in \mathbb{H}_d(\tau),\ \tau \in \Delta\},$$

waarbij $s|_\tau$ de beperking van s tot de sferische driehoek τ is.

6.2 Sferische PS splines

De Powell–Sabin 6-split Δ^{PS} van een sferische driehoeksverfijning Δ wordt analoog gedefinieerd als de PS 6-split van een vlakke driehoeksverfijning. Het klassieke resultaat van Powell en Sabin kan uitgebreid worden naar de sferische splineruimten die we zonet geïntroduceerd hebben. Zij g_i en h_i onafhankelijke eenheidsvectoren die liggen in het raakvlak aan S in hoekpunt $V_i \in \Delta$, $i = 1, \ldots, N$. Gegeven is een willekeurige verzameling van triplets $(\alpha_i, \beta_i, \gamma_i)$, $i = 1, \ldots, N$. We tonen aan dat er een unieke sferische PS spline $s(v) \in S^1_2(\Delta^{PS})$ bestaat zodanig dat

$$s(V_i) = \alpha_i, \quad D_{g_i} s(V_i) = \beta_i, \quad D_{h_i} s(V_i) = \gamma_i$$

voor alle $i = 1, \ldots, N$. Bijgevolg is de dimensie van de sferische splineruimte $S^1_2(\Delta^{PS})$ gelijk aan $3N$.

6.3 Een B-spline basis voor sferische PS spline ruimten

Als we voor elk hoekpunt V_i in Δ getallen $(\alpha_{ij}, \beta_{ij}, \gamma_{ij})$, $j = 1, 2, 3$, kiezen die een verzameling van 3 lineair onafhankelijke triplets vormen, dan heeft elke $s(v) \in S^1_2(\Delta^{PS})$ een unieke voorstelling

$$s(v) = \sum_{i=1}^{N} \sum_{j=1}^{3} c_{ij} B_{ij}(v)$$

waarbij de B-splines $B_{ij}(v)$ gedefinieerd zijn als de unieke oplossing van het interpolatieprobleem

$$B_{ij}(V_k) = \delta_{ik}\alpha_{ij}, \quad D_{g_i}B_{ij}(V_k) = \delta_{ik}\beta_{ij}, \quad D_{h_i}B_{ij}(V_k) = \delta_{ik}\gamma_{ij}.$$

Door een goede keuze van de triplets $(\alpha_{ij}, \beta_{ij}, \gamma_{ij})$ kunnen we B-splines creëren met bepaalde nuttige eigenschappen zoals stabiliteit, het vormen van een eenheidspartitie, rakende controledriehoeken, enzovoort.

6.4 Preconditioners op de bol

De constructie van geneste sferische Powell–Sabin spline ruimten is volledig analoog aan het bivariate geval. We kunnen dyadische, triadische of $\sqrt{3}$-subdivisie gebruiken. Eveneens kunnen we, volledige analoog aan het bivariate geval, een suboptimale hiërarchische basis preconditioner en een optimale BPX-preconditioner construeren voor vierde orde elliptische partiële differentiaalvergelijkingen op de bol. De bewijzen die we hiervan geven zijn echter geen triviale uitbreiding van het bivariate geval, maar zijn gebaseerd op de expliciete constructie van de sferische B-splines.

7 Besluit

7.1 Belangrijkste bijdragen

- We bewijzen dat de B-spline basis een stabiele basis vormt voor de Powell–Sabin spline ruimte voor alle L_p normen met $0 < p \leq \infty$.
- We tonen aan dat de Hermite interpolerende Powell–Sabin spline een gegeven functie en haar afgeleiden optimaal benaderd.
- We tonen aan dat de standaard hiërarchische basis een multiresolutie analyse vormt voor de Banach ruimte $C^1(\overline{\Omega})$. Deze basis is zwak stabiel met betrekking tot de norm in $C^1(\overline{\Omega})$, maar sterk stabiel met betrekking tot de norm in de deelruimten $H^s(\Omega)$ met $s \in (2, \frac{5}{2})$.
- Bijgevolg is de hiërarchische basis geschikt voor de compressie van oppervlakken. We leiden a priori foutengrenzen af die scherp zijn.
- We bewijzen dat de hiërarchische basis suboptimaal is als preconditioner voor vierde orde elliptische partiële differentiaalvergelijkingen. Nauw verwant is de BPX-preconditioner en we tonen aan dat deze preconditioner optimaal is.
- We constueren een nieuwe basis voor $S_2^1(\Delta^{PS})$ door gebruik te maken van Lagrange interpolatie. De bijhorende hiërarchische basis is stabiel voor $H^s(\Omega)$ met $s \in (1, \frac{5}{2})$.

- We gebruiken het lifting schema om wavelets te construeren. Dit is werk tesamen met Evelyne Vanraes.

- Door middel van Fouriertechnieken kunnen we de stabiliteit van de wavelets onderzoeken. We breiden enkele bestaande resultaten uit naar een algemener geval.

- Op uniforme rooster construeren we lokale prewavelets voor $S_2^1(\Delta^{PS})$. Deze wavelet basis is stabiel voor $H^s(\Omega)$ met $s \in (-\frac{5}{2}, \frac{5}{2})$.

- We werken een elegante manier uit om de ruimte van Powell–Sabin splines te definiëren op het oppervlak van de bol in $\mathbb{R}^3$.

- Bijgevolg vinden we een hiërarchische basis preconditioner en een BPX-preconditioner voor vierde orde elliptische partiële differentiaalvergelijkingen op de bol.

7.2 Suggesties voor verder onderzoek

- De sferische "shallow water equations" zijn een verzameling vergelijkingen die de beweging beschrijven van een dunne laag gas of vloeistof op het oppervlak van de bol. We hebben reeds een framework beschreven voor de constructie van eindige elementen op de bol en we hebben optimale preconditioners ontworpen voor elliptische vergelijkingen op de bol. Het zou de moeite waard zijn om eens een iets moeilijker probleem aan te pakken, zoals de sferische "shallow water equations".

- De constructie van multivariate wavelets op willekeurige driehoeksverdelingen is zeer moeilijk. Tot nu toe bestaat er nog steeds geen C^1 continue wavelet basis op een willekeurige driehoeksverdeling die sterk stabiel is voor de L_2 norm.

- We hebben reeds een semi-orthogonale basis gecreëerd voor de ruimte van Powell–Sabin splines waarbij de basisfuncties compacte drager hebben. Misschien is het mogelijk om een lokale orthogonale basis te creëren.

- Door het lifting schema te gebruiken kan men spline wavelets op de bol construeren.

- We hebben steeds de ruimte van Powell–Sabin splines op de PS 6-split gebruikt om preconditioners af te leiden. Men kan ook andere C^1 spline ruimten gebruiken. Het zou interessant zijn om deze verschillende preconditioners numeriek met mekaar te vergelijken.

- Het $\sqrt{3}$-subdivisie schema laat zeer gemakkelijk lokale subdivisie toe. Adaptieve eindige elementen methoden voor elliptische vergelijkingen zijn in de praktijk vaak beter dan niet-adaptieve methoden. Men zou een optimale adaptieve eindige elementen methode voor vierde orde elliptische partiële differentiaalvergelijkingen kunnen afleiden, zowel in het vlak als op de bol.

Contents

Notations

The following list contains some of the notations and symbols used in this dissertation, together with a brief explanation. The numbers at the end of each line indicate the page where the notation is explained or used for the first time. The list starts with arbitrary symbols, Greek symbols, and then proceeds more or less alphabetically.

List of symbols

ψ_l	set of wavelet functions at resolution level l 45
$\boldsymbol{\psi}_l$	row vector of wavelet functions at resolution level l .94
$\psi_{k,l}$	wavelet function (vector) 45
Ξ_l	Lagrange interpolation set at resolution level l 82
Ω	bounded (polygonal) domain 3
$\partial\Omega$	boundary of Ω 3
$\omega_r(\cdot,\cdot)_p$	modulus of smoothness 160
$a(\cdot,\cdot)$	bilinear form 4
$\mathcal{A}$	positive definite self-adjoint operator 4
$A_q^s\left(L_p(\Omega)\right)$	auxiliary space 51
A_α	mask coefficient matrix 99
$A_{\xi,l}$	area of the support of $B_{\xi,l}$ 84
A_l	low pass filter operator, subdivision matrix 35
$\widetilde{A}_l$	dual low pass filter operator 95
B_l	high pass filter operator 95
$\widetilde{B}_l$	dual high pass filter operator 95
$\mathcal{B}$	Banach space 39
$B_q^s\left(L_p(\Omega)\right)$	Besov space 51
$b_1(\cdot), b_2(\cdot), b_3(\cdot)$	barycentric coordinates, trihedral coordinates 12
B_{ij}	PS B-spline 15
$B_{ij,l}$	PS B-spline at resolution level l 35
B_{ijk}^d	Bernstein polynomial of degree d 12
$B_{\xi,l}$	PS B-spline of Lagrange type at resolution level l .. 83
c_{ij}	coefficient of B_{ij} 15
$c_{ij,l}$	coefficient of $B_{ij,l}$ 35
c_{ijk}	Bézier ordinate 12
c_ξ	coefficient of $B_{\xi,l}$ 83
$\mathcal{C}$	preconditioner 5
$E_l(f,\Omega)$	local error of approximation 161
g_l	spline wavelet component at resolution level l 46
$H^k(\Omega)$	Sobolev space with integer smoothness k 4
$H^s(\Omega)$	Sobolev space with fractional smoothness s 49
I_l	index set 31
$\mathcal{I}$	Hermite interpolant 26
$\mathcal{I}_l$	Hermite interpolant at resolution level l 46
J_l	index set 45
l	resolution level 35
$\mathcal{L}_l$	Lagrange interpolant at resolution level l 86
$\mathrm{Lip}(\delta,\Omega)$	space of δ-Lipschitz functions 59
M	dilation matrix 99
M_i	molecule of vertex V_i 15
N_l	number of vertices in Δ_l 35

p_d	bivariate polynomial of degree d	3
$\mathcal{P}_d$	bivariate polynomials of degree d	11
$P(\omega)$	symbol	100
$\mathcal{Q}_l$	projection operator	39
s_f	smoothness exponent of f	99
S_l	spline space at resolution level l	31
$S_d^r(\Delta)$	polynomial spline space	11
$S_2^1(\Delta^{PS})$	Powell–Sabin spline space	14
s_l	spline in the spline space S_l	35
$\mathrm{spec}(\cdot)$	spectrum of an operator	101
T	triangle	14
$\|T\|$	diameter of triangle T	28
T_P	transition operator	100
T_s	standard 2-simplex	24
$\mathcal{T}$	trihedron	131
$\mathscr{T}$	control triangle	16
t_i	PS-triangle	16
V_i	vertex	12
W_l	wavelet space at resolution level l	39
$W_p^k(\Omega)$	Sobolev space	27

Abbreviations

BPX	Bramble–Pasciak–Xu
CAGD	Computer Aided Geometric Design
CG	Conjugate Gradient
HB	Hierarchical Basis
MRA	Multiresolution Analysis
PDE	Partial Differential Equation
PS	Powell–Sabin

Chapter 1

Introduction

The conjugate gradient method is a very efficient solver for large linear systems arising from the Galerkin method for elliptic boundary value problems, provided that these systems have been suitably preconditioned. During the past 15 years very efficient preconditioners have become available [11, 30, 31, 33, 65, 103, 131] that achieve optimal multigrid complexity. In this dissertation we explore the potential of these techniques for fourth order elliptic problems.

1.1 A boundary value problem in 1D

Let us first explain the principles of *multilevel preconditioning* by means of a simple example. Consider the two-point boundary value problem

$$-u'' = f \quad \text{on} \quad \Omega := [0,1], \quad u(0) = u(1) = 0. \tag{1.1}$$

Although (1.1) is a simple problem for which many simple solution methods exist, we use a finite element Galerkin method to solve (1.1). The advantages of a Galerkin method are the ability to cope with complicated domains and the fact that the use of compactly supported basis functions leads to sparse stiffness matrices. Hence, the resulting system of linear equations can be solved efficiently with an iterative method.

We start from the standard *weak formulation*

$$\langle u', v' \rangle = \langle f, v \rangle, \quad v \in H_0^1([0,1]), \tag{1.2}$$

i.e. we multiply both sides of (1.1) by smooth test functions that vanish on $\partial\Omega$, the boundary of Ω, and then we integrate by parts. Here $\langle \cdot, \cdot \rangle$ is the standard L_2 inner product and $H_0^1([0,1])$ is the closure of all C^∞

functions with compact support in $(0,1)$ relative to the norm $\|f\|_{H^1([0,1])} := \|f\|_{L_2([0,1])} + \|f'\|_{L_2([0,1])}$. Note that the weak formulation requires less regularity than the original equation. The latter form makes sense even when u and v belong to the Sobolev space $H_0^1([0,1])$, and whenever f is only a distribution in the dual space $\left(H_0^1([0,1])\right)'$.

In order to solve (1.2) we employ piecewise linear continuous functions as building blocks to approximate the solution. We define trial spaces $S_l \subset H_0^1([0,1])$ that are spanned by so-called hat functions

$$\phi_{k,l}(\cdot) := 2^{l/2}\Phi(2^l \cdot -k), \quad k = 0, \ldots, 2^l, \tag{1.3}$$

with $\Phi(x)$ the generator ,

$$\Phi(x) := \begin{cases} 1+x, & -1 \le x \le 0, \\ 1-x, & 0 \le x \le 1, \\ 0, & \text{otherwise.} \end{cases} \tag{1.4}$$

With the spaces S_l defined, the Galerkin conditions

$$\langle u_l', v' \rangle = \langle f, v \rangle, \quad u_l = \sum_k c_k \phi_{k,l}, \quad v \in S_l$$

give rise to a linear system of equations

$$A_{\phi_l} c = b_{\phi_l}, \tag{1.5}$$

where A_{ϕ_l} is the stiffness matrix relative to the basis functions $\phi_{k,l}$, b_{ϕ_l} is a vector with $(b_{\phi_l})_k = \langle f, \phi_{k,l} \rangle$, and c is a vector of unknown coefficients relative to the basis functions $\phi_{k,l}$. In this particular case the stiffness matrix A_{ϕ_l} is tridiagonal, such that (1.5) is efficiently solvable without the use of an iterative method. This is not the case anymore for higher dimensional problems, so we will proceed by applying an iterative method to (1.5).

The performance of an iterative scheme for a symmetric positive definite system is known to depend on the spectral condition number κ of the system matrix. Here, the condition number κ is given by the maximum eigenvalue divided by the minimum eigenvalue, see also (1.11). It can easily be shown that the condition number of A_{ϕ_l} grows like 2^{2l} with the resolution level l. This growth can be explained by noting that the second order derivative in (1.1) treats highly oscillatory functions very differently from slowly varying functions, and the spaces S_l contain functions with frequency ranging between 1 and 2^l, see [31, Sec. 10.3] for a rigorous proof. A high condition number slows down the convergence speed of the iterative method. Therefore, it is of primary importance to precondition the linear system.

The discussion in the previous paragraph motivates the split of S_l into subspaces consisting of functions with fixed frequency. Then, on each subspace, the differential operator would be well conditioned. This is the

essence of multilevel preconditioning. The key is that the main building block is refinable. In this particular example we have indeed that

$$\begin{aligned}\Phi(x) &= \frac{1}{2}\Phi(2x+1) + \Phi(2x) + \frac{1}{2}\Phi(2x-1),\\ \phi_{k,l} &= \frac{1}{\sqrt{2}}\left(\frac{1}{2}\phi_{2k-1,l+1} + \phi_{2k,l+1} + \frac{1}{2}\phi_{2k+1,l+1}\right),\end{aligned}$$

so the spaces S_l are nested, i.e.

$$S_0 \subset S_1 \subset S_2 \subset \cdots .$$

One can now build a multilevel basis for S_n by keeping the basis functions on the lower levels and adding additional basis functions in a complement space between two successive spaces S_l and S_{l+1}. This means that we look for a suitable basis for the complement space W_l with

$$S_{l+1} = S_l \oplus W_l.$$

The space S_{l+1} is spanned by the basis functions of S_l and the basis functions of the complement space W_l. In our example the simplest complement spaces are those spanned by the hat functions corresponding to the new nodes that are added when going from a coarse level to a finer level. The resulting multilevel basis is better known under the name *hierarchical basis* [129]. For the specific case of (1.1) one can check that the stiffness matrix relative to the hierarchical basis is diagonal and a simple diagonal scaling would yield uniformly bounded condition numbers independent of the resolution level l and thus independent on the mesh size. For two dimensions we do not have a diagonal stiffness matrix anymore, but it turns out that the hierarchical stiffness matrices can still be preconditioned by diagonal scaling to obtain condition numbers that only increase logarithmically with the resolution level. Moreover, later on, we will derive several multiscale bases that perform better than the hierarchical basis.

1.2 Elliptic boundary value problems

Let p_{2k} be a polynomial of degree $2k$ on $\mathbb{R}^d$, with d the spatial dimension. Denote by $p_{2k}(D)$ the differential operator where each variable is replaced by the corresponding partial derivative. We are interested in solving boundary value problems of the form

$$p_{2k}(D)u = f \quad \text{on} \quad \Omega, \qquad Bu = 0 \quad \text{on} \quad \partial\Omega, \tag{1.6}$$

where B is a suitable trace operator expressing the boundary conditions, and $\Omega \subset \mathbb{R}^d$ has a local Lipschitz continuous boundary $\partial\Omega$. The weak

formulation of (1.6) is given by

$$a(u,v) = \langle f, v\rangle \quad \text{for all } v \in H^k_B(\Omega), \tag{1.7}$$

where $a(\cdot,\cdot)$ is the *bilinear form* induced by (1.6), and $H^k_B(\Omega)$ is a suitable subspace of the *Sobolev space* $H^k(\Omega)$ depending on the boundary conditions in terms of the operator B. The reader is referred to Section A.1 for the definition of a Sobolev space. We assume that the partial differential operator is *elliptic*, which can be expressed by the equivalence

$$a(v,v) \sim \|v\|^2_{H^k(\Omega)}, \quad v \in H^k_B(\Omega). \tag{1.8}$$

We always mean by $a \sim b$ that $a \lesssim b$ and $a \gtrsim b$ hold, where $a \lesssim b$ means that a can be bounded by a constant multiple of b uniformly in any parameters on which a, b may depend, and $a \gtrsim b$ means $b \lesssim a$. We will also refer to $\|\cdot\|^2_{H^k(\Omega)}$ as the *energy norm* induced by the bilinear form $a(\cdot,\cdot)$. The ellipticity condition (1.8) implies, by the Theorem of Lax–Milgram (see, e.g., [132]), the existence of a unique solution u to the problem (1.7) for all $f \in \big(H^k_B(\Omega)\big)'$. Here the prime denotes that $\big(H^k_B(\Omega)\big)'$ is the dual function space of $H^k_B(\Omega)$.

Denote by S_l a (finite or infinite dimensional) subspace of $H^k_B(\Omega)$, and let $\mathcal{A}$ denote the positive definite self-adjoint operator on S_l that is uniquely defined by

$$a(u,v) = \langle \mathcal{A}u, v\rangle_{S_l' \times S_l}, \quad v \in S_l. \tag{1.9}$$

The operator $\mathcal{A}$ maps the function space S_l into the topological dual function space S_l', and $\langle\cdot,\cdot\rangle_{S_l'\times S_l}$ is the dual form. We have to solve the linear operator equation

$$\mathcal{A}u = b \tag{1.10}$$

for some $u \in S_l$, where $b \in S_l'$ is defined by $\langle b, v\rangle_{S_l'\times S_l} = \langle f, v\rangle_{S_l'\times S_l}$, $v \in S_l$. The conjugate gradient method is a very efficient solver for large linear systems arising from problems such as (1.10). However, because of stability reasons, it is necessary that these systems have been suitably preconditioned. The extreme eigenvalues of some linear self-adjoint positive definite operator $\mathcal{Q}$ can be characterized by

$$\begin{aligned}
\lambda_{\min}(\mathcal{Q}) &= \min_{v\in S_l, v\neq 0} \frac{\langle \mathcal{Q}v, v\rangle_{S_l'\times S_l}}{\langle v, v\rangle_{S_l'\times S_l}}, \\
\lambda_{\max}(\mathcal{Q}) &= \max_{v\in S_l, v\neq 0} \frac{\langle \mathcal{Q}v, v\rangle_{S_l'\times S_l}}{\langle v, v\rangle_{S_l'\times S_l}},
\end{aligned}$$

and the *spectral condition number* of $\mathcal{Q}$ is given by

$$\kappa(\mathcal{Q}) = \frac{\lambda_{\max}(\mathcal{Q})}{\lambda_{\min}(\mathcal{Q})}. \tag{1.11}$$

It is known (see, e.g., [33, 74]) that if for some constants $0 < \gamma, \Gamma < \infty$ and some positive definite self-adjoint linear invertible operator $\mathcal{C}$

$$\gamma \langle \mathcal{C}^{-1}u, u\rangle_{S_l' \times S_l} \leq a(u,u) \leq \Gamma \langle \mathcal{C}^{-1}u, u\rangle_{S_l' \times S_l} \text{ for all } u \in S_l, \tag{1.12}$$

then the spectral condition number $\kappa(\mathcal{C}^{1/2}\mathcal{A}\mathcal{C}^{1/2})$ is bounded by Γ/γ.

Let us represent the operator $\mathcal{A}$ by the stiffness matrix

$$A_{\phi_l} := (a(\phi_{i,l}, \phi_{j,l}))_{i,j \in I_l}$$

with respect to some typical nodal basis $\phi_l := \{\phi_{i,l} \mid i \in I_l\}$ of S_l. Then it is known that the spectral condition number $\kappa(A_{\phi_l})$ of A_{ϕ_l} grows at least like $(\#I_l)^{2k/d}$, see, e.g., [120, Chap. 5] for spatial dimension $d = 1$. In order to precondition the system

$$A_{\phi_l} c = b_{\phi_l}, \quad (b_{\phi_l})_i := \langle f, \phi_{i,l}\rangle, \ i \in I_l, \tag{1.13}$$

one can perform a change of basis. So let $\psi := \{\psi_j \mid j \in J\}$, $\#J = \#I_l$, be another basis of S_l, and L be the transfer matrix between the two bases. Then we can transform the stiffness matrix with respect to the nodal basis into the stiffness matrix with respect to ψ_l by

$$A_\psi = L^T A_{\phi_l} L.$$

Now, suppose that the equivalence

$$k_1 \sum_{j \in J} |d_j|^2 \leq \left\| \sum_{j \in J} d_j \psi_j \right\|^2_{H^k(\Omega)} \leq k_2 \sum_{j \in J} |d_j|^2 \tag{1.14}$$

holds, then by (1.8) and (1.12) we find that

$$\kappa(A_\psi) \lesssim \frac{k_2}{k_1}.$$

Suppose that the quotient k_2/k_1 is small compared to the bound $(\#I_l)^{2k/d}$, then LL^T is a candidate for a preconditioner. Ideally k_1 and k_2 are constants, such that $\kappa(A_\psi) = \mathcal{O}(1)$.

1.3 Preconditioners

Several approaches exist to construct a suitable preconditioner for systems arising from discretizations of elliptic operator equations, such as the *hierarchical basis preconditioner* [129] and the closely related *Bramble–Pasciak–Xu preconditioner* [11]. In both cases the preconditioning is realized through a change of basis, as explained in the previous section. Originally, these preconditioners were formulated for second order problems on two-dimensional planar domains, such as the model problem

$$-\Delta u + qu = f \text{ on } \Omega, \quad u = 0 \text{ on } \partial\Omega, \tag{1.15}$$

where $\Omega \subset \mathbb{R}^2$ is a polygonal domain. The bilinear form $a(\cdot,\cdot)$ induced by the model problem (1.15) satisfies (1.8) with $k = 1$, and a suitable basis for preconditioning should satisfy (1.14) for $H^1(\Omega)$ such that the quotient k_2/k_1 does not increase too fast with the resolution level. The growth rate of the condition numbers for the hierarchical basis preconditioner was shown to be logarithmic in the size of the problem in [129]. Moreover, it was proved there that this bound is sharp. For the Bramble–Pasciak–Xu preconditioner initially only a logarithmic upper bound was established in [11]. Later an uniformly bounded condition number was established in [33, 103].

Also wavelet bases can be used for preconditioning purposes. Jaffard [65] has obtained a number of interesting results applicable to elliptic boundary value problems. Essentially his results imply that linear elliptic boundary value problems preconditioned by a suitable normalized wavelet basis yield uniformly bounded condition numbers independent of the resolution level.

Numerical experiments in [71, 81, 82] show that for the *Poisson problem*, i.e. $q = 0$ in (1.15), the Bramble–Pasciak–Xu preconditioner is superior to the wavelet Galerkin methods. Both the number of iterations needed to ensure a desired accuracy, and the cost of each iteration are higher for the wavelet methods. The situation changes for, e.g., so-called *Helmholtz problems*, where the value of $q > 0$ increases. Here the additional zero order term starts to affect stability, and the efficiency of the Bramble–Pasciak–Xu scheme starts to deteriorate. What happens is that, for large q, the zero order term qu becomes more important than the second order term Δu. Therefore, in practical situations, we have

$$a(\cdot,\cdot) \sim \|\cdot\|_{L_2(\Omega)}$$

instead of (1.8) with $k = 1$. In contrast to the Bramble–Pasciak–Xu preconditioner, wavelet based preconditioners are more *robust* for the class of problems (1.15). Wavelets often form a Riesz basis for a larger range of Sobolev spaces including $L_2(\Omega)$, so that the zero-order term qu is handled better.

Robustness is an important issue, and it favors the wavelet based discretization methods. However, one should also compare the optimal wavelet method with multiplicative multigrid schemes, which are usually more efficient than the additive counterparts (we note that the Bramble–Pasciak–Xu scheme is in fact an additive multigrid preconditioner). The performance of multigrid methods is best understood with respect to uniform mesh refinements. However, in many practical cases singularities in the data or the domain geometry may necessitate very high local resolutions, making discretizations on uniform grids unsuitable due to memory requirements. Such singularities can be handled by adaptive refinement. By their very nature, wavelet representations have a naturally built in adaptivity, and a nice theory has been developed by Cohen, Dahmen and DeVore [18, 19, 20] with regard to the following goal: keep the computational work proportional to the number of significant terms in the wavelet expansion of the searched solution, see also [7, 13, 21, 24, 27, 34]. Wavelets are much more sophisticated tools than conventional discretizations and their potential may eventually lead to competitive or even superior schemes compared to multiplicative multigrid.

1.4 The scope of this thesis

In this thesis we focus on the construction of preconditioners for fourth order elliptic problems. More specifically, as model problem we consider the *biharmonic equation* with *Dirichlet boundary conditions*, i.e.

$$\Delta^2 u = f \text{ on } \Omega, \quad u = \frac{\partial u}{\partial n} = 0 \text{ on } \partial\Omega, \tag{1.16}$$

where n is the outward normal to $\partial\Omega$. The biharmonic equation is encountered in plate bending problems (u is the Airy stress function), and it is also used to describe slow flows of viscous incompressible fluids (u is the stream function). Note that, due to different boundary regimes for plate bending, from an applied point of view mixtures of all kind of boundary conditions are possible. For simplicity we will only consider Dirichlet boundary conditions.

The hierarchical basis preconditioner and Bramble–Pasciak–Xu preconditioner could also be established for fourth order elliptic equations [36, 102]. As in the second order case, the hierarchical basis preconditioner yields logarithmic rates, while the Bramble–Pasciak–Xu preconditioner gives uniformly bounded condition numbers. The underlying bases consist of C^1 continuous conforming element spaces on regular partitions of the underlying domain, such as C^1 piecewise cubics and quintics in [36], and C^1 piecewise quadratics and cubics in [102]. In this thesis we will consider another

kind of C^1 piecewise conforming finite elements: the C^1 piecewise quadratic Powell–Sabin splines on the Powell–Sabin 6-split (in [102] PS splines were used on a PS 12-split). The spline spaces that we consider have a much lower dimension than the spaces spanned by the C^1 finite elements considered in [36, 102]. Moreover, our constructions are straightforward and simple to implement. Furthermore we will see later that our constructions can be elegantly extended to spline spaces on the surface of the two-sphere.

In Chapter 2 we briefly recall the fundamental theory of Bernstein–Bézier polynomials and we introduce the space of Powell–Sabin splines. We summarize the construction of a class of B-spline bases for PS splines, developed by Dierckx [48], that form a partition of unity. Then we prove that these B-spline bases are stable, i.e., the L_p norm of a PS spline is of the same magnitude as the discrete l_p norm of its coefficients in the B-spline representation. The stability depends on the smallest angle in the underlying triangulation and on a variable that is inherent to the actual B-spline basis that is used from the class. Furthermore we show that sufficiently smooth functions and their derivatives are approximated up to optimal order by the Hermite interpolating PS spline.

Chapter 3 starts with spline subdivision schemes for Powell–Sabin spline surfaces as developed in [126]. We are now able to calculate the B-spline representation of a surface on a refinement of the initial triangulation. We prove that the resulting nested sequence of PS spline spaces forms a multiresolution analysis for the Banach space $C^1(\overline{\Omega})$ and we introduce the corresponding hierarchical basis. We show that the hierarchical basis is weakly stable with respect to the norm in $C^1(\overline{\Omega})$, but for certain subspaces of $C^1(\overline{\Omega})$ we prove strong stability. As an immediate consequence of these stability results we find that the hierarchical basis preconditioner yields condition numbers for the problem (1.16) that increase logarithmically with the problem size, as expected. Key ingredients are the construction of suitable interpolation operators, and Jackson and Bernstein estimates that are derived in Appendix B. Next we investigate how the hierarchical basis performs as a surface compression tool. Strong stability indicates that small coefficients in the hierarchical representation can be omitted, and this feature forms the main idea for a very simple surface compression algorithm. Following the framework developed by DeVore *et al.* in [43] we derive optimal a priori error bounds with respect to the L_∞ norm. The last part of this chapter is dedicated to a Bramble–Pasciak–Xu preconditioner that is optimal for problems of the form (1.16), and we numerically compare this BPX preconditioner with the HB preconditioner.

In Chapter 4 we construct a Lagrange basis for the space of Powell–Sabin splines with homogeneous boundary conditions, and we prove that this basis is stable and local. We also consider the multiresolution setting, and prove that the hierarchical basis of Lagrange basis functions is stable with respect

to the norm in the Sobolev spaces $H^s(\Omega)$ with $s \in (1, \frac{5}{2})$. This stability range is larger than the stability range for the hierarchical basis of Hermite type from the previous chapter, and leads to a more robust preconditioner.

In Chapter 5 we present a general construction method for wavelets on arbitrary domains that are suitable for preconditioning systems arising from elliptic variational problems. First we give a short overview of the principles of lifting. Furthermore we explain how wavelets can be created on arbitrary domains and we discuss the design of the second lifting step, the update, in detail. Then we theoretically investigate the Riesz basis property in the Sobolev space $H^s(\mathbb{R}^d)$ of a given hierarchical system with Fourier techniques. Crucial here is the derivation of the smoothness of the dual system. In order to be able to use Fourier techniques we will only consider the shift-dilation invariant setting of a multiresolution analysis, although realistic applications require other settings. Then we explicitly construct wavelets with the lifting scheme and we investigate their stability with the Fourier techniques described before. Linear spline wavelets are treated in one and two dimensions, and we also construct Powell–Sabin spline wavelets. Furthermore we provide some numerical experiments that confirm the theory. Next we briefly discuss a strategy to construct stable wavelets on uniform grids. Using this strategy we find connections with other constructions in the literature. Finally we give an explicit construction of compactly supported Powell–Sabin spline prewavelets on the uniform hexagonal grid. The obtained prewavelet basis is stable in the Sobolev spaces $H^s(\Omega)$ for $|s| < \frac{5}{2}$.

Chapter 6 is devoted to elliptic PDEs on the sphere. In Section 6.2 we introduce homogeneous and spherical spline spaces which will allow us to create bases on the sphere. More specifically we consider C^1 continuous piecewise quadratic spherical spline spaces of Powell–Sabin type in Section 6.3. In order to apply the theory from Section 1.2 we need suitable basis functions for these spaces that are stable in some sense. In Section 6.4, we present an algorithm to extend bivariate PS B-splines to spherical PS B-splines. Furthermore we prove that certain important properties of the bivariate basis such as stability are inherited by the spherical B-splines. Then, in Section 6.5, we construct a weakly stable hierarchical basis on the sphere, and in Section 6.6 we construct optimal BPX preconditioners for 2nd and 4th order elliptic PDEs on the sphere and we provide some numerical experiments.

Finally we give an overview of the contributions, conclusions and suggestions fur further research in Chapter 7.

Chapter 2

Powell–Sabin splines

2.1 Introduction

In [36, 102] several C^1 conforming finite element spaces are investigated for the numerical treatment of fourth order elliptic problems, such as C^1 piecewise quadratics on a Powell–Sabin 12-split, C^1 piecewise cubics on Clough–Tocher triangles and on quandrangulations, and C^1 piecewise quintics of Argyris-type. In this dissertation we consider C^1 piecewise quadratics on a Powell–Sabin 6-split, because their patch structure is not very complicated, and because the space that they span has low dimension compared to the constructions in [36, 102].

Let Δ be an arbitrary *triangulation* of a subset $\Omega \in \mathbb{R}^2$ with polygonal boundary $\partial\Omega$. The *polynomial spline space* $S_d^r(\Delta)$ is defined as

$$S_d^r(\Delta) := \{s \in C^r(\Omega) \mid s|_\tau \in \mathcal{P}_d \text{ for all } \tau \in \Delta\}, \tag{2.1}$$

where $d > r \geq 0$ are given integers and $\mathcal{P}_d$ is the *space of bivariate polynomials of total degree* $\leq d$. Determining the dimension of spline spaces $S_d^r(\Delta)$ is a nontrivial task for $r > 0$, and can only be done for general triangulations Δ when $d \geq 3r + 2$, see [66]. A common solution for the case $d < 3r + 2$ is the use of split triangulations: each triangle is split into smaller triangles in a structured manner and the dimension of that refined triangulation can uniquely be determined. In this chapter we study C^1 continuous piecewise quadratic splines, i.e. $r = 1$ and $d = 2$. Because there exists no solution for general triangulations, we restrict ourselves to the *Powell–Sabin 6-split* Δ^{PS} of Δ. The corresponding splines are called *Powell–Sabin splines* [107].

Section 2.2 gives a very short introduction to the Bernstein–Bézier representation of polynomials on triangles and Section 2.3 introduces the space of Powell–Sabin splines. Then, in Section 2.4, we review a class of B-spline

bases of PS splines introduced by Dierckx [48]. Several other bases than the one described in this section are around in the literature [5, 77, 110]. Their main drawback is that they do not form a convex partition of unity. If properly normalized, these B-spline bases are stable with respect to the L_p norm for all $1 \leq p \leq \infty$ and with respect to the L_p *quasi-norms* for all $0 < p < 1$. We note that a quasi-norm satisfies the same properties as a norm, except that the triangle inequality is replaced by the weaker form

$$\|x + y\| \lesssim \|x\| + \|y\|,$$

see, e.g., [44]. We have published these stability results in [90, 93] and we reproduce the proofs in Section 2.5. Finally, in Section 2.6, we prove that sufficiently smooth functions and their derivatives are approximated up to optimal order by the Hermite interpolating PS spline. This result is published in our paper [91].

2.2 Bernstein–Bézier polynomials

Consider a non–degenerated triangle $\tau(V_1, V_2, V_3)$ in a plane, having vertices V_i with Cartesian coordinates (x_i, y_i), $i = 1, 2, 3$. This triangle will be called the *domain triangle*. Let v be an arbitrary point in $\mathbb{R}^2$ with Cartesian coordinates (x, y). We define the *barycentric coordinates* $b_1(v), b_2(v), b_3(v)$ of v with respect to τ as the unique solution to the system

$$\begin{bmatrix} x_1 & x_2 & x_3 \\ y_1 & y_2 & y_3 \\ 1 & 1 & 1 \end{bmatrix} \begin{bmatrix} b_1(v) \\ b_2(v) \\ b_3(v) \end{bmatrix} = \begin{bmatrix} x \\ y \\ 1 \end{bmatrix}. \tag{2.2}$$

Each polynomial $p_d(v) \in \mathcal{P}_d$ on τ has a unique representation

$$p_d(v) = \sum_{i+j+k=d} c_{ijk} B^d_{ijk}(v), \tag{2.3}$$

with

$$B^d_{ijk}(v) := \frac{d!}{i!j!k!} b_1^i(v) b_2^j(v) b_3^k(v) \tag{2.4}$$

the *Bernstein polynomials* on the triangle [55]. The coefficients c_{ijk} are called the *Bézier ordinates*, and the *Bézier domain points* ξ_{ijk} are defined as the points with barycentric coordinates $(\frac{i}{d}, \frac{j}{d}, \frac{k}{d})$ with respect to τ. By associating each ordinate c_{ijk} with the domain point ξ_{ijk} we can display this Bernstein–Bézier representation schematically, as in Figure 2.1. The linear interpolant of the *Bézier control points* $(\xi_{ijk}, c_{ijk}) \in \mathbb{R}^3$ is called the *Bézier control net*, and this control net mimics the shape of the Bernstein–Bézier surface $z = p_d(v)$, see Figure 2.2.

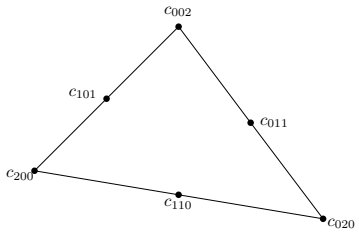

Figure 2.1: Positions of the Bézier ordinates for $d = 2$.

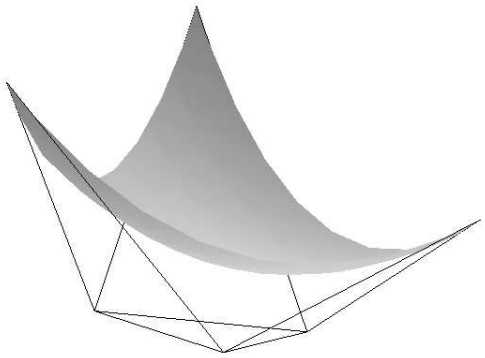

Figure 2.2: A quadratic Bernstein–Bézier surface with its control net.

2.3 The space of Powell–Sabin splines

Consider a simply connected subset $\Omega \subset \mathbb{R}^2$ with polygonal boundary $\partial\Omega$. Suppose we have a conforming triangulation Δ of Ω that consists of triangles T_j , $j = 1, \ldots, t$, and vertices V_i with Cartesian coordinates (x_i, y_i), $i = 1, \ldots, N$. The Powell–Sabin 6-split Δ^{PS} of Δ divides each triangle T_j into six smaller triangles with a common vertex. It can be constructed as follows (see Figure 2.3):

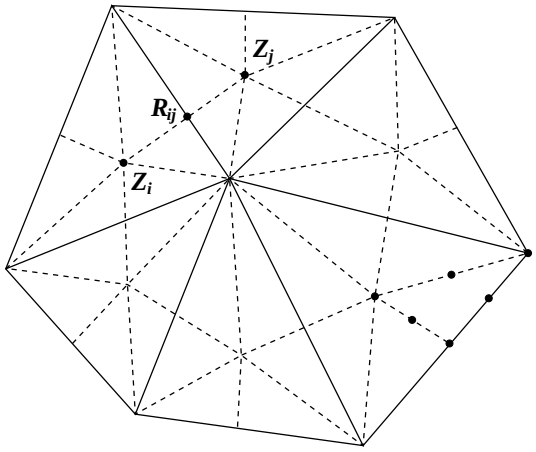

Figure 2.3: A PS 6-split Δ^{PS}.

1. Choose an interior point Z_j for each triangle T_j, so that if two triangles T_i and T_j have a common edge, the line joining Z_i and Z_j intersects this common edge at a point R_{ij} between its vertices. We will choose Z_j as the incenter of triangle T_j.
2. Join the points Z_j to the vertices of T_j.
3. For each edge of T_j
   - which belongs to the boundary $\partial\Omega$, join Z_j to some point on the edge. We choose the middle point of the edge.
   - which is common to a triangle T_i, join Z_j to R_{ij}.

Now we consider the space of piecewise quadratic C^1 continuous polynomials on Ω, the *Powell–Sabin splines*. This space is denoted by

$$S_2^1(\Delta^{PS}) := \{s \in C^1(\Omega) \mid s|_\tau \in \mathcal{P}_2 \text{ for all } \tau \in \Delta^{PS}\}. \tag{2.5}$$

Each of the $6t$ triangles resulting from the PS–refinement becomes the domain triangle of a quadratic Bernstein–Bézier polynomial, i.e. we choose $d = 2$ in Equation (2.3) and (2.4), as indicated for one subtriangle in Figure 2.3. Powell and Sabin [107] showed that the following interpolation problem:

$$s(V_k) = f_k, \quad D_x s(V_k) = f_{xk}, \quad D_y s(V_k) = f_{yk}, \quad k = 1, \ldots, N, \quad (2.6)$$

has a unique solution $s(x, y)$ in $S_2^1(\Delta^{PS})$. Hence, the dimension of the space $S_2^1(\Delta^{PS})$ equals $3N$.

2.4 A B-spline representation

Dierckx [48] presented a *B-spline representation* for Powell–Sabin splines

$$s(x, y) = \sum_{i=1}^{N} \sum_{j=1}^{3} c_{ij} B_{ij}(x, y) \quad , \quad (x, y) \in \Omega, \quad (2.7)$$

where the B-splines form a convex partition of unity on Ω, i.e.

$$B_{ij}(x, y) \geq 0 \text{ for all } (x, y) \in \Omega, \quad (2.8)$$

$$\sum_{i=1}^{N} \sum_{j=1}^{3} B_{ij}(x, y) = 1 \text{ for all } (x, y) \in \Omega. \quad (2.9)$$

Furthermore these basis functions have local support: $B_{ij}(x, y)$ vanishes outside the so-called *molecule* or *1-ring* M_i of vertex V_i, which is the union of all triangles T_k in Δ containing V_i. Figure 2.4 shows such a PS B-spline.

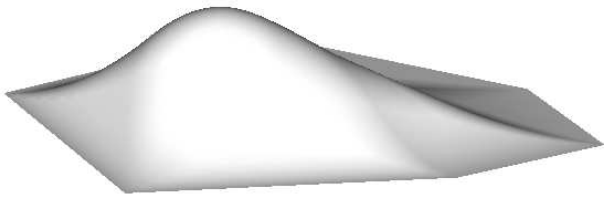

Figure 2.4: A PS B-spline surface.

The basis functions $B_{ij}(x, y)$ can be obtained as follows: find three linearly independent triplets of real numbers $(\alpha_{ij}, \beta_{ij}, \gamma_{ij})$, $j = 1, 2, 3$, for each

vertex V_i. $B_{ij}(x, y)$ is the unique solution of the interpolation problem (2.6) with $(f_k, f_{xk}, f_{yk}) = (\delta_{ki}\alpha_{ij}, \delta_{ki}\beta_{ij}, \delta_{ki}\gamma_{ij})$, where δ_{ki} is the *Kronecker delta*. The triplets $(\alpha_{ij}, \beta_{ij}, \gamma_{ij})$, $j = 1, 2, 3$, must be determined in such a way that Equations (2.8) and (2.9) are satisfied. We use the algorithm from [48]:

1. For each vertex $V_i \in \Delta$, find its *PS-points*. These are the immediately surrounding Bézier domain points of the vertex V_i, and vertex V_i itself. Figure 2.5 shows the PS-points $L, \tilde{L}, L'$ and V_1 for the vertex V_1 in the triangle $T(V_1, V_2, V_3)$.

2. For each vertex V_i, find a triangle $t_i(Q_{i1}, Q_{i2}, Q_{i3})$ that contains all the PS-points of V_i from all the triangles T_k in the molecule M_i. These triangles t_i, $i = 1, \ldots, N$, are called *PS-triangles* and we denote their vertices with $Q_{ij}(X_{ij}, Y_{ij})$. Figure 2.5 also shows such a PS-triangle t_1.

3. Three linearly independent triplets of real numbers $(\alpha_{ij}, \beta_{ij}, \gamma_{ij})$, $j = 1, 2, 3$, can be derived from the PS-triangle t_i of a vertex V_i as follows:

$$
\begin{aligned}
&(\alpha_{i1}, \alpha_{i2}, \alpha_{i3}) \text{ are the barycentric coordinates of} \\
&V_i \text{ with respect to } t_i, \\
&(\beta_{i1}, \beta_{i2}, \beta_{i3}) = \left(\frac{Y_{i2} - Y_{i3}}{e}, \frac{Y_{i3} - Y_{i1}}{e}, \frac{Y_{i1} - Y_{i2}}{e} \right), \\
&(\gamma_{i1}, \gamma_{i2}, \gamma_{i3}) = \left(\frac{X_{i3} - X_{i2}}{e}, \frac{X_{i1} - X_{i3}}{e}, \frac{X_{i2} - X_{i1}}{e} \right),
\end{aligned}
$$

   where

$$
e := \begin{vmatrix} X_{i1} & Y_{i1} & 1 \\ X_{i2} & Y_{i2} & 1 \\ X_{i3} & Y_{i3} & 1 \end{vmatrix}.
$$

A useful byproduct for CAGD purposes is the notion of *control triangles*. First, we define the *PS-control points* as

$$
C_{ij}(X_{ij}, Y_{ij}, c_{ij}). \tag{2.10}
$$

For fixed i, they constitute a triangle $\mathscr{T}_i(C_{i1}, C_{i2}, C_{i3})$ that is tangent to the surface at $(V_i, s(V_i))$, see Figure 2.6. The projection of the control triangles $\mathscr{T}_i$ in the (x, y) plane are the PS-triangles t_i. For later use we note that the area of a PS-triangle t_i equals

$$
\mathrm{vol}(t_i) = \frac{1}{2|\beta_{i1}\gamma_{i2} - \gamma_{i1}\beta_{i2}|} = \frac{|e|}{2}. \tag{2.11}
$$

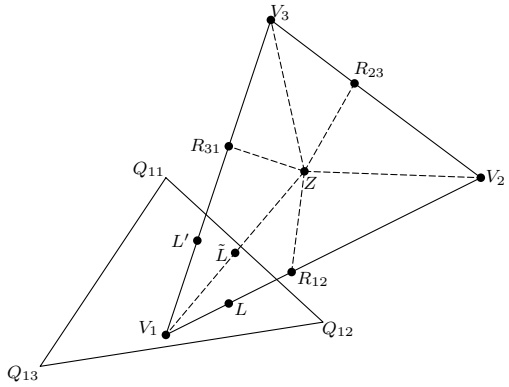

Figure 2.5: PS-points L, L', $\tilde{L}$, V_1 for V_1, and a corresponding PS-triangle $t_1(Q_{11}, Q_{12}, Q_{13})$.

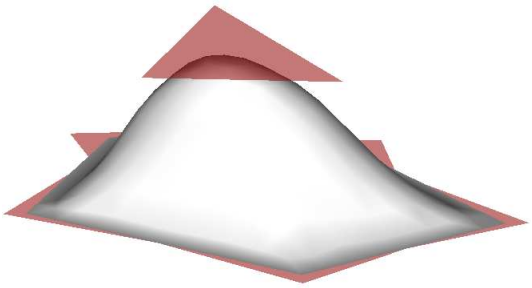

Figure 2.6: A PS spline surface with control triangles.

2.5 Stability of the B-spline basis

In this section we prove that the set of basis functions $\{B_{ij} \mid i = 1, \ldots, N,\ j = 1, 2, 3\}$ forms a stable basis for $S_2^1(\Delta^{PS})$. Stability is very important for a spline basis. This property guarantees that a small perturbation on the coefficients does not lead to a large perturbation on the surface itself. As we will see throughout this thesis, several applications rely on the stability of the underlying basis, see, e.g., (1.14).

Definition 2.5.1. *Let $\mathcal{B}$ be a Banach space, and let $\|\cdot\|_v$ be some yet unspecified vector norm. The basis $\{B_{ij} \mid i = 1, \ldots, N,\ j = 1, 2, 3\}$ is said to form a stable basis for the norm in $\mathcal{B}$ if for any coefficient vector $c := (c_{ij})_{ij}$*

$$\|c\|_v \sim \left\| \sum_{i=1}^{N} \sum_{j=1}^{3} c_{ij} B_{ij} \right\|_{\mathcal{B}}, \tag{2.12}$$

and the constants of equivalence depend only on the smallest angle in the underlying triangulation.

We show that (2.12) holds for all L_p norms with corresponding l_p vector norm for all $0 < p \leq \infty$. As already mentioned in the introduction, for $p < 1$ we do not really have a norm but a quasi-norm. Before we prove the main theorems, we introduce some lemmas and notation.

Let T be a triangle, then

$$\begin{aligned}
\rho_T &:= \text{the radius of the largest disk contained in } T,\\
\mathrm{vol}(T) &:= \text{the area of triangle } T,\\
e_{\max}(T) &:= \text{the longest edge in } T,\\
\theta_T &:= \text{the smallest angle in } T,\\
\theta_{\Delta^{PS}} &:= \text{the smallest angle in } \Delta^{PS},\\
\theta_{\Delta} &:= \text{the smallest angle in } \Delta.
\end{aligned}$$

The first lemma gives an upper bound for $\|D_x s\|_{L_\infty(\tau)}$ and $\|D_y s\|_{L_\infty(\tau)}$, where τ is a triangle in the PS-refinement Δ^{PS}. This is some kind of Markov inequality [95]. Several versions can be found in [16], see also [76, Lemma 4.2]. We give a proof here because we want to derive the exact bounding constants for this particular case of bivariate quadratic polynomials.

Lemma 2.5.2. *Suppose $s \in S_2^1(\Delta^{PS})$. Consider a triangle τ of the PS-refinement Δ^{PS} of Δ. Then*

$$\|D_x s\|_{L_\infty(\tau)} \leq \frac{12}{\rho_\tau} \|s\|_{L_\infty(\tau)}$$

and

$$\|D_y s\|_{L_\infty(\tau)} \leq \frac{12}{\rho_\tau}\|s\|_{L_\infty(\tau)}.$$

Proof. We can write $s|_\tau$ in its unique Bézier representation:

$$s(x,y) = \sum_{i+j+k=2} c_{ijk} B^2_{ijk}(x,y), \quad \forall (x,y) \in \tau.$$

Denote the vertices of τ as $V_i(x_i, y_i)$, $i = 1, 2, 3$. Let $u = V_2 - V_1 = (x_2 - x_1,\ y_2 - y_1)$ and $v = V_3 - V_1 = (x_3 - x_1,\ y_3 - y_1)$ define two vectors. Then the directional derivatives of s at $(x, y) \in \tau$ with respect to the directions u respectively v are given by

$$\begin{aligned} D_u s(x,y) &= (x_2 - x_1) D_x s(x,y) + (y_2 - y_1) D_y s(x,y), \\ D_v s(x,y) &= (x_3 - x_1) D_x s(x,y) + (y_3 - y_1) D_y s(x,y). \end{aligned}$$

Solving for $D_x s(x, y)$ and $D_y s(x, y)$ gives

$$\begin{aligned} D_x s(x,y) &= \frac{(y_3 - y_1) D_u s(x,y) - (y_2 - y_1) D_v s(x,y)}{x_1 y_2 + x_2 y_3 + x_3 y_1 - x_1 y_3 - x_2 y_1 - x_3 y_2}, \\ D_y s(x,y) &= \frac{(x_2 - x_1) D_v s(\tau) - (x_3 - x_1) D_u s(x,y)}{x_1 y_2 + x_2 y_3 + x_3 y_1 - x_1 y_3 - x_2 y_1 - x_3 y_2}, \end{aligned}$$

from which we find that

$$\|D_x s\|_{L_\infty(\tau)} \leq \frac{|y_3 - y_1|}{2\,\mathrm{vol}(\tau)}\|D_u s\|_{L_\infty(\tau)} + \frac{|y_2 - y_1|}{2\,\mathrm{vol}(\tau)}\|D_v s\|_{L_\infty(\tau)}.$$

The area $\mathrm{vol}(\tau)$ is bounded below by

$$\rho_\tau |y_3 - y_1| \leq \mathrm{vol}(\tau), \qquad \rho_\tau |y_2 - y_1| \leq \mathrm{vol}(\tau).$$

Substituting in the previous equation gives

$$\|D_x s\|_{L_\infty(\tau)} \leq \frac{1}{2\rho_\tau}(\|D_u s\|_{L_\infty(\tau)} + \|D_v s\|_{L_\infty(\tau)}).$$

The estimate for $\|D_y s\|_{L_\infty(\tau)}$ can be established in the same way.
Vector u has barycentric coordinates $(-1, 1, 0)$. The directional derivative of s at $(x, y) \in \tau$ with respect to direction u is given by [56]

$$D_u s(x,y) = 2 \sum_{i+j+k=1} (-c_{i+1,jk} + c_{i,j+1,k}) B^1_{ijk}(x,y).$$

We now have

$$\|D_u s\|_{L_\infty(\tau)} \leq \max_{(x,y)} \left(2 \sum_{i+j+k=1} (2\|c\|_\infty) B^1_{ijk}(x,y) \right) = 4\|c\|_\infty.$$

The same reasoning gives an analogous estimate for $\|D_v s\|_{L_\infty(\tau)}$. Combining these two estimates yields

$$\|D_x s\|_{L_\infty(\tau)} \leq \frac{4}{\rho_\tau}\|c\|_\infty$$

and

$$\|D_y s\|_{L_\infty(\tau)} \leq \frac{4}{\rho_\tau}\|c\|_\infty.$$

It suffices to prove that

$$\|c\|_\infty \leq 3\|s\|_{L_\infty(\tau)}.$$

Define

$$\xi := \left\{ \left(\frac{i}{2}, \frac{j}{2}, \frac{k}{2} \right) \;\middle|\; i+j+k=2,\ i,j,k \geq 0 \right\}$$

as the set of Bézier domain points. Then

$$(s(\xi))_\xi = \left(B^2_{ijk}(\xi)\right)_{\xi,ijk} \cdot (c_{ijk})_{ijk}$$

holds, where $(s(\xi))_\xi$ and $(c_{ijk})_{ijk}$ are 6×1 vectors, and $\left(B^2_{ijk}(\xi)\right)_{\xi,ijk}$ is a 6×6 matrix. Since interpolation at the Bézier domain points ξ by polynomials in $\mathcal{P}_2$ is unique, $\left(B^2_{ijk}(\xi)\right)_{\xi,ijk}$ is invertible, and we find

$$\begin{aligned}\|c\|_\infty &\leq \| \left(B^2_{ijk}(\xi)\right)^{-1}_{\xi,ijk} \|_\infty \cdot \| \left(s(\xi)\right)_\xi \|_\infty \\ &\leq \| \left(B^2_{ijk}(\xi)\right)^{-1}_{\xi,ijk} \|_\infty \cdot \|s\|_{L_\infty(\tau)}.\end{aligned}$$

It can easily be verified that $\left\| \left(B^2_{ijk}(\xi)\right)^{-1}_{\xi,ijk} \right\|_\infty = 3.$ □

Now we introduce a definition and a lemma that deal with the choice of the PS-triangles. Obviously there are infinitely many possibilities for a PS-triangle because the only condition is that it contains the appropriate PS-triangle points. It is important to choose small PS-triangles in the construction of the basis functions. The control points will be closer to the surface, which gives the user more local control. Therefore Definition 2.5.3 introduces a constant K that reflects the size and shape of the PS-triangles. One can always find PS-triangles that satisfy $K = 1$, and in practice K will be typically smaller than 1. If PS-triangles with minimal area are used, then K can be bounded in function of the smallest angle in the triangulation, see Proposition 2.5.8.

Definition 2.5.3. *Let D_i be the smallest disk with vertex V_i as center that contains all the PS-triangle points of V_i as in Figure 2.7 and denote its radius as r_i. For each vertex V_i we define K_i as the smallest value such that there exists an equilateral triangle t_{D_i} with barycenter V_i and inradius $K_i r_i$ that contains the actual PS-triangle t_i. Define K as the maximum of all constants K_i in the vertices V_i of Δ.*

Note that any triangle t_{D_i} with barycenter V_i and inradius $K_i r_i$ with $K_i \geq 1$ is a valid PS-triangle for V_i. Therefore, in practical situations, we only use PS-triangles t_i for which $K_i \leq 1$, and thus $K \leq 1$.

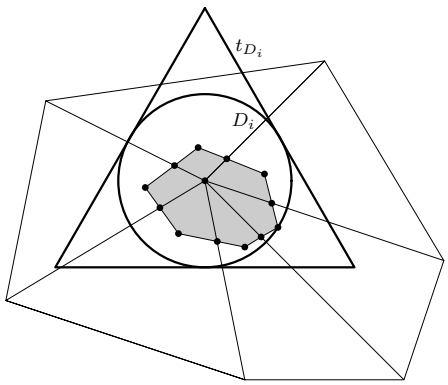

Figure 2.7: The disk D_i and an equilateral triangle t_{D_i} for $K_i = 1$.

Lemma 2.5.4. *Denote the PS-triangle point with the longest distance to vertex V_i as L and define $\tau_L \in \Delta^{PS}$ as either one of the two triangles in Δ^{PS} that contain the PS-triangle point L. Then*

$$\frac{|e_{\max}(t_i)|}{|e_{\max}(\tau_L)|} \leq \sqrt{3}K.$$

Proof. By the definition of K there exists an equilateral triangle t_{D_i} that contains the PS-triangle t_i. Hence it is sufficient to prove that

$$\frac{|e_{\max}(t_{D_i})|}{|e_{\max}(\tau_L)|} \leq \sqrt{3}K.$$

Denote r_i as the radius of the disk D_i defined in Definition 2.5.3. Then

$$|e_{\max}(t_{D_i})| = 2\sqrt{3}K_i r_i \leq 2\sqrt{3}K r_i.$$

If we combine this inequality with the fact that

$$|e_{\max}(\tau_L)| \geq 2\|V_i - L\|_{l_2} = 2r_i,$$

then we have proven the lemma. □

Now we come to the main theorem of this section.

Theorem 2.5.5. *The B-spline basis for Powell–Sabin splines is a stable basis for the max norm, i.e., for any arbitrary coefficient vector c we have*

$$k_1\|c\|_\infty \leq \left\| \sum_{i=1}^{N} \sum_{j=1}^{3} c_{ij} B_{ij} \right\|_{L_\infty(\Omega)} \leq k_2 \|c\|_\infty,$$

with

$$k_1 = \left(1 + \frac{192\sqrt{3}K}{\tan(\theta_{\Delta^{PS}}/2)} \right)^{-1}, \quad k_2 = 1.$$

Proof. The right inequality follows immediately from (2.9). Let s be shorthand notation for the PS spline $\sum_{i=1}^{N} \sum_{j=1}^{3} c_{ij} B_{ij}$. Then we have that

$$\begin{bmatrix} s(V_i) \\ D_x s(V_i) \\ D_y s(V_i) \end{bmatrix} = \begin{bmatrix} \alpha_{i1} & \alpha_{i2} & \alpha_{i3} \\ \beta_{i1} & \beta_{i2} & \beta_{i3} \\ \gamma_{i1} & \gamma_{i2} & \gamma_{i3} \end{bmatrix} \begin{bmatrix} c_{i1} \\ c_{i2} \\ c_{i3} \end{bmatrix} =: Ac.$$

If we take into account that $\alpha_{i3} = 1 - \alpha_{i1} - \alpha_{i2}$, $\beta_{i3} = -\beta_{i1} - \beta_{i2}$, and $\gamma_{i3} = -\gamma_{i1} - \gamma_{i2}$, then we find that

$$A^{-1} = \begin{bmatrix} 1 & \eta_{i1} & \widetilde{\eta}_{i1} \\ 1 & \eta_{i2} & \widetilde{\eta}_{i2} \\ 1 & \eta_{i3} & \widetilde{\eta}_{i3} \end{bmatrix},$$

where

$$\eta_{ij} := \frac{\alpha_{i2}\gamma_{i1} - \alpha_{i1}\gamma_{i2} + \delta_{j1}\gamma_{i2} - \delta_{j2}\gamma_{i1}}{\beta_{i1}\gamma_{i2} - \beta_{i2}\gamma_{i1}}, \tag{2.13}$$

$$\tilde{\eta}_{ij} := \frac{\alpha_{i1}\beta_{i2} - \alpha_{i2}\beta_{i1} - \delta_{j1}\beta_{i2} + \delta_{j2}\beta_{i1}}{\beta_{i1}\gamma_{i2} - \beta_{i2}\gamma_{i1}}, \tag{2.14}$$

with δ_{ij} the Kronecker delta. Note that the volume of PS-triangle t_i is given by $\frac{1}{2|\beta_{i1}\gamma_{i2} - \beta_{i2}\gamma_{i1}|}$, see (2.11). We can find upper bounds for η_{ij} and $\widetilde{\eta}_{ij}$ by using the fact that $|\alpha_{ij}| \leq 1$ and $|\delta_{ij}| \leq 1$, and by using the explicit formulas for β_{ij} and γ_{ij}:

$$\begin{aligned} |\eta_{ij}| &\leq |\alpha_{i2}\gamma_{i1} - \alpha_{i1}\gamma_{i2} + \delta_{j1}\gamma_{i2} - \delta_{j2}\gamma_{i1}| \cdot 2\,\mathrm{vol}(t_i) \\ &\leq 2(|X_{i3} - X_{i2}| + |X_{i1} - X_{i3}|) \\ &\leq 4|e_{\max}(t_i)|. \end{aligned}$$

Similarly we find that $|\widetilde{\eta}_{ij}| \leq 4|e_{\max}(t_i)|$, and in combination with Lemma 2.5.4 we find

$$|\eta_{ij}|, |\widetilde{\eta}_{ij}| \leq 4\sqrt{3}K|e_{\max}(\tau_L)|, \tag{2.15}$$

for some $\tau_L \in \Delta^{PS}$ as defined in Lemma 2.5.4. Suppose that $\|c\|_\infty = |c_{ij}|$. Then

$$\|c\|_\infty = |s(V_i) + \eta_{ij} D_x s(V_i) + \widetilde{\eta}_{ij} D_y s(V_i)|.$$

If we use Lemma 2.5.2 we deduce that

$$\begin{aligned} \|c\|_\infty &\leq \|s\|_{L_\infty(\tau_L)} \left(1 + |\eta_{ij}|\frac{12}{\rho_{\tau_L}} + |\widetilde{\eta}_{ij}|\frac{12}{\rho_{\tau_L}}\right), \\ &\leq \|s\|_{L_\infty(\tau_L)} \left(1 + \frac{24}{\rho_{\tau_L}} 4\sqrt{3}K|e_{\max}(\tau_L)|\right). \end{aligned}$$

It is a well-known result from goniometry that

$$\rho_{\tau_L} = \tan(\theta_{\tau_L}/2)\frac{a + b - c}{2},$$

with a, b, and c the side lengths of the triangle τ_L. Side length c corresponds to the side opposite to the angle θ_{τ_L}, and thus has the smallest value. The following inequalities hold:

$$\frac{2}{\tan(\theta_{\tau_L})} = \frac{a + b - c}{\rho_{\tau_L}} \geq \frac{|e_{\max}(\tau_L)|}{\rho_{\tau_L}}. \tag{2.16}$$

We find that

$$\|c\|_\infty \leq \|s\|_{L_\infty(\Omega)} \left(1 + \frac{192\sqrt{3}K}{\tan(\theta_{\Delta^{PS}}/2)}\right).$$

□

Note that it is also possible to give coefficients k_1 and k_2 in Theorem 2.5.5 that depend only on the smallest angle θ_Δ in Δ. This is an immediate consequence of the inequality $\theta_{\Delta^{PS}} \geq \theta_\Delta \sin(\theta_\Delta)/4$, which is established in [77].

We will now extend Theorem 2.5.5 to arbitrary L_p norms. First we need the following lemma.

Lemma 2.5.6. *Consider a triangle $T_i \in \Delta$ such that $V_i \in T_i$, and let M_i be the molecule of vertex V_i. Then,*

$$\text{vol}(T_i) \sim \text{vol}(M_i),$$

with constants of equivalence that depend at most on the smallest angle θ_Δ in the triangulation Δ.

Proof. Let T_j be another triangle in M_i, then

$$\frac{\mathrm{vol}(T_i)}{\mathrm{vol}(T_j)} \leq \frac{\pi |e_{\max}(T_i)|^2}{\pi \rho_{T_j}^2}. \tag{2.17}$$

Let e and $\hat{e}$ be two edges of the same triangle T_i, then $\sin(\theta_\Delta)|e| \leq |\hat{e}|$. If we iterate this principle we find that

$$|e_{\max}(T_i)| \leq \sin(\theta_\Delta)^{-(\pi/\theta_\Delta+1)} |e_{\max}(T_j)|, \tag{2.18}$$

because there always exists a sequence of edges of maximum length $\lfloor \pi/\theta_\Delta + 1 \rfloor$ between the two edges $e_{\max}(T_i)$ and $e_{\max}(T_j)$, since the maximum number of triangles in the molecule M_i is bounded by $2\pi/\theta_\Delta$. If we combine (2.17) and (2.18) we find

$$\frac{\mathrm{vol}(T_i)}{\mathrm{vol}(T_j)} \lesssim \frac{|e_{\max}(T_j)|^2}{\rho_{T_j}^2}.$$

The righthand side can be bounded by an expression only depending on θ_Δ by using a similar reasoning as in (2.16). Hence

$$\mathrm{vol}(T_i) \sim \mathrm{vol}(T_j).$$

Since the number of triangles in M_i is bounded we have proven the lemma. □

Corollary 2.5.7. *Under a suitable normalization we find that the B-spline basis for PS splines is a stable basis for the L_p norm with $0 < p \leq \infty$, i.e.*

$$\left\| \sum_{i=1}^{N} \sum_{j=1}^{3} c_{ij} B_{ij} \right\|_{L_p(\Omega)} \sim \left(\sum_{i=1}^{N} \sum_{j=1}^{3} |c_{ij}|^p \,\mathrm{vol}(M_i) \right)^{1/p}, \tag{2.19}$$

with M_i the molecule of vertex V_i.

Proof. Let $s := \sum_{i=1}^{N} \sum_{j=1}^{3} c_{ij} B_{ij}$. From Theorem 2.5.5 we get

$$|c_{ij}| \lesssim \|s\|_{L_\infty(T_i)}$$

with $T_i \in \Delta$ such that $V_i \in T_i$. By mapping T_i to the standard simplex $T_s := \{(x,y) \,|\, 0 \leq x, y \leq 1,\, x+y \leq 1\}$, and using the fact that all norms on a finite dimensional space are equivalent, we infer

$$\|s\|_{L_\infty(T_i)} \lesssim \mathrm{vol}(T_i)^{-1/p} \|s\|_{L_p(T_i)}.$$

Now, using Lemma 2.5.6, we get

$$\left(\sum_{i=1}^{N} \sum_{j=1}^{3} |c_{ij}|^p \,\mathrm{vol}(M_i) \right)^{1/p} \lesssim \left(\sum_{i=1}^{N} \sum_{j=1}^{3} \|s\|_{L_p(T_i)}^p \right)^{1/p} \lesssim \|s\|_{L_p(\Omega)}.$$

The other inequality follows from the observation that

$$\left|\sum_{i=1}^{N}\sum_{j=1}^{3} c_{ij}B_{ij}(x,y)\right|^p \lesssim \sum_{i=1}^{N}\sum_{j=1}^{3} |c_{ij}|^p |B_{ij}(x,y)|^p,$$

which holds because at any $(x,y) \in \Omega$ there are at most 9 non-zero B-splines. We find that

$$\begin{aligned}
\|s\|^p_{L_p(\Omega)} &= \int_\Omega \left|\sum_{i=1}^{N}\sum_{j=1}^{3} c_{ij}B_{ij}(x,y)\right|^p dxdy \\
&\lesssim \sum_{i=1}^{N}\sum_{j=1}^{3} |c_{ij}|^p \int_\Omega |B_{ij}(x,y)|^p dxdy \\
&\lesssim \sum_{i=1}^{N}\sum_{j=1}^{3} |c_{ij}|^p \,\mathrm{vol}(M_i).
\end{aligned}$$

□

Proposition 2.5.8. *Suppose that the basis functions* $\{B_{ij} \mid i = 1,\dots,N,\ j = 1,2,3\}$ *have PS-triangles with minimal area. Then the equivalence constants in Theorem 2.5.5 depend only on the smallest angle* $\theta_{\Delta^{PS}}$ *in the PS-refinement* Δ^{PS}.

Proof. It is sufficient to prove that there exists a set of triangles t_{D_i}, such that the corresponding K can be bounded in function of the smallest angle $\theta_{\Delta^{PS}}$, with K the constant defined in Definition 2.5.3. Let us concentrate on triangle $\tau_L \in \Delta^{PS}$, with τ_L as defined in Lemma 2.5.4. Then, from geometry, we know that

$$\rho_{\tau_L} = \frac{2\,\mathrm{vol}(\tau_L)}{a + b + c}$$

with a, b, c the side lengths of triangle τ_L. Some simple computations yield

$$\mathrm{vol}(\tau_L) \geq \frac{\sin^2(\theta_{\Delta^{PS}})\|V_i - L\|^2_{l_2}}{2}, \quad a + b + c \leq (2 + \sin^{-1}(\theta_{\Delta^{PS}}))\|V_i - L\|_{l_2},$$

hence

$$\rho_{\tau_L} \geq \frac{\sin^2(\theta_{\Delta^{PS}})\|V_i - L\|_{l_2}}{2 + \sin^{-1}(\theta_{\Delta^{PS}})}. \tag{2.20}$$

Now, choose

$$K = \frac{|e_{\max}(t_i)|}{2\sqrt{3}\|V_i - L\|_{l_2}}, \tag{2.21}$$

then the PS-triangle t_i is contained in an equilateral triangle t_{D_i} with side length $2\sqrt{3}K\|V_i - L\|_{l_2}$, cfr. Definition 2.5.3, and the bounds in Theorem 2.5.5 hold with the K given in (2.21). The area of PS-triangle t_i can be bounded below by combining (2.20) and (2.21),

$$\mathrm{vol}(t_i) \geq \frac{\sqrt{3}K \sin^2(\theta_{\Delta^{PS}})\|V_i - L\|_{l_2}^2}{2 + \sin^{-1}(\theta_{\Delta^{PS}})}.$$

On the other hand, there exists a valid equilateral PS-triangle with area $3\sqrt{3}\|V_i - L\|_{l_2}^2$ (see, e.g., the PS-triangle depicted in Figure 2.7) . Thus, we find that

$$K \leq \frac{6 + 3\sin^{-1}(\theta_{\Delta^{PS}})}{\sin^2(\theta_{\Delta^{PS}})},$$

otherwise we get a contradiction with the minimality of the area of PS-triangle t_i. □

2.6 Approximation power

In [76], Lai and Schumaker show how to construct stable approximation schemes in the bivariate spline spaces $S_d^r(\Delta)$ with $d \geq 3r + 2$ which achieve *optimal approximation power*, i.e., the error of approximation is of the order $|\Delta|^{d+1}$ with $|\Delta|$ the maximum of the diameters of the triangles in Δ. The diameter of a triangle T is denoted as $|T|$ and it equals the diameter of the smallest disk containing T. In this section we extend their results to the spline space $S_2^1(\Delta^{PS})$. Our approach is different from the one in [76], since we make use of the Bramble–Hilbert lemma [10].

Let us define the quasi-interpolant operator $\mathcal{I} : C^1(\overline{\Omega}) \to S_2^1(\Delta^{PS})$ by

$$\mathcal{I}f := \sum_{i=1}^{N}\sum_{j=1}^{3} \mu_{ij}(f)B_{ij}, \tag{2.22}$$

where the μ_{ij} are linear functionals of the form

$$\mu_{ij}(f) := f(V_i) + \eta_{ij}D_x f(V_i) + \widetilde{\eta}_{ij}D_y f(V_i), \tag{2.23}$$

with η_{ij}, $\widetilde{\eta}_{ij}$ as in (2.13) resp. (2.14). It is easy to check that

$$\mathcal{I}s = s, \quad \forall s \in S_2^1(\Delta^{PS}),$$

and

$$\mathcal{I}f(V_i) = f(V_i), \quad \nabla\mathcal{I}f(V_i) = \nabla f(V_i), \quad i = 1, \ldots, N.$$

Note that this quasi-interpolant $\mathcal{I}$ is just the *Hermite interpolant* of f in the space $S_2^1(\Delta^{PS})$. This Hermite interpolant can also be expressed, e.g.,

in the Hermite basis from [110] as follows. Setting e_1 and e_2 as the unit directions corresponding to the coordinate axes, we have

$$\mathcal{I}f = \sum_{i=1}^{n} (f(V_i)\phi_i + \nabla f(V_i)e_1\chi_i + \nabla f(V_i)e_2\psi_i)$$

where $\phi_i, \chi_i, \psi_i \in S_2^1(\Delta^{PS})$ and $\phi_i(V_j) = \nabla\chi_i(V_j)e_1 = \nabla\psi_i(V_j)e_2 = \delta_{ij}$, the other Hermite data being zero. See also [94] for other kinds of PS quasi-interpolants.

The Hermite interpolant $\mathcal{I}$ plays a crucial role in characterizing the approximation power of Powell–Sabin splines. We prove in Theorem 2.6.2 that the PS spline $\mathcal{I}f$ approximates the function f up to optimal order, provided that f is sufficiently smooth. The crucial ingredient of the proof is the Bramble–Hilbert lemma. We refer to Section A.1 for the definition of the Sobolev space $W_p^k(\Omega)$.

Lemma 2.6.1 (Bramble–Hilbert [10]). *Let Ω be a bounded domain in $\mathbb{R}^2$ with diameter $|\Omega|$, let f be a function in $W_p^k(\Omega)$, and let F be a linear functional on $C^j(\Omega)$ with $0 \le j < k$ satisfying*

1. *$|F(f)| \lesssim \sum_{n=0}^{j} |\Omega|^n |f|_{n,\Omega}$, where*

$$|f|_{n,\Omega} := \sup_{(x,y)\in\Omega} \sum_{\alpha+\beta=n} |D_x^\alpha D_y^\beta f(x,y)|,$$

2. *$F(q) = 0$ for all polynomials q such that $D_x^\alpha D_y^\beta q = 0$ for all $\alpha+\beta = k$.*

Then for $p > 2/(k-j)$ we have

$$|F(f)| \lesssim |\Omega|^{k-2/p} |f|_{W_p^k(\Omega)}.$$

Theorem 2.6.2. *Let $0 \le \alpha+\beta \le 1$ and $p > 1$, or $\alpha+\beta = 2$ and $p > 2$. For every $f \in W_p^3(\Omega)$,*

$$\|D_x^\alpha D_y^\beta (f - \mathcal{I}f)\|_{L_p(\Omega)} \lesssim |\Delta|^{3-\alpha-\beta} |f|_{W_p^3(\Omega)}.$$

Here $|\Delta|$ is the maximum of the diameters of the triangles in Δ and $\mathcal{I}$ is the Hermite interpolant defined in (2.22)*. The bounding constant depends at most on the smallest angle $\theta_{\Delta^{PS}}$ in the PS-refinement Δ^{PS}.*

Proof. Fix (x, y) in a triangle $T \in \Delta$. By Theorem 2.5.5,

$$\begin{aligned} |\mathcal{I}f(x,y)| &\le \sum_{i|V_i\in T} \sum_{j=1}^{3} |\mu_{ij}(f)| B_{ij}(x,y) \\ &\le \max_{i|V_i\in T, j} |f(V_i) + \eta_{ij} D_x f(V_i) + \tilde{\eta}_{ij} D_y f(V_i)|. \end{aligned} \quad (2.24)$$

From (2.15) we infer

$$|\eta_{ij}|, |\widetilde{\eta}_{ij}| \lesssim |T|, \tag{2.25}$$

with $|T|$ the diameter of triangle T. By substituting the upper bounds for η_{ij} and $\tilde{\eta}_{ij}$ in Equation (2.24) we find that

$$|\mathcal{I}f(x,y)| \lesssim \|f\|_{L_\infty(T)} + |T| \sup_{(x,y)\in T} (|D_x f(x,y)| + |D_y f(x,y)|).$$

This immediately implies

$$|\mathcal{I}f(x,y) - f(x,y)| \lesssim \sum_{n=0}^{1} |T|^n |f|_{n,T},$$

with $|f|_{n,T}$ as defined in Lemma 2.6.1. The Bramble–Hilbert lemma implies

$$|\mathcal{I}f(x,y) - f(x,y)| \lesssim |T|^{3-2/p} |f|_{W_p^3(T)},$$

provided that $p > 1$. We find that

$$\begin{aligned} \|\mathcal{I}f - f\|_{L_p(T)} &= \left(\int_T |\mathcal{I}f(x,y) - f(x,y)|^p dxdy \right)^{1/p} \\ &\lesssim |T|^{3-2/p} |f|_{W_p^3(T)} \cdot (\mathrm{vol}(T))^{1/p} \\ &\lesssim |T|^3 |f|_{W_p^3(T)}. \end{aligned}$$

By summing over all triangles we get

$$\begin{aligned} \|\mathcal{I}f - f\|_{L_p(\Omega)} &= \left(\sum_{T\in\Delta} \|\mathcal{I}f - f\|^p_{L_p(T)} \right)^{1/p} \\ &\lesssim |\Delta|^3 \left(\sum_{T\in\Delta} |f|^p_{W_p^3(T)} \right)^{1/p} \\ &\lesssim |\Delta|^3 |f|_{W_p^3(\Omega)}. \end{aligned}$$

These equations establish the theorem for $\alpha = \beta = 0$ and for arbitrary $p > 1$.

Suppose $1 \leq \alpha + \beta \leq 2$. Let $\tau \in \Delta^{PS}$, then $\mathcal{I}f|_\tau$ is just a bivariate polynomial of total degree at most 2. The Markov inequality

$$\|D_x^\alpha D_y^\beta \mathcal{I}f\|_{L_\infty(\tau)} \lesssim \rho_\tau^{-\alpha-\beta} \|\mathcal{I}f\|_{L_\infty(\tau)} \tag{2.26}$$

holds. The proof of (2.26) is similar to the proof of Lemma 2.5.2, see, e.g., [16] or [76]. The inequality

$$\rho_\tau^{-1} \lesssim |\tau|^{-1}$$

can be deduced from (2.16). Using techniques from the proof of Lemma 2.5.6 we find

$$|\tau|^{-1} \lesssim |T|^{-1}$$

with $T \in \Delta$ such that τ is contained in T. Hence, for any $(x, y) \in T$,

$$|D_x^\alpha D_y^\beta \mathcal{I} f(x,y)| \lesssim |T|^{-\alpha-\beta} \left(|f|_{0,T} + |T||f|_{1,T} \right),$$

and

$$|D_x^\alpha D_y^\beta \mathcal{I} f(x,y) - D_x^\alpha D_y^\beta f(x,y)| \lesssim |T|^{-\alpha-\beta} \sum_{n=0}^{\alpha+\beta} |T|^n |f|_{n,T}.$$

The remainder of the proof is similar to the case $\alpha = \beta = 0$. □

Chapter 3

The hierarchical basis

3.1 Introduction

The starting point for the idea of hierarchical bases is a *nested sequence of finite dimensional spaces* of real-valued functions

$$S_0 \subset S_1 \subset S_2 \subset \cdots \subset S_n \subset \cdots . \tag{3.1}$$

As n increases, the resolution (i.e. level of detail) of functions in S_n increases. Each space S_n has a finite basis and a set of functions

$$\bigcup_{l=0}^{n} \{\phi_{k,l}\}_{k \in I_l}$$

is a hierarchical basis for S_n given that

$$\bigcup_{l=0}^{m} \{\phi_{k,l}\}_{k \in I_l}$$

is a basis for S_m for each $m = 0, 1, \ldots, n$. Here I_l denotes a yet unspecified index set. Every $s \in S_n$ can be written in the form

$$s = \sum_{l=0}^{n} \sum_{k \in I_l} c_{k,l} \phi_{k,l}$$

and the partial sums

$$s_m = \sum_{l=0}^{m} \sum_{k \in I_l} c_{k,l} \phi_{k,l}$$

are functions in the spaces S_m for each $m = 0, 1, \ldots, n$.

This idea, the hierarchical representation of functions, essentially goes back to a paper [54] by Georg Faber published in 1909 in "Mathematische Annalen". Faber's idea spread out through many parts of applied mathematics. The wavelet transform [96], for instance, is widely used nowadays in signal analysis and image processing. Subspace decompositions of finite element spaces, like Faber's decomposition, are an indispensable tool in the construction and analysis of fast solvers [129].

In Section 3.2 we discuss a dyadic, triadic and $\sqrt{3}$ subdivision scheme for PS splines as in [126]. These schemes yield nested spline spaces in the sense of (3.1). The rest of the chapter mainly summarizes the work that was done in our paper [90]. In Section 3.3 we prove that the corresponding hierarchical basis forms a multiresolution analysis for the Banach space $C^1(\overline{\Omega})$. Although the hierarchical basis is only weakly stable with respect to the norm in $C^1(\overline{\Omega})$, we prove strong stability for certain subspaces of Sobolev type in Section 3.4. These proofs are based on techniques from the theory of approximation spaces, see, e.g., [45, 124]. As a result, we find that the hierarchical basis as preconditioner for the model problem (1.16) yields logarithmically growing condition numbers with the size of the problem. Then, in Section 3.5, we consider a very simple surface compression algorithm. Although surface compression is not immediately related to the main topic of this thesis: preconditioning, we find it useful to investigate in some sense the compression properties of the hierarchical basis. We derive optimal a priori error bounds for surface compression with respect to the L_∞ norm, see [43, 90]. We explain how this surface compression algorithm can be viewed as a greedy algorithm for best N-term nonlinear approximation [42]. We note that best N-term nonlinear approximation is one of the main tools for the adaptive wavelet schemes from [18, 19, 20], and, therefore, Section 3.5 can be viewed as a first step in developing adaptive schemes for the solution of fourth order elliptic equations, although we will not explore this any further. Finally, in Section 3.6, we proceed with the results from Section 3.4, and, by adding redundant basis functions to the standard hierarchical basis, we derive a Bramble–Pasciak–Xu-preconditioner [11] that is optimal for the model problem (1.16). Moreover we numerically compare the BPX preconditioner with the HB preconditioner.

3.2 Powell–Sabin spline subdivision

The goal of PS spline subdivision is to calculate the B-spline representation (2.7) of a PS spline surface on a refinement Δ_1 of the given triangulation Δ_0. The new basis functions after subdivision have smaller support and, thus, give more local control for manipulating surfaces. So, assume that some

initial triangulation Δ_0 is given. If we can find a refinement procedure that yields nested sequences

$$\Delta_0 \subset \Delta_1 \subset \Delta_2 \subset \cdots \tag{3.2}$$
$$\Delta_0^{PS} \subset \Delta_1^{PS} \subset \Delta_2^{PS} \subset \cdots \tag{3.3}$$

then we immediately find Powell–Sabin spline spaces $S_l := S_2^1(\Delta_l^{PS})$, $l \geq 0$, that are nested, i.e. (3.1) holds.

In the previous chapter we derived some stability results in terms of the smallest angle in the underlying triangulation Δ_l^{PS}. Starting from a uniform initial triangulation Δ_0 it is clear that the smallest angle in Δ_l^{PS} for an arbitrary $l > 0$ cannot become arbitrarily small, provided a regular refinement strategy is used. In fact, in the uniform case, the minimal angle in Δ_l^{PS} equals $\pi/6$. For arbitrary initial triangulations Δ_0 we do believe that there always exists a nested sequence of triangulations such that the smallest angle in Δ_l^{PS} is at least a fixed $\theta > 0$ independent of l, but we cannot prove this. Intuitively one can argue that such a nested sequence exists by looking at a uniform triangulation and then use perturbation arguments. For most applications later on we will assume that the nested sequences (3.2) and (3.3) are *regular*, which means that the minimum angle of any triangle in any Δ_l remains bounded away from zero and that

$$(\#\Delta_l)^{-1/2} \lesssim \min_{T\in\Delta_l} |T| \leq \max_{T\in\Delta_l} |T| \lesssim (\#\Delta_l)^{-1/2}, \qquad l \in \mathbb{N}_0, \tag{3.4}$$

where $|T|$ is the diameter of triangle T, and $\#\Delta_l$ denotes the number of triangles in Δ_l. Automatically the same holds for the triangles in the PS-refinement

$$(\#\Delta_l)^{-1/2} \lesssim \min_{\tau\in\Delta_l^{PS}} |\tau| \leq \max_{\tau\in\Delta_l^{PS}} |\tau| \lesssim (\#\Delta_l)^{-1/2}, \qquad l \in \mathbb{N}_0.$$

The most obvious choice for creating nested sequences (3.2) is *dyadic subdivision*. In this scheme a new vertex is inserted on every edge between two old vertices and every original triangle is split into four new triangles, hence $(\#\Delta_l)^{-1/2} \sim 2^{-l}$. In order to satisfy (3.3) we place those new vertices on each edge at the position of the intersection with the PS-refinement, see Figure 3.1. Note that this dyadic refinement principle can not be used for arbitrary initial triangulations Δ_0. For example in Figure 3.1, the interior point Z_{ijk} of the PS-refinement of the original triangle must lie inside the middle new triangle $T(V_{ij}, V_{jk}, V_{ki})$. This condition is easily violated when Δ_0 is highly irregular.

Therefore Vanraes *et al.* considered a *triadic subdivision* scheme [126]. The principle is shown in Figure 3.2. Here a new vertex is placed at the position of the interior point Z_{ijk} in the PS-refinement, and two new vertices

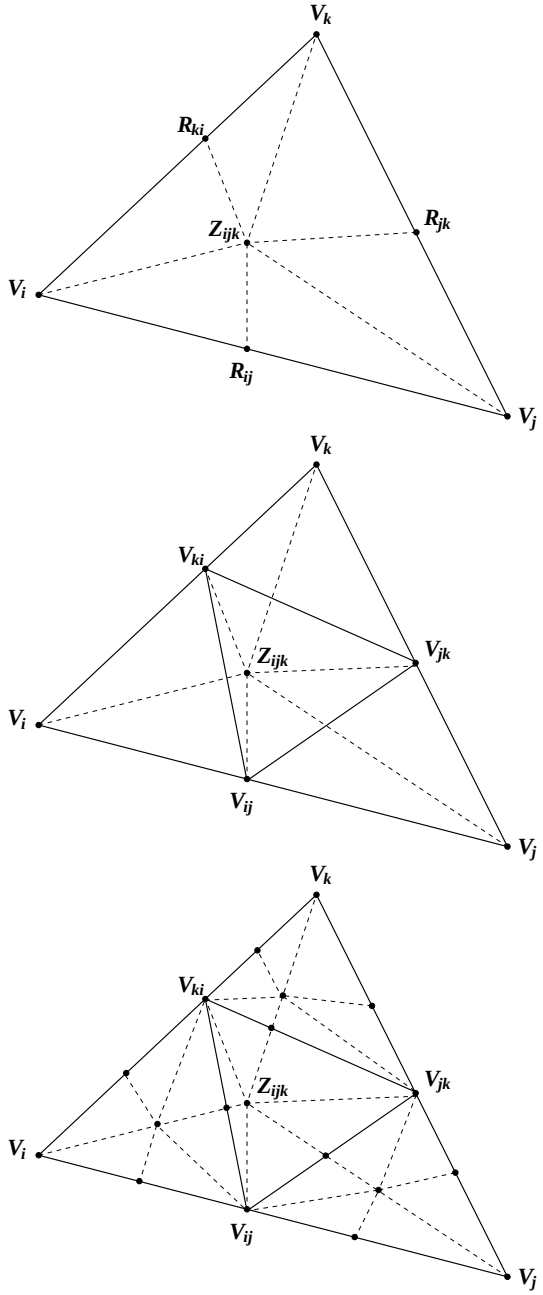

Figure 3.1: Principle of dyadic refinement. We place a new vertex on each edge at the position of the intersection with the PS-refinement.

are inserted on each edge, one at each side of the intersection with the PS-refinement. Every original triangle is split into nine new triangles, hence $(\#\Delta_l)^{-1/2} \sim 3^{-l}$. With this refinement procedure it is always possible to create nested sequences (3.2) and (3.3) for any initial triangulation Δ_0.

A PS spline $s_l \in S_l$ can now be represented as

$$s_l = \sum_{i=1}^{N_l} \sum_{j=1}^{3} c_{ij,l} B_{ij,l}, \tag{3.5}$$

where N_l denotes the number of vertices in Δ_l, and $B_{ij,l}$ represents a B-spline on Δ_l with corresponding coefficient $c_{ij,l}$. The subscript l denotes the resolution level . If the refinement is regular (3.4), then Corollary 2.5.7 holds with $\mathrm{vol}(M_i) \sim (\#\Delta_l)^{-1}$. It is convenient to use matrix notation for the following. We write a Powell–Sabin spline $s_l \in S_l$ as $s_l = \boldsymbol{\phi}_l c_l$, where $\boldsymbol{\phi}_l$ denotes the row vector of basis functions $B_{ij,l}$ and c_l the column vector with the coefficients $c_{ij,l}$. Because the spaces S_l are nested there exists a *subdivision matrix* A_l such that $\boldsymbol{\phi}_l = \boldsymbol{\phi}_{l+1} A_l$, or equivalently $c_{l+1} = A_l c_l$. Such a subdivision matrix A_l can be written in block matrix form as

$$A_l = \begin{bmatrix} O_l \\ N_l \end{bmatrix}.$$

We distinguish between a part O_l that computes the coefficients of the new basis functions on the finer triangulation Δ_{l+1} associated with old vertices (i.e. vertices that also belong to Δ_l), and a part N_l that computes the coefficients of the new basis functions associated with vertices in $\Delta_{l+1} \setminus \Delta_l$. Note that, by the definition/construction of the B-splines $B_{ij,l}$, the square matrix O_l is always invertible.

Remark 3.2.1. *In [126] an algorithm is given that automatically constructs control triangles* (2.10) *for the basis functions at the next resolution level. Furthermore the resulting subdivision formula are convex combinations, i.e. the rows of O_l and N_l contain a finite number of elements, each of them positive but smaller than one, and each row sums up to one. Hence the subdivision algorithm presented in [126] is stable.*

We split $\boldsymbol{\phi}_{l+1}$ in functions $\boldsymbol{\phi}^o_{l+1}$ associated with the old vertices (i.e. the vertices in Δ_l) and functions $\boldsymbol{\phi}^n_{l+1}$ associated with the new vertices that are added when going from Δ_l to Δ_{l+1},

$$\boldsymbol{\phi}_{l+1} = [\boldsymbol{\phi}^o_{l+1} \quad \boldsymbol{\phi}^n_{l+1}].$$

Theorem 3.2.2. *For each $m \geq 0$, the set of splines*

$$\boldsymbol{\phi}_0 \cup \bigcup_{l=1}^{m} \boldsymbol{\phi}^n_l \tag{3.6}$$

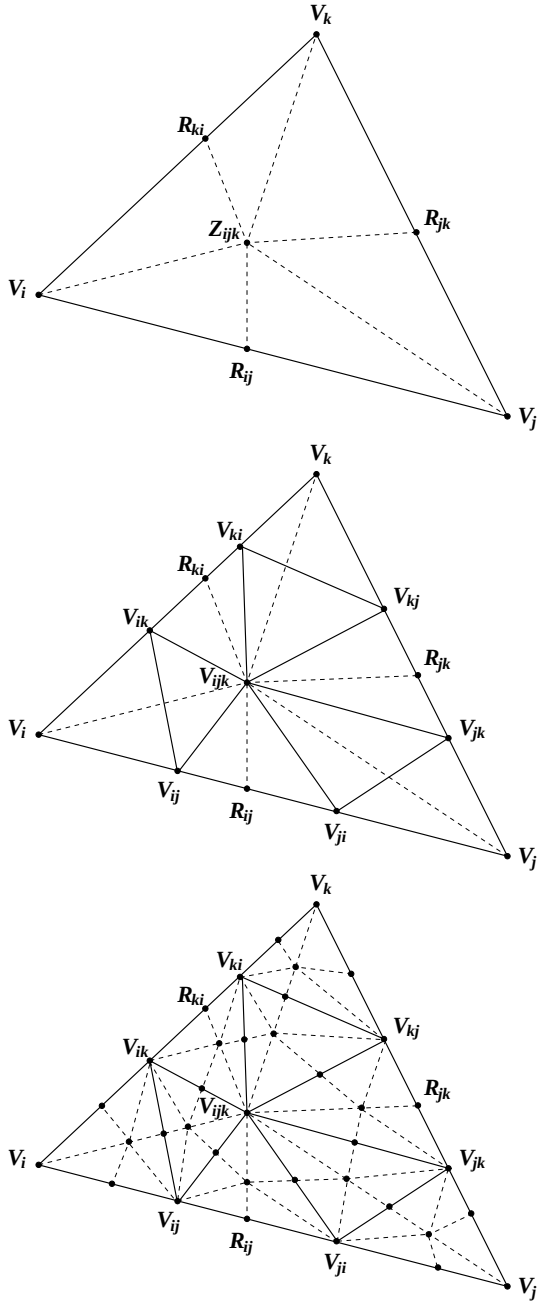

Figure 3.2: Principle of triadic refinement. We place a new vertex at the position of the interior point in the PS-refinement and two new vertices on each edge, one at each side of the intersection with the PS-refinement.

forms a (hierarchical) basis for S_m.

Proof. From the previous we know that

$$\begin{bmatrix} \boldsymbol{\phi}_l & \boldsymbol{\phi}_{l+1}^n \end{bmatrix} = \boldsymbol{\phi}_{l+1} \begin{bmatrix} O_l & 0 \\ N_l & 1 \end{bmatrix}.$$

Because O_l is invertible we get

$$\begin{bmatrix} (O_l)^{-1} & 0 \\ -N_l\,(O_l)^{-1} & 1 \end{bmatrix} \begin{bmatrix} \boldsymbol{\phi}_l & \boldsymbol{\phi}_{l+1}^n \end{bmatrix} = \boldsymbol{\phi}_{l+1}.$$

Hence for all l we have proven that the set of functions $\begin{bmatrix} \boldsymbol{\phi}_l & \boldsymbol{\phi}_{l+1}^n \end{bmatrix}$ forms a basis for the space S_l. The theorem follows by induction. □

One of the points of criticism in this construction is the use of the triadic refinement, which is prohibitive in many real-world applications because the number of degrees of freedom grows too rapidly with the number of refinement levels. However, it is possible to work around the triadic refinement. There is another possible refinement strategy that is very close to the triadic refinement. Note that the nested sequences (3.2) and (3.3) are in fact a little bit too restrictive to create nested PS spline spaces. It is sufficient to demand that only (3.3) holds, and that we replace (3.2) by

$$\{V_i \in \Delta_0\} \subset \{V_i \in \Delta_1\} \subset \{V_i \in \Delta_2\} \subset \cdots .$$

It was pointed out by Vanraes *et al.* in [126] that applying a $\sqrt{3}$ *refinement scheme* also yields nested PS spline spaces. Applying the $\sqrt{3}$ scheme twice yields a triadic scheme. The $\sqrt{3}$ scheme was first introduced by Kobbelt [72] and Labsik and Greiner [75]. Instead of splitting each edge and performing a 1-to-4 split for each triangle (dyadic refinement), we compute a new vertex for each triangle and retriangulate the old and new vertices. A $\sqrt{3}$ scheme performs slower topological refinement than dyadic refinement, the number of triangles only triples each step. So we have a finer gradation of hierarchy levels. Figure 3.3 shows the principle of $\sqrt{3}$ refinement. Note that at the boundary special constructions are necessary. Another interesting point about the $\sqrt{3}$ scheme is that it allows for local refinement. The scheme can be applied locally to one triangle and the resulting locally refined spline space is nested into the previous coarser spline space in a natural way. In [114] Speleers proposes a parameter driven heuristic for refinement propagation in order to avoid triangle degeneration after applying local $\sqrt{3}$-subdivision.

In this thesis we will always use the triadic refinement scheme to prove certain approximation or stability properties, unless stated otherwise. However, the results remain valid for the dyadic and $\sqrt{3}$ subdivision schemes, with some minor modifications.

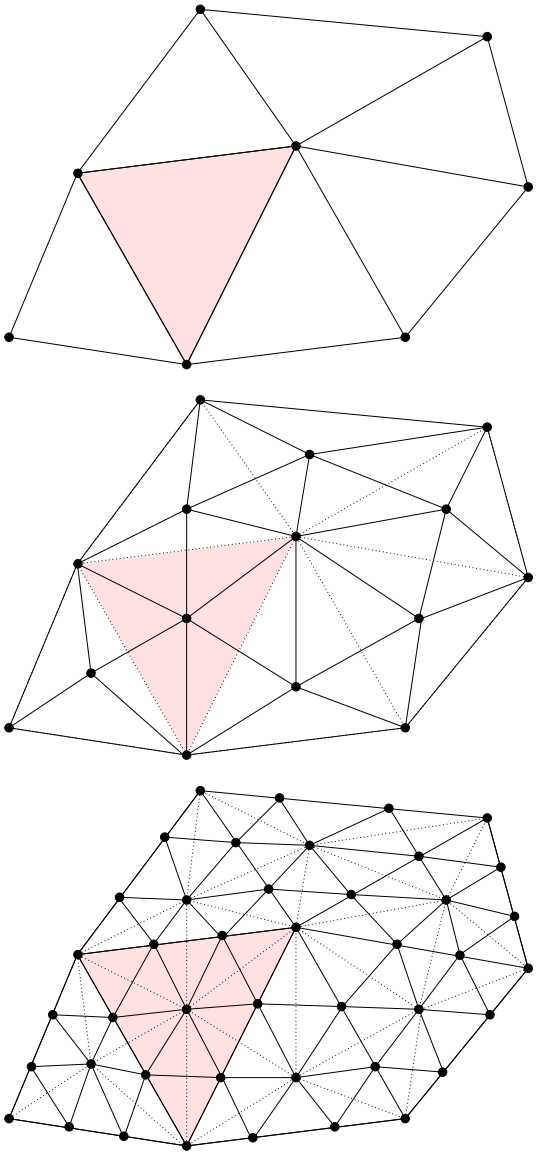

Figure 3.3: Principle of $\sqrt{3}$ refinement. The PS-refinements are not shown. Each time we place the new vertices at the position of the interior point in the PS-refinement. Applying the $\sqrt{3}$ scheme twice results in triadic refinement.

3.3 Multiresolution analysis

In this section we relate the hierarchical basis (3.6) to the following fairly general definition of a *multiresolution analysis* given in [14, 28, 29].

Definition 3.3.1. *A multiresolution analysis consists of*

1. *A Banach space $\mathcal{B}$ of functions defined on a bounded subset $\Omega \subset \mathbb{R}^2$ with associated norm $\|\cdot\|_{\mathcal{B}}$.*

2. *A nested sequence of subspaces $S_0 \subset S_1 \subset S_2 \subset \cdots \subset \mathcal{B}$ that are dense in $\mathcal{B}$,*
$$\overline{\bigcup_{l=0}^{\infty} S_l} = \mathcal{B}.$$

3. *A collection of uniformly bounded operators*
$$\mathcal{Q}_l : \mathcal{B} \to S_l$$
with the properties
$$\begin{aligned} \mathcal{Q}_l \mathcal{Q}_l &= \mathcal{Q}_l, \\ \mathcal{Q}_l \mathcal{Q}_{l+1} &= \mathcal{Q}_l, \\ \mathcal{Q}_l(\mathcal{B}) &= S_l \end{aligned}$$
for all integers $l \geq 0$.

We are interested in how much an approximation $f_l \in S_l$ of a given function $f \in \mathcal{B}$ changes when progressing to the next higher resolution S_{l+1}. Therefore we look for suitable complement spaces W_l such that

$$S_{l+1} = S_l \oplus W_l$$

as well as for stable bases of W_l by which one can describe the differences between the approximations $f_l \in S_l$ and $f_{l+1} \in S_{l+1}$. With the projectors $\mathcal{Q}_l$ given, we can define these complement spaces as

$$W_l := \{s \in S_{l+1} | \mathcal{Q}_l s = 0\}.$$

Hence we get a decomposition of $\mathcal{B}$ as the direct sum

$$\mathcal{B} = S_0 \oplus W_0 \oplus W_1 \oplus W_2 \oplus \cdots .$$

Obviously we are interested in PS spline spaces, so consider nested triangulations (3.2) and (3.3), obtained by regular triadic refinement, and let S_l be the PS spline space $S_2^1(\Delta_l^{PS})$. We will look for a suitable Banach space

$\mathcal{B}$ and suitable operators $\mathcal{Q}_l$ such that we get a multiresolution analysis in the sense of Definition 3.3.1.

Recall the Hermite interpolant $\mathcal{I} : C^1(\overline{\Omega}) \to S_2^1(\Delta^{PS})$ defined in (2.22). We extend this operator to the multilevel setting: define $\mathcal{I}_l : C^1(\overline{\Omega}) \to S_l$ by

$$\mathcal{I}_l f := \sum_{i=1}^{N_l} \sum_{j=1}^{3} \mu_{ij,l}(f) B_{ij,l}, \tag{3.7}$$

where the $\mu_{ij,l}$ are linear functionals of the form

$$\mu_{ij,l}(f) := f(V_i) + \eta_{ij,l} D_x f(V_i) + \widetilde{\eta}_{ij,l} D_y f(V_i), \tag{3.8}$$

with $\eta_{ij,l}$, $\widetilde{\eta}_{ij,l}$ as in (2.13) resp. (2.14) (with obvious modification). By the regularity (3.4), by the fact that $(\#\Delta_l)^{-1/2} \sim 3^{-l}$, and by (2.15),

$$|\eta_{ij,l}|, |\widetilde{\eta}_{ij,l}| \lesssim 3^{-l}. \tag{3.9}$$

We have

$$\mathcal{I}_l s_l = s_l, \quad \forall s_l \in S_l,$$

and

$$\mathcal{I}_l f(V_i) = f(V_i), \quad \nabla \mathcal{I}_l f(V_i) = \nabla f(V_i), \quad i = 1, \ldots, N_l.$$

These operators $\mathcal{I}_l$ will play the role of the operator $\mathcal{Q}_l$ in Definition 3.3.1. Remark that the complement spaces

$$W_l := \{s \in S_{l+1} | \mathcal{I}_l s = 0\}$$

are spanned by the set

$$\{B_{ij,l+1} \mid i \text{ such that } V_i \in \Delta_{l+1} \setminus \Delta_l,\ j = 1, 2, 3\}.$$

Thus, decomposing S_{n+1} as $S_0 \oplus \bigoplus_{l=0}^{n} W_l$ is equivalent to writing each $s \in S_{n+1}$ in its hierarchical basis representation.

As Banach space $\mathcal{B}$ we take $C^1(\overline{\Omega})$, the space of functions defined on $\overline{\Omega}$ that are continuous and have continuous first derivatives in $\overline{\Omega}$. There is a natural norm for $C^1(\overline{\Omega})$ that is defined as

$$\|f\|_{C^1(\overline{\Omega})} := \max \left\{ \|f\|_{L_\infty(\Omega)}, \|D_x f\|_{L_\infty(\Omega)}, \|D_y f\|_{L_\infty(\Omega)} \right\} \tag{3.10}$$

and every function f in $C^1(\overline{\Omega})$ satisfies $\|f\|_{C^1(\overline{\Omega})} < \infty$.

The following proposition shows that the operators $\mathcal{I}_l$ from (3.7) are suitable for constructing a multiresolution analysis.

Proposition 3.3.2. *For each $l \geq 0$ we have*

$$\mathcal{I}_l \mathcal{I}_{l+1} = \mathcal{I}_l.$$

Proof. From the construction of $\mathcal{I}_l$ we know that

$$\mathcal{I}_{l+1} f(V_k) = f(V_k), \qquad \nabla \mathcal{I}_{l+1} f(V_k) = \nabla f(V_k), \qquad \forall\ V_k \in \Delta_{l+1}.$$

Then it is also obvious that

$$\mathcal{I}_l \mathcal{I}_{l+1} f(V_k) = f(V_k), \qquad \nabla \mathcal{I}_l \mathcal{I}_{l+1} f(V_k) = \nabla f(V_k), \qquad \forall\ V_k \in \Delta_l \subset \Delta_{l+1},$$

and

$$\mathcal{I}_l f(V_k) = f(V_k), \qquad \nabla \mathcal{I}_l f(V_k) = \nabla f(V_k), \qquad \forall\ V_k \in \Delta_l \subset \Delta_{l+1}.$$

From the uniqueness of the interpolation problem (2.6) we conclude that $\mathcal{I}_l \mathcal{I}_{l+1} = \mathcal{I}_l$. □

In the next proposition we prove that the operators $\mathcal{I}_l$ are uniformly bounded.

Proposition 3.3.3. *For every $f \in C^1(\overline{\Omega})$ and every point $(x, y) \in \overline{\Omega}$ the inequalities*

$$|\mathcal{I}_l f(x,y)| \lesssim \|f\|_{C^1(\overline{\Omega})}, \tag{3.11}$$

$$|D_x \mathcal{I}_l f(x,y)| \lesssim \|f\|_{C^1(\overline{\Omega})}, \tag{3.12}$$

$$|D_y \mathcal{I}_l f(x,y)| \lesssim \|f\|_{C^1(\overline{\Omega})} \tag{3.13}$$

hold. Therefore the operators $\mathcal{I}_l$ are uniformly bounded in $C^1(\overline{\Omega})$.

Proof. The inequalities

$$\begin{aligned} |\mathcal{I}_l f(x,y)| &\leq \max_{i,j} |\mu_{ij,l}(f)| \left| \sum_{i=1}^{N_l} \sum_{j=1}^{3} B_{ij,l}(x,y) \right| \\ &\lesssim \|f\|_{C^1(\overline{\Omega})} \end{aligned} \tag{3.14}$$

hold because of (2.9), (3.8) and (3.9). The other two inequalities (3.12) and (3.13) are similar. We only give the proof of the first one. We have

$$\begin{aligned} |D_x \mathcal{I}_l f(x,y)| &= \left| \sum_{i=1}^{N_l} \sum_{j=1}^{3} \mu_{ij,l}(f) D_x B_{ij,l}(x,y) \right| \\ &\lesssim \left| \sum_{i=1}^{N_l} \sum_{j=1}^{3} f(V_i) D_x B_{ij,l}(x,y) \right| \\ &\quad + \left| \sum_{i=1}^{N_l} \sum_{j=1}^{3} 3^{-l} \|f\|_{C^1(\overline{\Omega})} D_x B_{ij,l}(x,y) \right|. \end{aligned}$$

Now suppose that (x, y) belongs to triangle $T \in \Delta_l$ with vertices V_1, V_2 and V_3. Then we deduce from the local support of the basis functions that

$$\begin{aligned} |D_x \mathcal{I}_l f(x,y)| &\lesssim \left| \sum_{i=1}^{3} \sum_{j=1}^{3} f(V_i) D_x B_{ij,l}(x,y) \right| \\ &\quad + \left| \sum_{i=1}^{3} \sum_{j=1}^{3} 3^{-l} \|f\|_{C^1(\overline{\Omega})} D_x B_{ij,l}(x,y) \right|. \end{aligned} \tag{3.15}$$

From the Markov inequality for polynomials in $\mathcal{P}_2$ (see, e.g., Lemma 2.5.2, [16] or [76]), and the regularity (3.4) it follows that

$$|D_x B_{ij,l}(x,y)| \lesssim 3^l. \tag{3.16}$$

Hence the second part of (3.15) can be bounded by a constant multiple of $\|f\|_{C^1(\overline{\Omega})}$. Now we need to prove that the first part is also bounded by a constant multiple of $\|f\|_{C^1(\overline{\Omega})}$. Hereto we use the equality

$$\sum_{i=1}^{3} \sum_{j=1}^{3} D_x B_{ij,l}(x,y) = 0, \tag{3.17}$$

which follows immediately from (2.9). Using (3.17) and the mean-value theorem the first part of (3.15) can be bounded by

$$\begin{aligned} &\left| \sum_{i=1}^{3} \sum_{j=1}^{3} f(V_i) D_x B_{ij,l}(x,y) \right| \\ &= \left| \sum_{j=1}^{3} \left(f(V_2) - f(V_1)\right) D_x B_{2j,l}(x,y) + \left(f(V_3) - f(V_1)\right) D_x B_{3j,l}(x,y) \right| \\ &\lesssim \left| \sum_{j=1}^{3} D_{\beta^1} f(\xi^1) 3^{-l} D_x B_{2j,l}(x,y) + D_{\beta^2} f(\xi^2) 3^{-l} D_x B_{3j,l}(x,y) \right|, \end{aligned}$$

where ξ^1 and ξ^2 are points on the line segments $[V_1, V_2]$ resp. $[V_1, V_3]$, and β^1 and β^2 are unit directions that point from V_1 to V_2 resp. V_3. From the Markov inequality (3.16) we deduce that $|D_x \mathcal{I}_l f(x,y)| \lesssim \|f\|_{C^1(\overline{\Omega})}$. □

The following proposition is the last step in showing that the spaces $\cup_{l \geq 0} S_l$ form a multiresolution analysis. We verify that every function in $C^1(\overline{\Omega})$ can be approximated by functions from $\cup_{l \geq 0} S_l$ with arbitrarily small error.

Proposition 3.3.4. *The space $\cup_{l\geq 0} S_l$ is dense in the Banach space $C^1(\overline{\Omega})$ with norm $\|\cdot\|_{C^1(\overline{\Omega})}$.*

Proof. It is sufficient to show that $\lim_{l\to\infty} \|f - \mathcal{I}_l f\|_{C^1(\overline{\Omega})} = 0$ for every function $f \in C^1(\overline{\Omega})$. As in the proof of Proposition 3.3.3 let (x, y) be an arbitrary point in triangle $T \in \Delta_l$ with vertices V_1, V_2 and V_3. Then from (2.9), (3.8), (3.9) and the mean-value theorem we find

$$\begin{aligned}
&|f(x,y) - \mathcal{I}_l f(x,y)| \\
&= \left| f(x,y) \sum_{i=1}^{3}\sum_{j=1}^{3} B_{ij,l}(x,y) - \sum_{i=1}^{3}\sum_{j=1}^{3} \mu_{ij,l}(f) B_{ij,l}(x,y) \right| \\
&\lesssim \left| \sum_{i=1}^{3}\sum_{j=1}^{3} \left(f(x,y) - f(V_i)\right) B_{ij,l}(x,y) \right| \\
&\quad + \left| \sum_{i=1}^{3}\sum_{j=1}^{3} \|f\|_{C^1(\overline{\Omega})}\, 3^{-l} B_{ij,l}(x,y) \right| \qquad (3.18) \\
&\lesssim \left| \sum_{i=1}^{3}\sum_{j=1}^{3} D_{\beta^i} f(\xi^i) 3^{-l} B_{ij,l}(x,y) \right| + \|f\|_{C^1(\overline{\Omega})}\, 3^{-l} \\
&\lesssim \|f\|_{C^1(\overline{\Omega})}\, 3^{-l},
\end{aligned}$$

and we obtain that $\lim_{l\to\infty} \|f - \mathcal{I}_l f\|_{L_\infty(\Omega)} = 0$, where ξ_i denotes a point on the line segment connecting V_i with (x, y), and β_i is the unit direction that points from V_i to (x, y). Now we prove that the derivatives of $\mathcal{I}_l f$ converge to the derivatives of f. We only give the proof for the derivative with respect to x. Denote the Cartesian coordinates of vertex $V_k \in \Delta_l$ with (x_k, y_k). Then the equations

$$\begin{aligned}
x &= \sum_{i=1}^{N_l}\sum_{j=1}^{3} (x_i + \eta_{ij,l}) B_{ij,l}(x,y), \\
y &= \sum_{i=1}^{N_l}\sum_{j=1}^{3} (y_i + \widetilde{\eta}_{ij,l}) B_{ij,l}(x,y)
\end{aligned}$$

hold. If we take the derivative with respect to x and we evaluate in $(x, y) \in T$

then we infer

$$1 = \sum_{i=1}^{3}\sum_{j=1}^{3}(x_i + \eta_{ij,l})D_x B_{ij,l}(x,y), \tag{3.19}$$

$$0 = \sum_{i=1}^{3}\sum_{j=1}^{3}(y_i + \widetilde{\eta}_{ij,l})D_x B_{ij,l}(x,y). \tag{3.20}$$

If we use (3.19) and (3.20) we can deduce that

$$\begin{aligned} e &= |D_x f(x,y) - D_x \mathcal{I}_l f(x,y)| \\ &= \Bigg| D_x f(x,y)\left(\sum_{i=1}^{3}\sum_{j=1}^{3}(x_i + \eta_{ij,l})D_x B_{ij,l}(x,y)\right) \\ &\quad + D_y f(x,y)\left(\sum_{i=1}^{3}\sum_{j=1}^{3}(y_i + \widetilde{\eta}_{ij,l})D_x B_{ij,l}(x,y)\right) \\ &\quad - \sum_{i=1}^{3}\sum_{j=1}^{3}\left(f(V_i) + \eta_{ij,l}D_x f(V_i) + \widetilde{\eta}_{ij,l}D_y f(V_i)\right)D_x B_{ij,l}(x,y)\Bigg|. \end{aligned}$$

If we use (3.17) we can rewrite e as

$$\begin{aligned} e &= \Bigg| \sum_{i=1}^{3}\sum_{j=1}^{3}\left(D_x f(x,y) - D_x f(V_i)\right)\eta_{ij,l}D_x B_{ij,l}(x,y) \\ &\quad + \sum_{i=1}^{3}\sum_{j=1}^{3}\left(D_y f(x,y) - D_y f(V_i)\right)\widetilde{\eta}_{ij,l}D_x B_{ij,l}(x,y) \\ &\quad + D_x f(x,y)\sum_{j=1}^{3}\Big((x_2 - x_1)D_x B_{2j,l}(x,y) + (x_3 - x_1)D_x B_{3j,l}(x,y)\Big) \\ &\quad + D_y f(x,y)\sum_{j=1}^{3}\Big((y_2 - y_1)D_x B_{2j,l}(x,y) + (y_3 - y_1)D_x B_{3j,l}(x,y)\Big) \\ &\quad - \sum_{j=1}^{3}\Big((f(V_2) - f(V_1))D_x B_{2j,l}(x,y) + (f(V_3) - f(V_1))D_x B_{3j,l}(x,y)\Big)\Bigg| \end{aligned}$$

and from (3.9), (3.16) and the mean-value theorem we get

$$\begin{aligned} e \lesssim & \left| \sum_{i=1}^{3} \sum_{j=1}^{3} (D_x f(x,y) - D_x f(V_i)) \right| \\ & + \left| \sum_{i=1}^{3} \sum_{j=1}^{3} (D_y f(x,y) - D_y f(V_i)) \right| \\ & + \left| \sum_{j=1}^{3} \left(\langle \nabla f(x,y) - \nabla f(\xi^1), V_2 - V_1 \rangle D_x B_{2j}(x,y) \right. \right. \\ & \left. \left. + \langle \nabla f(x,y) - \nabla f(\xi^2), V_3 - V_1 \rangle D_x B_{3j}(x,y) \right) \right|, \end{aligned} \tag{3.21}$$

where ξ^1 and ξ^2 are points on the line segments $[V_1, V_2]$ resp. $[V_1, V_3]$, and $\langle \cdot, \cdot \rangle$ is the usual dot product. The upper bound in (3.21) goes to 0 as $l \to \infty$ because of the uniform continuity of the partial derivatives of f. □

Remark 3.3.5. *Propositions 3.3.3 and 3.3.4 are inherent to the spline spaces S_l and do not depend on any particular basis. One can prove these propositions using any basis for S_l that is stable in the sense of Definition 2.5.1, such as for instance the Hermite basis of [110].*

3.4 Stability of the hierarchical basis

Suppose that we are given a multiresolution analysis in the sense of Definition 3.3.1 and a corresponding decomposition

$$\mathcal{B} = S_0 \oplus W_0 \oplus W_1 \oplus W_2 \oplus \cdots,$$

as well as stable bases $\psi_l := \{\psi_{k,l} | k \in J_l\}$ for W_l by which one can describe the differences between the approximations $f_l \in S_l$ and $f_{l+1} \in S_{l+1}$. Here J_l denotes an index set. We will refer to the complement spaces W_l as wavelet spaces and the functions $\psi_{k,l} \in W_l$ as *wavelets* , despite the fact that they might not have a vanishing moment (which is for instance the case for the hierarchical basis). The spaces S_l are spanned by bases $\phi_l := \{\phi_{k,l} | k \in I_l\}$ with I_l an index set. We refer to the functions $\phi_{k,l}$ as *scaling functions*. Then any $f_n \in S_n$ can be written in single scale representation

$$f_n = \sum_{k \in I_n} c_{k,n} \phi_{k,n} \tag{3.22}$$

or in multiscale representation

$$f_n = \sum_{l=-1}^{n-1} \sum_{k \in J_l} d_{k,l} \psi_{k,l}, \tag{3.23}$$

where we have set for simplicity $\psi_{-1} := \phi_0$, $J_{-1} := I_0$. Because the spaces S_l are dense in $\mathcal{B}$, every function $f \in \mathcal{B}$ has a representation (3.23) with $n \to \infty$.

The decomposition (3.23) is particularly useful if the norm of f in some L_p space or Sobolev space can be determined solely by examining the size of the coefficients $d_{k,l}$ because we do not want that the overall shape of the surface changes when a small coefficient $d_{k,l}$ vanishes. In other words, we want that the multiscale basis forms a *strongly stable basis* for some L_p space or Sobolev space.

Definition 3.4.1. *Let $\mathcal{B}$ be a Banach space with a multiresolution analysis and corresponding multiscale basis $\mathbf{\Psi} := \bigcup_{l=-1}^{\infty} \psi_l$. The multiscale basis $\mathbf{\Psi}$ is said to form a weakly stable basis for $\mathcal{B}$ if for each $n \geq 0$*

$$C_1^{-1} \left\| (d_{k,l})_{l \in K_n, k \in J_l} \right\|_v \leq \left\| \sum_{l \in K_n} \sum_{k \in J_l} d_{k,l} \psi_{k,l} \right\|_{\mathcal{B}} \leq C_2 \left\| (d_{k,l})_{l \in K_n, k \in J_l} \right\|_v$$

where $\| \cdot \|_v$ is some vector norm, $K_n := \{-1, \ldots, n-1\}$, and the constants C_1 and C_2 have at most polynomial growth in n. If the constants C_1 and C_2 are independent of n, the basis is said to be strongly stable.

Let us return to the MRA (Multiresolution Analysis) for $C^1(\overline{\Omega})$ developed in the previous section, i.e. the spaces S_l are defined as the PS spline spaces $S_2^1(\Delta_l^{PS})$, and the operators $\mathcal{Q}_l$ from Definition 3.3.1 are the Hermite interpolation operators $\mathcal{I}_l$ from (3.7). The multiscale representation (3.23) is in this situation just the representation with respect to the hierarchical basis from Section 3.2.

We prove that under a suitable normalization the hierarchical basis of PS splines forms a weakly stable basis for $C^1(\overline{\Omega})$. Define the index sets

$$I_l := \{(i,j) \mid i = 1, \ldots, N_l,\ j = 1,2,3\}, \tag{3.24}$$

$$J_l := \{(i,j) \mid V_i \in \Delta_{l+1} \setminus \Delta_l, j = 1,2,3\}, \tag{3.25}$$

with $J_{-1} := I_0$. We need the following lemma.

Lemma 3.4.2. *Let g_l be the wavelet component of f in W_l given by*

$$g_l = \mathcal{I}_{l+1} f - \mathcal{I}_l f = \sum_{(i,j) \in I_{l+1}} c_{ij,l+1} B_{ij,l+1} = \sum_{(i,j) \in J_l} d_{ij,l} B_{ij,l+1},$$

with f in $C^1(\overline{\Omega})$. Then the coefficients $c_{ij,l+1}$ and $d_{ij,l}$ are bounded by

$$|c_{ij,l+1}| \lesssim 3^{-l} \|g_l\|_{C^1(\overline{\Omega})} \lesssim 3^{-l} \|f\|_{C^1(\overline{\Omega})} .$$

$$|d_{ij,l}| \lesssim 3^{-l} \|g_l\|_{C^1(\overline{\Omega})} \lesssim 3^{-l} \|f\|_{C^1(\overline{\Omega})} .$$

Furthermore we have that the estimates

$$\|g_l\|_{L_\infty(\Omega)} \lesssim 3^l \|c_{l+1}\|_\infty , \quad \|g_l\|_{L_\infty(\Omega)} \lesssim 3^l \|d_l\|_\infty ,$$

$$\|D_x g_l\|_{L_\infty(\Omega)} \lesssim 3^l \|c_{l+1}\|_\infty , \quad \|D_x g_l\|_{L_\infty(\Omega)} \lesssim 3^l \|d_l\|_\infty ,$$

$$\|D_y g_l\|_{L_\infty(\Omega)} \lesssim 3^l \|c_{l+1}\|_\infty , \quad \|D_y g_l\|_{L_\infty(\Omega)} \lesssim 3^l \|d_l\|_\infty$$

hold where $\|c_{l+1}\|_\infty := \max_{(i,j)\in I_{l+1}} \{|c_{ij,l+1}|\}$ and $\|d_l\|_\infty := \max_{(i,j)\in J_l} \{|d_{ij,l}|\}$.

Proof. Because g_l satisfies $\mathcal{I}_l g_l = 0$ we know that

$$g_l(V_k) = 0, \quad \nabla g_l(V_k) = 0, \quad \text{for all } V_k \in \Delta_l.$$

Because $g_l \in W_l \subset S_{l+1}$ we have $\mathcal{I}_{l+1} g_l = g_l$ which yields $c_{ij,l+1} = \mu_{ij,l+1}(g_l)$ by (3.7) and by (3.8) we find that

$$c_{ij,l+1} = 0 \quad \text{for all} \quad \{i \mid V_i \in \Delta_l\}. \tag{3.26}$$

Choose i such that $V_i \in \Delta_{l+1} \setminus \Delta_l$. Let k be such that $V_k \in \Delta_l$ and such that V_i and V_k are contained in the same triangle $T \in \Delta_l$. Then

$$\begin{aligned} |c_{ij,l+1}| &= |g_l(V_i) + \eta_{ij,l+1} D_x g_l(V_i) + \widetilde{\eta}_{ij,l+1} D_y g_l(V_i)| \\ &\lesssim |g_l(V_i) - g_l(V_k)| + 3^{-l} \|g_l\|_{C^1(\overline{\Omega})} \\ &\lesssim 3^{-l} \|g_l\|_{C^1(\overline{\Omega})}, \end{aligned}$$

where the last step follows from the mean-value theorem. Because the operator $\mathcal{I}_l$ is bounded in $C^1(\overline{\Omega})$ (Proposition 3.3.3) we find that $|c_{ij,l+1}| \lesssim 3^{-l} \|f\|_{C^1(\overline{\Omega})}$.

From Theorem 2.5.5 we immediately find that

$$\|g_l\|_{L_\infty(\Omega)} \lesssim \|c_{l+1}\|_\infty \leq 3^l \|c_{l+1}\|_\infty .$$

Let (x, y) be an arbitrary point in triangle $T \in \Delta_{l+1}$ with vertices V_1, V_2

and V_3. Then the inequalities

$$\begin{aligned} |D_x g_l(x,y)| &= \left| \sum_{i=1}^{3}\sum_{j=1}^{3} c_{ij,l+1} D_x B_{ij,l+1}(x,y) \right| \\ &\leq \|c_{l+1}\|_\infty \sum_{i=1}^{3}\sum_{j=1}^{3} |D_x B_{ij,l+1}(x,y)| \\ &\lesssim \|c_{l+1}\|_\infty \sum_{i=1}^{3}\sum_{j=1}^{3} 3^{l+1} \\ &\lesssim 3^l \|c_{l+1}\|_\infty \end{aligned}$$

hold. We have used the Markov inequality (3.16). This yields

$$\|D_x g_l\|_{L_\infty(\Omega)} \lesssim 3^l \|c_{l+1}\|_\infty$$

and the proof for $\|D_y g_l\|_{L_\infty(\Omega)}$ is similar.

From (3.26) and the fact that the multiscale basis is a hierarchical basis, we easily infer

$$\|c_{l+1}\|_\infty = \|d_l\|_\infty.$$

□

Most of the work for proving stability in $C^1(\overline{\Omega})$ is done in Lemma 3.4.2.

Theorem 3.4.3. *Let f be a function in $C^1(\overline{\Omega})$ and define the wavelet components $g_l \in W_l$ as*

$$g_l = \mathcal{I}_{l+1} f - \mathcal{I}_l f = \sum_{(i,j)\in J_l} d_{ij,l} B_{ij,l+1}.$$

Then, under a suitable normalization, the hierarchical basis is a weakly stable basis for $C^1(\overline{\Omega})$, because the following inequalities hold:

$$\max_{l\leq n} \left\|3^l d_l\right\|_\infty \lesssim \|\mathcal{I}_{n+1} f - \mathcal{I}_0 f\|_{C^1(\overline{\Omega})} \lesssim n \max_{l\leq n} \left\|3^l d_l\right\|_\infty . \tag{3.27}$$

Proof. Suppose $\max_{l\leq n} \left\|3^l d_l\right\|_\infty = \|3^r d_r\|_\infty$. Then from Lemma 3.4.2 we find

$$\begin{aligned} \max_{l\leq n} \left\|3^l d_l\right\|_\infty &\lesssim \|\mathcal{I}_{r+1} f - \mathcal{I}_r f\|_{C^1(\overline{\Omega})} \\ &\lesssim \|\mathcal{I}_{r+1} f - \mathcal{I}_0 f\|_{C^1(\overline{\Omega})} + \|\mathcal{I}_r f - \mathcal{I}_0 f\|_{C^1(\overline{\Omega})} \end{aligned}$$

Because $\mathcal{I}_{r+1}\mathcal{I}_{n+1}f = \mathcal{I}_{r+1}f$ and $\mathcal{I}_{r+1}\mathcal{I}_0 f = \mathcal{I}_0 f$ we deduce that

$$\begin{aligned}\max_{l\leq n}\left\|3^l d_l\right\|_\infty &\lesssim \|\mathcal{I}_{r+1}\mathcal{I}_{n+1}f - \mathcal{I}_{r+1}\mathcal{I}_0 f\|_{C^1(\overline{\Omega})} + \|\mathcal{I}_r\mathcal{I}_{n+1}f - \mathcal{I}_r\mathcal{I}_0 f\|_{C^1(\overline{\Omega})} \\ &\lesssim \left(\|\mathcal{I}_{r+1}\|_{C^1(\overline{\Omega})} + \|\mathcal{I}_r\|_{C^1(\overline{\Omega})}\right)\|\mathcal{I}_{n+1}f - \mathcal{I}_0 f\|_{C^1(\overline{\Omega})}\end{aligned}$$

which yields

$$\max_{l\leq n}\left\|3^l d_l\right\|_\infty \lesssim \|\mathcal{I}_{n+1}f - \mathcal{I}_0 f\|_{C^1(\overline{\Omega})}$$

because of Proposition 3.3.3. Using Lemma 3.4.2 the right inequality in (3.27) follows from

$$\|\mathcal{I}_{n+1}f - \mathcal{I}_0 f\|_{C^1(\overline{\Omega})} \leq \sum_{l=0}^{n}\|g_l\|_{C^1(\overline{\Omega})} \lesssim \sum_{l=0}^{n}\left\|3^l d_l\right\|_\infty .$$

□

So, unfortunately, not all functions in $C^1(\overline{\Omega})$ can be characterized by the coefficients of their representation with respect to the hierarchical basis. Therefore we will now look for certain subspaces of the Banach space $C^1(\overline{\Omega})$ for which the hierarchical basis is a strongly stable basis. These subspaces are the Sobolev spaces $H^s(\Omega)$ with $s \in (2, \frac{5}{2})$. We refer to Section A.1 to recall the definition of a Sobolev space. Crucial for the stability proof are estimates of Jackson and Bernstein type. The proofs of these estimates can be found in Appendix B.

We have shown that the operator $\mathcal{I}_l$ from (3.7) is suitable for constructing an MRA. This same operator will play a key role in proving strong stability.

Lemma 3.4.4. *The Sobolev space $H^s(\Omega)$ with $s > 2$ is a subset of $C^1(\overline{\Omega})$. Therefore the operator $\mathcal{I}_l$ is bounded on $H^s(\Omega)$ with $s > 2$.*

Proof. Because Ω is a bounded domain with polygonal boundary we have that Ω satisfies the strong local Lipschitz property and the uniform cone property, see, e.g., [1]. From Theorems 5.4 and 7.58 in [1] the embeddings

$$H^s(\Omega) \subset W^2_{2/(3-s)} \subset C^1(\overline{\Omega})$$

hold for $2 < s < 3$. The case $s = 3$ follows immediately from Theorem 5.4 in [1] and the case $s > 3$ is obtained from the embedding $H^s(\Omega) \subset H^3(\Omega)$. The boundedness of $\mathcal{I}_l$ follows from Proposition 3.3.3. □

The operator $\mathcal{I}_l$ is only useful if there exist function spaces for which $\mathcal{I}_l f$ converges to f in some L_p norm as the resolution level l increases. From Theorem 2.6.2 we know already that this holds for all $f \in W^3_p(\Omega)$, $p > 1$. The following lemma extends these results.

Lemma 3.4.5. *For each $f \in H^s(\Omega)$, $s > 2$, and arbitrary $p \geq 1$ we have that*

$$\|f - \mathcal{I}_l f\|_{L_p(\Omega)} \to 0 \quad as \quad l \to \infty.$$

Proof. First we consider the case $2 < s \leq 3$. Let (x, y) be some arbitrary point in triangle $\tau \in \Delta_l^{PS}$. From (3.18) we immediately get that

$$|f(x,y) - \mathcal{I}_l f(x,y)| \lesssim \|f\|_{L_\infty(\tau)} + 3^{-l} \|f\|_{C^1(\overline{\tau})}.$$

Then the Bramble–Hilbert lemma [10] (Lemma 2.6.1) implies

$$|f(x,y) - \mathcal{I}_l f(x,y)| \lesssim (3^{-l})^{2-2/q} |f|_{W_q^2(\tau)}$$

for arbitrary $q > 2$. If we take $q = 2/(3-s)$ then Theorem 7.58 in [1] yields $H^s(\tau) \subset W_q^2(\tau)$ for $2 < s < 3$, and Theorem 5.4 in [1] yields $H^3(\tau) \subset W_q^2(\tau)$. So

$$|f(x,y) - \mathcal{I}_l f(x,y)| \lesssim 3^{-l(s-1)} |f|_{H^s(\tau)}.$$

By using (3.4) we find that

$$\begin{aligned} \|f - \mathcal{I}_l f\|_{L_p(\tau)} &= \left(\int_\tau |f(x,y) - \mathcal{I}_l f(x,y)|^p \, dxdy \right)^{1/p} \\ &\lesssim 3^{-l(s-1)} |f|_{H^s(\tau)} 3^{-2l/p}. \end{aligned}$$

Then taking the sum over all triangles $\tau \in \Delta_l^{PS}$ yields

$$\|f - \mathcal{I}_l f\|_{L_p(\Omega)}^p = \sum_{\tau \in \Delta_l^{PS}} \|f - \mathcal{I}_l f\|_{L_p(\tau)}^p \lesssim 3^{-lp(s-1+2/p)} \sum_{\tau \in \Delta_l^{PS}} |f|_{H^s(\tau)}^p,$$

and using the fact that $\#\{\tau \in \Delta_l^{PS}\} \sim 3^{2l}$ implies

$$\|f - \mathcal{I}_l f\|_{L_p(\Omega)}^p \lesssim 3^{-lp(s-1+2/p)} 3^{2l} |f|_{H^s(\Omega)}^p,$$

hence

$$\|f - \mathcal{I}_l f\|_{L_p(\Omega)} \lesssim 3^{-l(s-1)} |f|_{H^s(\Omega)}.$$

The case $s > 3$ follows from the embedding $H^s(\Omega) \subset H^3(\Omega)$. □

From Lemma 3.4.5 we known that each function $f \in H^s(\Omega)$, $s > 2$, can be decomposed as

$$f = \sum_{l=0}^{\infty} g_l, \qquad g_l \in S_l,$$

in the sense of L_p. Moreover, we can use the decomposition

$$f = \sum_{l=0}^{\infty} (\mathcal{I}_l - \mathcal{I}_{l-1}) f,$$

with $\mathcal{I}_{-1} := 0$.

We now introduce auxiliary spaces $A_q^s(L_p(\Omega))$. Under certain conditions these auxiliary spaces can be related to Besov spaces, which implies that the norm of an auxiliary space is equivalent to the norm of its corresponding Besov space. This important property is needed for proving stability. An introduction to Besov spaces can be found in Section A.2.

Definition 3.4.6. *A function $f \in L_p(\Omega)$ belongs to $A_q^s(L_p(\Omega))$ for some fixed $s \geq 0$, $1 \leq p, q \leq \infty$ if there exists a sequence $g_l \in S_l$, $l = 0, 1, \ldots$ such that $f = \sum_{l=0}^{\infty} g_l$ in the sense of L_p, and $\|\{3^{ls}\|g_l\|_{L_p(\Omega)}\}\|_{l_q} < \infty$. The norm on $A_q^s(L_p(\Omega))$ is defined as*

$$\|f\|_{A_q^s(L_p(\Omega))} = \inf \left(\sum_{l=0}^{\infty} \left[3^{ls} \|g_l\|_{L_p(\Omega)} \right]^q \right)^{1/q}$$

where the infimum must be taken with respect to all admissible representations $\sum_{l=0}^{\infty} g_l$ of f. With an admissible representation we mean that $\lim_{n\to\infty} \|f - \sum_{l=0}^{n} g_l\|_{L_p} = 0$.

So in order to work with the abstract $A_q^s(L_p(\Omega))$-spaces, we relate them to the more convenient function spaces of Besov type , see Section A.2. The following fact can be extracted from the results in [102].

Proposition 3.4.7. *Suppose the nested spaces $\{S_l\}_{l=0}^{\infty}$ satisfy Jackson estimates (B.9) for all $f \in L_p(\Omega)$, as well as Bernstein estimates (B.10) for $r = 3$, then for $1 \leq p, q \leq \infty$, $s > 0$*

$$A_q^s(L_p(\Omega)) \cong B_q^s(L_p(\Omega)), \qquad 0 < s < 2 + \frac{1}{p}. \tag{3.28}$$

The space $B_q^s(L_p(\Omega))$ is a Besov space, and the notation $\cong$ indicates the equivalence between the two function spaces.

If we take $p = q = 2$ then Proposition 3.4.7 is not valid for $s > \frac{5}{2}$, so it reduces the range of Sobolev spaces $H^s(\Omega)$ for which the hierarchical basis is possibly strongly stable from $s > 2$ to $s \in (2, \frac{5}{2})$, since the equivalence (3.28) is crucial for proving stability. Equation (A.5) and Proposition 3.4.7 yield

$$\|f\|_{H^s(\Omega)}^2 \sim \inf_{g_l \in S_l : f = \sum_l g_l} \sum_{l=0}^{\infty} 3^{2ls} \|g_l\|_{L_2(\Omega)}^2, \qquad 0 < s < \frac{5}{2}. \tag{3.29}$$

Using the norm equivalence (3.29) we can now prove the following theorem which is inspired by the work in [36] and [41]. This theorem is the most important step in proving stability in $H^s(\Omega)$.

Theorem 3.4.8. *Choose $s \in (2, \frac{5}{2})$. Then it holds that*

$$\|f\|^2_{H^s(\Omega)} \sim \sum_{l=0}^{\infty} 3^{2ls} \|(\mathcal{I}_l - \mathcal{I}_{l-1})f\|^2_{L_2(\Omega)}, \qquad f \in H^s(\Omega). \tag{3.30}$$

Proof. Because of the norm equivalence (3.29) it is sufficient to prove that

$$\inf_{g_l \in S_l : f = \sum_l g_l} \sum_{l=0}^{\infty} 3^{2ls} \|g_l\|^2_{L_2(\Omega)} \sim \sum_{l=0}^{\infty} 3^{2ls} \|(\mathcal{I}_l - \mathcal{I}_{l-1})f\|^2_{L_2(\Omega)}.$$

Since $(\mathcal{I}_l - \mathcal{I}_{l-1})f \in S_l$ and $\sum_{l=0}^{\infty}(\mathcal{I}_l - \mathcal{I}_{l-1})f = f$ the inequality "$\lesssim$" is trivial and we will concentrate on the inequality "$\gtrsim$". Let $f = \sum_{l=0}^{\infty} g_l$ with $g_l \in S_l$. Since the operators $\mathcal{I}_l$ are projectors and the spaces S_l are nested, we have $(\mathcal{I}_l - \mathcal{I}_{l-1})S_n = 0$ when $n \leq l-1$. Moreover the operators $\mathcal{I}_l$ also satisfy

$$\|\mathcal{I}_l s_n\|_{L_2(\Omega)} \lesssim 3^{2(n-l)} \|s_n\|_{L_2(\Omega)}, \quad s_n \in S_n, \quad n \geq l. \tag{3.31}$$

Indeed, from (3.8) and (3.9) we get

$$\|\mathcal{I}_l s_n\|_{L_\infty(T)} \lesssim \|s_n\|_{L_\infty(T)} + 3^{-l} \|D_x s_n\|_{L_\infty(T)} + 3^{-l} \|D_y s_n\|_{L_\infty(T)},$$

with $T \in \Delta_l$. Then we use the Markov inequality (Lemma 2.5.2) and the regularity (3.4) and we obtain

$$\|\mathcal{I}_l s_n\|_{L_\infty(T)} \lesssim \|s_n\|_{L_\infty(T)} + 3^{-l}3^n \|s_n\|_{L_\infty(T)} \lesssim 3^{n-l} \|s_n\|_{L_\infty(T)}.$$

Now (3.31) can be deduced by using Theorem 2.5.5 and Corollary 2.5.7.

From the properties above and the Cauchy–Schwartz inequality we have

$$\begin{aligned}
&\sum_{n,n'=0}^{\infty} \sum_{l=0}^{\infty} 3^{2ls} \langle (\mathcal{I}_l - \mathcal{I}_{l-1})g_n, (\mathcal{I}_l - \mathcal{I}_{l-1})g_{n'} \rangle_{L_2(\Omega)} \\
&= \sum_{n,n'=0}^{\infty} \sum_{l=0}^{\min\{n,n'\}} 3^{2ls} \langle (\mathcal{I}_l - \mathcal{I}_{l-1})g_n, (\mathcal{I}_l - \mathcal{I}_{l-1})g_{n'} \rangle_{L_2(\Omega)} \\
&\leq \sum_{n,n'=0}^{\infty} \sum_{l=0}^{\min\{n,n'\}} 3^{2ls} \left(\|\mathcal{I}_l g_n\|_{L_2(\Omega)} + \|\mathcal{I}_{l-1} g_n\|_{L_2(\Omega)} \right) \\
&\qquad\qquad \cdot \left(\|\mathcal{I}_l g_{n'}\|_{L_2(\Omega)} + \|\mathcal{I}_{l-1} g_{n'}\|_{L_2(\Omega)} \right) \\
&\lesssim \sum_{n,n'=0}^{\infty} \sum_{l=0}^{\min\{n,n'\}} 3^{2ls} 3^{2(n+n')-4l} \|g_n\|_{L_2(\Omega)} \|g_{n'}\|_{L_2(\Omega)}.
\end{aligned}$$

The last expression can be rewritten as

$$\sum_{n,n'=0}^{\infty} \sum_{l=0}^{\min\{n,n'\}} 3^{(s-2)(2l-n-n')}(3^{ns}\|g_n\|_{L_2(\Omega)})(3^{n's}\|g_{n'}\|_{L_2(\Omega)}),$$

which is equivalent to

$$\sum_{n,n'=0}^{\infty} 3^{(s-2)(2\min\{n,n'\}-n-n')}(3^{ns}\|g_n\|_{L_2(\Omega)})(3^{n's}\|g_{n'}\|_{L_2(\Omega)}).$$

The factor $3^{(s-2)(2\min\{n,n'\}-n-n')}$ becomes very small if $|n-n'| \gg 0$. In fact, the infinite matrix $[3^{(s-2)(2\min\{n,n'\}-n-n')}]_{n,n'\in\mathbb{N}}$ defines a bounded mapping on l_2. Therefore

$$\sum_{n,n'=0}^{\infty} 3^{(s-2)(2\min\{n,n'\}-n-n')}(3^{ns}\|g_n\|_{L_2(\Omega)})(3^{n's}\|g_{n'}\|_{L_2(\Omega)})$$

$$\lesssim \sum_{n=0}^{\infty} 3^{2ns}\|g_n\|^2_{L_2(\Omega)}.$$

Since the splitting $f = \sum_{l=0}^{\infty} g_l$ was arbitrary, we have derived that

$$\inf_{g_l\in S_l: f=\sum_l g_l} \sum_{n,n'=0}^{\infty}\sum_{l=0}^{\infty} 3^{2ls}\langle(\mathcal{I}_l-\mathcal{I}_{l-1})g_n,(\mathcal{I}_l-\mathcal{I}_{l-1})g_{n'}\rangle_{L_2(\Omega)}$$

$$\lesssim \inf_{g_l\in S_l: f=\sum_l g_l} \sum_{n=0}^{\infty} 3^{2ns}\|g_n\|^2_{L_2(\Omega)}.$$

Because $f \in A_2^s(L_2(\Omega))$ (Proposition 3.4.7) we know that the right expression is bounded. Then from the derivation made above it follows that the left expression is absolutely convergent and we are allowed to write that

$$\begin{aligned}
&\inf_{g_l\in S_l: f=\sum_l g_l} \sum_{n,n'=0}^{\infty}\sum_{l=0}^{\infty} 3^{2ls}\langle(\mathcal{I}_l-\mathcal{I}_{l-1})g_n,(\mathcal{I}_l-\mathcal{I}_{l-1})g_{n'}\rangle_{L_2(\Omega)}\\
&= \inf_{g_l\in S_l: f=\sum_l g_l} \sum_{l=0}^{\infty}\sum_{n,n'=0}^{\infty} 3^{2ls}\langle(\mathcal{I}_l-\mathcal{I}_{l-1})g_n,(\mathcal{I}_l-\mathcal{I}_{l-1})g_{n'}\rangle_{L_2(\Omega)}\\
&= \sum_{l=0}^{\infty} 3^{2ls}\|(\mathcal{I}_l-\mathcal{I}_{l-1})f\|^2_{L_2(\Omega)}.
\end{aligned}$$

The last step is obtained by moving the summation over n and n' inside the L_2 inner product, and by using the linearity of the operators $\mathcal{I}_l$. We conclude that

$$\sum_{l=0}^{\infty} 3^{2ls} \|(\mathcal{I}_l - \mathcal{I}_{l-1})f\|^2_{L_2(\Omega)} \lesssim \inf_{g_l \in S_l : f = \sum_l g_l} \sum_{l=0}^{\infty} 3^{2ls} \|g_l\|^2_{L_2(\Omega)}.$$

□

Proving that the hierarchical basis is a strongly stable basis for $H^s(\Omega)$ with $2 < s < \frac{5}{2}$ involves only a few steps now.

Corollary 3.4.9. *The multiscale basis*

$$\bigcup_{l=0}^{\infty} \{3^{l(1-s)} B_{ij,l} \mid (i,j) \in J_{l-1}\}$$

is a strongly stable basis for $H^s(\Omega)$, $2 < s < \frac{5}{2}$.

Proof. Since, from Corollary 2.5.7, the set $\{3^l B_{ij,l} \mid (i,j) \in J_{l-1}\}$ is an L_2-stable basis for W_{l-1} we find from Theorem 3.4.8 that

$$\begin{aligned} \|f\|^2_{H^s(\Omega)} &\sim \sum_{l=0}^{\infty} 3^{2ls} \| \sum_{(i,j)\in J_{l-1}} c_{ij,l} 3^l B_{ij,l} \|^2_{L_2(\Omega)} \\ &\sim \sum_{l=0}^{\infty} 3^{2ls} \sum_{(i,j)\in J_{l-1}} |c_{ij,l}|^2. \end{aligned}$$

Hence,

$$\left\| \sum_{l=0}^{\infty} \sum_{(i,j)\in J_{l-1}} c_{ij,l} 3^{l(1-s)} B_{ij,l} \right\|^2_{H^s(\Omega)} \sim \sum_{l=0}^{\infty} \sum_{(i,j)\in J_{l-1}} |c_{ij,l}|^2.$$

□

Let us now consider the model problem (1.16). The weak variational form is given by

$$\langle \Delta u, \Delta v \rangle =: a(u,v) = \langle f, v \rangle \quad \text{for all } v \in H^2_0(\Omega), \tag{3.32}$$

where $a(\cdot,\cdot)$ is the bilinear form induced by (1.16). Because of the Dirichlet boundary conditions we have that

$$a(v,v) \sim \|v\|^2_{H^2(\Omega)} \quad \text{for all } v \in H^2_0(\Omega),$$

and the condition number of the stiffness matrix for (1.16) with respect to the hierarchical basis is determined by the stability of the hierarchical basis with respect to the norm in $H^2(\Omega)$, see Section 1.2. Unfortunately, the space $H^2(\Omega)$ is not included in Theorem 3.4.8 and Corollary 3.4.9, which implies that the hierarchical basis is not a strongly stable basis for $H^2(\Omega)$, but we can prove the following suboptimal results.

Theorem 3.4.10. *The multiscale basis*

$$\bigcup_{l=0}^{\infty}\{3^{-l}B_{ij,l} \mid (i,j) \in J_{l-1}\}$$

is a weakly stable basis for $H^2(\Omega)$,

$$n^{-2}\sum_{l=0}^{n}\sum_{(i,j)\in J_{l-1}}|c_{ij,l}|^2 \lesssim \left\|\sum_{l=0}^{n}3^{-l}\sum_{(i,j)\in J_{l-1}}c_{ij,l}B_{ij,l}\right\|^2_{H^2(\Omega)} \lesssim \sum_{l=0}^{n}\sum_{(i,j)\in J_{l-1}}|c_{ij,l}|^2.$$

Proof. Suppose that $s = \sum_{l=0}^{n} g_l$ with each $g_l \in S_l$. Starting from (3.31) and the Cauchy–Schwartz inequality we derive that

$$\begin{aligned}
&\sum_{l=0}^{n}3^{4l}\|(\mathcal{I}_l-\mathcal{I}_{l-1})s\|_{L_2(\Omega)}\\
&\quad=\sum_{m,m'=0}^{n}\sum_{l=0}^{\min\{m,m'\}}3^{4l}\langle(\mathcal{I}_l-\mathcal{I}_{l-1})g_m,(\mathcal{I}_l-\mathcal{I}_{l-1})g_{m'}\rangle_{L_2(\Omega)}\\
&\quad\lesssim\sum_{m,m'=0}^{n}\sum_{l=0}^{\min\{m,m'\}}3^{4l}3^{2(m+m')-4l}\|g_m\|_{L_2(\Omega)}\|g_{m'}\|_{L_2(\Omega)}\\
&\quad\lesssim\sum_{m,m'=0}^{n}\min\{m,m'\}\left(3^{2m}\|g_m\|_{L_2(\Omega)}\right)\left(3^{2m'}\|g_{m'}\|_{L_2(\Omega)}\right)\\
&\quad\lesssim n^2\sum_{m=0}^{n}3^{4m}\|g_m\|^2_{L_2(\Omega)}.
\end{aligned}$$

Since the splitting $s = \sum_{l=0}^{n} g_l$ was arbitrary, we have derived that

$$n^{-2}\sum_{l=0}^{n}3^{4l}\|(\mathcal{I}_l-\mathcal{I}_{l-1})s\|_{L_2(\Omega)} \lesssim \inf_{g_m\in S_m:s=\sum_m g_m}\sum_{m=0}^{n}3^{4m}\|g_m\|^2_{L_2(\Omega)}.$$

Of course the inequality

$$\inf_{g_m \in S_m : s = \sum_m g_m} \sum_{m=0}^{n} 3^{4m} \|g_m\|^2_{L_2(\Omega)} \lesssim \sum_{l=0}^{n} 3^{4l} \|(\mathcal{I}_l - \mathcal{I}_{l-1})s\|_{L_2(\Omega)}$$

also holds. Furthermore, by (3.29),

$$\inf_{g_m \in S_m : s = \sum_m g_m} \sum_{m=0}^{n} 3^{4m} \|g_m\|^2_{L_2(\Omega)} \sim \|s\|^2_{H^2(\Omega)},$$

and similar reasoning as in the proof of Corollary 3.4.9 yields the desired result. □

From Theorem 3.4.10 and the theory in Section 1.2 we find that the condition number of the stiffness matrix for the problem (1.16) with respect to the hierarchical basis is of the order n^2, with n the maximum resolution level. Equivalently, we can say that the condition number is of the order $|\log h|^2$ with h the mesh size of the underlying triangulation Δ_n.

3.5 Nonlinear approximation and surface compression

Nowadays surfaces in Computer Aided Geometric Design are often described with millions of control parameters. These control parameters can for instance arise from measurements of a physical model. *Surface compression*, which is in fact a tradeoff between maintaining accuracy and reduction of the amount of data, is essential in these settings.

Nonlinear approximation [42] means that the approximants do not come from fixed linear spaces (such as for instance the spline space S_l), but the idea is that the elements used in the approximation are allowed to depend on the function being approximated. The standard problem is the problem of N-term approximation where one fixes a basis and looks to approximate the target function by a linear combination of N terms of the basis. When the basis is a wavelet-type basis, then N-term approximation is the starting point for compression algorithms. Nonlinear approximation explains the thresholding and quantization strategies used in compression and noise removal, and it explains precisely which surfaces/images can be compressed well by certain thresholding and quantization strategies.

In [43] a surface compression algorithm was given by means of multiscale decompositions of certain box splines and error bounds were given in terms of the smoothness of the input surface. The theory behind the surface compression algorithm comes from the field of nonlinear approximation. The

purpose of this section is to extend these ideas to the case of a multiresolution analysis over triangles, based on quadratic Hermite interpolation.

In the previous sections we have sufficiently demonstrated that Powell–Sabin multiscale decompositions are suitable for surface compression. We have proved that the norm of f in several smoothness classes can be determined from the size of the coefficients in the multiscale decomposition. In this section we consider a simple surface compression algorithm and we give an error bound for the approximation of f by its compressed multiscale decomposition. The most natural norm for compression is the L_∞ norm, so our approximation results take place in this norm. These results are obtained by following the framework given in [43], adapted to the special case of PS splines.

Not all functions f are suitable for compression by Powell–Sabin splines. If we use the operator $\mathcal{I}_l$ (3.7) to project given functions f into S_l, then we need at least that the gradient ∇f is well defined at the vertices $V_i \in \Delta_l$. However we would also like to compress continuous functions f for which $\mathcal{I}_l f$ might not be well defined. Therefore we construct a new operator $\mathcal{I}_l^\nabla$ that only uses values of the given function f. It suffices to approximate the gradient $\nabla f(V_i)$ by a linear combination of values of f such that the approximation is exact for quadratic polynomials. Let V_i, R_i and Z_i denote the vertices of a triangle $\tau \in \Delta_l^{PS}$ as in Figure 3.4. Then we can estimate the gradient $\nabla f(V_i)$ by

$$\nabla_l f(V_i) := \begin{bmatrix} R_i^x - V_i^x & R_i^y - V_i^y \\ Z_i^x - V_i^x & Z_i^y - V_i^y \end{bmatrix}^{-1} \begin{bmatrix} 4f(\frac{V_i+R_i}{2}) - 3f(V_i) - f(R_i) \\ 4f(\frac{V_i+Z_i}{2}) - 3f(V_i) - f(Z_i) \end{bmatrix} \tag{3.33}$$

and because $s_l \in S_l$ is a quadratic polynomial on each triangle $\tau \in \Delta_l^{PS}$ we find that

$$\nabla s_l(V_i) = \nabla_l s_l(V_i). \tag{3.34}$$

Indeed, first note that the Bézier ordinates (Figure 2.1) of the unique quadratic polynomial that interpolates the given function f at the position of the Bézier ordinates, are given by

$$\begin{array}{rclcrcl} c_{200} &=& f(V_i), & & c_{110} &=& 2f(\frac{V_i+R_i}{2}) - \frac{f(V_i)}{2} - \frac{f(R_i)}{2}, \\ c_{020} &=& f(R_i), & & c_{011} &=& 2f(\frac{R_i+Z_i}{2}) - \frac{f(R_i)}{2} - \frac{f(Z_i)}{2}, \\ c_{002} &=& f(Z_i), & & c_{101} &=& 2f(\frac{V_i+Z_i}{2}) - \frac{f(V_i)}{2} - \frac{f(Z_i)}{2}. \end{array}$$

Define the directions $u := R_i - V_i$ and $v := Z_i - V_i$, then

$$\begin{bmatrix} D_u s \\ D_v s \end{bmatrix} = \begin{bmatrix} R_i^x - V_i^x & R_i^y - V_i^y \\ Z_i^x - V_i^x & Z_i^y - V_i^y \end{bmatrix} \begin{bmatrix} D_x s \\ D_y s \end{bmatrix}$$

and (3.33) follows from the equations

$$\begin{aligned} D_u s(V_i) &= 2(-c_{200} + c_{110}) = 4f(\frac{V_i + R_i}{2}) - 3f(V_i) - f(R_i), \\ D_v s(V_i) &= 2(-c_{200} + c_{101}) = 4f(\frac{V_i + Z_i}{2}) - 3f(V_i) - f(Z_i). \end{aligned}$$

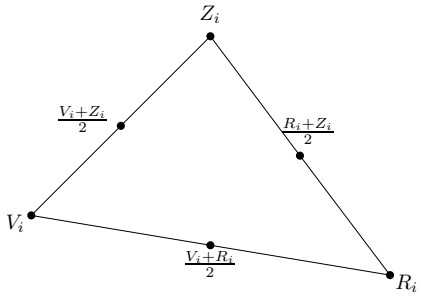

Figure 3.4: A triangle $\tau \in \Delta^{PS}$ that contains vertex $V_i \in \Delta$.

Note that

$$\begin{bmatrix} R_i^x - V_i^x & R_i^y - V_i^y \\ Z_i^x - V_i^x & Z_i^y - V_i^y \end{bmatrix}^{-1} = \frac{1}{\mathrm{vol}(\tau)} \begin{bmatrix} Z_i^y - V_i^y & V_i^y - R_i^y \\ V_i^x - Z_i^x & R_i^x - V_i^x \end{bmatrix}$$

which yields

$$|\nabla_l f(V_i)| \lesssim 3^l \, \|f\|_{L_\infty(\tau)} \, . \tag{3.35}$$

Thus we define the operator $\mathcal{I}_l^\nabla$ analogous to the operator $\mathcal{I}_l$ from (3.7) with the minor modification that we replace $\nabla f(V_i)$ by the approximation $\nabla_l f(V_i)$. Because of (3.34) it is easy to see that the operators $\mathcal{I}_l^\nabla$ satisfy $\mathcal{I}_l^\nabla s_l = s_l$ and

$$\mathcal{I}_l^\nabla f(V_i) = f(V_i), \qquad \nabla \mathcal{I}_l^\nabla f(V_i) = \nabla_l f(V_i), \qquad i = 1, \ldots, N_l.$$

Furthermore, from (3.35) we find that $|\mathcal{I}_l^\nabla f(x,y)| \lesssim \|f\|_{L_\infty(\Omega)}$ for arbitrary $(x,y) \in \Omega$, so the operator $\mathcal{I}_l^\nabla$ is uniformly bounded in $C^0(\overline{\Omega})$.

Still not all functions f are suitable for compression by Powell–Sabin splines. We need at least that the functions are C^0 such that $\mathcal{I}_l^\nabla f$ is well defined. Furthermore we would like that f can be represented as

$$f = \sum_{l=0}^{\infty} \sum_{(i,j) \in J_{l-1}} c_{ij,l} B_{ij,l} \tag{3.36}$$

with convergence in L_∞, where J_l is defined as in (3.25). Therefore we are particularly interested in functions f lying in Besov spaces that are

embedded in $B^{\delta}_{\infty}\left(L_{\infty}(\Omega)\right) = \mathrm{Lip}(\delta, \Omega)$ for $\delta > 0$. For the remainder of this section we define

$$\nu := \frac{2}{s} \text{ and } \delta := \frac{2}{\nu} - \frac{2}{\sigma} \tag{3.37}$$

for some $\sigma \geq 0$. If $\sigma > \nu$ then we have $\delta > 0$.

Lemma 3.5.1. *Let $s > 0$ and $\sigma > \nu$, then*

$$B^{s}_{\sigma}\left(L_{\sigma}(\Omega)\right) \subset B^{\delta}_{\infty}\left(L_{\infty}(\Omega)\right) = \mathrm{Lip}(\delta, \Omega).$$

Proof. The case $\sigma \geq 1$ follows immediately from Theorems 7.69 and 7.70 in [1]. For the case $\sigma < 1$ we can use Theorems 12.3, 12.5 and 12.7 from [46]. □

Lemma 3.5.1 guarantees that $\mathcal{I}_l^{\nabla} f$ is well defined for all $f \in B^{s}_{\sigma}\left(L_{\sigma}(\Omega)\right)$ given that $\sigma > \nu$. The following corollary validates the representation (3.36) with convergence in L_{∞} for all $f \in B^{s}_{\sigma}\left(L_{\sigma}(\Omega)\right)$, $\sigma > \nu$.

Corollary 3.5.2. *Assume the constants ν, s, δ, σ satisfy* (3.37)*. For all $f \in B^{s}_{\sigma}\left(L_{\sigma}(\Omega)\right)$ with $s < 3$, all $\sigma > \nu$, and arbitrary $l \geq 0$ we have that*

$$\left\| f - \mathcal{I}_l^{\nabla} f \right\|_{L_{\infty}(\Omega)} \lesssim 3^{-\delta l} \left| f \right|_{B^{s}_{\sigma}(L_{\sigma}(\Omega))}.$$

Proof. Since $\mathcal{I}_l^{\nabla}$ is bounded on $C^0(\overline{\Omega})$ we find that

$$\begin{aligned} \left\| f - \mathcal{I}_l^{\nabla} f \right\|_{L_{\infty}(\Omega)} &\leq \inf_{g \in S_l} \left(\|f - g\|_{L_{\infty}(\Omega)} + \left\| \mathcal{I}_l^{\nabla}(g - f) \right\|_{L_{\infty}(\Omega)} \right) \\ &\leq \left(1 + \left\| \mathcal{I}_l^{\nabla} \right\|_{L_{\infty}(\Omega)} \right) \inf_{g \in S_l} \|f - g\|_{L_{\infty}(\Omega)} \\ &\lesssim \inf_{g \in S_l} \|f - g\|_{L_{\infty}(\Omega)} \end{aligned}$$

and from applying Corollary B.1.3 to the right hand side of the previous equation, we get

$$\left\| f - \mathcal{I}_l^{\nabla} f \right\|_{L_{\infty}(\Omega)} \lesssim \omega_3(f, 3^{-l})_{\infty}. \tag{3.38}$$

By (A.4) and Lemma 3.5.1 we know that

$$3^{\delta l} \omega_3(f, 3^{-l})_{\infty} \lesssim |f|_{B^{\delta}_{\infty}(L_{\infty}(\Omega))} \lesssim |f|_{B^{s}_{\sigma}(L_{\sigma}(\Omega))}.$$

□

Suppose we are given a function $f \in B^s_\sigma\left(L_\sigma(\Omega)\right)$, $\sigma > \nu$ that represents the surface that is being compressed. The surface compression algorithm is as follows: Let K be such that $f \approx \mathcal{I}^\nabla_K f$, then we obtain the decomposition

$$f \approx \sum_{l=0}^{K} \sum_{(i,j)\in J_l} c_{ij,l} B_{ij,l}.$$

At all levels $l \geq 0$ we only retain those coefficients $c_{ij,l}$ that satisfy $|c_{ij,l}| > \epsilon/(2K+2)$.

We will need some estimation for the constant K, i.e. the maximum number of resolution levels. Suppose we are looking for a compressed approximant S of f such that

$$\|f - S\|_{L_\infty(\Omega)} \leq \epsilon.$$

Corollary 3.5.2 gives us an a priori bound for the number of resolution levels. Choose K such that

$$\left\|f - \mathcal{I}^\nabla_K f\right\|_{L_\infty(\Omega)} \leq \epsilon/2, \tag{3.39}$$

then we find that

$$K \geq \frac{1}{\delta \log 3} \log\left(\frac{2C\,|f|_{B^s_\sigma(L_\sigma(\Omega))}}{\epsilon}\right) \tag{3.40}$$

where C is the equivalence constant in Corollary 3.5.2.

From (2.9) we find that

$$\sum_{(i,j)\in J_{l-1}} |B_{ij,l}| \leq 1.$$

If we retain only the coefficients $c_{ij,l}$ of $\mathcal{I}^\nabla_K f$ that satisfy $|c_{ij,l}| > \frac{\epsilon}{2(K+1)}$, then

$$\left\|\mathcal{I}^\nabla_K f - S\right\|_{L_\infty(\Omega)} \leq \epsilon/2 \tag{3.41}$$

because the maximal error is given by

$$\frac{\epsilon}{2(K+1)} \sum_{l=0}^{K} \sum_{(i,j)\in J_{l-1}} B_{ij,l} \leq \frac{\epsilon}{2}.$$

From (3.39) and (3.41) we deduce that

$$\|f - S\|_{L_\infty(\Omega)} \leq \left\|f - \mathcal{I}^\nabla_K f\right\|_{L_\infty(\Omega)} + \left\|\mathcal{I}^\nabla_K f - S\right\|_{L_\infty(\Omega)} \leq \epsilon. \tag{3.42}$$

We will now examine the coefficients $c_{ij,l}$. We have that

$$(\mathcal{I}_{l+1} - \mathcal{I}_l)\mathcal{I}_K^{\triangledown} f = \sum_{(i,j)\in J_l} c_{ij,l+1} B_{ij,l+1},$$

and from (3.4) and the construction of the projectors $\mathcal{I}_l$ we infer

$$|c_{ij,l+1}| \lesssim \|\mathcal{I}_K^{\triangledown} f\|_{L_\infty(\tau_i)} \sim \|f\|_{L_\infty(\tau_i)}$$

with τ_i a triangle in Δ_l^{PS} such that $\operatorname{supp} B_{ij,l} \cap \tau_i \neq 0$. Now let $\pi \in \mathcal{P}_2$ be an arbitrary bivariate polynomial of degree at most 2. Then

$$(\mathcal{I}_{l+1} - \mathcal{I}_l)\mathcal{I}_K^{\triangledown} f = (\mathcal{I}_{l+1} - \mathcal{I}_l)(\mathcal{I}_K^{\triangledown} f - \pi),$$

so we also find that

$$|c_{ij,l+1}| \lesssim \inf_{\pi\in\mathcal{P}_2} \|f - \pi\|_{L_\infty(\tau_i)}$$

The following lemma gives an upper bound for magnitude of the coefficients $c_{ij,l+1}$ in function of $|f|_{B_\sigma^s(L_\sigma(\Omega))}$.

Lemma 3.5.3. *Assume the constants ν, s, δ, σ satisfy* (3.37). *Let $s < 3$ and let $f \in B_\sigma^s(L_\sigma(\Omega))$. Then the coefficients $c_{ij,l+1}$ in the decomposition (3.36) satisfy*

$$|c_{ij,l+1}| \lesssim 3^{-l\delta} |f|_{B_\sigma^s(L_\sigma(\tau_i))} \tag{3.43}$$

for all $\sigma > \nu$.

Proof. From the derivation above and Whitney's Theorem (see, e.g., [16, 119]) we infer

$$|c_{ij,l+1}| \lesssim \omega_3(f, 3^{-l})_\infty,$$

and the same reasoning as in the proof of Corollary 3.5.2 yields

$$|c_{ij,l+1}| \lesssim 3^{-l\delta} |f|_{B_\sigma^s(L_\sigma(\tau_i))}.$$

□

We now give a bound for the number of terms N in the compressed approximant S such that the error remains bounded by the threshold ϵ.

Theorem 3.5.4. *Assume the constants ν, s, δ, σ satisfy* (3.37). *Let f be a function in $B_\sigma^s(L_\sigma(\Omega))$ with $s < 3$ and such that $|f|_{B_\sigma^s(L_\sigma(\Omega))} \leq 1$ for some $\sigma > \nu$. Then the surface compression algorithm provides an approximation S such that*

$$\|f - S\|_{L_\infty(\Omega)} \leq \epsilon \tag{3.44}$$

and

$$N \lesssim \epsilon^{-2/s} \tag{3.45}$$

where N represents the number of terms in S.

Proof. Under the assumptions of the theorem, the bound for K (3.40) does not depend on f anymore. We already know that (3.44) is true, see (3.42). Let $N(l)$ denote the number of terms at resolution level l, then a trivial bound for $N(l)$ is

$$N(l) \lesssim 9^l \tag{3.46}$$

which follows from the fact that we have used triadic refinement to create the nested subspaces $\{S_l\}_{l=0}^{\infty}$. We give another bound for $N(l)$. We know that each coefficient $c_{ij,l+1}$ in S satisfies $|c_{ij,l+1}| > \epsilon/(2K+2)$ but we have also the upper bound (3.43). If we raise $c_{ij,l+1}$ to the power σ and sum over all $m \in J_l$ then we obtain that

$$\begin{aligned} N(l)\left(\frac{\epsilon}{2(K+1)}\right)^{\sigma} < \sum_{(i,j)\in J_l} |c_{ij,l+1}|^{\sigma} &\lesssim \sum_{(i,j)\in J_l} 3^{-\sigma l\delta}\,|f|^{\sigma}_{B^s_{\sigma}(L_\sigma(\tau_i))} \\ &\lesssim 3^{-\sigma l\delta}\,|f|^{\sigma}_{B^s_{\sigma}(L_\sigma(\Omega))}. \end{aligned}$$

Under the assumption $|f|_{B^s_{\sigma}(L_\sigma(\Omega))} \leq 1$ we find

$$N(l) \lesssim \epsilon^{-\sigma} 3^{-\sigma l\delta}. \tag{3.47}$$

From (3.46) and (3.47) we find for an arbitrary integer k that

$$N \lesssim \sum_{l=1}^{k} 9^l + \sum_{l=k}^{K} \epsilon^{-\sigma} 3^{-\sigma l\delta} \lesssim 9^k + \epsilon^{-\sigma} 3^{-\sigma k\delta}.$$

Choose k such that $9^k \sim \epsilon^{-\sigma} 3^{-\sigma k\delta}$, then $N \lesssim 9^k$. Furthermore we deduce that $9^k 3^{\sigma k\delta} = 3^{2k\left(1+\frac{\sigma\delta}{2}\right)} \sim \epsilon^{-\sigma}$ and that $9^k \sim \epsilon^{-\sigma/\left(1+\frac{\sigma\delta}{2}\right)} = \epsilon^{-2/s}$, so

$$N \lesssim 9^k \sim \epsilon^{-2/s}.$$

□

The following corollary is the main result of this section. It is a direct consequence of Theorem 3.5.4.

Corollary 3.5.5. *Assume the constants ν, s, δ, σ satisfy* (3.37)*. If $f \in B^s_{\sigma}(L_\sigma(\Omega))$ with $s < 3$, and $N \in \mathbb{N}$ is given, then one can choose the*

threshold ϵ and the maximum resolution level K such that the compression algorithm generates an approximant S to f with at most N terms and

$$\|f - S\|_{L_\infty(\Omega)} \lesssim |f|_{B^s_\sigma(L_\sigma(\Omega))} N^{-s/2}$$

for arbitrary $\sigma > \nu$.

Proof. This proof is the same as the proof of Corollary 5.4 in [43] but we give it here for completeness. Let $\epsilon := C^{s/2} N^{-s/2} |f|_{B^s_\sigma(L_\sigma(\Omega))}$ with C the bounding constant from (3.45). If we apply the algorithm to f and ϵ we get a compressed approximant S. If we apply the algorithm to $\frac{f}{|f|_{B^s_\sigma(L_\sigma(\Omega))}}$ and $\frac{\epsilon}{|f|_{B^s_\sigma(L_\sigma(\Omega))}}$ then the algorithm returns $\frac{S}{|f|_{B^s_\sigma(L_\sigma(\Omega))}}$ as compressed approximant. From Theorem 3.5.4 the number of terms in S does not exceed $C\left(\frac{\epsilon}{|f|_{B^s_\sigma(L_\sigma(\Omega))}}\right)^{-2/s}$ which is equal to N. □

We can compare the error bound for the compressed approximant S of f to an error bound for the linear approximant $\mathcal{I}_l^\nabla f$. If each approximation has N coefficients then we have that

$$\|f - S\|_{L_\infty(\Omega)} \lesssim N^{-s/2} |f|_{B^s_\sigma(L_\sigma(\Omega))}, \quad s < 3, \tag{3.48}$$

and

$$\left\|f - \mathcal{I}_l^\nabla f\right\|_{L_\infty(\Omega)} \lesssim N^{-s/2} |f|_{B^s_\infty(L_\infty(\Omega))}, \quad s < 3, \tag{3.49}$$

for all $f \in B^s_\sigma(L_\sigma(\Omega))$ and for all $\sigma > \nu$. The error bound for $\mathcal{I}_l^\nabla f$ follows immediately from Corollary 3.5.2 and $N \sim 9^l$. These error bounds (3.48) and (3.49) show that $\|f - S\|_{L_\infty(\Omega)} = \mathcal{O}(N^{-s/2})$ if f has s "derivatives" in L_σ while $\|f - \mathcal{I}_l^\nabla f\|_{L_\infty(\Omega)} = \mathcal{O}(N^{-s/2})$ if f has s "derivatives" in L_∞ which is a much stricter requirement. It can often happen that the right hand side of (3.48) is finite for certain values of s for which the right hand side of (3.49) is infinite. This is best illustrated by Figure 3.5. Each point in the $(1/p, s)$-plane corresponds to a smoothness space describing smoothness s measured in L_p. The spaces located left of the fat line are embedded in L_∞. The spaces of smoothness on the vertical line above L_∞ (i.e. the s-axis) are essentially those spaces whose elements can be approximated with accuracy $\mathcal{O}(N^{-s/2})$ by approximants from regular meshes, i.e. linear approximation. On the other hand, the spaces on the critical embedding line are characterized by nonlinear approximation like best N-term approximation. Thus, while moving to the right in the figure, the smoothness spaces admit increasingly stronger singularities, but this loss of regularity can be compensated by nonlinear approximation such that the same convergence

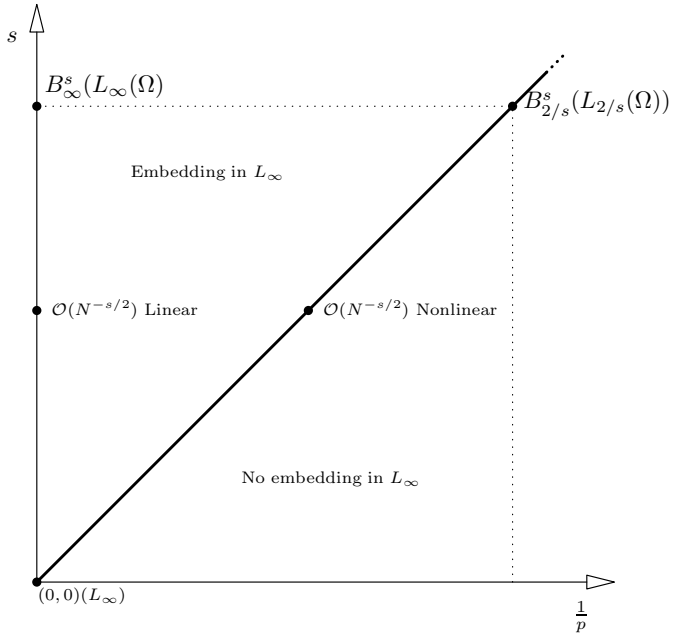

Figure 3.5: Topography of smoothness spaces

rate, i.e. $\mathcal{O}(N^{-s/2})$, is retained, provided that we stay to the left side of the critical embedding line.

To demonstrate the accuracy of the error bounds we performed experiments with several test functions. In all cases we choose Δ_0 as the triangulation that is constructed by dividing the unit square $[0,1]^2 \in \mathbb{R}^2$ by its bisector in two triangles. We selected the following bivariate test functions

given by

$$\begin{aligned}
f_1(x,y) &= 0.75\exp\left[-\frac{(9x-2)^2+(9y-2)^2}{4}\right] \\
&\quad +0.75\exp\left[-\frac{(9x+1)^2}{49}-\frac{(9y+1)^2}{10}\right] \\
&\quad +0.5\exp\left[-\frac{(9x-7)^2+(9y-3)^2}{4}\right] \\
&\quad -0.2\exp\left[-(9x-4)^2-(9y-7)^2\right], \\
f_2(x,y) &= 9(x-y)\left(\exp\left[-\frac{1}{9}\left((x-y)^2\right)^{1/8}\right]-1\right), \\
f_3(x,y) &= 97(x-0.5)\tanh\left[\frac{1}{97}((x-0.5)^2+(y-0.5)^2)^{1/4}\right], \\
f_4(x,y) &= \exp\left[-|x-y|\right], \\
f_5(x,y) &= \left((2x-1)^2+(2y-1)^2\right)^{1/4}.
\end{aligned}$$

Function f_1 is Franke's test function [57] and it is smooth everywhere. Function f_2 is C^1 but its partial derivatives have singularities on the line $y = x$. Function f_3 is also C^1 but its partial derivatives have a cusp singularity at $(1/2, 1/2)$. Function f_4 is only Lipschitz continuous and it has singularities on the line $y = x$. And finally function f_5 is C^0 (not Lipschitz) with a cusp singularity at $(1/2, 1/2)$. Because the error bound (3.48) is valid for all Besov spaces $B^s_\sigma(L_\sigma(\Omega))$ as long as $\sigma > \nu$ we will base our discussion on the Besov spaces $B^s_\nu(L_\nu(\Omega))$ which are close to $B^s_\sigma(L_\sigma(\Omega))$ (take $\sigma = \nu + \epsilon$ and let $\epsilon \to 0_+$).

For the function f_1 we do not expect much advantage from the compressed approximant to the linear approximant. Because f_1 is C^∞ the norms $|f_1|_{B^s_\sigma(L_\sigma(\Omega))}$ and $|f_1|_{B^s_\infty(L_\infty(\Omega))}$ are comparable for all $\sigma > 0$.

For the function f_2 we compute that $\left|(\Delta^3_h f_2)(x,y)\right| \approx |h|^{5/4}$ in a band of width $|h|$ along the line $y = x$. It follows that

$$\omega_3(f_2,t)_\nu \approx t^{5/4+1/\nu}, \quad 0 < t < 1, \quad 0 < \nu \le \infty.$$

Therefore we have that $f_2 \in B^s_\nu(L_\nu(\Omega))$ provided that $s < \frac{5}{2}$ while $f_2 \in B^s_\infty(L_\infty(\Omega))$ provided $s < \frac{5}{4}$.

The 3-th order difference $\left|(\Delta^3_h f_3)(x,y)\right|$ is approximately equal to $|h^{3/2}|$ in a disc with diameter $|h|$ around $(1/2, 1/2)$. This yields $\omega_3(f_3,t)_\nu \approx t^{3/2+2/\nu}$ and $f_3 \in B^s_\nu(L_\nu(\Omega))$ for all $s < 3$ while $f_3 \in B^s_\infty(L_\infty(\Omega))$ provided $s < \frac{3}{2}$.

The function f_4 has singularities along the line $y = x$ and similar computations as before yield $\omega_3(f_4,t)_\nu \approx t^{1+1/\nu}$. Therefore the function f_4 is in $B^s_\nu(L_\nu(\Omega))$ provided that $s < 2$ and f_4 is in $B^s_\infty(L_\infty(\Omega))$ for $s < 1$.

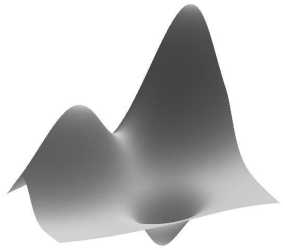

(a) Original

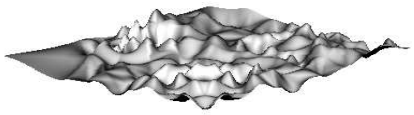

(b) $N = 181$

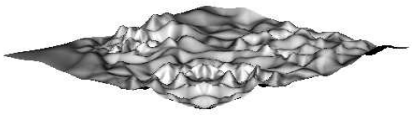

(c) $N = 232$

Figure 3.6: Test function f_1 and the residuals of two compressed approximants.

The last function f_5 has a cusp singularity in $(1/2, 1/2)$ and the modulus of smoothness $\omega_3(f_5, t)_\nu \approx t^{1/2+2/\nu}$. Therefore the function f_5 is in all of the spaces $B^s_\sigma(L_\sigma(\Omega))$ for all $s < 3$, while f_5 is in the spaces $B^s_\infty(L_\infty(\Omega))$ only for $s < 1/2$.

Table 3.1 presents the error of approximation produced by the compression algorithm for various numbers of coefficients. Note that for test function f_5 we have shown less data than for the other test functions. This is due to the fact that the error with respect to f_5 only starts to increase when we have less than 1000 coefficients. This is because the cusp singularity cannot be approximated up to arbitrary precision by the C^1 splines. Table 3.2 compares the nonlinear error rates (3.48) to the experimental error rates and shows how much is gained with respect to linear approximation.

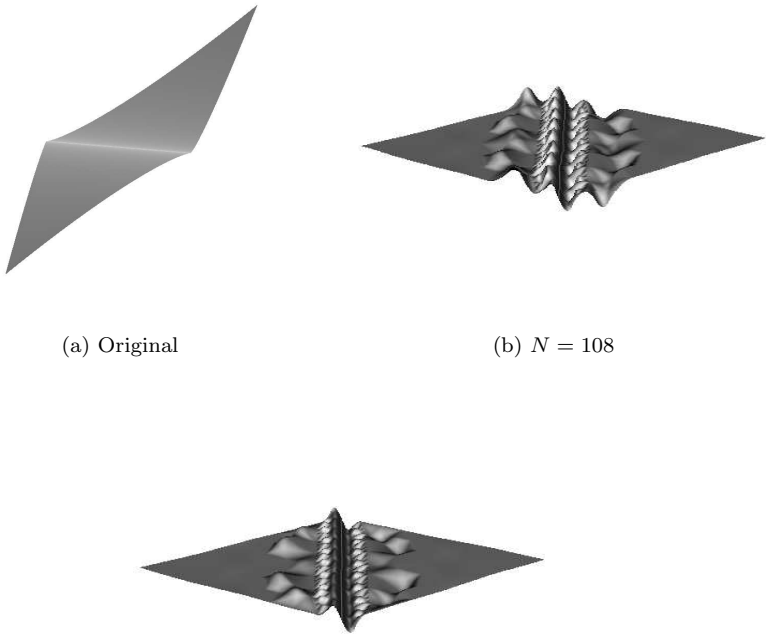

(a) Original (b) $N = 108$

(c) $N = 152$

Figure 3.7: Test function f_2 and the residuals of two compressed approximants.

Figures 3.6 up to 3.10 depict the original test functions together with the residual of some compressed approximants. Notice the large artefacts in Fig. 3.9 (b) and (c). Because the bisector of the unit square $[0, 1]^2$ is an edge of the initial triangulation Δ_0, our compression algorithm needs a lot of derivative information on this bisector (which coincides with the ridge). Therefore, at one side of the ridge, we get a very good approximation because the derivatives are estimated well, and on the other side we get the artefacts.

Finally let us make a comparison with other similar methods in the literature. Since the construction of multivariate wavelets on arbitrary triangulations is very challenging, and, except for box spline spaces, little is known yet about higher order spline spaces, we will restrict ourselves to a

Test function	Error	Number of coefficients
f_1	5.94×10^{-5}	6666
	1.01×10^{-4}	4156
	4.36×10^{-4}	1455
	6.06×10^{-4}	1175
	1.17×10^{-3}	944
	4.71×10^{-3}	340
	6.45×10^{-3}	258
	8.00×10^{-3}	232
	1.17×10^{-2}	181
f_2	6.55×10^{-6}	5610
	1.34×10^{-5}	4838
	4.30×10^{-5}	4094
	1.67×10^{-4}	2664
	5.54×10^{-4}	1156
	1.51×10^{-3}	474
	3.36×10^{-3}	272
	6.35×10^{-3}	152
	1.02×10^{-2}	108
f_3	1.12×10^{-5}	2174
	5.67×10^{-5}	798
	9.12×10^{-5}	498
	1.83×10^{-4}	336
	4.15×10^{-4}	198
	6.01×10^{-4}	174
	8.97×10^{-4}	148
	1.10×10^{-3}	116
	2.10×10^{-3}	74
f_4	1.10×10^{-5}	2232
	4.99×10^{-4}	1949
	7.87×10^{-4}	1691
	2.42×10^{-3}	1477
	4.27×10^{-3}	725
	6.42×10^{-3}	499
	1.19×10^{-2}	246
	2.25×10^{-2}	125
	3.68×10^{-2}	81
f_5	4.26×10^{-4}	1006
	5.02×10^{-4}	868
	1.02×10^{-3}	578
	4.45×10^{-3}	216
	1.08×10^{-2}	114
	4.53×10^{-2}	48

Table 3.1: Errors and number of coefficients for the surface compression algorithm applied to the test functions f_1, f_2, f_3, f_4 and f_5.

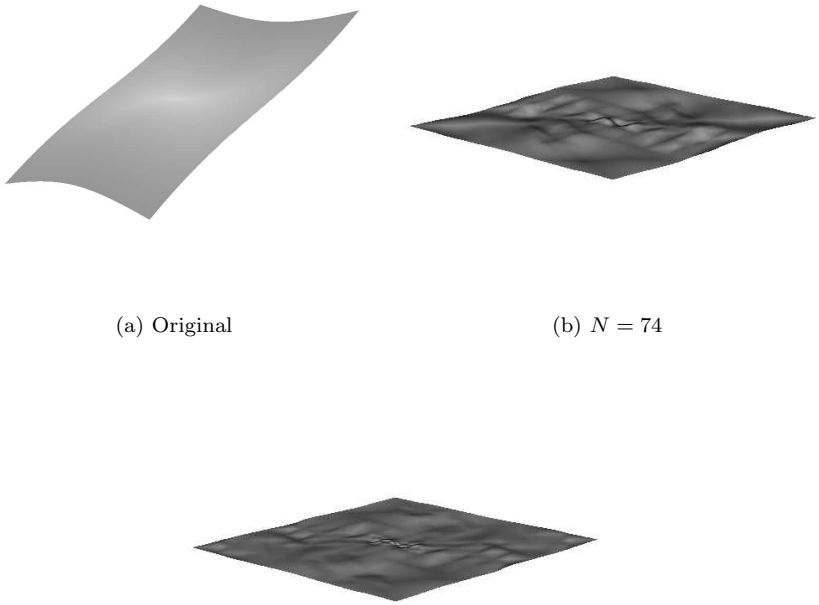

(a) Original (b) $N = 74$

(c) $N = 116$

Figure 3.8: Test function f_3 and the residuals of two compressed approximants.

comparison with the results of [43]. Here C^2 continuous box splines on uniform partitions are used. As can be deduced form (3.48), the best rate that we can get with the compression method presented here is $\mathcal{O}(N^{-3/2})$. Recall that the fact that $s < 3$ in (3.48) is a direct consequence of the C^1 continuity of the splines that we use. If we compress a function $f \in B^s_\sigma\left(L_\sigma(\Omega)\right)$ with some $s > 3$, then our compression algorithm treats this function f as a member of $B^s_\sigma\left(L_\sigma(\Omega)\right)$ with $s = 3$. In comparison, the best compression rate that can be achieved with the C^2 box splines of [43] is $\mathcal{O}(N^{-2})$, due to the smoother splines that are used. Table 3.3 shows the error of approximation produced by the compression method from [43] for the test functions f_4 and f_5. The experimental rates for f_4 and f_5 are given by $3.36N^{-1.01}$ resp. $604N^{-2.00}$. Note that both compression algorithms give almost equal

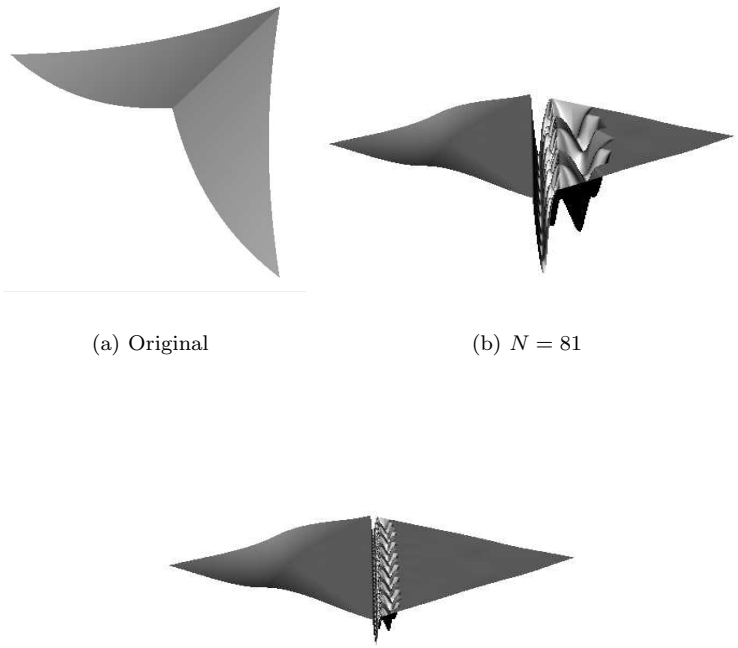

(a) Original (b) $N = 81$

(c) $N = 246$

Figure 3.9: Test function f_4 and the residuals of two compressed approximants.

results for test function f_4. For test function f_5 the compression algorithm of [43] gives an error rate of $\mathcal{O}(N^{-2})$ which is superior to our error rate, although our method gives better results for N small.

3.6 The BPX-preconditioner

In this section we construct a Bramble–Pasciak–Xu-type preconditioner [11] for the model problem (1.16), and we compare this preconditioner numerically with the suboptimal hierarchical basis preconditioner from Section 3.4.

Let $\mathcal{Q}_l$, $l = 0, 1, \ldots$, be a sequence of projectors on the PS spline space

	Linear approximation	Nonlinear approximation	Experimental compression rate
f_1	$\mathcal{O}(N^{-3/2})$	$\mathcal{O}(N^{-3/2})$	$29.8N^{-1.51}$
f_2	$\mathcal{O}(N^{-5/8})$	$\mathcal{O}(N^{-5/4})$	$3.68N^{-1.26}$
f_3	$\mathcal{O}(N^{-3/4})$	$\mathcal{O}(N^{-3/2})$	$1.19N^{-1.47}$
f_4	$\mathcal{O}(N^{-1/2})$	$\mathcal{O}(N^{-1})$	$3.37N^{-1.03}$
f_5	$\mathcal{O}(N^{-1/4})$	$\mathcal{O}(N^{-3/2})$	$24.0N^{-1.62}$

Table 3.2: Error rates for the test functions f_1, f_2, f_3, f_4 and f_5.

Test function	Error	Number of coefficients
f_4	1.60×10^{-3}	1934
	6.49×10^{-3}	482
	1.30×10^{-2}	237
	2.59×10^{-2}	116
	4.22×10^{-2}	80
f_5	1.38×10^{-3}	618
	2.76×10^{-3}	463
	1.38×10^{-2}	222
	2.69×10^{-2}	163
	7.13×10^{-2}	91
	1.05×10^{-1}	70

Table 3.3: Errors and number of coefficients for the surface compression algorithm from [43] applied to the test functions f_4 and f_5. (Results extracted from [43])

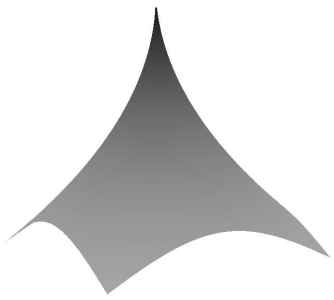

(a) Original

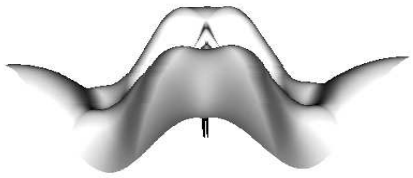

(b) $N = 48$

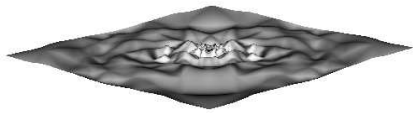

(c) $N = 216$

Figure 3.10: Test function f_5 and the residuals of two compressed approximants.

S_l that are orthogonal with respect to the standard L_2 inner product and let $\mathcal{Q}_{-1} \equiv 0$. Suppose $s_n \in S_n$. Then (3.29) immediately implies

$$\|s_n\|^2_{H^s(\Omega)} \sim \sum_{l=0}^{n} 3^{2ls} \|(\mathcal{Q}_l - \mathcal{Q}_{l-1})f\|^2_{L_2(\Omega)}, \quad 0 < s < \frac{5}{2}, \tag{3.50}$$

see [45, 102] for a rigorous proof. In view of (1.12) let us define the self-adjoint positive definite operator $\mathcal{C}_n^{-1}$ on S_n by

$$\langle \mathcal{C}_n^{-1} u, v\rangle = \sum_{l=0}^{n} 3^{4l} \langle (\mathcal{Q}_l - \mathcal{Q}_{l-1})u, (\mathcal{Q}_l - \mathcal{Q}_{l-1})v\rangle, \quad \forall v \in S_n, \tag{3.51}$$

and let $\mathcal{A}_n$ be the operator defined by (1.9) for $a(\cdot,\cdot)$ the bilinear form

induced by the model problem (1.16), i.e.

$$a(u,v) = \langle \Delta u, \Delta v \rangle.$$

Because of the Dirichlet boundary condition, the ellipticity condition

$$a(v,v) \sim \|v\|^2_{H^2(\Omega)}, \quad \forall v \in H^2_0(\Omega),$$

holds, and by (3.50) and (1.12) we find that

$$\kappa(\mathcal{C}_n^{1/2} \mathcal{A}_n \mathcal{C}_n^{1/2}) = \mathcal{O}(1). \tag{3.52}$$

Note that, by (3.51), we have

$$\mathcal{C}_n^{-1} := \sum_{l=0}^{n} 3^{4l} (\mathcal{Q}_l - \mathcal{Q}_{l-1}). \tag{3.53}$$

Indeed, by the L_2-orthogonality of the operators $\mathcal{Q}_l$ we find

$$\begin{aligned} \langle \mathcal{C}_n^{-1} u, v \rangle &= \langle \sum_{l=0}^{n} 3^{4l} (\mathcal{Q}_l - \mathcal{Q}_{l-1}) u, v \rangle \\ &= \langle \sum_{l=0}^{n} 3^{4l} (\mathcal{Q}_l - \mathcal{Q}_{l-1}) u, \sum_{j=0}^{n} (\mathcal{Q}_j - \mathcal{Q}_{j-1}) v \rangle \\ &= \sum_{l=0}^{n} 3^{4l} \langle (\mathcal{Q}_l - \mathcal{Q}_{l-1}) u, (\mathcal{Q}_l - \mathcal{Q}_{l-1}) v \rangle. \end{aligned}$$

Using techniques developed in [74] we now replace $\mathcal{C}_n$ by a computationally simpler preconditioner $\widehat{\mathcal{C}}_n$ given by

$$\widehat{\mathcal{C}}_n := \sum_{l=0}^{n} 3^{2l} \sum_{i=1}^{N_l} \sum_{j=1}^{3} \langle \cdot, B_{ij,l} \rangle B_{ij,l}. \tag{3.54}$$

We will show that $\widehat{\mathcal{C}}_n$ is spectrally equivalent to $\mathcal{C}_n$. We say that two operators $\mathcal{X}$ and $\mathcal{Y}$ are spectrally equivalent if

$$\frac{\langle \mathcal{X} v, v \rangle}{\langle v, v \rangle} \sim \frac{\langle \mathcal{Y} v, v \rangle}{\langle v, v \rangle}.$$

By the orthogonality of the projectors $\mathcal{Q}_l$ one finds from (3.53) that

$$\mathcal{C}_n = \sum_{l=0}^{n} 3^{-4l} (\mathcal{Q}_l - \mathcal{Q}_{l-1}).$$

Because of the decaying scaling factors we can replace $\mathcal{C}_n$ by the spectrally equivalent operator

$$\widetilde{\mathcal{C}}_n := \sum_{l=0}^{n} 3^{-4l} \mathcal{Q}_l.$$

From Corollary 2.5.7, we have the equivalence

$$\left\| \sum_{i=1}^{N_l} \sum_{j=1}^{3} c_{ij,l} B_{ij,l} \right\|_{L_2}^2 \sim 3^{-2l} \sum_{i=1}^{N_l} \sum_{j=1}^{3} |c_{ij,l}|^2,$$

and by the Riesz property (see, e.g., [30]) this implies the existence of a dual basis $\{\widetilde{B}_{ij,l}\}$ such that

$$\left\| \sum_{i=1}^{N_l} \sum_{j=1}^{3} c_{ij,l} \widetilde{B}_{ij,l} \right\|_{L_2}^2 \sim 3^{2l} \sum_{i=1}^{N_l} \sum_{j=1}^{3} |c_{ij,l}|^2.$$

The orthogonal projector $\mathcal{Q}_l$ has the representation

$$\mathcal{Q}_l f = \sum_{i=1}^{N_l} \sum_{j=1}^{3} \langle f, B_{ij,l} \rangle \widetilde{B}_{ij,l}.$$

Hence,

$$\langle \mathcal{Q}_l f, f \rangle = \langle \mathcal{Q}_l f, \mathcal{Q}_l f \rangle = \|\mathcal{Q}_l f\|_{L_2}^2 \sim 3^{2l} \sum_{i=1}^{N_l} \sum_{j=1}^{3} |\langle f, B_{ij,l} \rangle|^2 = \langle \widehat{\mathcal{Q}}_l f, f \rangle,$$

with

$$\widehat{\mathcal{Q}}_l := 3^{2l} \sum_{i=1}^{N_l} \sum_{j=1}^{3} \langle \cdot, B_{ij,l} \rangle B_{ij,l},$$

which shows that $\widehat{\mathcal{C}}_n$ defined in (3.54) is spectrally equivalent to $\mathcal{C}_n$ such that, by (3.52),

$$\kappa(\widehat{\mathcal{C}}_n^{1/2} \mathcal{A}_n \widehat{\mathcal{C}}_n^{1/2}) = \mathcal{O}(1).$$

In other words, the BPX-preconditioner works with a frame of redundant basis functions, instead of a basis.

In the paper [61] Griebel shows that the conjugate gradient (CG) method for the semidefinite system that arises from the Galerkin scheme using the nodal basis functions of the finest level and of all coarser levels of discretization, is equivalent to the BPX-preconditioned CG method for the linear system that arises from the Galerkin scheme using only the nodal

basis functions of the finest level. We will briefly sketch the proof here. The interested reader is referred to [61].

As in Section 3.2, let $\boldsymbol{\phi}_n$ denote the row vector of basis functions $B_{ij,n}$ at level n, and let A_n denote the subdivision matrix. Then

$$[\boldsymbol{\phi}_0 \quad \boldsymbol{\phi}_1] = \boldsymbol{\phi}_1[A_0 \quad I_1],$$

with I_1 the $\dim S_1 \times \dim S_1$ identity matrix. If $T_1 := [A_0 \quad I_1]$ then we find in a similar way

$$[\boldsymbol{\phi}_0 \quad \boldsymbol{\phi}_1 \quad \boldsymbol{\phi}_2] = \boldsymbol{\phi}_2[A_1T_1 \quad I_2].$$

Again, if $T_2 := [A_1T_1 \quad I_2]$, then

$$[\boldsymbol{\phi}_0 \quad \boldsymbol{\phi}_1 \quad \boldsymbol{\phi}_2 \quad \boldsymbol{\phi}_3] = \boldsymbol{\phi}_3[A_2T_2 \quad I_3]$$

and so on. Now, using the nodal basis functions $B_{ij,n}$ at the fixed resolution level n, the Galerkin approach leads to the linear system of equations $L_nu_n = f_n$, where $(L_n)_{3i+j,3k+l} = a(B_{ij,n}, B_{kl,n})$, with $a(\cdot,\cdot)$ the bilinear form induced by the elliptic PDE, and $(f_n)_{3k+l} = \langle f, B_{kl,n}\rangle$. If we use the nodal basis functions of the finest level and of all coarser levels, then the Galerkin approach leads to the enlarged system of equations $L_n^E w_n^E = f_n^E$, where $(L_n^E)^{l_1,l_2}_{3i+j,3k+l} = a(B_{ij,l_1}, B_{kl,l_2})$ and $(f_n^E)^{l_2}_{3k+l} = \langle f, B_{kl,l_2}\rangle$, with $l_1, l_2 = 0, \ldots, n$. Note that, to compute L_n^E, it is not necessary to explicitly compute $a(B_{ij,l_1}, B_{kl,l_2})$ and $\langle f, B_{kl,l_2}\rangle$ which involves integration on all levels $0, \ldots, n$, but we can use

$$L_n^E = (T_n)^T L_n T_n, \qquad f_n^E = (T_n)^T f_n. \tag{3.55}$$

The matrix L_n^E is relatively densely populated, but in practical implementations it is not necessary to know the matrix explicitly. We only need the matrix vector multiplication $L_n^E w_n^E$, such that the product representation (3.55) can be used, which can be computed in $\mathcal{O}(\dim S_n)$ operations. The matrix L_n^E is semidefinite and has the same rank as the matrix L_n. The system $L_n^E w_n^E = f_n^E$ is solvable, but it has numerous different solutions. However, for two different solution $w_n^{E,1}$ and $w_n^{E,2}$,

$$T_n w_n^{E,1} = T_n w_n^{E,2} = u_n$$

holds, where u_n is the unique solution of the system $L_nu_n = f_n$. Therefore, it is sufficient to compute just one solution of the enlarged semidefinite system to obtain via T_n the unique solution of the system $L_nu_n = f_n$.

Now we consider the diagonally preconditioned CG method for the enlarged semidefinite system. A major task in the CG method is the computation of the residual

$$r_n^E = f_n^E - L_n^E w_n^E$$

of the semidefinite system for a given w_n^E. Using (3.55) we find

$$r_n^E = (T_n)^T f_n = (T_n)^T L_n (T_n) w_n^E = (T_n)^T (f_n - L_n u_n) = (T_n)^T r_n.$$

Let D_n^E be a diagonal matrix that we use as a preconditioner. With D_n^E-preconditioning we must compute $(r_n^E)^T D_n^E r_n^E$ in the preconditioned CG algorithm. Since $r_n^E = (T_n)^T r_n$ we find that

$$(r_n^E)^T D_n^E r_n^E = r_n^T T_n D_n^E (T_n)^T r_n.$$

Hence, the D_n^E-preconditioned CG algorithm for solving $L_n^E w_n^E = f_n^E$ is equivalent to the CG algorithm with preconditioner $T_n D_n^E (T_n)^T$ for solving $L_n u_n = f_n$.

Now consider the BPX-preconditioner (3.54). If we apply the preconditioner to the residual r_n we get

$$\widehat{\mathcal{C}}_n r_n = \sum_{l=0}^{n} \sum_{i=1}^{N_l} \sum_{j=1}^{3} 3^{2l} \langle r_n, B_{ij,l} \rangle B_{ij,l}.$$

This preconditioner can easily be expressed in terms of the enlarged linear system $L_n^E w_n^E = f_n^E$. Computation of the residual $r_n^E = f_n^E - L_n^E w_n^E$ produces

$$r_n^E = (T_n)^T r_n = \left(r^{(1)^T} \quad r^{(2)^T} \cdots \; r^{(n-1)^T} \quad r^{n^T} \right)^T,$$

where

$$(r^{(l)})_{3i+j} = \langle r_n, B_{ij,l} \rangle B_{ij,l}, \quad l = 0, \ldots, n.$$

The BPX-preconditioner resembles just a multiplication of the residual r_n^E with a diagonal matrix D_n^E where the diagonal entries are given by the scaling factors 3^{2l}. In [130] Yserentant suggested to replace the scaling factors 3^{2l} by $1/a(B_{ij,l}, B_{ij,l})$, which leads to the so-called multilevel diagonal scaling preconditioner. This preconditioner is further analyzed in [128, 133]. Multilevel diagonal scaling can be expected to work better in practice than BPX for non-model problems since it reflects more closely the properties of the problem. However, for elliptic problems with constant coefficients it is equivalent to BPX up to a constant multiple. In our implementation we have used the multilevel diagonal scaling.

Let us take a look at the condition numbers of the D_n^E-preconditioned semidefinite system. Of course, the conventional condition number is infinity because the matrix L_n^E is singular. In [61] it is shown that the condition numbers of the preconditioned enlarged and original systems are the same, provided that a generalized condition number is used that considers the preconditioned matrix restricted to the orthogonal complement of its null

space. In practice this means that the generalized condition number that we use is given by

$$\kappa((D_n^E)^{1/2} L_n^E (D_n^E)^{1/2}) = \lambda_{\max}/\lambda_{\min},$$

where $\lambda_{\max}$ denotes the largest eigenvalue of $(D_n^E)^{1/2} L_n^E (D_n^E)^{1/2}$ and $\lambda_{\min}$ its smallest non-zero eigenvalue, and

$$\kappa(\widehat{\mathcal{C}}_n^{1/2} \mathcal{A}_n \widehat{\mathcal{C}}_n^{1/2}) = \kappa((D_n^E)^{1/2} L_n^E (D_n^E)^{1/2})$$

holds.

For the hierarchical basis preconditioner we use a similar strategy. Denote by L_n^{HB} the stiffness matrix that uses only the basis functions in the hierarchical basis. Then

$$L_n^{HB} = (T_n^{HB})^T L_n T_n^{HB}$$

holds, with

$$T_n^{HB} = \begin{bmatrix} A_n & 0 \\ 0 & I \end{bmatrix} \begin{bmatrix} A_{n-1} & 0 \\ 0 & I \end{bmatrix} \cdots \begin{bmatrix} A_0 & 0 \\ 0 & I \end{bmatrix}.$$

Let us numerically solve the problem (1.16) with the right hand side f such that the exact solution u is given by $u(x,y) = (x(1-x)y(1-y))^2$. Table 3.4 shows the results. We have used a nested iteration conjugate gradient method to solve the problem, i.e., by means of an outer iteration loop going from a coarse resolution level to the finest resolution level $n_{\max}$ we compute the solution at each level with the conjugate gradient method and we use the solution obtained at the previous coarser level as an initial guess. At each level we stop the conjugate gradient iteration if the energy norm (H^2-norm) of the residual is proportional to the discretization error. By Theorem 2.6.2 we know that this discretization error measured in the H^2-norm is of $\mathcal{O}(h)$ with h the mesh size. In [35] arguments are given for the fact that nested iteration is an asymptotically optimal method in the sense that it provides the solution u at the finest resolution level $n_{\max}$ up to discretization error in an overall amount of $\mathcal{O}(N_{n_{\max}})$ operations, provided that an optimal preconditioner is used. The optimality of nested iteration combined with an optimal preconditioner is also explained in any good multigrid textbook.

The first column in Table 3.4 contains the resolution level n. Then we distinguish between the results for the BPX preconditioner and the results for the hierarchical basis preconditioner. For each preconditioner we display the spectral condition number κ of the system matrix for the linear system of equations that is solved. Moreover we show the H^2-norm of the residuals corresponding to the approximate solution, and the number of iterations that are needed on this level to reach discretization error accuracy.

	BPX			HB		
n	κ	residual	#	κ	residual	#iter
2	125.4	1.1066e-05	16	207.7	1.0121e-05	22
3	176.9	3.5235e-06	16	492.6	2.9262e-06	39
4	216.9	8.4733e-07	17	950.4	1.1454e-06	52
5	236.1	3.4569e-07	15	1584.6	3.9780e-07	79

Table 3.4: Iteration history for problem (1.16).

Remark 3.6.1. *Any basis for S_l that is stable in the sense of Definition 2.5.1 gives rise to an optimal BPX preconditioner and suboptimal HB preconditioner for* (1.16)*.*

Remark 3.6.2. *Computing the H^2-norm of the residual is easy. In fact we have that*

$$\begin{aligned}
\|u_n - u\|_{H^2} &\sim \|\mathcal{A}u_n - f\|_{(H^2)'} \\
&= \left\| \sum_{l=0}^{n} \sum_{i=1}^{N_l} \sum_{j=1}^{3} \langle B_{ij,l}, \mathcal{A}(u_l - u)\rangle B^*_{ij,l} \right\|_{(H^2)'} \\
&\sim \sum_{l=0}^{n} 3^{2l} \sum_{i=1}^{N_l} \sum_{j=1}^{3} |\langle B_{ij,l}, \mathcal{A}(u_l - u)\rangle|^2 \\
&= \sum_{l=0}^{n} 3^{2l} \sum_{i=1}^{N_l} \sum_{j=1}^{3} \left(\langle B_{ij,l}, \mathcal{A}u_l\rangle - \langle B_{ij,l}, f\rangle\right)^2 .
\end{aligned}$$

Here $\{B^*_{ij,l}\}_{ijl}$ is the dual frame to $\{B_{ij,l}\}_{ijl}$. The first equivalence is due to the ellipticity of the operator $\mathcal{A}$. The second equivalence is because the dual frame is a Riesz frame for the dual function space $\left(H^2\right)'$. The last expression is just the l_2 norm of the residual of the system (1.13) *with respect to the suitably normalized frame $\{B_{ij,l}\}_{ijl}$. This trick only works for elliptic PDEs, because the first equivalence above makes use of the ellipticity condition* (1.8)*.*

Chapter 4

A hierarchical basis of Lagrange type

4.1 Introduction

In the previous chapter we constructed a hierarchical basis by using the Hermite interpolant $\mathcal{I}_l$. Therefore the range of stability is restricted to values $s > 2$, since, by the Sobolev embedding theorem, this Hermite interpolant is only well defined for functions in $H^s(\Omega)$, $s > 2$, cfr. Lemma 3.4.4. With this in mind, the construction of hierarchical bases based on C^1 finite elements of *Lagrange type* instead of Hermite type should allow to enlarge the range of stability from $s \in (2, \frac{5}{2})$ to $s \in (1, \frac{5}{2})$. Recently Davydov and Stevenson [41] constructed such hierarchical Riesz bases for $H^s(\Omega), s \in (1, \frac{5}{2})$, based on a Lagrange type interpolation operator for C^1 piecewise cubic polynomials on certain triangulations obtained from checkerboard quadrangulations.

In this chapter we construct hierarchical Riesz bases for C^1 piecewise quadratic polynomials on Powell–Sabin triangulations. Inspired by the work of Davydov and Stevenson we look how we can extend the range of stability from $s \in (2, \frac{5}{2})$ to $s \in (1, \frac{5}{2})$ by using a Lagrange interpolation operator. While the construction of Davydov and Stevenson is rather technical, especially near the domain boundary, our construction is easier and straightforward. The work in this chapter is published in our paper [89].

In Section 4.2 we construct a Lagrange basis for the space of Powell–Sabin splines with homogeneous boundary conditions, and we prove that this basis is stable and local. Section 4.3 is devoted to the construction of a $H^s(\Omega)$ stable hierarchical basis for $s \in (1, \frac{5}{2})$. The corresponding hierarchical basis preconditioner is an optimal preconditioner for the model problem (1.16).

4.2 A stable local Lagrange-type basis for nested PS spline spaces

Let Ω be a domain in $\mathbb{R}^2$ with polygonal boundary for which there exists a conforming triangulation Δ_0 such that

(a) $\Omega = \bigcup_{T\in\Delta_0} T$,

(b) the intersection of any two different triangles in Δ_0 is either empty or a common edge or vertex,

(c) all interior vertices have degree six,

(d) all triangles in Δ_0 can be colored black and white in such a way that every interior vertex in Δ_0 belongs to exactly one black triangle.

Such a triangulation can be constructed for any domain with a polygonal boundary. First we create a so-called checkerboard quadrangulation [100] for Ω. This is a quadrangulation consisiting of quadrilaterals with largest interior angle less than π, and the quadrilaterals can be colored black and white in such a way that any two quadrilaterals sharing an edge have the opposite color. If we allow triangles at the boundary, see Figure 4.1, then such a checkerboard triangulation can always be constructed for a polygonal domain, see [41] for a proof. Note that all interior vertices in the checkerboard quadrangulation are of degree four. Next we construct a triangulation by adding the north-west south-east diagonal to each quadrilateral in the quadrangulation, see Figure 4.2. Note that all interior vertices have degree six. A suitable coloring can be obtained easily by applying a regular coloring pattern since, by construction, our triangulation has a "regular" pattern, i.e. looking closely at Figure 4.2 we see a distorted uniform triangulation. So construct a regular coloring pattern satisfying (d) for a uniform triangulation and apply that pattern to the constructed triangulation. Let Δ_1 be the triadic refinement of Δ_0, see Figure 3.2. It is trivially checked that Δ_1 still satisfies (a)–(d). By induction, each triangulation Δ_l satisfies the properties (a)–(d). We define $\Delta_l^\bullet$ as the subset of Δ_l consisting of the black triangles, and Δ_l° as $\Delta_l \setminus \Delta_l^\bullet$.

We are interested in the multiscale spaces $S_l \subset S_2^1(\Delta_l^{PS})$ satisfying homogeneous boundary conditions, i.e.

$$S_l := \left\{ s \in C^1(\overline{\Omega}) \mid s|_\tau \in \mathcal{P}_2 \text{ for all } \tau \in \Delta_l^{PS}, s = D_x s = D_y s = 0 \text{ on } \partial\Omega \right\}.$$

The spaces S_l are nested:

$$S_0 \subset S_1 \subset \cdots \subset S_l \subset \cdots .$$

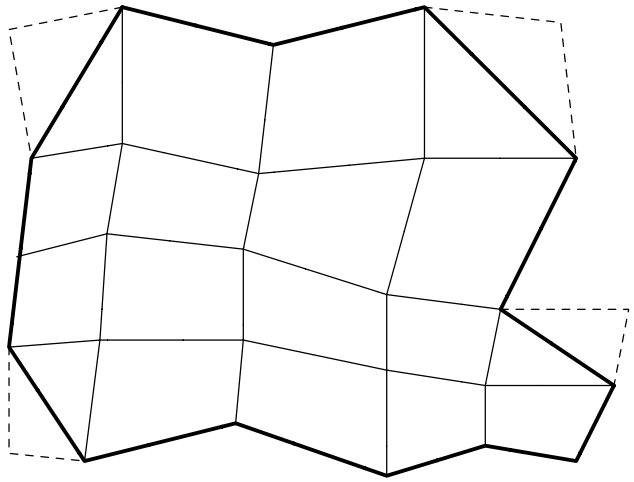

Figure 4.1: Checkerboard quadrangulation without coloring.

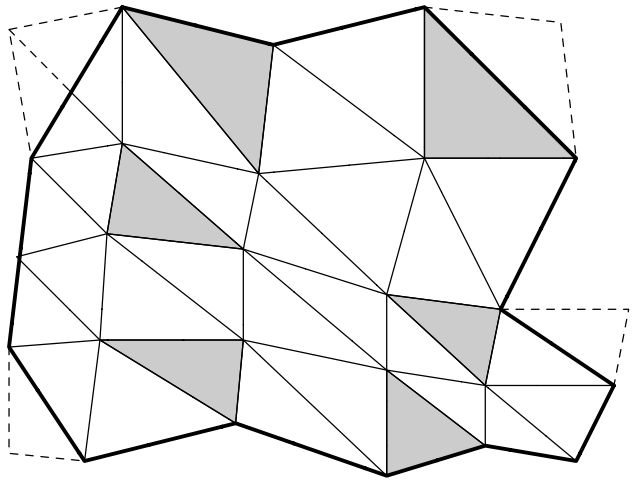

Figure 4.2: Construction of a suitable triangulation.

The remainder of this section is devoted to the construction of a suitable Lagrange basis for the spaces S_l.

For each interior vertex $V_i \in \Delta_l$ we have a corresponding triangle $T_{V_i} \in \Delta_l^\bullet$. Define $D_l(V_i)$ as the set $\{V_i, V_{ij}, V_{ik}\}$, with V_{ij} and V_{ik} chosen such that the triangle $T(V_i, V_{ij}, V_{ik})$ belongs to the triadic refinement of triangle $T_{V_i} \in \Delta_l^\bullet$, see Figure 4.3. Define Ξ_l as the union of all sets $D_l(V_i)$, i.e.

$$\Xi_l := \bigcup_{V_i \in \Delta_l \setminus \partial\Omega} D_l(V_i).$$

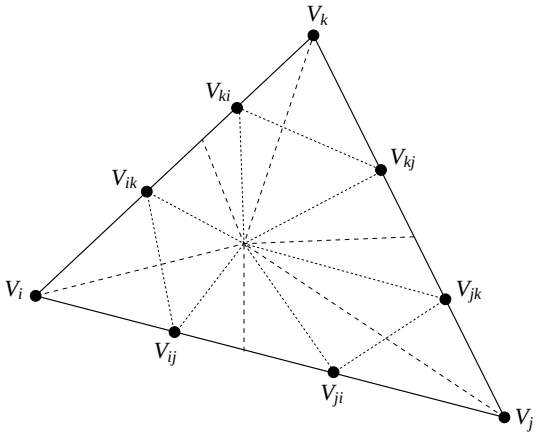

Figure 4.3: With each interior vertex $V_i \in \Delta_l$ we associate the set $D_l(V_i) := \{V_i, V_{ij}, V_{ik}\}$. The figure also depicts the sets $D_l(V_j) := \{V_j, V_{jk}, V_{ji}\}$ and $D_l(V_k) := \{V_k, V_{ki}, V_{kj}\}$ (assuming that V_j and V_k are interior vertices) .

Theorem 4.2.1. *The set Ξ_l is a Lagrange interpolation set for S_l, $l \geq 0$, i.e., for any arbitrary function f in $C^0(\Omega)$ there exists a unique spline $s \in S_l$ such that*

$$s(\xi) = f(\xi), \qquad \xi \in \Xi_l.$$

Moreover,

$$\|s\|_{L_\infty(T)} \lesssim \max\{|f(\xi)| \mid \xi \in \Xi_l \cap \mathrm{star}(T)\}, \qquad T \in \Delta_l, \tag{4.1}$$

with $\mathrm{star}(T)$ *the union of all triangles in Δ_l having at least one vertex in common with T. The bounding constant in (4.1) depends at most on the smallest angle in the triangulation Δ_l^{PS}.*

Proof. From the classical work of Powell and Sabin [107] we know that the dimension of the spline space $S_2^1(\Delta_l^{PS})$ equals $3N_l$ with N_l the number of vertices in Δ_l. Let $N_l = N_l^i \cup N_l^b$ with N_l^i the number of interior vertices and with N_l^b the number of boundary vertices. The spline spaces S_l satisfy homogeneous boundary conditions, therefore we find that $\dim S_l = 3N_l^i = \#\Xi_l$. Proving that the set Ξ_l is a Lagrange interpolation set is now equivalent to the statement that $s(\xi) = 0$, $\xi \in \Xi_l$, implies $s = 0$. So let s be in S_l with $s(\xi) = 0$ for all $\xi \in \Xi_l$.

Suppose that e is an edge of a triangle in $\Delta_l^\bullet$ that contains four interpolation points. Then, from the univariate theory, this set of four interpolation points on e is a Lagrange interpolation set for the space of quadratic C^1 spline on this edge e with one interior knot in e. Therefore, we find that $s|_e = 0$ holds for all edges e in Δ that contain exactly four Lagrange interpolation points.

Next, consider an edge e of a triangle in $\Delta_l^\bullet$ that contains only two interpolation points. Then one endpoint of this edge is on the boundary of the domain and we have homogeneous boundary conditions in this endpoint. Again, from the univariate theory, we find that $s|_e = 0$ holds. Similarly we find that $s|_e = 0$ for all edges e of the triangles in $\Delta_l^\bullet$ that do not contain any interpolation points.

We have now proven that $s|_e = 0$ for all edges $e \in \Delta_l^\bullet$. Therefore, we immediately deduce that the function value and the gradient of s vanish at all vertices in Δ_l, and the classical interpolation conditions of Powell and Sabin imply that $s = 0$.

Now we prove (4.1) in a similar way. From the univariate theory we find that

$$\|s\|_{L_\infty(e)} \lesssim \max\{|f(\xi)| \mid \xi \in \Xi_l \cap e\}$$

for each edge $e \in \Delta_l^\bullet$. Hence, because of the C^1 continuity conditions, (4.1) follows.

□

Next, we define the *Lagrange basis functions* $B_{\xi,l}$, $\xi \in \Xi_l$, for the space S_l. They are the unique solutions of the interpolation problem

$$B_{\xi,l}(\zeta) = \delta_{\xi,\zeta}, \quad \forall \xi, \zeta \in \Xi_l,$$

with $\delta_{\xi,\zeta}$ the Kronecker delta. By Theorem 4.2.1, this interpolation problem is well defined and the basis functions $B_{\xi,l}$ satisfy

$$\operatorname{supp} B_{\xi,l} \subset \operatorname{star}(T), \qquad \xi \in T \subset \Delta_l^\bullet,$$

and

$$\|B_{\xi,l}\|_{L_\infty(\Omega)} \sim 1.$$

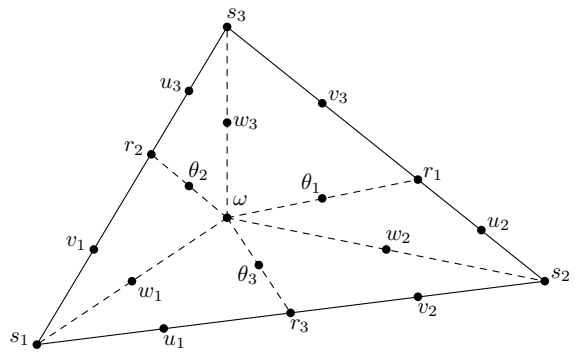

Figure 4.4: The Powell–Sabin macro-element.

It is a simple exercise to show that

$$\left\| \sum_{\xi \in \Xi_l} c_\xi B_{\xi,l} \right\|_{L_\infty(\Omega)} \sim \|\mathbf{c}\|_\infty . \tag{4.2}$$

Figure 4.5 depicts the typical forms of these Lagrange basis functions.

Define $A_{\xi,l}$ as the area of the support of the corresponding basis function $B_{\xi,l}$.

Theorem 4.2.2. *Let $s_l \in S_l$ be given by $\sum_{\xi \in \Xi_l} c_\xi B_{\xi,l} A_{\xi,l}^{-1/p}$, then for any $1 \le p \le \infty$ we have*

$$\|s_l\|_{L_p(\Omega)} \sim \|c\|_{l_p} := \left(\sum_{\xi \in \Xi_l} |c_\xi|^p \right)^{1/p} . \tag{4.3}$$

The constants of equivalence depend at most on the smallest angle in the triangulation Δ_l^{PS}.

Proof. For $p = \infty$ the normalization factor $A_{\xi,l}^{-1/p}$ equals one and we find (4.2). Next, we treat the case $1 \le p < \infty$. Choose a triangle $T \in \Delta_l$ and let $I_T := \{\xi \mid \operatorname{supp} B_{\xi,l} \cap T \neq 0\}$. Let $1/p + 1/q = 1$, then by Hölder's inequality

$$\begin{aligned} \int_T |s_l|^p \, d\omega &= \int_T \left| \sum_{\xi \in I_T} c_\xi B_{\xi,l} A_{\xi,l}^{-1/p} \right|^p d\omega \\ &\le \sum_{\xi \in I_T} |c_\xi|^p \int_T \left(\sum_{\xi \in I_T} B_{\xi,l}^q A_{\xi,l}^{-q/p} \right)^{p/q} d\omega. \end{aligned}$$

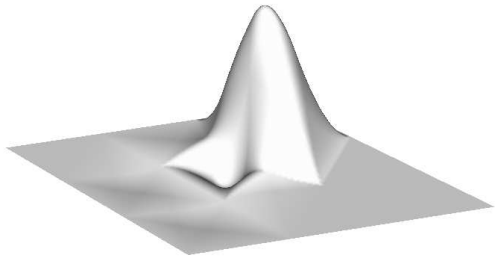

(a)

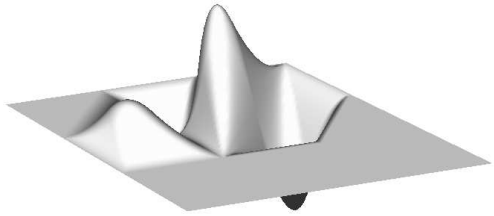

(b)

Figure 4.5: (a) Basis function $B_{\xi,l}$ with ξ corresponding to a vertex in Δ_l. (b) Basis function $B_{\xi,l}$ with ξ corresponding to a vertex in $\Delta_{l+1} \setminus \Delta_l$.

Since $\#I_T \leq 9$ and $B_{\xi,l}$ is uniformly bounded by a constant C

$$\int_T |s_l|^p \, d\omega \leq C^p 9^{p/q} \max_{\xi \in I_T} \frac{\mathrm{vol}(T)}{A_{\xi,l}} \sum_{\xi \in I_T} |c_\xi|^p \leq C^p 9^p \sum_{\xi \in I_T} |c_\xi|^p \, .$$

We sum over all triangles $T \in \Delta_l$. A certain c_ξ can appear more than once on the right-hand side and the number of times it appears can be bounded by the maximum number of triangles in the support of $B_{\xi,l}$. We find

$$\|s_l\|_{L_p(\Omega)} = \left(\sum_{T \in \Delta_l} \int_T |s_l|^p d\omega \right)^{1/p} \lesssim \left(\sum_{\xi \in \Xi_l} |c_\xi|^p \right)^{1/p} ,$$

which proves the upper bound in (4.3).

To prove the lower bound, we use the fact that all norms on a finite dimensional vector space are equivalent (in our case this is the finite dimensional space of bivariate polynomials of degree 2). Consider a triangle

$T \in \Delta_l$ and the standard simplex $T_s := \{(x,y) \mid 0 \le x,y \le 1, x+y \le 1\}$. We know that $\|s_l\|_{L_\infty(T_s)} \lesssim \|s_l\|_{L_p(T_s)}$ and therefore $\|s_l\|_{L_\infty(T)} \lesssim \mathrm{vol}(T)^{-1/p} \|s_l\|_{L_p(T)}$. Note that from (4.2)

$$\|s_l\|_{L_\infty(T)} \sim \max_{\xi \in I_T} \left| c_\xi A_{\xi,l}^{-1/p} \right|,$$

therefore

$$\begin{aligned} \sum_{\xi \in I_T} |c_\xi|^p &\le \max_{\zeta \in I_T} A_{\zeta,l} \sum_{\xi \in I_T} \left| c_\xi A_{\xi,l}^{-1/p} \right|^p \le 9 \max_{\zeta \in I_T} A_{\zeta,l} \max_{\xi \in I_T} \left| c_\xi A_{\xi,l}^{-1/p} \right|^p \\ &\lesssim \max_{\zeta \in I_T} A_{\zeta,l} \|s_l\|_{L_\infty(T)}^p \lesssim \max_{\zeta \in I_T} \frac{A_{\zeta,l}}{\mathrm{vol}(T)} \|s_l\|_{L_p(T)}^p \end{aligned}$$

From similar reasoning as in the proof of Lemma 2.5.6 we easily deduce that $\max_{\zeta \in I_T} \frac{A_{\zeta,l}}{\mathrm{vol}(T)} \lesssim 1$. Summing over all triangles $T \in \Delta_l$ yields

$$\sum_{\xi \in \Xi_l} |c_\xi|^p \le \sum_{T \in \Delta_l} \sum_{\xi \in I_T} |c_\xi|^p \lesssim \|s_l\|_{L_p(\Omega)}^p$$

which proves the lower bound in (4.3). □

4.3 C^1 hierarchical Riesz bases for $H_0^s(\Omega)$ with $s \in (1, \frac{5}{2})$

In the previous section we constructed a hierarchical basis of Lagrange type on arbitrary polygonal domains and we derived some stability results at most depending on the smallest angle in the underlying triangulation Δ_l^{PS}. We now assume that the nested sequences (3.2) and (3.3) are regular.

Let us introduce the interpolant operator $\mathcal{L}_l : C^0(\Omega) \to S_l$ that is defined as

$$\mathcal{L}_l f := \sum_{\xi \in \Xi_l} f(\xi) B_{\xi,l}. \tag{4.4}$$

It is obvious that this operator returns the unique spline function in S_l that interpolates the given function f at the positions of the $\xi \in \Xi_l$. We show that this operator is suitable for constructing a multiresolution analysis in the sense of Definition 3.3.1.

As Banach space $\mathcal{B}$ we take $C_0^0(\Omega)$, the space of C^0 continuous functions that vanish on $\partial\Omega$, and its associated norm is the L_∞ norm. By Theorem 4.2.2 for $p = \infty$ and (4.4), we get $\|\mathcal{L}_l f\|_{L_\infty(\Omega)} \lesssim \|f\|_{L_\infty(\Omega)}$, so the operator $\mathcal{L}_l$ is uniformly bounded in $C_0^0(\Omega)$. Proving that the spaces S_l are dense in

$C_0^0(\Omega)$ is equivalent to proving that $\lim_{l\to\infty} \|f - \mathcal{L}_l f\|_{L_\infty(\Omega)} = 0$. Let (x, y) be an arbitrary point in triangle $T \in \Delta_l^\bullet$ with $T \cap \partial\Omega = \emptyset$. Then

$$\begin{aligned} |f(x,y) - \mathcal{L}_l f(x,y)| &= |f(x,y) \sum_{\xi\in\Xi_l} B_{\xi,l}(x,y) - \sum_{\xi\in\Xi_l} f(\xi) B_{\xi,l}(x,y)| \\ &= |\sum_{\xi\in\Xi_l} (f(x,y) - f(\xi)) B_{\xi,l}(x,y)|, \end{aligned}$$

and, provided that $B_{\xi,l}(x,y) \neq 0$, $f(x,y) - f(\xi)$ goes to zero as $l \to \infty$ because f is continuous. Similar arguments hold when $T \cap \partial\Omega \neq \emptyset$ or when $T \in \Delta_l^\circ$, so the spaces S_l are dense in $C_0^0(\Omega)$. The last property, $\mathcal{L}_l\mathcal{L}_{l+1} = \mathcal{L}_l$, follows immediately from the fact that the sets Ξ_l are nested, i.e.

$$\Xi_0 \subset \Xi_1 \subset \cdots \subset \Xi_l \subset \cdots .$$

Since for $l \geq 0$, the sets $\{B_{l,\xi} \mid \xi \in \Xi_l \setminus \Xi_{l-1}\}$ are L_∞-stable bases for the spaces $\mathrm{Im}(\mathcal{L}_l - \mathcal{L}_{l-1})$, we find that $\bigcup_{l=0}^\infty \{B_{l,\xi} \mid \xi \in \Xi_l \setminus \Xi_{l-1}\}$ is a weakly L_∞-stable hierarchical basis for $C_0^0(\Omega)$. The remainder of this section is devoted to the proof of the fact that

$$\bigcup_{l=0}^{\infty} \left\{ 3^{(1-s)l} B_{\xi,l} \mid \xi \in \Xi_l \setminus \Xi_{l-1} \right\}$$

is a strongly stable Riesz basis for $H_0^s(\Omega)$ for any $s \in (1, \frac{5}{2})$. The operators $\mathcal{L}_l$ will be essential tools. Note that, by the Sobolev embedding theorem, $\mathcal{L}_l$ is only well defined on $H_0^s(\Omega)$ given that $s > 1$.

Lemma 4.3.1. *For each $f \in H_0^s(\Omega)$, $s > 1$, and arbitrary $p > 0$ we have that*

$$\|f - \mathcal{L}_l f\|_{L_p(\Omega)} \to 0 \quad \textit{as} \quad l \to \infty.$$

Proof. Suppose that $1 < s < 2$. Let (x, y) be some arbitrary point in triangle $T \in \Delta_l$. A simple calculation yields

$$|f(x,y) - \mathcal{L}_l f(x,y)| \lesssim \|f\|_{L_\infty(T)} .$$

Then the Bramble–Hilbert lemma [10] (Lemma 2.6.1) and Theorem 7.58 in [1] imply

$$|f(x,y) - \mathcal{L}_l f(x,y)| \lesssim 3^{-l(s-1)} |f|_{H^s(T)} .$$

Using (3.4), we get

$$\begin{aligned} \|f - \mathcal{L}_l f\|_{L_p(T)} &= \left(\int_T |f(x,y) - \mathcal{L}_l f(x,y)|^p \, dxdy \right)^{1/p} \\ &\lesssim 3^{-l(s-1)} |f|_{H^s(T)} 3^{-2l/p}, \end{aligned}$$

and some elementary calculations yield

$$\|f - \mathcal{L}_l f\|_{L_p(\Omega)} \lesssim 3^{-l(s-1+2/p)} \, |f|_{H^s(\Omega)} .$$

The case $s = 2$ can be proven using the same techniques, and the case $s > 2$ follows from the fact that $H^s(\Omega) \subset H^{s-1}(\Omega)$. □

From Lemma 4.3.1 we know that each function $f \in H_0^s(\Omega)$, $s > 1$, can be decomposed as

$$f = \sum_{l=0}^{\infty} g_l, \qquad g_l \in S_l,$$

in the sense of L_p. Moreover, we can use the decomposition

$$f = \sum_{l=0}^{\infty} (\mathcal{L}_l - \mathcal{L}_{l-1}) f,$$

with $\mathcal{L}_{-1} := 0$.

Recall Proposition 3.4.7. Using the norm equivalence (3.28) we can now prove the following theorem, which is essentially the same as Theorem 3.4.8. The proof is inspired by the work in [36] and [41].

Theorem 4.3.2. *For any $s \in (1, \frac{5}{2})$, it holds that*

$$\|f\|^2_{H^s(\Omega)} \sim \sum_{l=0}^{\infty} 3^{2ls} \|(\mathcal{L}_l - \mathcal{L}_{l-1}) f\|^2_{L_2(\Omega)}, \qquad f \in H_0^s(\Omega).$$

Proof. Because of the norm equivalence (3.28) it is sufficient to prove that

$$\inf_{g_l \in S_l : f = \sum_l g_l} \sum_{l=0}^{\infty} 3^{2ls} \|g_l\|^2_{L_2(\Omega)} \sim \sum_{l=0}^{\infty} 3^{2ls} \|(\mathcal{L}_l - \mathcal{L}_{l-1}) f\|^2_{L_2(\Omega)}.$$

Since $(\mathcal{L}_l - \mathcal{L}_{l-1}) f \in S_l$ and $\sum_{l=0}^{\infty} (\mathcal{L}_l - \mathcal{L}_{l-1}) f = f$ the inequality "$\lesssim$" is trivial and we will concentrate on the inequality "$\gtrsim$". Let $f = \sum_{l=0}^{\infty} g_l$ with $g_l \in S_l$. Since the operators $\mathcal{L}_l$ are projectors and the spaces S_l are nested, we have $(\mathcal{L}_l - \mathcal{L}_{l-1}) S_n = 0$ when $n \leq l - 1$. Moreover the operators $\mathcal{L}_l$ also satisfy

$$\|\mathcal{L}_l s_n\|_{L_2(\Omega)} \lesssim 3^{n-l} \|s_n\|_{L_2(\Omega)}, \quad s_n \in S_n. \tag{4.5}$$

Indeed, from the construction of $\mathcal{L}_l$ and (3.4) we easily get

$$\|\mathcal{L}_l s_n\|_{L_\infty(T)} \lesssim \|s_n\|_{L_\infty(T)}, \quad T \in \Delta_l.$$

Then (4.5) can be deduced by using (4.2) and Theorem 4.2.2.

From the properties above and the Cauchy–Schwarz inequality we have

$$\begin{aligned}
&\sum_{n,n'=0}^{\infty}\sum_{l=0}^{\infty} 3^{2ls}\langle(\mathcal{L}_l-\mathcal{L}_{l-1})g_n,(\mathcal{L}_l-\mathcal{L}_{l-1})g_{n'}\rangle_{L_2(\Omega)}\\
&\quad=\sum_{n,n'=0}^{\infty}\sum_{l=0}^{\min\{n,n'\}} 3^{2ls}\langle(\mathcal{L}_l-\mathcal{L}_{l-1})g_n,(\mathcal{L}_l-\mathcal{L}_{l-1})g_{n'}\rangle_{L_2(\Omega)}\\
&\quad\le\sum_{n,n'=0}^{\infty}\sum_{l=0}^{\min\{n,n'\}} 3^{2ls}\left(\|\mathcal{L}_l g_n\|_{L_2(\Omega)}+\|\mathcal{L}_{l-1}g_n\|_{L_2(\Omega)}\right)\\
&\qquad\qquad\cdot\left(\|\mathcal{L}_l g_{n'}\|_{L_2(\Omega)}+\|\mathcal{L}_{l-1}g_{n'}\|_{L_2(\Omega)}\right)\\
&\quad\lesssim\sum_{n,n'=0}^{\infty}\sum_{l=0}^{\min\{n,n'\}} 3^{2ls}3^{n+n'-2l}\|g_n\|_{L_2(\Omega)}\|g_{n'}\|_{L_2(\Omega)}.
\end{aligned}$$

The last expression can be rewritten as

$$\sum_{n,n'=0}^{\infty}\sum_{l=0}^{\min\{n,n'\}} 3^{(s-1)(2l-n-n')}(3^{ns}\|g_n\|_{L_2(\Omega)})(3^{n's}\|g_{n'}\|_{L_2(\Omega)}),$$

which is equivalent to

$$\sum_{n,n'=0}^{\infty} 3^{(s-1)(2\min\{n,n'\}-n-n')}(3^{ns}\|g_n\|_{L_2(\Omega)})(3^{n's}\|g_{n'}\|_{L_2(\Omega)}).$$

The factor $3^{(s-1)(2\min\{n,n'\}-n-n')}$ becomes very small if $|n-n'|\gg 0$. In fact, the infinite matrix $[3^{(s-1)(2\min\{n,n'\}-n-n')}]_{n,n'\in\mathbb{N}}$ defines a bounded mapping on l_2. Therefore

$$\begin{aligned}
&\sum_{n,n'=0}^{\infty} 3^{(s-1)(2\min\{n,n'\}-n-n')}(3^{ns}\|g_n\|_{L_2(\Omega)})(3^{n's}\|g_{n'}\|_{L_2(\Omega)})\\
&\qquad\lesssim\sum_{n=0}^{\infty}3^{2ns}\|g_n\|^2_{L_2(\Omega)}.
\end{aligned}$$

Since the splitting $f=\sum_{l=0}^{\infty}g_l$ was arbitrary, we have derived that

$$\begin{aligned}
&\inf_{g_l\in S_l:f=\sum_l g_l}\sum_{n,n'=0}^{\infty}\sum_{l=0}^{\infty}3^{2ls}\langle(\mathcal{L}_l-\mathcal{L}_{l-1})g_n,(\mathcal{L}_l-\mathcal{L}_{l-1})g_{n'}\rangle_{L_2(\Omega)}\\
&\qquad\lesssim\inf_{g_l\in S_l:f=\sum_l g_l}\sum_{n=0}^{\infty}3^{2ns}\|g_n\|^2_{L_2(\Omega)}.
\end{aligned}$$

Because $f \in A_2^s(L_2(\Omega))$ (Proposition 3.4.7) we know that the right expression is bounded. Then from the derivation made above it follows that the left expression is absolutely convergent and we are allowed to write that

$$\begin{aligned}
&\inf_{g_l \in S_l : f = \sum_l g_l} \sum_{n,n'=0}^{\infty} \sum_{l=0}^{\infty} 3^{2ls} \langle (\mathcal{L}_l - \mathcal{L}_{l-1}) g_n, (\mathcal{L}_l - \mathcal{L}_{l-1}) g_{n'} \rangle_{L_2(\Omega)} \\
&= \inf_{g_l \in S_l : f = \sum_l g_l} \sum_{l=0}^{\infty} \sum_{n,n'=0}^{\infty} 3^{2ls} \langle (\mathcal{L}_l - \mathcal{L}_{l-1}) g_n, (\mathcal{L}_l - \mathcal{L}_{l-1}) g_{n'} \rangle_{L_2(\Omega)} \\
&= \sum_{l=0}^{\infty} 3^{2ls} \| (\mathcal{L}_l - \mathcal{L}_{l-1}) f \|_{L_2(\Omega)}^2 .
\end{aligned}$$

We conclude that

$$\sum_{l=0}^{\infty} 3^{2ls} \| (\mathcal{L}_l - \mathcal{L}_{l-1}) f \|_{L_2(\Omega)}^2 \lesssim \inf_{g_l \in S_l : f = \sum_l g_l} \sum_{l=0}^{\infty} 3^{2ls} \| g_l \|_{L_2(\Omega)}^2 .$$

□

Since, by Theorem 4.2.2, the subsets $\left\{ 3^l B_{\xi,l} \mid \xi \in \Xi_l \setminus \Xi_{l-1} \right\}$ form an L_2-stable Riesz basis for $\mathrm{Im}(\mathcal{L}_l - \mathcal{L}_{l-1})$, we find from Theorem 4.3.2 that

$$\begin{aligned}
\| f \|_{H^s(\Omega)}^2 &\sim \sum_{l=0}^{\infty} 3^{2ls} \left\| \sum_{\xi \in \Xi_l \setminus \Xi_{l-1}} c_\xi 3^l B_{\xi,l} \right\|_{L_2(\Omega)}^2 \\
&\sim \sum_{l=0}^{\infty} 3^{2ls} \sum_{\xi \in \Xi_l \setminus \Xi_{l-1}} |c_\xi|^2 .
\end{aligned}$$

Hence,

$$\left\| \sum_{l=0}^{\infty} \sum_{\xi \in \Xi_l \setminus \Xi_{l-1}} c_\xi 3^{l(1-s)} B_{\xi,l} \right\|_{H^s(\Omega)}^2 \sim \sum_{l=0}^{\infty} \sum_{\xi \in \Xi_l \setminus \Xi_{l-1}} |c_\xi|^2, \quad s \in (1, \frac{5}{2}). \tag{4.6}$$

This result immediately implies that, by the theory from Section 1.2, the corresponding hierarchical basis preconditioner is optimal for fourth order elliptic equations.

Remark 4.3.3. *A local Lagrange interpolating scheme on Powell–Sabin triangulations was developed in [101] which is similar to our construction. The construction in [101] was not placed in a multiresolution context, but a similar reasoning as above can be applied. The basis functions in [101] have*

a larger support sometimes, but, on the other hand, their construction holds for arbitrary initial triangulations Δ_0. By merging the approach described above and the approach in [101] one can easily create a hierarchical basis starting from an arbitrary initial triangulation Δ_0 that is stable with respect to the norm in $H^s(\Omega)$ for all $s \in (1, \frac{5}{2})$.

Remark 4.3.4. *As already mentioned in the introduction, experience in the second-order case shows that often the BPX scheme is superior to most HB and wavelet schemes derived from the same MRA, and equally cheap in its implementation. There is no implementation of this HB-type preconditioner, but a similar picture would probably emerge when compared to the BPX preconditioner.*

Chapter 5

Optimal wavelet preconditioners

5.1 Introduction

In recent years wavelets have become a well-appreciated discretization tool for solving elliptic variational problems, see, e.g., [21, 24, 29, 33, 65, 71, 105]. In this chapter we present a general construction method for wavelets on arbitrary domains that are suitable for preconditioning systems arising from elliptic variational problems.

Section 5.2 gives a short overview of the principles of multiresolution analysis and lifting [40, 121, 122, 123]. Furthermore we explain how wavelets can be created on arbitrary domains and we discuss the design of the second lifting step, the update, in detail, which is joint work with colleague Evelyne Vanraes and published in our paper [125]. Section 5.3 contains theoretic material to investigate the Riesz basis property in the Sobolev space $H^s(\mathbb{R}^d)$ of a given hierarchical system. Crucial here is the derivation of the smoothness of the dual system. In order to be able to use Fourier techniques we will only consider the shift-dilation invariant setting of a multiresolution analysis, although realistic applications require other settings. Recently there has been a growing interest in the numerical computation of the smoothness of refinable functions (or function vectors), see, e.g., [22, 39, 67, 108] and references therein. However, a necessary condition in those papers is that the refinable functions (vectors) exist in L_2. From [121] it appears that the duals arising from the lifting scheme do not necessarily satisfy this condition: it is possible that they only exist in distributional sense in L_2. This difficulty was dealt with by Lorentz and Oswald for the single function refinable case. In their paper [82] they provide sharp stability estimates

for systems where the duals do not belong to L_2. Our main result in this section is Theorem 5.3.4 which extends the result of Lorentz and Oswald to refinable function vectors, and it is published in our paper [88]. In Section 5.4 we explicitly construct wavelets using the method from Section 5.2 and we investigate their stability using the theoretical framework from Section 5.3. Piecewise linear and quadratic spline wavelets are treated in one or two dimensions. Furthermore we numerically compare the constructed wavelet systems to standard finite element hierarchical bases. These numerical experiments confirm the theory. Then, in Section 5.5, we briefly discuss a strategy to construct stable wavelets on uniform grids. Using this strategy we find connections with other constructions in the literature. Finally, in Section 5.6, we give an explicit construction of compactly supported Powell–Sabin spline prewavelets on the uniform hexagonal grid, see our paper [87]. The obtained prewavelet basis is stable in the Sobolev spaces $H^s(\Omega)$ for $|s| < \frac{5}{2}$, see, e.g., [104].

5.2 Multiscale decomposition on non-uniform grids

Let Ω be a bounded polygonal domain in $\mathbb{R}^d$ or $\mathbb{R}^d$ itself, with d the spatial dimension, and suppose that we are given a sequence $S_0 \subset S_1 \subset S_2 \subset \cdots \subset L_2(\Omega)$ of closed spline subspaces S_l of $L_2(\Omega)$ where each S_l has the form $S_l = \text{span}\{\phi_{k,l} | k \in I_l\}$, and we refer to the spline functions $\phi_{k,l}$ as *scaling functions*. It will be convenient to use matrix notation. Define $\boldsymbol{\phi}_l$ as the row vector of all scaling functions $\phi_{k,l}$, $k \in I_l$. We assume that the scaling functions form an L_2 Riesz basis for S_l, i.e.

$$\|\boldsymbol{\phi}_l c\|_{L_2}^2 \sim c^T c. \tag{5.1}$$

Because the spaces S_l are nested there exists a subdivision matrix A_l such that $\boldsymbol{\phi}_l = \boldsymbol{\phi}_{l+1} A_l$. Such a subdivision matrix A_l can be written in block matrix form as

$$A_l = \begin{bmatrix} O_l \\ N_l \end{bmatrix}.$$

We distinguish a part O_l that computes the coefficients of the basis functions on the finer grid associated with old vertices, and a part N_l that computes the coefficients of the basis functions on the finer grid associated with new vertices. Each space S_{l+1} contains splines on a finer grid than the previous coarser space S_l and therefore can describe more detail of a surface. These details are captured in an algebraic complement W_l such that $S_l \oplus W_l = S_{l+1}$. We will refer to the basis functions of W_l as *wavelets* and we denote $\boldsymbol{\psi}_l$ as the row vector of all wavelets that span W_l. The relation between $\boldsymbol{\psi}_l$

and $\boldsymbol{\phi}_{l+1}$ is given by a filter B_l , i.e. $\boldsymbol{\psi}_l = \boldsymbol{\phi}_{l+1} B_l$. In order to go from a coarse grid to a finer grid we use a regular refinement. This implies that there exists a constant ρ such that $\mathrm{diam}(\mathrm{supp}\, \phi_{k,l}) \sim \rho^{-j}$. Typically we have $\rho = 2$ (dyadic refinement).

The main idea is to start with a hierarchical basis and apply a local correction process on the scaling functions at each level in order to achieve certain stability properties (1.14) for the wavelets. This technique fits in the framework of both the *lifting scheme* [122] and the *stable completion technique* [14]. We split $\boldsymbol{\phi}_{l+1}$ in functions $\boldsymbol{\phi}^o_{l+1}$ associated with old grid points and functions $\boldsymbol{\phi}^n_{l+1}$ associated with new grid points when going from S_l to S_{l+1}, i.e.

$$\boldsymbol{\phi}_{l+1} = [\boldsymbol{\phi}^o_{l+1} \quad \boldsymbol{\phi}^n_{l+1}].$$

The wavelets $\boldsymbol{\psi}_l$ are then initially defined as $\boldsymbol{\phi}^n_{l+1}$, and

$$B_l = \begin{bmatrix} 0 \\ I \end{bmatrix}.$$

We have now made a choice for the complement space W_l. This construction gives us a set of biorthogonal filter operators $\{A_l, B_l, \widetilde{A}_l, \widetilde{B}_l\}$ such that

$$\begin{aligned} [\boldsymbol{\phi}_l \quad \boldsymbol{\psi}_l] &= \boldsymbol{\phi}_{l+1}[A_l \quad B_l], \\ [\boldsymbol{\phi}_l \quad \boldsymbol{\psi}_l] \begin{bmatrix} \widetilde{A}_l \\ \widetilde{B}_l \end{bmatrix} &= \boldsymbol{\phi}_{l+1}, \\ \begin{bmatrix} \widetilde{A}_l \\ \widetilde{B}_l \end{bmatrix} [A_l \quad B_l] &= I. \end{aligned} \tag{5.2}$$

We also find dual scaling functions $\widetilde{\boldsymbol{\phi}}_l$ (that mainly consist of Dirac distributions and differential operators) and dual wavelets $\widetilde{\boldsymbol{\psi}}_l$ satisfying

$$[\widetilde{\boldsymbol{\phi}}_l \quad \widetilde{\boldsymbol{\psi}}_l] = \widetilde{\boldsymbol{\phi}}_{l+1}[\widetilde{A}_l^T \quad \widetilde{B}_l^T], \tag{5.3}$$

and they are biorthogonal in the sense that

$$\begin{aligned} &\langle \widetilde{\phi}_{k,l}, \phi_{k',l} \rangle = \delta_{k,k'}, \quad &&\langle \widetilde{\psi}_{m,l}, \psi_{m',l} \rangle = \delta_{m,m'}, \\ &\langle \widetilde{\phi}_{k,l}, \psi_{m,l} \rangle = 0, &&\langle \widetilde{\psi}_{m,l}, \phi_{k,l} \rangle = 0. \end{aligned} \tag{5.4}$$

As discussed before it can be desirable to have another complement space with certain properties. The new wavelet functions can be found by projecting the $\boldsymbol{\phi}^n_{l+1}$ into the desired complement space W_l along S_l, i.e. $\boldsymbol{\psi}_l = \boldsymbol{\phi}^n_{l+1} - \boldsymbol{\phi}_l C_l$. For each wavelet function there is a corresponding column in the *lifting matrix* C_l. The possibly nonzero entries in this column together will be called the *stencil* for that wavelet function. Note that if

there are no zero entries in C_l, the wavelets will have the whole domain Ω as their support.

The *semiorthogonal* construction orthogonalizes the new basis functions $\boldsymbol{\psi}_l$ to S_l. The lifting matrix C_l is found as the solution of the linear system $C_l = \langle \boldsymbol{\phi}_l, \boldsymbol{\phi}_l \rangle^{-1} \langle \boldsymbol{\phi}_l, \boldsymbol{\phi}_{l+1} \rangle$. Although this construction process produces a stable multiscale basis, the wavelets are not practically useful because they are globally supported on Ω. However, the semiorthogonal lifting matrix has exponential off-diagonal decay [113, Lemma 5.2]. This motivates the use of *local semiorthogonalization* [83]. This construction method fixes the stencil in advance in order to have local support for the wavelet functions. Hence, a wavelet function on a new grid point is updated by the scaling functions of some neighbouring old grid points. The lifting matrix orthogonalizes the wavelets to their predefined set of scaling functions. Unfortunately this method does not yield stable multiscale bases. Hereto we need at least one *vanishing moment*, which implies that the dual scaling functions reproduce constants, a necessary condition for stability [112]. This leads to an overdetermined system because we do not have sufficient degrees of freedom. However, as already briefly mentioned in [83], enforcing a vanishing moment is easy. During the partial orthogonalization process, one simply adds a linear constraint that forces the wavelet to have a vanishing moment. This will be our approach here. Once the lifting matrix is chosen we find a new set of biorthogonal filter operators $\{A_l, B_l - A_l C_l, \widetilde{A}_l + C_l \widetilde{B}_l, \widetilde{B}_l\}$ satisfying similar relations as above.

Theorem 5.2.1. *Suppose that the scaling functions satisfy $\phi_{k,l} \geq 0$ for all k, l. Then for each level l, the set of wavelets $\boldsymbol{\psi}_l$ that have one vanishing moment and are as orthogonal as possible in a least squares sense with respect to the scaling functions in their predefined update stencil, forms an L_2 Riesz basis of W_l.*

Proof. Denote the one level wavelet transform filters as M_l, i.e.

$$[\boldsymbol{\phi}_l \quad \boldsymbol{\psi}_l] = \boldsymbol{\phi}_{l+1} M_l.$$

We show that $\|M_l\|_2, \|M_l^{-1}\|_2 = \mathcal{O}(1)$, uniformly in l. Then, by (5.1), the theorem follows. The filters M_l and M_l^{-1} can be factored as

$$M_l = \begin{bmatrix} O_l & 0 \\ 0 & I \end{bmatrix} \cdot \begin{bmatrix} I & 0 \\ N_l & I \end{bmatrix} \cdot \begin{bmatrix} I & -C_l \\ 0 & I \end{bmatrix}$$

and

$$M_l^{-1} = \begin{bmatrix} I & C_l \\ 0 & I \end{bmatrix} \cdot \begin{bmatrix} I & 0 \\ -N_l & I \end{bmatrix} \cdot \begin{bmatrix} O_l^{-1} & 0 \\ 0 & I \end{bmatrix}.$$

Hence it is sufficient to prove that $\|C_l\|_2, \|N_l\|_2, \|O_l\|_2, \|O_l^{-1}\|_2 = \mathcal{O}(1)$. Because of (5.1) one can show, using results from [14], that $\|N_l\|_2, \|O_l\|_2, \|O_l^{-1}\|_2 =$

$\mathcal{O}(1)$. It remains to check whether the update is stable, i.e. $\|C_l\|_2 = \mathcal{O}(1)$. For band matrices with uniformly bounded bandwidth, the 1-norm and the 2-norm are equivalent uniformly in the dimensions of the matrix. Therefore it is sufficient to show that $\|C_l\|_1 \sim \max_{ij} |(C_l)_{ij}|$ is uniformly bounded. Let us focus on the update of a particular wavelet function $\psi_{m,l}$, where m represents a new grid point. The update involves a set of neighbouring scaling functions corresponding to old grid points. Let us denote these scaling functions by $\{\phi_{k,l} | k \in U_m\}$ with U_m an index set representing the old grid points and U_m satisfies by construction $\#U_m \lesssim 1$. Define the Gram matrix G as $G := (\langle \phi_{k_1,l}, \phi_{k_2,l} \rangle_{L_2})_{k_1,k_2 \in U_m}$. The update step solves the following overdetermined system

$$G \cdot c = b \quad \text{with} \quad b = (\langle \phi_{k,l}, \phi_{m,l+1} \rangle_{L_2})_{k \in U_m},$$

$$(\langle 1, \phi_{k,l} \rangle_{L_2})_{k \in U_m} c = \langle 1, \phi_{m,l+1} \rangle_{L_2}$$

in a constrained least squares sense such that the vanishing moment condition is satisfied. Hence the column vector c, that is part of the lifting matrix C_l, satisfies

$$\begin{aligned} &G \cdot c = b + \epsilon \quad \text{with } \epsilon \text{ the least squares error,} \\ &(\langle 1, \phi_{k,l} \rangle_{L_2})_{k \in U_m} c = \langle 1, \phi_{m,l+1} \rangle_{L_2}. \end{aligned} \tag{5.5}$$

Suppose that $\{\phi^*_{k,l} | k \in U_m\}$ is a dual base for $\{\phi_{k,l} | k \in U_m\}$, i.e.

$$\langle \phi^*_{k_1,l}, \phi_{k_2,l} \rangle_{L_2} = \delta_{k_1,k_2},$$

and suppose that $\phi^*_{k,l} =: \sum_{n \in U_m} b_{k,n} \phi_{n,l}$, then $G^{-1} = (b_{k,n})_{k,n \in U_m}$ and

$$\|\phi^*_{k,l}\|^2_{L_2} = \langle \phi^*_{k,l}, \phi^*_{k,l} \rangle_{L_2} = \left\langle \phi^*_{k,l}, \sum_{n \in U_m} b_{k,n} \phi_{n,l} \right\rangle_{L_2} = b_{k,k}. \tag{5.6}$$

From the L_2 stability of the scaling functions (5.1) it follows that

$$\sum_{n \in U_m} b^2_{k,n} \lesssim \|\phi^*_{k,l}\|^2_{L_2}.$$

So $\sum_{n \in U_m} b^2_{k,n} \lesssim b_{k,k}$ and we derive $b^2_{k,n} \lesssim b_{k,k}$. For $k = n$ this becomes $b_{k,k} \lesssim 1$. Combining these two yields

$$|b_{k,n}| \lesssim 1. \tag{5.7}$$

Due to (5.5)

$$\|c\|_\infty \leq \|G^{-1}\|_\infty (\|b\|_\infty + \|\epsilon\|_\infty). \tag{5.8}$$

Combining (5.6), (5.7) and (5.8) gives

$$\|c\|_\infty \lesssim \|\epsilon\|_\infty. \tag{5.9}$$

Suppose that we choose for the column vector c a solution in which all the entries c_k, $k \in U_m$, are equal to zero, except for one entry c_n, $n \in U_m$. From the vanishing moment condition we find

$$c_n = \frac{\langle 1, \phi_{m,l+1} \rangle_{L_2}}{\langle 1, \phi_{n,l} \rangle_{L_2}}.$$

Because the scaling functions form a Riesz basis of L_2 and because they are positive, we can deduce that

$$\langle 1, \phi_{m,l+1} \rangle \lesssim \langle 1, \phi_{k,l} \rangle, \tag{5.10}$$

and thus $|c_k| \lesssim 1$ for all $k \in U_m$, independent of the level l, and $\|\epsilon\|_2 = \|G \cdot c - b\|_2 \lesssim 1$. Since the least squares method finds a c that minimizes $\|G \cdot c - b\|_2$, we have $\|\epsilon\|_\infty \lesssim 1$ and from (5.9) we get $\max_{ij} |(C_l)_{ij}| \lesssim 1$. □

Remark 5.2.2. *Note that we only use the positivity of the scaling functions to prove that* (5.10) *holds. Theorem 5.2.1 is also true for several other constructions for which $\phi_{k,l} \geq 0$ not necessarily holds. One only has to validate* (5.10) *for the specific set of scaling functions at hand. One can, for instance, use a reasoning as follows. A necessary condition for* (5.1) *to hold is the reproduction of polynomials of degree 0, see for instance [112]. In the shift invariant case this implies that the generator Φ satisfies $\langle 1, \Phi \rangle_{L_2} \neq 0$. Therefore, by perturbation arguments, on can show that $\langle 1, \phi_{k,l} \rangle_{L_2} \neq 0$ for all k and l, and* (5.10) *holds.*

Remark 5.2.3. *Suppose that the scaling functions reproduce polynomials of degree $N-1$. Then, using the local semiorthogonalization philosophy, we can demand up to N vanishing moments. If the update stencil is too small, the update coefficients in C_l might be unbounded. Simoens [113] gives examples of this phenomenon in the one-dimensional case and proposes a stabilized variant.*

5.3 Stability over all levels

Theorem 5.2.1 does not imply that the multiscale basis $\bigcup_{l=0}^{\infty} \boldsymbol{\psi}_l$ is a uniformly stable Riesz basis for $L_2(\Omega)$. More generally, we are interested in the range of s for which the multiscale basis $\bigcup_{l=0}^{\infty} \boldsymbol{\psi}_l$ forms a Riesz basis for the Sobolev space $H^s(\Omega)$. The range of such s is determined by the Sobolev regularity of the scaling functions $\phi_{k,l}$ and the Sobolev regularity

of the dual scaling functions $\widetilde{\phi}_{k,l}$. The Sobolev regularity or smoothness of an arbitrary function f on Ω is measured by the critical exponent

$$s_f := \sup\{s : f \in H^s(\Omega)\}.$$

It is known from [29] that if $\phi_{k,l}, \widetilde{\phi}_{k,l} \in L_2(\Omega)$ have compact support, then the multiscale basis $\bigcup_{l=0}^{\infty} \boldsymbol{\psi}_l$ is a Riesz basis for $H^s(\Omega)$ for all s with $-s_{\widetilde{\phi}_{k,l}} < s < s_{\phi_{k,l}}$ and that this interval is sharp.

Realistic applications often require a multilevel basis on bounded domains Ω, such that the nested spaces S_l are not shift-dilation invariant. However, for our stability analysis we will assume a shift-dilation invariant setting for our multilevel basis, because this allows us to obtain estimates for the Sobolev regularity. We start with a geometric refinement described by the *dilation matrix* M which is of the form $M := \sigma I_d$, with σ an integer greater than 1, and denote $m := |\det M| = \sigma^d$. Let $\lambda_k + M\mathbb{Z}^d$ be the m distinct elements of $\mathbb{Z}^d/(M\mathbb{Z}^d)$, with $\lambda_0 = 0$. Define the sets

$$\Lambda := \{\lambda_k, k = 0, \ldots, m-1\}, \quad \Lambda' := \Lambda \setminus \{\lambda_0\}.$$

In the most general case we find a multilevel system

$$\boldsymbol{\Psi} := \{\Phi(x-\alpha), m^{l/2}\Psi^{\lambda}(M^l x - \alpha), \alpha \in \mathbb{Z}^d, l = 0, 1, \ldots, \ \lambda \in \Lambda'\}, \quad (5.11)$$

where

$$\Phi(x) = (\phi_1(x), \phi_2(x), \ldots, \phi_r(x))^T, \quad \Psi^{\lambda}(x) = \left(\psi_1^{\lambda}(x), \psi_2^{\lambda}(x), \ldots, \psi_r^{\lambda}(x)\right)^T$$

are $r \times 1$ function vectors on $\mathbb{R}^d$ that satisfy *vector refinement equations* of the form

$$\Phi(x) = \sum_{\alpha \in \mathbb{Z}^d} A_\alpha \Phi(Mx - \alpha), \quad (5.12)$$

$$\Psi^{\lambda}(x) = \sum_{\alpha \in \mathbb{Z}^d} A_\alpha^{\lambda} \Phi(Mx - \alpha), \quad (5.13)$$

with $\{A_\alpha\}_\alpha$ and $\{A_\alpha^{\lambda}\}_\alpha$ finitely supported sequences of $r \times r$ *mask coefficient matrices* .

We now introduce a lot of new notation and some theorems to estimate the range of stability for some given multilevel system.

Taking the Fourier transform of both sides of (5.12), we obtain

$$\widehat{\Phi}(\omega) = P(M^{-T}\omega)\widehat{\Phi}(M^{-T}\omega), \qquad \omega \in \mathbb{R}^d,$$

and

$$P(\omega) := m^{-1} \sum_{\alpha \in \mathbb{Z}^d} A_\alpha e^{-i\alpha\cdot\omega}, \qquad \omega \in \mathbb{R}^d,$$

is the *symbol* associated with (5.12). Here $P(\omega)$ is an $r \times r$ matrix function. Its entries are trigonometric polynomials with real coefficients. It is well-known that if $P(0)$ satisfies *Condition E*, i.e., 1 is a simple eigenvalue of $P(0)$ and all other eigenvalues of $P(0)$ lie inside the open unit disk, then there exists a unique compactly supported distributional solution vector $\Phi(u)$ satisfying (5.12) and $\Phi(0) = y_R$, with y_R (y_L) the normalized right (left) eigenvector of $P(0)$ associated with eigenvalue 1, see [106].

Without loss of generality we assume that the support of the symbol $P(\omega)$ is in the cube $[-N, N]^d$ for some fixed $N \geq 0$, so $A_\alpha = 0$ for all $\alpha \notin [-N, N]^d$. Let

$$K := \left(\sum_{l=1}^{\infty} M^{-l}([-2N, 2N]^d) \right) \cap \mathbb{Z}^d.$$

Define the torus $\mathbb{T} := [0, 2\pi]^d$ and let $C_0(\mathbb{T})^{r\times r}$ denote the space of all $r \times r$ matrix functions with trigonometric polynomial entries. For a given refinement equation with symbol $P(\omega) \in C_0(\mathbb{T})^{r\times r}$ we define the associated *transition operator* T_P on $C_0(\mathbb{T})^{r\times r}$ by

$$T_P H(\omega) := \sum_{k=0}^{m-1} P(M^{-T}(\omega+2\pi\lambda_l))H(M^{-T}(\omega+2\pi\lambda_l))P(M^{-T}(\omega+2\pi\lambda_l))^*.$$

Define

$$\mathbb{H} := \{H(\omega) \in C_0(\mathbb{T}^d)^{r\times r} : H(\omega) = \sum_{\alpha\in K} H_\alpha e^{-i\alpha\cdot\omega}\},$$

then $\mathbb{H}$ is invariant under T_P. Furthermore we know from [63, 68] that the eigenfunctions of T_P corresponding to nonzero eigenvalues lie in $\mathbb{H}$. So it is sufficient to consider the restriction of T_P to $\mathbb{H}$ in order to study the eigenvalues and eigenfunctions of T_P.

Let us define the refinement operator R_P on $L_2(\mathbb{R}^d)^{r\times 1}$ by

$$R_P F := \sum_{\alpha\in\mathbb{Z}^d} A_\alpha F(M\cdot -\alpha),$$

then Φ solves (5.12) if $R_P\Phi = \Phi$. The *cascade algorithm* [39] consists in the repeated application of R_P. If for some compactly supported initial $F \in L_2(\mathbb{R}^d)^{r\times 1}$ the cascade algorithm converges in the L_2 norm, then the vector function obtained in the limit is an $L_2(\mathbb{R}^d)^{r\times 1}$-solution of (5.12). The following theorem gives necessary but sufficient conditions to guarantee that (5.12) has a solution in L_2.

Theorem 5.3.1. *The cascade algorithm associated with the symbol $P(\omega)$ converges in the L_2 norm if and only if $P(\omega)$ satisfies sum rules of order 1, i.e.,*

$$y_L P(2\pi M^{-T}\lambda_k) = 0, \quad k = 1, \ldots, m-1,$$

and the transition operator T_P satisfies Condition E.

Proofs can be found in [63, 79, 112]. Note that the requirement that $P(\omega)$ satisfies sum rules of order 1 is equivalent to the requirement that the shifts of the solution Φ of (5.12) reproduce polynomials of degree 0. The following theorem is the main result of the paper [67], and it can be used to estimate the smoothness of the solution to (5.12).

Theorem 5.3.2. *Let $\Phi \in L_2(\mathbb{R}^d)^{r\times 1}$ be the normalized solution of (5.12) with symbol $P(\omega)$. Suppose the highest degree of polynomials reproduced by Φ is $k-1$. Let*

$$E_k := \{\eta_j\sigma^{-\mu}, \overline{\eta}_j\sigma^{-\mu} : |\mu| < k, j = 2, \ldots, r\} \cup \{\sigma^{-\mu} : |\mu| < 2k\},$$

with $\mu = (\mu_1, \ldots, \mu_d) \in \mathbb{N}_0^d$, $\sigma^{-\mu} := \sigma^{-\mu_1}\cdots\sigma^{-\mu_d}$ and $\{\eta_1, \ldots, \eta_r\} := \operatorname{spec}(P(0))$, where $\eta_1 = 1$ and $\eta_j \neq 1$ for $j = 2, \ldots, r$. Here $\operatorname{spec}(\cdot)$ denotes the spectrum. Define

$$\rho_k := \max\{|\nu| : \nu \in \operatorname{spec}(T_P|_{\mathbb{H}}) \setminus E_k\}.$$

Then

$$s_\Phi \geq -\frac{d}{2}\log_m \rho_k.$$

If Φ is L_2-stable then we have equality:

$$s_\Phi = -\frac{d}{2}\log_m \rho_k.$$

Suppose that the multilevel system (5.11) is a Riesz basis of $L_2(\mathbb{R}^d)$. Then equations (5.2) and (5.3) yield a dual system

$$\widetilde{\mathbf{\Psi}} := \{\widetilde{\Phi}(x-\alpha), m^{l/2}\widetilde{\Psi}^\lambda(M^l x - \alpha), \alpha \in \mathbb{Z}^d, l = 0, 1, \ldots, \ \lambda \in \Lambda'\}$$

which is also a Riesz basis of $L_2(\mathbb{R}^d)$ satisfying (5.4). Furthermore

$$\widetilde{\Phi}(x) = \sum_{\alpha\in\mathbb{Z}^d} \widetilde{A}_\alpha \widetilde{\Phi}(Mx-\alpha), \quad \widetilde{\Psi}^\lambda(x) = \sum_{\alpha\in\mathbb{Z}^d} \widetilde{A}_\alpha^\lambda \widetilde{\Phi}(Mx-\alpha).$$

The following theorem is due to Dahmen [29].

Theorem 5.3.3. *Assume that $\mathbf{\Psi}$ and $\widetilde{\mathbf{\Psi}}$ are dual Riesz bases in $L_2(\mathbb{R}^d)$ with compactly supported basis functions. In particular the symbols $P(\omega)$ and $\widetilde{P}(\omega)$ of the scaling functions Φ resp. $\widetilde{\Phi}$ are trigonometric polynomials (i.e. they have finitely supported masks $(A_\alpha)_\alpha, (\widetilde{A}_\alpha)_\alpha$). Then the regularity exponents of Φ and $\widetilde{\Phi}$ are positive, and*

$$\begin{aligned} \mathbf{\Psi} \text{ is a Riesz basis in } H^s(\mathbb{R}^d) &\quad\Leftrightarrow\quad -s_{\widetilde{\Phi}} < s < s_\Phi, \\ \widetilde{\mathbf{\Psi}} \text{ is a Riesz basis in } H^s(\mathbb{R}^d) &\quad\Leftrightarrow\quad -s_\Phi < s < s_{\widetilde{\Phi}}, \end{aligned}$$

where s_Φ and $s_{\widetilde{\Phi}}$ are the smoothness exponents of Φ resp. $\widetilde{\Phi}$.

Theorem 5.3.3 is not always applicable because it assumes that $\widetilde{\Phi} \in L_2(\mathbb{R}^d)^{r\times 1}$, which can be checked by Theorem 5.3.1. Generally we do not know in advance whether our multilevel system $\mathbf{\Psi}$ of the form (5.11) is an L_2 Riesz basis. Therefore, it is possible that the dual system only exists in distributional sense in L_2 which is not sufficient. In that case we cannot use Theorem 5.3.2 either to compute $s_{\widetilde{\Phi}}$. This problem was solved by Lorentz and Oswald in [82] for the case $r = 1$. For the remainder of this section we will treat here the more general case $r \geq 1$ which is a generalization of the results in [82]. We prove the following theorem.

Theorem 5.3.4. *Assume that $\mathbf{\Psi}$ and $\widetilde{\mathbf{\Psi}}$ only contain compactly supported basis functions. If $\widetilde{s} := -\frac{d}{2}\log_m \widetilde{\rho} \leq 0$ satisfies $-\widetilde{s} < s_\Phi$ with $\widetilde{\rho} := \max\{|\nu| : \nu \in \operatorname{spec}(T_{\widetilde{P}}\big|_{\mathbb{H}})\}$, then the multilevel system $\mathbf{\Psi}$ of the form (5.11) is a Riesz basis in $H^s(\mathbb{R}^d)$ for all s in the interval*

$$-\widetilde{s} < s < s_\Phi.$$

Furthermore, $\mathbf{\Psi}$ is not a Riesz basis in $H^s(\mathbb{R}^d)$ for any $s < -\widetilde{s}$.

First we introduce some notation and we prove some auxiliary lemmas. Suppose that $(c_\alpha)_\alpha$ is a sequence of $r\times 1$ vectors, then we denote the periodic function vector

$$c(\omega) := \sum_{\alpha\in\mathbb{Z}^d} c_\alpha e^{-i\alpha\cdot\omega}$$

by the same letter. Likewise we have

$$c^T(\omega) := \sum_{\alpha\in\mathbb{Z}^d} c_\alpha^T e^{-i\alpha\cdot\omega}.$$

We introduce the matrix function

$$L(\omega) := \left(P^{\lambda_j}(\omega + 2\pi M^{-T}\lambda_i)\right)_{i,j\in\Lambda},$$

which is invertible for all $\omega \in \mathbb{T}$ if and only if $\{\Phi(x-\alpha), \Psi(x-\alpha), \alpha \in \mathbb{Z}^d\}$ is an L_2 Riesz basis in S_1, see [118, Theorem 13]. For our purposes this is satisfied, see Theorem 5.2.1. From (5.2) and (5.3) we get

$$L^{-1}(\omega) = \left(\widetilde{P}^{\lambda_i}(\omega + 2\pi M^{-T}\lambda_j)^*\right)_{i,j\in\Lambda}. \tag{5.14}$$

Lemma 5.3.5. *Consider the unique decomposition of $v_1 \in S_1$:*

$$v_1 := \sum_{\alpha\in\mathbb{Z}^d} c_\alpha^T \Phi(M\cdot - \alpha) = v_0 + w_1,$$

with

$$v_0 := \sum_{\beta\in\mathbb{Z}^d} (d_\beta^{\lambda_0})^T \Phi(\cdot - \beta) \in S_0, \qquad w_1 := \sum_{\lambda\in\Lambda'}\sum_{\beta\in\mathbb{Z}^d} (d_\beta^{\lambda})^T \Psi(\cdot - \beta) \in W_1.$$

Then, with

$$\begin{aligned} c(\omega) &:= \sum_{\alpha\in\mathbb{Z}^d} c_\alpha e^{-i\alpha\cdot\omega}, \\ d^{\lambda_0}(\omega) &:= \sum_{\beta\in\mathbb{Z}^d} d_\beta^{\lambda_0} e^{-i\beta\cdot\omega}, \end{aligned}$$

we have that

$$d^{\lambda_0}(M\omega) = m^{-1}\sum_{j=0}^{m-1} \widetilde{P}(\omega + 2\pi M^{-T}\lambda_j)^* c(\omega + 2\pi M^{-T}\lambda_j). \tag{5.15}$$

Proof. This is a straightforward generalization of Equation (41) in [82]. Some algebra using (5.12) and (5.13) gives

$$v_0 + w_1 = \sum_{\alpha\in\mathbb{Z}^d}\left(\sum_{\lambda\in\Lambda}\sum_{\beta\in\mathbb{Z}^d} (d_\beta^\lambda)^T A_{\alpha - M\beta}^\lambda\right)\Phi(M\cdot - \alpha),$$

with $A_\alpha^{\lambda_0} := A_\alpha$. Hence,

$$c_\alpha^T = \sum_{\lambda\in\Lambda}\sum_{\beta\in\mathbb{Z}^d} (d_\beta^\lambda)^T A_{\alpha - M\beta}^\lambda.$$

Since M is defined as σI_d we have that $M\beta\cdot\omega = \beta\cdot M\omega$ and we infer

$$c(\omega)^T = m\sum_{\lambda\in\Lambda} (d^\lambda)^T(M\omega) P^\lambda(\omega).$$

Substituting the arguments $\omega + 2\pi M^{-T}\lambda_j$ we get

$$\begin{aligned}
\mathbf{c}^T(\omega) &= \left(c^T(\omega + 2\pi M^{-T}\lambda_j)\right)_{j=0}^{m-1} \\
&= m\left(\sum_{i=0}^{m-1}(d^{\lambda_i})^T(M\omega)P^{\lambda_i}(\omega + 2\pi M^{-T}\lambda_j)\right)_{j=0}^{m-1} \\
&= m\left((d^{\lambda_i})^T(M\omega)\right)_{i=0}^{m-1}\cdot\left(P^{\lambda_i}(\omega + 2\pi M^{-T}\lambda_j\right)_{i,j=0}^{m-1} \\
&= m\ \mathbf{d}^T(M\omega)\cdot L^T(\omega),
\end{aligned}$$

where $\mathbf{c}^T(\omega)$ and $\mathbf{d}^T(M\omega)$ are $1 \times rm$ row vectors. We find that

$$\mathbf{d}(M\omega) = m^{-1}L^{-1}(\omega)\mathbf{c}(\omega)$$

and (5.15) follows from (5.14). □

Let us define the projection operators

$$\mathcal{Q}_l f := \sum_{\alpha\in\mathbb{Z}^d}\langle\widetilde{\Phi}(M^l\cdot-\alpha), f\rangle_{L_2}\Phi(M^l\cdot-\alpha).$$

These operators satisfy $\mathcal{Q}_l\mathcal{Q}_{l+k} = \mathcal{Q}_l$ for all $0 \le l, k < \infty$. We also define the following norm on $C_0(\mathbb{T})^{r\times r}$:

$$\|T_P^k H\|_\infty := \sum_{1\le i,j\le r}\sup_{\omega\in\mathbb{T}}\{|e_i^T T_P^k H(\omega)e_j|\},$$

with e_i, e_j the i-th resp. j-th column of I_r, and

$$\|\ T_P^k\big|_{\mathbb{H}}\ \|_\infty := \sup_{H\in\mathbb{H}}\frac{\|T_P^k H\|_\infty}{\|H\|_\infty}.$$

Lemma 5.3.6. *For arbitrary $k > 0$ we have the norm equivalence*

$$\|\ \mathcal{Q}_l\big|_{S_{l+k}}\ \|_{L_2}^2 = \|\ \mathcal{Q}_0\big|_{S_k}\ \|_{L_2}^2 \sim \|T_{\tilde{P}}^k I_r\|_\infty.$$

Proof. First we show that $\|\ \mathcal{Q}_0\big|_{S_1}\ \|_{L_2}^2 \sim \|T_{\tilde{P}}I_r\|_\infty$. Define v_0, v_1 and w_1 as in Lemma 5.3.5. Then, by the Riesz basis property of $\{\Phi(M^l\cdot-\alpha), \alpha\in\mathbb{Z}^d\}$ and because $\{e^{i\alpha\cdot\omega}, \alpha\in\mathbb{Z}^d, \omega\in\mathbb{T}\}$ is an orthonormal basis for $L_2(\mathbb{T})$,

$$\|\ \mathcal{Q}_0\big|_{S_1}\ \|_{L_2}^2 = \sup_{v_1\neq 0}\frac{\|\mathcal{Q}_0 v_1\|_{L_2}^2}{\|v_1\|_{L_2}^2} \sim m\sup_{c\neq 0}\frac{\|d^{\lambda_0}\|_{F(\mathbb{T})}^2}{\|c\|_{F(\mathbb{T})}^2},$$

where

$$\|d\|_{F(\mathbb{T})}^2 := \sum_{1\le j\le r}\|d_j\|_{L_2(\mathbb{T})}^2$$

is the Frobenius norm of the function vector $d(\omega) = [d_1(\omega) \cdots d_r(\omega)]^T$. Note that we have the equivalence

$$\max_j \|d_j\|^2_{L_2(\mathbb{T})} \le \|d\|^2_{F(\mathbb{T})} \le r \max_j \|d_j\|^2_{L_2(\mathbb{T})}. \tag{5.16}$$

Now we use Lemma 5.3.5, Equation (5.16), and Hölder's inequality to derive that

$$\begin{aligned}
& m\|d\|^2_{F(\mathbb{T})} \\
&= m^2\|d(M\cdot)\|^2_{F(M^{-T}\mathbb{T})} \\
&= \|\sum_{k=0}^{m-1} \widetilde{P}(\omega + 2\pi M^{-T}\lambda_k)^* c(\omega + 2\pi M^{-T}\lambda_k)\|^2_{F(M^{-T}\mathbb{T})} \\
&\sim \max_j \int_{M^{-T}\mathbb{T}} \left| \sum_{k=0}^{m-1} \sum_{i=1}^{r} \widetilde{P}_{ij}(\overline{\omega + 2\pi M^{-T}\lambda_k}) c_i(\omega + 2\pi M^{-T}\lambda_k) \right|^2 d\omega \\
&\le \max_j \int_{M^{-T}\mathbb{T}} \left(\sum_{k=0}^{m-1} \sum_{i=1}^{r} |\widetilde{P}_{ij}(\omega + 2\pi M^{-T}\lambda_k)|^2 \right) \\
&\quad \cdot \left(\sum_{k=0}^{m-1} \|c(\omega + 2\pi M^{-T}\lambda_k)\|^2_{l_2} \right) d\omega \\
&\le \sum_{i,j=1}^{r} \left\| \sum_{k=0}^{m-1} \widetilde{P}_{ij}(\omega + 2\pi M^{-T}\lambda_k) \widetilde{P}_{ij}(\overline{\omega + 2\pi M^{-T}\lambda_k}) \right\|_{L_\infty(M^{-T}\mathbb{T})} \\
&\quad \cdot \int_{M^{-T}\mathbb{T}} \left(\sum_{k=0}^{m-1} \|c(\omega + 2\pi M^{-T}\lambda_k)\|^2_{l_2} \right) d\omega \\
&= \|T_{\widetilde{P}} I_r\|_\infty \cdot \|c\|^2_{F(\mathbb{T})}.
\end{aligned}$$

Thus we have $\| \mathcal{Q}_0|_{S_1} \|^2_{L_2} \lesssim \|T_{\widetilde{P}} I_r\|_\infty$. Since Hölder's inequality is a sharp estimate we can find a function vector $c(\omega)$ such that

$$\begin{aligned}
m\|d\|^2_{F(\mathbb{T})} \sim \max_j \int_{M^{-T}\mathbb{T}} & \left(\sum_{k=0}^{m-1} \sum_{i=1}^{r} |\widetilde{P}_{ij}(\omega + 2\pi M^{-T}\lambda_k)|^2 \right) \\
& \cdot \left(\sum_{k=0}^{m-1} \|c(\omega + 2\pi M^{-T}\lambda_k)\|^2_{l_2} \right) d\omega.
\end{aligned}$$

Indeed, take $c(\omega) = a(\omega) \left(\widetilde{P}_{ij}(\omega)\right)_{i=1}^{r}$ with $a(\omega)$ an arbitrary measurable function on $M^{-T}\mathbb{T}$. Now choose $a(\omega)$ as the characteristic function of the

set of all $\omega \in M^{-T}\mathbb{T}$ for which for arbitrary i, j

$$\sum_{k=0}^{m-1} |\widetilde{P}_{ij}(\omega + 2\pi M^{-T}\lambda_k)|^2 \geq (1-\epsilon) \left\| \sum_{k=0}^{m-1} |\widetilde{P}_{ij}(\omega + 2\pi M^{-T}\lambda_k)|^2 \right\|_{L_\infty(M^{-T}\mathbb{T})}$$

and let $\epsilon \to 0$. We find

$$\begin{aligned} m\|d\|^2_{F(\mathbb{T})} &\sim \max_j \sum_{i=1}^{r} \left\| \sum_{k=0}^{m-1} |\widetilde{P}_{ij}(\omega + 2\pi M^{-T}\lambda_k)|^2 \right\|_{L_\infty(M^{-T}\mathbb{T})} \\ &\quad \cdot \int_{M^{-T}\mathbb{T}} \left(\sum_{k=0}^{m-1} \|c(\omega + 2\pi M^{-T}\lambda_k)\|^2_{l_2} \right) d\omega \\ &\sim \|T_{\widetilde{P}} I_r\|_\infty \cdot \|c\|^2_{F(\mathbb{T})}. \end{aligned}$$

Hence $\| \mathcal{Q}_0|_{S_1} \|^2_{L_2} \sim \|T_{\widetilde{P}} I_r\|_\infty$. By iterating Lemma 5.3.5 one obtains

$$\| \mathcal{Q}_0|_{S_k} \|^2_{L_2} \sim \|T^k_{\widetilde{P}} I_r\|_\infty$$

in the same way. This concludes the proof. □

Proof of Theorem 5.3.4. It follows from properties of the spectral radius and Lemma 5.3.6 that

$$\|\mathcal{Q}_l v_{l+k}\|^2_{L_2} \lesssim \sigma^{-2\widetilde{s}k} \|v_{l+k}\|^2_{L_2}, \qquad l, k \in \mathbb{N}, \quad v_{l+k} \in S_{l+k}. \tag{5.17}$$

Indeed, we have the equality $\widetilde{\rho} = \lim_{k\to\infty} \|(T_{\widetilde{P}}|_{\mathbb{H}})^k\|^{1/k}_\infty$. Choose an $\epsilon > 0$. The spectral radius of the operator $(\widetilde{\rho} + \epsilon)^{-1} T_{\widetilde{P}}|_{\mathbb{H}}$ is strictly smaller than one. Therefore we find that

$$\lim_{k\to\infty} \|((\widetilde{\rho} + \epsilon)^{-1} T_{\widetilde{P}}|_{\mathbb{H}})^k\|_\infty = 0,$$

such that for arbitrary $k > 0$ there exists a constant C_ϵ for which

$$\|((\widetilde{\rho} + \epsilon)^{-1} T_{\widetilde{P}}|_{\mathbb{H}})^k\|_\infty < C_\epsilon,$$

or

$$\|(T_{\widetilde{P}}|_{\mathbb{H}})^k\|_\infty \lesssim (\widetilde{\rho} + \epsilon)^k.$$

Because $I_r \in \mathbb{H}$ and $\|I_r\|_\infty \sim 1$ we find from Lemma 5.3.6 that

$$\|\mathcal{Q}_l v_{l+k}\|^2_{L_2} \lesssim (\widetilde{\rho} + \epsilon)^k \|v_{l+k}\|^2_{L_2}.$$

By definition of $\widetilde{s}$ and by taking a sufficiently small $\epsilon > 0$ we find (5.17).

It is by now well known, see, e.g., Proposition 3.4.7 or [105, Lemma 2], that

$$\|f\|_{H^s}^2 \sim \inf_{v_l \in S_l : f = \sum_l v_l} \sum_{l=0}^{\infty} \sigma^{2ls} \|v_l\|_{L_2}^2 \tag{5.18}$$

for all $0 < s < s_\Phi$. Because of the norm equivalence (5.18) it is sufficient to show that

$$\inf_{v_l \in S_l : v_n = \sum_l v_l} \sum_{l=0}^{n} \sigma^{2ls} \|v_l\|_{L_2}^2 \sim \sum_{l=0}^{n} \sigma^{2ls} \|(\mathcal{Q}_l - \mathcal{Q}_{l-1}) v_n\|_{L_2}^2$$

for all $-\widetilde{s} < s < s_\Phi$ which follows from standard techniques as used in Theorems 3.4.8 and 4.3.2. This equivalence implies the H^s Riesz basis property for the finite set

$$\mathbf{\Psi}_n := \{\Phi(x-\alpha), \sigma^{l(d/2-s)} \Psi^\lambda(M^l x - \alpha), \alpha \in \mathbb{Z}^d, l = 0, 1, \ldots, n,\ \lambda \in \Lambda'\}.$$

Then we let $n \to \infty$ to obtain the H^s Riesz basis property for the (normalized) multilevel system $\mathbf{\Psi}$.

Now suppose that $s < -\widetilde{s}$. Let $s' \in (s, -\widetilde{s})$. Similar to the derivation of Equation (5.17) we can now find a sequence $v_n \in S_n$ with $n \to \infty$ such that $\|\mathcal{Q}_0 v_n\|_{L_2}^2 \gtrsim \sigma^{2s'n} \|v_n\|_{L_2}^2$. Using (5.18) we obtain

$$\begin{aligned} \|v_n\|_{H^s} &\lesssim \inf_{v_l \in S_l : v_n = \sum_l v_l} \sum_{l=0}^{n} \sigma^{2ls} \|v_l\|_{L_2}^2 \lesssim \sigma^{2n(s-s')} \|\mathcal{Q}_0 v_n\|_{L_2}^2 \\ &\lesssim \sigma^{2n(s-s')} \left(\|\mathcal{Q}_0 v_n\|_{L_2}^2 + \sum_{l=1}^{n} \sigma^{2ls} \|(\mathcal{Q}_l - \mathcal{Q}_{l-1}) v_n\|_{L_2}^2 \right). \end{aligned}$$

The factor $\sigma^{2n(s-s')}$ goes exponentially fast to zero as $n \to \infty$. Therefore the equivalence

$$\|v_n\|_{H^s} \sim \sum_{l=0}^{n} \sigma^{2ls} \|(\mathcal{Q}_l - \mathcal{Q}_{l-1}) v_n\|_{L_2}^2$$

does not hold. This establishes Theorem 5.3.4.

□

Remark 5.3.7. *Q. Jiang and P. Oswald have written Matlab routines for numerically estimating smoothness exponents, see their papers [69] and [70].*

5.4 Explicit constructions

Many real-world applications require multilevel bases on bounded domains Ω and discretization spaces S_l that are not shift-invariant. Therefore we will construct wavelet bases in this section using the construction method described in Section 5.2. On the other hand, from a theoretical point of view we are interested in determining the range of Sobolev exponents for which these systems do form a Riesz basis. The theory developed in Section 5.3 gives such estimates for shift-invariant MRAs on $\mathbb{R}^d$. The following constructions are therefore explicitly derived on a uniform grid in order to be able to compute the range of stability. The numerical stability results for uniform grids that we obtain give estimates for the range of stability on non-uniform grids.

5.4.1 Linear spline wavelets on $\mathbb{R}$

The shifts

$$\phi_{k,l} = \Phi(2^l \cdot - k), \qquad k \in \mathbb{Z},$$

of the generating function

$$\Phi(t) = \begin{cases} 1+t, & -1 \le t \le 0, \\ 1-t, & 0 \le t \le 1, \\ 0, & \text{else} \end{cases}$$

form a basis of the space of linear splines S_l with knots at $2^{-l}k$, $k \in \mathbb{Z}$. Furthermore the scaled set $\{2^{l/2}\phi_{k,l}, k \in \mathbb{Z}\}$ satisfies the Riesz basis property (5.1). The wavelets $\psi_{k,l}$ are initially defined as $\psi_{k,l} := \phi_{2k+1,l+1}$. It is easy to see that a scaling function $\phi_{k,l}$ corresponds to an old knot at $2^{-l}k$ while a wavelet function $\psi_{l,k}$ corresponds to a new knot at $2^{-l}k + 1/2$. We fix the update stencil in advance in order to have local support for the wavelet functions in W_l. A wavelet function $\psi_{k,l} \in W_l$ corresponding to a new knot $2^{-l}k + 1/2$ is updated by the two neighbouring scaling functions in S_l corresponding to the two neighbouring old knots $2^{-l}k$ and $2^{-l}(k+1)$. Applying the construction method described in Section 5.2 we find that

$$\psi_{k,l} = \phi_{2k+1,l+1} - \frac{1}{4}\phi_{k,l} - \frac{1}{4}\phi_{k+1,l}, \qquad k \in \mathbb{Z},$$

which is the CDF(2,2) wavelet [23]. The scaling functions and the duals satisfy the refinement relation

$$\begin{aligned}\Phi(t) &= \Phi(2t) + \frac{1}{2}\left(\Phi(2t-1) + \Phi(2t+1)\right), \qquad t \in \mathbb{R} \\ \widetilde{\Phi}(t) &= \frac{3}{2}\widetilde{\Phi}(2t) + \frac{1}{2}\left(\widetilde{\Phi}(2t-1) + \widetilde{\Phi}(2t+1)\right) \\ &\quad -\frac{1}{4}\left(\widetilde{\Phi}(2t-2) + \widetilde{\Phi}(2t+2)\right), \quad t \in \mathbb{R}.\end{aligned}$$

It is well-known that $s_\Phi = 1.5$. So we only need to investigate the Sobolev regularity of the dual scaling function $\widetilde{\phi}$. Using Theorem 5.3.2 we compute in Matlab that $s_{\widetilde{\Phi}} \approx 0.440765$. We used the software from Remark 5.3.7 and double checked the results in Maple. From Theorem 5.3.3, the linear spline wavelets are a Riesz basis for $H^s(\mathbb{R})$ with $-0.440765 < s < 1.5$. Figure 5.1 depicts Φ, Ψ and $\widetilde{\Phi}$. Note that, on uniform grids, the wavelets have two vanishing moments, although our construction method only demands one vanishing moment.

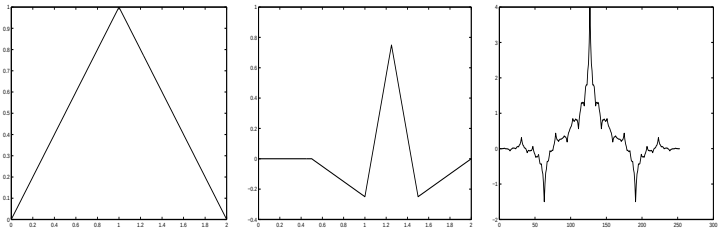

(a) Φ (b) Ψ (c) $\widetilde{\Phi}$

Figure 5.1: Linear spline wavelet on $\mathbb{R}$.

Suppose that we do not demand a vanishing moment, but that we orthogonalize the wavelet $\psi_{k,l}$ to $\phi_{k,l}$ and $\phi_{k+1,l}$. Then we find that

$$\psi_{k,l} = \phi_{2k+1,l+1} - \frac{3}{10}\phi_{k,l} - \frac{3}{10}\phi_{k+1,l}, \qquad k \in \mathbb{Z},$$

which yields a Riesz basis for $H^s(\mathbb{R})$ with $0.064715 < s < 1.5$. As expected we do not get an L_2 stable Riesz basis.

In the introduction we motivated the use of wavelets for solving elliptic equations. Consider the two-point boundary value problem

$$-u'' + qu = f \quad \text{on} \quad \Omega := [0,2], \qquad u(0) = u(2) = 0. \tag{5.19}$$

If we take $f(x) = e^x(x^2(1-x) + 2x(1+q) - 2)$, then $u(x) = e^x x(2-x)$ is the exact solution. For the discretizations and solvers we use the linear finite element hierarchical basis and the linear wavelet basis constructed above. Near the boundary the wavelets are corrected following the strategy of Section 5.2 subjected to the boundary constraints. For instance, in the uniform setting we find that $\psi_{k,l} = \phi_{2k+1,l+1} - \frac{1}{2}\phi_{k,l}$ near the right boundary. To solve the boundary value problem we employ a nested iteration conjugate gradient method with as extra preconditioner the diagonal of the stiffness matrix. In fact, the extra diagonal preconditioner makes sure that the basis functions are suitably normalized. Tables 5.1 and 5.2 show the condition numbers κ of the related stiffness matrices, the error norms of the residuals corresponding to the approximate solutions, and the iteration numbers, for the cases $q = 1$ resp. $q = 10^8$. See Section 3.6 for a detailed explanation of the structure of these types of tables. It is well known that for problems with q small wavelet basis methods perform slightly worse than traditional finite element preconditioners, as can be seen in Table 5.1. The situation changes when the value of q is increased. The better behaviour for the wavelet basis is due to its L_2-stability which becomes more important for large q, because a large zero-order term in (5.19) affects the energy norm.

	Linear wavelets			Linear FEM		
n	residual	#	κ	residual	#	κ
4	2.3826e-04	6	4.2707	1.3960e-04	2	1.2880
5	1.1810e-04	6	4.6169	3.5487e-05	2	1.2887
6	1.3758-04	5	4.8821	8.8724e-06	2	1.2889
7	4.5134e-05	5	5.0910	4.5287e-05	1	1.2890
8	2.7058e-05	4	5.2576	7.3693e-06	1	1.2890
9	1.1858e-05	4	5.3925	2.4101e-06	1	1.2890
10	4.1122e-06	4	5.5031	5.2695e-07	1	1.2890
11	4.4043e-06	3	5.5949	1.4313e-07	1	1.2890
12	1.6728e-06	3	5.6717	3.4457e-08	1	1.2890

Table 5.1: Iteration history for problem (5.19), $q = 1$.

5.4.2 Linear spline wavelets on $\mathbb{R}^2$

Let Δ by a type-1 triangulation, i.e. a triangulation formed by a rectangular partition plus northeast diagonals. Define the dilation matrix $M := 2I_2$. Each scaling function $\phi_{k,0}$ takes the value 1 at vertex $k \in \Delta$ and is zero at all other vertices. Let S_l be the space of linear splines with vertices at $M^{-l}\Delta$. We update a wavelet at a new vertex m in $M^{-l-1}\Delta$ by the four old vertices $k_1, \ldots, k_4$ in $M^{-l}\Delta$ that define the two triangles $T(k_1, k_2, k_3)$ and $T(k_1, k_2, k_4)$ in $M^{-l}\Delta$ with common edge $[k_1, k_2]$ containing m. We find

	Linear wavelets			Linear FEM		
n	residual	#	κ	residual	#	κ
4	2.5106e-04	6	6.1018	4.9987e-04	9	120.9161
5	1.6339e-04	5	6.6487	1.2481e-04	13	287.7855
6	1.3260e-04	4	7.1602	5.9980e-05	14	667.1219
7	3.4732e-05	4	7.5836	5.5237e-05	10	1.5158e+03
8	2.1101e-05	3	7.9610	3.5013e-05	16	3.3852e+03
9	1.6646e-05	2	8.2814	1.9165e-05	35	7.4039e+03
10	6.5550e-06	2	8.5351	8.2853e-06	7	1.5504e+04
11	2.5265e-06	2	8.6829	3.9577e-06	29	2.8954e+04
12	1.3461e-06	3	8.7174	2.2209e-06	69	4.3179e+04

Table 5.2: Iteration history for problem (5.19), $q = 10^8$.

that

$$\psi_{m,l} = \phi_{m,l+1} - \frac{13}{80}\left(\phi_{k_1,l} + \phi_{k_2,l}\right) + \frac{3}{80}\left(\phi_{k_3,l} + \phi_{k_4,l}\right).$$

The scaling functions and the dual scaling functions satisfy

$$\begin{aligned}
\Phi(x) &= \Phi(Mx) + \frac{1}{2}\sum_{k\in K_1}\Phi(Mx-k), \qquad x \in \mathbb{R}^2,\\
\widetilde{\Phi}(x) &= \frac{41}{20}\widetilde{\Phi}(Mx) + \frac{13}{20}\sum_{k\in K_1}\widetilde{\Phi}(Mx-k) - \frac{7}{40}\sum_{k\in K_2}\widetilde{\Phi}(Mx-k)\\
&\quad -\frac{3}{20}\sum_{k\in K_3}\widetilde{\Phi}(Mx-k),\ x \in \mathbb{R}^2,
\end{aligned}$$

with

$$\begin{aligned}
K_1 &:= \{(0,1),(1,0),(-1,0),(0,-1),(1,-1),(-1,1)\},\\
K_2 &:= \{(0,2),(2,0),(-2,0),(0,-2),(2,-2),(-2,2)\},\\
K_3 &:= \{(1,1),(-1,-1),(-1,2),(-2,1),(1,-2),(2,-1)\}.
\end{aligned}$$

We find that $s_\Phi = 1.5$ and $s_{\widetilde{\Phi}} \approx 0.328857$ using Theorem 5.3.2. The bivariate linear spline wavelets are a Riesz basis for $H^s(\mathbb{R}^2)$ with $-0.328857 < s < 1.5$, and in the uniform setting they have two vanishing moments. Figure 5.2 depicts Φ, Ψ and $\widetilde{\Phi}$.

Consider the elliptic problem

$$-\Delta u + qu = f \quad \text{on} \quad \Omega := [0,1]^2, \qquad u|_{\partial\Omega} = 0, \tag{5.20}$$

with $f(x,y) = 2y(1-y) + 2x(1-x) + qx(1-x)y(1-y)$. Then $u(x,y) = x(1-x)y(1-y)$ is the exact solution. For the discretizations and solvers we use the linear finite element hierarchical basis of Yserentant [129] which is suboptimal, the above constructed bivariate linear spline wavelet basis,

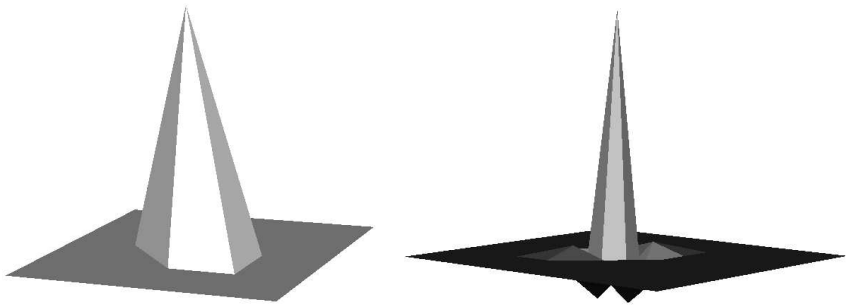

(a) Φ (b) Ψ

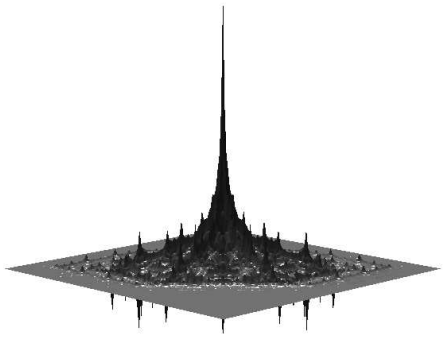

(c) $\widetilde{\Phi}$

Figure 5.2: Linear spline wavelet on $\mathbb{R}^2$.

and the BPX preconditioner from [11]. Near the boundary we correct the wavelets such that they satisfy the boundary conditions. We can do this easily by only using scaling functions in the update stencil that do not intersect with the domain boundary. The boundary wavelets still have at least one vanishing moment and are as orthogonal as possible with respect to the scaling functions in the update stencil. To solve the elliptic problem we employ a nested iteration preconditioned conjugate gradient method with preconditioner the diagonal of the stiffness matrix. Tables 5.3 and 5.4 show the results for the cases $q = 1$ resp. $q = 10^8$.

	BPX			Linear wavelets			HB		
n	residual	#	κ	residual	#	κ	residual	#	κ
2	2.4722e-5	8	7.82	1.2454e-5	10	9.57	1.8931e-5	9	10.65
3	9.6674e-6	10	9.47	1.0494e-5	12	12.66	8.3467e-6	12	19.64
4	3.3323e-6	11	10.88	4.3585e-6	13	14.88	4.4168e-6	14	32.04
5	1.2316e-6	12	12.06	2.7091e-6	13	16.50	3.0692e-6	15	47.41
6	8.8959e-7	12	13.06	8.6482e-7	14	17.74	1.2663e-6	18	65.74

Table 5.3: Iteration history for problem (5.20), $q = 1$.

	BPX			Linear wavelets			HB		
n	residual	#	κ	residual	#	κ	residual	#	κ
2	1.2421e-3	5	6.47	1.3974e-3	8	14.62	1.5714e-3	8	108.24
3	6.5035e-4	7	10.71	1.1266e-3	10	19.40	1.0239e-3	10	607.60
4	3.1799e-4	9	14.82	3.6792e-4	13	23.90	4.3267e-4	23	3.13e+3
5	3.0483e-4	10	18.83	2.9078e-4	14	27.74	2.9046e-4	39	1.53e+4
6	1.3945e-4	12	22.76	1.1941e-4	17	31.04	1.5280e-4	97	7.25e+4

Table 5.4: Iteration history for problem (5.20), $q = 10^8$.

5.4.3 Powell–Sabin spline wavelets on $\mathbb{R}^2$

Define the hexagonal lattice Δ in $\mathbb{R}^2$ as the image of $\mathbb{Z}^2$ under

$$\Gamma := \begin{bmatrix} 1 & -1/2 \\ 0 & \sqrt{3}/2 \end{bmatrix}, \tag{5.21}$$

and let Δ^{PS} be its PS-refinement by drawing in the additional grid lines $y = l$, $y = \frac{\sqrt{3}}{3}(x + m)$, and $y = -\frac{\sqrt{3}}{3}(x + n)$, $l, m, n \in \mathbb{Z}$, see Figure 5.3.

Define a function vector $\Phi = [\phi_1, \phi_2, \phi_3]^T$, where the functions ϕ_i, $i = 1, 2, 3$, are the unique solutions in $S_2^1(\Delta^{PS})$ of the Hermite interpolation problem

$$\begin{aligned} (\phi_1(V_j), \phi_2(V_j), \phi_3(V_j)) &= \delta_{0j}\,(1/3, 1/3, 1/3)\,, \\ (D_x\phi_1(V_j), D_x\phi_2(V_j), D_x\phi_3(V_j)) &= \delta_{0j}\,(-4/3, 2/3, 2/3)\,, \\ (D_y\phi_1(V_j), D_y\phi_2(V_j), D_y\phi_3(V_j)) &= \delta_{0j}\left(0, -2\sqrt{3}/3, 2\sqrt{3}/3\right), \end{aligned}$$

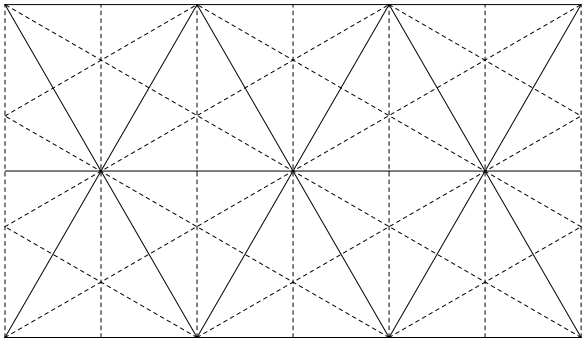

Figure 5.3: Hexagonal lattice Δ (black lines) with Powell–Sabin 6-split Δ^{PS} (black and dotted lines).

with V_0 some vertex in Δ. Then the integer translates under Γ of the basis functions ϕ_i form a basis for $S_2^1(\Delta^{PS})$. In fact, the functions ϕ_i correspond with the basis functions from [48] where the PS-triangle is chosen as in Figure 5.4, hence all results from Chapter 2 apply.

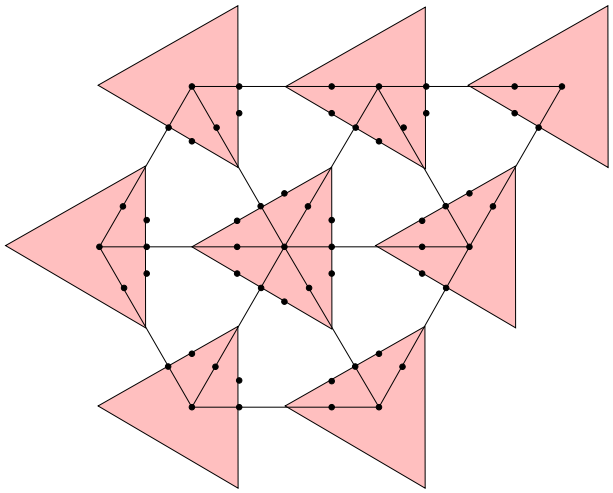

Figure 5.4: PS-triangles with PS-points in a hexagonal triangulation.

Define the 2×2 dilation matrix $M := 3I_2$, then we consider the refinement $\Delta_l := M^{-l}\Delta$, and the corresponding PS 6-split $\Delta_l^{PS} := M^{-l}\Delta^{PS}$. In general, the basis function vectors on all standard refinements Δ_l of Δ can

be written as

$$\phi_{k,l}(x) = \Phi(M^l x - \Gamma k), \qquad k \in \mathbb{Z}^2, \quad x \in \mathbb{R}^2,$$

and the set $\left\{3^l \phi_{k,l} \mid k \in \mathbb{Z}^2\right\}$ forms an L^2-stable basis of S_l, see Corollary 2.5.7. The scaling vector Φ satisfies a matrix refinement equation of the form

$$\Phi(x) = \sum_{k \in \mathbb{Z}^2} A_k \Phi(Mx - \Gamma k), \quad x \in \mathbb{R}^2, \tag{5.22}$$

where the 3×3 mask coefficient matrices A_k are given in Appendix C. The update stencil for the wavelet function vectors is different for a new vertex on the edge or a new vertex in the interior of an old triangle. Both stencils are shown in Figure 5.5. A wavelet function of a new vertex on an edge is updated by the scaling function vectors of the two neighbouring old vertices on that edge. Because there are three basis functions associated with each function vector, the width of this stencil is six. For the wavelet functions of a new vertex in the interior of an old triangle, the scaling function vectors on the corners of the triangle are used. This yields a stencil of width nine. After an extensive but straightforward computation we find that the dual

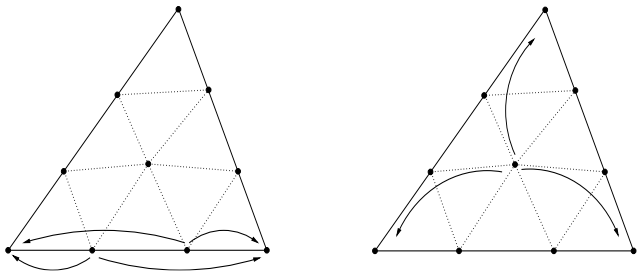

(a) vertex on edge (b) vertex in interior

Figure 5.5: The update stencil.

scaling function vectors satisfy the refinement equation

$$\widetilde{\Phi}(x) = \sum_{k \in \mathbb{Z}^2} \widetilde{A}_k \widetilde{\Phi}(Mx - \Gamma k), \quad x \in \mathbb{R}^2, \tag{5.23}$$

where the 3×3 mask coefficient matrices $\widetilde{A}_k$ are given in Appendix C. These dual function vectors exist in L_2 in distributional sense (the symbol $\widetilde{P}(\omega)$ satisfies Condition E: 1 is a simple eigenvalue of $\widetilde{P}(0)$ and all other

eigenvalues lie inside the open unit disk), but Theorem 5.3.1 is not satisfied. The transition operator $T_{\tilde{P}}$ does not satisfy Condition E. Hence we cannot use Theorem 5.3.2 to estimate the range of stability, but we use Theorem 5.3.4 and we find that these Powell–Sabin spline wavelets are a Riesz basis for $H^s(\mathbb{R}^2)$ for all $0.802774 < s < 2.5$. Figure 5.6 depicts Φ and Ψ.

Remark 5.4.1. *The same can be done for dyadically refined PS spline spaces, provided that the initial triangulation is not highly irregular, see the discussion in Section 3.2. On uniform triangulations we can show, by Theorem 5.3.4, that these wavelets are a Riesz basis for $H^s(\mathbb{R}^2)$ for all $0.431898 < s < 2.5$, see [84].*

5.5 Playing around on uniform grids

When a certain application does not require to work on a non-uniform grid, uniform grids are a much better choice, since all computations can be done in advance. The lifting scheme allows one to create wavelets with certain properties such as vanishing moments, symmetry, etc. The remaining degrees of freedom can be chosen in such a way that the range of stability is as large as possible by solving a minimization problem. Let us demonstrate this principle with an example. Consider the piecewise Hermite cubics defined by

$$\begin{aligned} \phi_1(x) &:= \begin{cases} (x+1)^2(-2x+1), & x \in [-1,0], \\ (1-x)^2(2x+1), & x \in [0,1] \end{cases} \\ \phi_2(x) &:= \begin{cases} (x+1)^2 x, & x \in [-1,0], \\ (1-x)^2 x, & x \in [0,1] \end{cases} . \end{aligned}$$

Integer translates of ϕ_1, ϕ_2 generate the space of C^1 piecewise cubic functions on $\mathbb{R}$ which interpolate function values and first derivatives at the integers. Define the generator $\Phi(x) = (\phi_1(x), \phi_2(x))^T$. Then $\Phi(x)$ satisfies the refinement equation

$$\Phi(x) = \begin{bmatrix} \frac{1}{2} & \frac{3}{4} \\ -\frac{1}{8} & -\frac{1}{8} \end{bmatrix} \Phi(2x+1) + \begin{bmatrix} 1 & 0 \\ 0 & \frac{1}{2} \end{bmatrix} \Phi(2x) + \begin{bmatrix} \frac{1}{2} & -\frac{3}{4} \\ \frac{1}{8} & -\frac{1}{8} \end{bmatrix} \Phi(2x-1).$$

The wavelets can be represented by the generator $\Psi(x) = (\psi_1(x), \psi_2(x))^T$. We define the update stencil for a new grid point as the two neighbouring coarser grid points. So we get

$$\Psi(x) = \Phi(2x-1) - \begin{bmatrix} \alpha_1 & \alpha_2 \\ \beta_1 & \beta_2 \end{bmatrix} \Phi(x) - \begin{bmatrix} \alpha_3 & \alpha_4 \\ \beta_3 & \beta_4 \end{bmatrix} \Phi(x-1).$$

Suppose that we want two vanishing moments, ψ_1 has to be symmetric, like ϕ_1, and ψ_2 has to be anti-symmetric, like ϕ_2. Then we need 6 degrees of

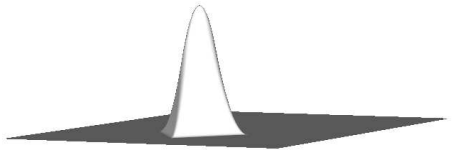

(a) Φ

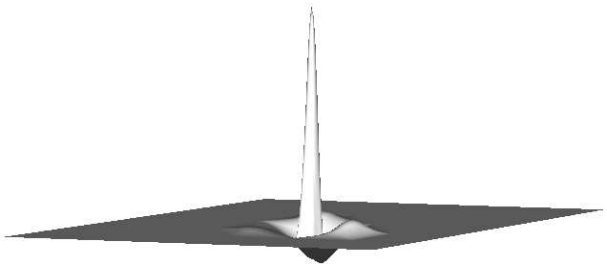

(b) Ψ (interior vertex)

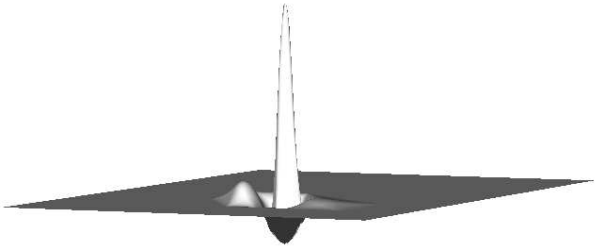

(c) Ψ (vertex on edge)

Figure 5.6: Powell–Sabin spline wavelet on $\mathbb{R}^2$.

freedom to satisfy these properties. Hence 2 degrees of freedom remain and the dual generator $\widetilde{\Phi}(x)$ satisfies the refinement equation

$$\begin{aligned}
\widetilde{\Phi}(x) &= \begin{bmatrix} -\frac{9}{40} - \frac{\beta_2}{5} & -\frac{7}{60} - \frac{\beta_2}{15} \\ \alpha_2 + \frac{3\beta_2}{2} & \frac{\alpha_2+\beta_2}{2} \end{bmatrix} \widetilde{\Phi}(2x+2) \\
&+ \begin{bmatrix} \frac{1}{2} & \frac{1}{30} - \frac{4\beta_2}{15} \\ -2\alpha_2 & 2\beta_2 \end{bmatrix} \widetilde{\Phi}(2x+1) \\
&+ \begin{bmatrix} \frac{29}{20} + \frac{2\beta_2}{5} & 0 \\ 0 & 4 - \alpha_2 + \beta_2 \end{bmatrix} \widetilde{\Phi}(2x) \\
&+ \begin{bmatrix} \frac{1}{2} & -\frac{1}{30} + \frac{4\beta_2}{15} \\ 2\alpha_2 & 2\beta_2 \end{bmatrix} \widetilde{\Phi}(2x-1) \\
&+ \begin{bmatrix} -\frac{9}{40} - \frac{\beta_2}{5} & \frac{7}{60} + \frac{\beta_2}{15} \\ -\alpha_2 - \frac{3\beta_2}{2} & \frac{\alpha_2+\beta_2}{2} \end{bmatrix} \widetilde{\Phi}(2x-2)
\end{aligned}$$

Theorems 5.3.3 and 5.3.4 characterize the range of stability, and Theorem 5.3.2 tells us how to compute the smoothness of $\widetilde{\Phi}(x)$. We use the minimization toolbox in Matlab to compute the optimal values (i.e. those values that give the largest range of stability) for the two remaining degrees of freedom α_2 and β_2 . We find $\alpha_2 = \frac{11}{7}$ and $\beta_2 = -\frac{6}{11}$, or

$$\Psi(x) = \Phi(2x-1) - \begin{bmatrix} \frac{1}{4} & \frac{11}{7} \\ -\frac{59}{660} & -\frac{6}{11} \end{bmatrix} \Phi(x) - \begin{bmatrix} \frac{1}{4} & -\frac{11}{7} \\ \frac{59}{660} & -\frac{6}{11} \end{bmatrix} \Phi(x-1).$$

These wavelets are stable for $H^s(\mathbb{R})$ with $-0.828823 < s < 2.5$. Figure 5.7 visualizes the constructed functions.

Note that these cubic Hermite spline wavelets are similar to the ones constructed in [32].

We conclude with a last example. Let us try to construct linear wavelets in $\mathbb{R}^2$ on the hexagonal lattice. We want them to have two vanishing moments, and we want hexagonal symmetry. If we use the same setting as in Section 5.4.2, then we initially have

$$\psi_{m,l} = \phi_{m,l+1} - \alpha_1\phi_{k_1,l} - \alpha_2\phi_{k_2,l} - \alpha_3\phi_{k_3,l} - \alpha_4\phi_{k_4,l}.$$

After some straightforward algebra we find that, in order to satisfy our wish list, we need three degrees of freedom out of four. Hence we keep one degree

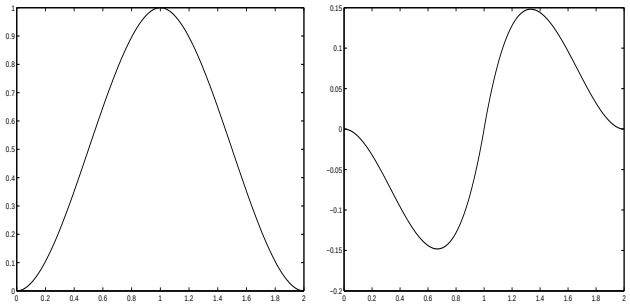

(a) ϕ_1 (b) ϕ_2

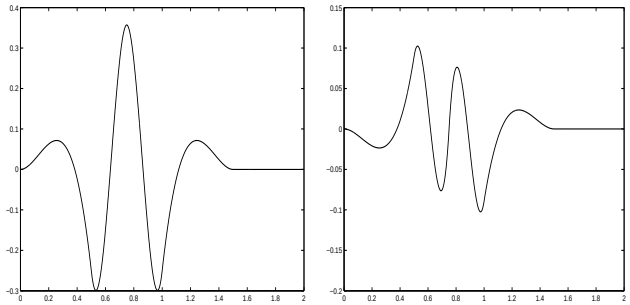

(c) ψ_1 (d) ψ_2

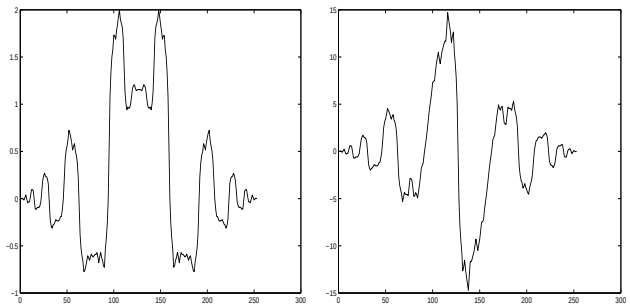

(e) $\widetilde{\phi}_1$ (f) $\widetilde{\phi}_2$

Figure 5.7: Cubic Hermite spline wavelets on $\mathbb{R}$.

of freedom to stabilize our wavelet. The dual $\widetilde{\Phi}(x)$ satisfies

$$\begin{aligned}\widetilde{\Phi}(x) &= (4-12\alpha_1)\widetilde{\Phi}(Mx) \\ &\quad +4\alpha_1 \sum_{k\in K_1} \widetilde{\Phi}(Mx-\Gamma k) \\ &\quad +(2\alpha_1-\frac{1}{2}) \sum_{k\in K_2} \widetilde{\Phi}(Mx-\Gamma k) \\ &\quad +(\frac{1}{2}-4\alpha_1) \sum_{k\in K_3} \widetilde{\Phi}(Mx-\Gamma k),\ x\in\mathbb{R}^2,\end{aligned}$$

with Γ as defined in (5.21). The optimal value for α_1 is computed with the optimization toolbox of Matlab and we find $\alpha_1 = \frac{3}{16}$. The resulting wavelet

$$\psi_{\lambda,l} = \phi_{\lambda,l+1} - \frac{3}{16}\left(\phi_{\gamma_1,l}+\phi_{\gamma_2,l}\right) + \frac{1}{16}\left(\phi_{\gamma_3,l}+\phi_{\gamma_4,l}\right)$$

is the same as the one constructed in [25] and the multilevel basis is a stable basis for $H^s(\mathbb{R}^2)$ with $-0.440765 < s < 1.5$.

5.6 Powell–Sabin spline prewavelets on uniform grids

Several (pre-)wavelet constructions on polygonal domains generate Riesz bases on H^s for s in a range around zero, see, e.g., [38, 116] and the constructions in Section 5.4.1 and Section 5.4.2. However, for most constructions at least a subset of the wavelets is only continuous, so that the range of stability is restricted to $s < \frac{3}{2}$, see, e.g., [38, 116]. The only available wavelet L_2-Riesz basis on general polygons for $s \geq \frac{3}{2}$ is the basis constructed in [37], but, from a practical point of view, this basis is very hard to construct. Note that the C^1 wavelet basis from Section 5.4.3 is only stable for Sobolev spaces with smoothness $s > 0.802774$. The wavelet basis that we present in this section is easy to construct, and it forms a Riesz basis for H^s, $|s| < \frac{5}{2}$, which makes it a useful basis for preconditioning all kinds of elliptic problems. It is however restricted to uniform triangulations. Another construction that provides a Riesz basis for H^s, $|s| < \frac{5}{2}$, is the cubic spline prewavelet basis on the uniform four-directional mesh [12]. The dimension of the cubic spline space in [12] is larger than the Powell–Sabin spline space that we use here, which gives more degrees of freedom in constructing prewavelets with certain properties, but at the cost of the construction complexity. The extra degrees of freedom are used to obtain symmetry properties. In comparison, the Powell–Sabin spline prewavelets have hexagonal symmetry for free.

The setting is almost the same as in Section 5.4.3. Define the hexagonal lattice Δ in $\mathbb{R}^2$ as the image of $\mathbb{Z}^2$ under Γ (5.21) and let Δ^{PS} be its PS-refinement, see Figure 5.3. Define a function vector $\Phi = [\phi_1, \phi_2, \phi_3]^T$, where the functions ϕ_i, $i = 1, 2, 3$, are the unique solution in $S_2^1(\Delta^{PS})$ of the Hermite interpolation problem

$$\begin{aligned}
(\phi_1(V_j), \phi_2(V_j), \phi_3(V_j)) &= \delta_{0j}\,(1/3, 1/3, 1/3)\,, \\
(D_x\phi_1(V_j), D_x\phi_2(V_j), D_x\phi_3(V_j)) &= \delta_{0j}\,(-4/3, 2/3, 2/3)\,, \\
(D_y\phi_1(V_j), D_y\phi_2(V_j), D_y\phi_3(V_j)) &= \delta_{0j}\left(0, -2\sqrt{3}/3, 2\sqrt{3}/3\right).
\end{aligned}$$

Then the integer translates under Γ of the basis functions ϕ_i form a basis for $S_2^1(\Delta^{PS})$. Define the 2×2 dilation matrix $M := 2I_2$, then we consider the dyadic refinement $\Delta_l := M^{-l}\Delta$, and the corresponding PS 6-split $\Delta_l^{PS} := M^{-l}\Delta^{PS}$. In general, the basis function vectors on all standard refinements Δ_l of Δ can be written as

$$\phi_{k,l}(x) = \Phi(M^l x - \Gamma k), \qquad k \in \mathbb{Z}^2, \quad x \in \mathbb{R}^2,$$

and the set $\left\{2^l\phi_{k,l} \mid k \in \mathbb{Z}^2\right\}$ forms an L^2-stable basis of S_l, see Corollary 2.5.7. The function vector Φ satisfies a matrix refinement equation of the form

$$\Phi(u) = \sum_{k\in\mathbb{Z}^2} A_k \Phi(Mu - \Gamma k), \quad u \in \mathbb{R}^2, \tag{5.24}$$

where A_k are 3×3 mask coefficient matrices. Moreover, $A_{(-1,-1)}$ and $A_{(0,-1)}$ are given by

$$\frac{1}{4}\begin{bmatrix} 1 & 0 & 2 \\ 0 & 1 & 2 \\ 0 & 0 & 0 \end{bmatrix}, \quad \frac{1}{4}\begin{bmatrix} 1 & 0 & 0 \\ 2 & 0 & 2 \\ 0 & 0 & 1 \end{bmatrix},$$

$A_{(-1,0)}$, $A_{(0,0)}$ and $A_{(0,1)}$ are given by

$$\frac{1}{4}\begin{bmatrix} 0 & 2 & 2 \\ 0 & 1 & 0 \\ 0 & 0 & 1 \end{bmatrix}, \quad \frac{1}{6}\begin{bmatrix} 4 & 1 & 1 \\ 1 & 4 & 1 \\ 1 & 1 & 4 \end{bmatrix}, \quad \frac{1}{4}\begin{bmatrix} 0 & 0 & 0 \\ 2 & 1 & 0 \\ 2 & 0 & 1 \end{bmatrix},$$

and $A_{(0,1)}$ and $A_{(1,1)}$ are given by

$$\frac{1}{4}\begin{bmatrix} 1 & 2 & 0 \\ 0 & 0 & 0 \\ 0 & 2 & 1 \end{bmatrix}, \quad \frac{1}{4}\begin{bmatrix} 1 & 0 & 0 \\ 0 & 1 & 0 \\ 2 & 2 & 0 \end{bmatrix},$$

see e.g. [127].

We are interested in complement spaces W_l of S_l such that

$$S_{l+1} = S_l \oplus^{\perp_{L_2}} W_l,$$

hence

$$L_2(\mathbb{R}^2) = \bigoplus_{l\in\mathbb{Z}}^{\perp_{L_2}} W_l.$$

We will refer to the basis functions of W_l as *prewavelets* or *semi-orthogonal* wavelets. Note that the prewavelets have three vanishing moments since constant, linear and quadratic polynomials are contained in the space S_l.

The construction of PS prewavelets consists of two steps, cfr. [115]. First we construct a dual basis

$$\{\widetilde{\phi}_{k,l} \mid k \in \Delta_l\} \subset S_{l+1} \tag{5.25}$$

for the basis $\left\{\phi_{k,l}\ \left(\|\phi_{k,l}\|^2_{L_2}\right)^{-1} \mid k \in \Delta_l\right\}$ of S_l, i.e.

$$\left\langle \widetilde{\phi}_{k,l}, \phi^T_{m,l} \right\rangle_{L_2} = \begin{cases} \|\phi_{k,l}\|^2_{L_2} & k = m, \\ 0 & k \neq m, \end{cases} \tag{5.26}$$

with $\|\phi_{k,l}\|^2_{L_2} := \mathrm{diag}(\langle \phi_{k,l}, \phi^T_{k,l}\rangle_{L_2})$. Since we search for a dual basis in the space S_{l+1} which is much larger than S_l, this basis is not unique. We will use this freedom to select a dual basis that is locally supported. Then, as the second step, for $m \in \Delta_{l+1} \setminus \Delta_l$ we define

$$\psi_{m,l} := \phi_{m,l+1} - \sum_{k\in\Delta_l} \left\langle \phi_{m,l+1}, \phi^T_{k,l} \right\rangle_{L_2} \left(\|\phi_{k,l}\|^2_{L_2}\right)^{-1} \widetilde{\phi}_{l,k}. \tag{5.27}$$

Note that, because of (5.25) and (5.26), $\psi_{m,l} \in S_{l+1} \bigcap S_l^{\perp_{L_2}}$.

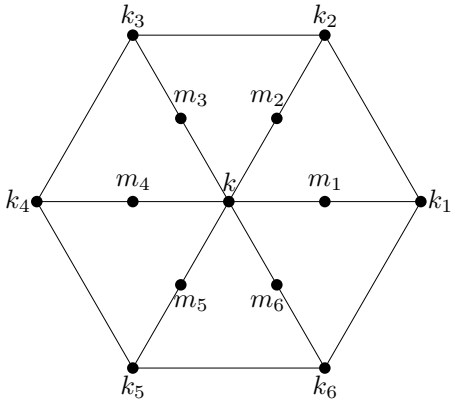

Figure 5.8: Grid around k.

Let $k \in \Delta_l$ and define $k_1, \ldots, k_6 \in \Delta_l$ and $m_1, \ldots, m_6 \in \Delta_{l+1}$ as in Figure 5.8. We look for a dual function vector $\widetilde{\phi}_{k,l}$ of the form

$$\widetilde{\phi}_{k,l} := \widetilde{A}_0 \phi_{k,l+1} + \sum_{i=1}^{6} \widetilde{A}_i \phi_{m_i,l+1}$$

that satisfies (5.26), where the $\widetilde{A}_i$ are 3×3 mask coefficient matrices. By construction we know that the support of each scaling vector $\phi_{k,l}$ is the set of all triangles in Δ_l that have $k \in \Delta_l$ as a common vertex. Note that, by construction, the support of $\widetilde{\phi}_{k,l}$ equals the support of $\phi_{k,l}$, see Figure 5.8. Therefore it is sufficient to solve the system

$$\begin{cases} \langle \widetilde{\phi}_{k,l}, \phi_{k,l}^T \rangle_{L_2} = \|\phi_{k,l}\|_{L_2}^2 & , \\ \langle \widetilde{\phi}_{k,l}, \phi_{k_i,l}^T \rangle_{L_2} = 0 & , \quad i = 1, \ldots, 6, \end{cases} \tag{5.28}$$

to obtain a dual basis. We have 63 equations and 63 unknown matrix entries. Since the system (5.28) is non-singular we find a unique solution,

$$\widetilde{A}_0 = \begin{bmatrix} \frac{382603}{41310} & -\frac{318649}{82620} & -\frac{318649}{82620} \\ -\frac{318649}{82620} & \frac{382603}{41310} & -\frac{318649}{82620} \\ -\frac{318649}{82620} & -\frac{318649}{82620} & \frac{382603}{41310} \end{bmatrix},$$

$$\widetilde{A}_1 = \begin{bmatrix} \frac{1691}{2754} & -\frac{551}{18360} & -\frac{551}{18360} \\ -\frac{779}{1836} & -\frac{608}{20655} & \frac{11761}{165240} \\ -\frac{779}{1836} & \frac{11761}{165240} & -\frac{608}{20655} \end{bmatrix},$$

$$\widetilde{A}_2 = \begin{bmatrix} \frac{10241}{82620} & \frac{4123}{18360} & -\frac{2204}{20655} \\ \frac{4123}{18360} & \frac{10241}{82620} & -\frac{2204}{20655} \\ -\frac{82783}{165240} & -\frac{82783}{165240} & \frac{6346}{20655} \end{bmatrix},$$

$$\widetilde{A}_3 = \begin{bmatrix} -\frac{608}{20655} & -\frac{779}{1836} & \frac{11761}{165240} \\ -\frac{551}{18360} & \frac{1691}{2754} & -\frac{551}{18360} \\ \frac{11761}{165240} & -\frac{779}{1836} & -\frac{608}{20655} \end{bmatrix},$$

$$\widetilde{A}_4 = \begin{bmatrix} \frac{6346}{20655} & -\frac{82783}{165240} & -\frac{82783}{165240} \\ -\frac{2204}{20655} & \frac{10241}{82620} & \frac{4123}{18360} \\ -\frac{2204}{20655} & \frac{4123}{18360} & \frac{10241}{82620} \end{bmatrix},$$

$$\widetilde{A}_5 = \begin{bmatrix} -\frac{608}{20655} & \frac{11761}{165240} & -\frac{779}{1836} \\ \frac{11761}{165240} & -\frac{608}{20655} & -\frac{779}{1836} \\ -\frac{551}{18360} & -\frac{551}{18360} & \frac{1691}{2754} \end{bmatrix},$$

$$\widetilde{A}_6 = \begin{bmatrix} \frac{10241}{82620} & -\frac{2204}{20655} & \frac{4123}{18360} \\ -\frac{82783}{165240} & \frac{6346}{20655} & -\frac{82783}{165240} \\ \frac{4123}{18360} & -\frac{2204}{20655} & \frac{10241}{82620} \end{bmatrix}.$$

Theorem 5.6.1. *The set*

$$\{2^{l+1}\widetilde{\phi}_{k,l} \mid k \in \Delta_l\} \cup \{2^{l+1}\phi_{m,l+1} \mid m \in \Delta_{l+1} \setminus \Delta_l\} \tag{5.29}$$

is a Riesz basis for the space S_{l+1}.

Proof. We know that $\{2^{l+1}\phi_{k,l+1} \mid k \in \Delta_{l+1}\}$ is a Riesz basis for S_{l+1}, see Corollary 2.5.7. Furthermore we have that the basis $\{2^{l+1}\phi_{k,l+1} \mid k \in \Delta_{l+1}\}$ can be transformed into the set (5.29) by a matrix operation of the form

$$M = \begin{bmatrix} K & L \\ 0 & I_n \end{bmatrix}, \tag{5.30}$$

where I_n denotes the $n \times n$ identity matrix with $n = \#\{m \in \Delta_{l+1} \setminus \Delta_l\}$. Note that we assume here that all basis function vectors are in a column vector. The matrix K has a block-structure of the form

$$K = \begin{bmatrix} \widetilde{A}_0 & 0 & 0 & \cdots \\ 0 & \widetilde{A}_0 & 0 & \cdots \\ 0 & 0 & \widetilde{A}_0 & \\ \vdots & \vdots & & \ddots \end{bmatrix},$$

and the matrix L is a sparse block-structured matrix with blocks $\widetilde{A}_i$, $i = 1, \ldots, 6$. Note that

$$M^{-1} = \begin{bmatrix} K^{-1} & -K^{-1}L \\ 0 & I_n \end{bmatrix}.$$

Clearly M is uniformly bounded and has full rank which proves our claim. □

For all l, for all $m \in \Delta_{l+1} \setminus \Delta_l$, we define the prewavelets $\psi_{m,l}$ as in (5.27). Note that these prewavelets are compactly supported. It is easily checked that $W_l = \text{span}\{\psi_{m,l} \mid m \in \Delta_{l+1} \setminus \Delta_l\}$. Indeed, suppose $w \in W_l$. Then by Theorem 5.6.1 we have

$$w = \sum_{m \in \Delta_{l+1} \setminus \Delta_l} c_m^T \phi_{m,l+1} + \sum_{k \in \Delta_l} c_k^T \widetilde{\phi}_{k,l},$$

or

$$[0 \quad 0 \quad 0] = \langle w, \phi_{k,l}^T \rangle_{L_2} = \sum_{m \in \Delta_{l+1} \setminus \Delta_l} c_m^T \langle \phi_{m,l+1}, \phi_{k,l}^T \rangle_{L_2} + c_k^T \|\phi_{k,l}\|_{L_2}^2,$$

which yields

$$c_k^T = - \sum_{m \in \Delta_{l+1} \setminus \Delta_l} c_m^T \langle \phi_{m,l+1}, \phi_{k,l}^T \rangle_{L_2} \left(\|\phi_{k,l}\|_{L_2}^2 \right)^{-1}$$

and we get

$$w = \sum_{m \in \Delta_{l+1} \setminus \Delta_l} c_m^T \psi_{m,l}.$$

Theorem 5.6.2. *The set*

$$\{2^{l+1}\psi_{m,l} \mid m \in \Delta_{l+1} \setminus \Delta_l\} \tag{5.31}$$

is a Riesz basis for the space W_l.

Proof. It is sufficient to show that

$$\left\| \sum_{m \in \Delta_{l+1} \setminus \Delta_l} c_m^T 2^{l+1} \psi_{m,l} \right\|_{L_2} \sim \|c\|_{l_2^{3\times 1}(\Delta_{l+1} \setminus \Delta_l)} .$$

With $l_2^{3\times 1}(\Delta)$ we denote the Banach space of all sequences of 3×1 vectors c_k for which $\sum_{k\in\Delta} \|c_k\|_{l_2}^2 < \infty$. By Theorem 5.6.1 and (5.27) it holds that

$$\begin{aligned}\left\| \sum_{m \in \Delta_{l+1} \setminus \Delta_l} c_m^T 2^{l+1} \psi_{m,l} \right\|_{L_2}^2 &\sim \sum_{m \in \Delta_{l+1} \setminus \Delta_l} c_m^T c_m \\ &+ \sum_{k \in \Delta_l} \left(\sum_{m \in \Delta_{l+1} \setminus \Delta_l} c_m^T \langle \phi_{m,l+1}, \phi_{k,l}^T \rangle_{L_2} \left(\|\phi_{k,l}\|_{L_2}^2 \right)^{-1} \right)^T \\ &\cdot \left(\sum_{m \in \Delta_{l+1} \setminus \Delta_l} c_m^T \langle \phi_{m,l+1}, \phi_{k,l}^T \rangle_{L_2} \left(\|\phi_{k,l}\|_{L_2}^2 \right)^{-1} \right) .\end{aligned}$$

Both for fixed $k \in \Delta_l$ or for fixed $m \in \Delta_{l+1} \setminus \Delta_l$ the number of nonzero inner products $\langle \phi_{m,l+1}, \phi_{k,l}^T \rangle_{L_2}$ is bounded above by an absolute constant. Furthermore it is straightforward to check that

$$0 \le \langle \phi_{m,l+1}, \phi_{k,l}^T \rangle_{L_2} \left(\|\phi_{k,l}\|_{L_2}^2 \right)^{-1} \le C$$

with C an absolute constant. This concludes the proof. □

Remark 5.6.3. *Note that the prewavelets $\psi_{m,l}$ and the dual functions $\widetilde{\phi}_{k,l}$ can be obtained as scaled translates of a finite subset of them. Indeed, we have that*

$$\begin{aligned}\psi_{m,l}(u) &= \Psi(M^l(u-m)), \quad m \in \Delta_{l+1} \setminus \Delta_l,\ u \in \mathbb{R}^2, \\ \widetilde{\phi}_{k,l}(u) &= \widetilde{\Phi}(M^l(u-k)), \quad k \in \Delta_l,\ u \in \mathbb{R}^2,\end{aligned}$$

with Ψ and $\widetilde{\Phi}$ a generating wavelet vector resp. a generating dual scaling vector. Therefore the inner products appearing in the construction above have to be computed only once. As a consequence of the hexagonal symmetry of Φ, both $\widetilde{\Phi}$ and Ψ have also hexagonal symmetry, i.e. the corresponding generating functions are invariant by a rotation of $2\pi/3$.

Remark 5.6.4. *We are interested in determining the exact range of Sobolev exponents s for which the prewavelet basis forms a Riesz basis for H^s. It turns out that the range of such s is determined by the Sobolev regularity $s(\Phi)$ of the scaling vector Φ, i.e. the wavelet system is a Riesz basis for H^s for all s with $-s_\Phi < s < s_\Phi$ and that this interval is sharp, cfr. [104]. We already know that PS splines are in the Sobolev spaces H^s for any $s < 5/2$, see Chapter 3.*

Remark 5.6.5. *The above construction can be used to construct prewavelets on bounded domains in $\mathbb{R}^2$ due to the explicit construction that we use.*

Finally we visualize a a dual scaling function and a prewavelet, see Figures 5.9 and 5.10.

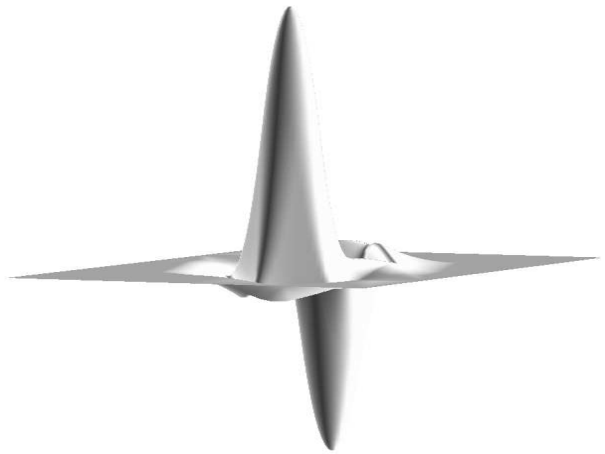

Figure 5.9: Dual scaling function.

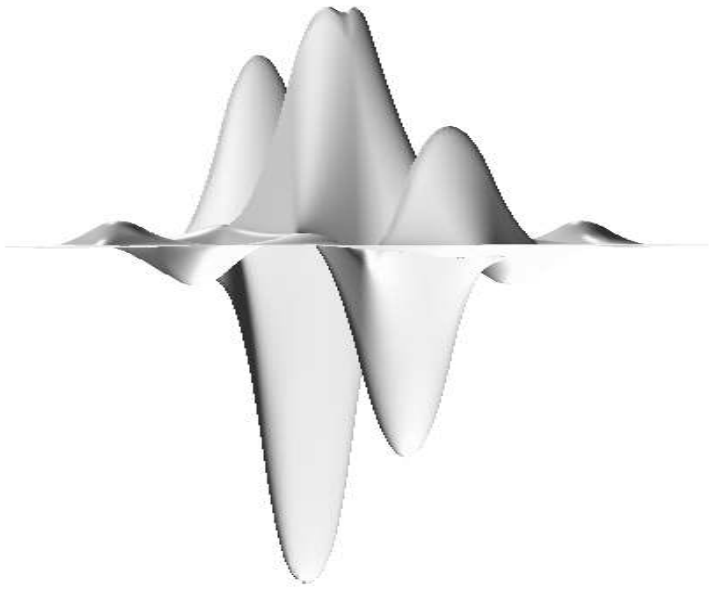

Figure 5.10: Prewavelet.

Chapter 6

Elliptic PDEs on the two–sphere

6.1 Introduction

The biharmonic equation on a sphere arises from several applications in physical geodesy, oceanography and meteorology, see, e.g., [15]. For instance, the stream function of incompressible Stokes flow, a widely used model equation in meteorology, is the solution of a biharmonic equation. The geometry of the sphere is a major obstacle in constructing a suitable approximation space for solving the biharmonic equation or any other partial differential equation. Often a transformation into spherical coordinates is used which gives rise to singularities at the "poles" of the sphere. Our approach to deal with the spherical geometry will be to work with homogeneous polynomials in the three-dimensional Cartesian space. In this way, operations such as integration and differentiation can be carried out directly within the usual context of Cartesian coordinates.

Let Ω be a subset of the unit sphere S in $\mathbb{R}^3$. We are interested in solving the boundary value problem

$$\Delta_S^2 u = f, \quad \text{on} \quad \Omega, \qquad u = \frac{\partial u}{\partial \overline{n}} = 0, \quad \text{on} \quad \partial\Omega, \tag{6.1}$$

where Δ_S is the *Laplace–Beltrami operator* on S, and $\overline{n}$ is the outward normal to $\partial\Omega$ tangent to S. In order to work with Cartesian coordinates it is important that we write down the Laplace–Beltrami operator in terms of the *tangential gradient*

$$\nabla_S u := \nabla \widetilde{u} - (n \cdot \nabla \widetilde{u}) n,$$

with $\widetilde{u}$ a smooth continuation of u to a neighborhood of S, and n the (outward) normal to the surface S. Note that $\nabla_S u$ depends on $u|_S$ only. The Laplace–Beltrami operator on S can now be defined as

$$\Delta_S := \nabla_S \cdot \nabla_S.$$

We also define the spherical Sobolev space $H^2(\Omega)$ [80, p. 37] that we shall use throughout this chapter. This is the smoothness space of functions that have weak tangential derivatives up to order two which are in $L_2(\Omega)$, i.e.

$$H^2(\Omega) = \left\{ u |\ u \in L_2(\Omega), \quad \nabla_S u \in L_2(\Omega), \quad \nabla_S (\nabla_S)^T u \in L_2(\Omega) \right\}. \tag{6.2}$$

With $H^2(\Omega)$ we can associate the norm

$$\|u\|_{H^2(\Omega)} := \|u\|_{L_2(\Omega)} + \|\nabla_S u\|_{L_2(\Omega)} + \left\|\nabla_S (\nabla_S)^T u\right\|_{L_2(\Omega)}, \tag{6.3}$$

and with $H_0^2(\Omega)$ we mean the closure of $C_0^\infty(\Omega)$, the space of C^∞ continuous functions with compact support in Ω, in $H^2(\Omega)$. We now formulate the basic existence of a solution for (6.1) (see, for example, [6, 52]). Suppose that $\partial\Omega \neq \emptyset$. For every $f \in L_2(\Omega)$ there exists a unique weak solution $u \in H_0^2(\Omega)$ of the problem (6.1), i.e. for every $v \in H_0^2(\Omega)$

$$\langle \Delta_S u, \Delta_S v \rangle_{L_2(\Omega)} = \langle f, v \rangle_{L_2(\Omega)}. \tag{6.4}$$

Suppose that $\partial\Omega = \emptyset$. For every $f \in L_2(\Omega)$ with $\int_S f \, d\omega = 0$ there exists a weak solution $u \in H^2(\Omega)$ of the problem $\Delta_S^2 u = f$, i.e. Equation (6.4) holds for all $v \in H^2(\Omega)$, and u is unique up to a constant.

All known constructions of C^1 hierarchical finite element bases (see [36, 41, 102], and the constructions in the previous chapters) have a planar parameter domain. In consequence, when solving the biharmonic equation (6.1) on the complete surface of the unit sphere S, difficulties will arise at the "poles" of the sphere when using these preconditioners. Therefore it is the objective of this chapter to construct a C^1 hierarchical basis with a spherical parameter domain that is suitable for the numerical treatment of the biharmonic equation on the sphere.

Equation (6.4) defines an energy norm $\|\cdot\|_E$ given by

$$\|\cdot\|_E := \langle \Delta_S \cdot\, , \Delta_S \cdot \rangle_{L_2(\Omega)}^{1/2}.$$

Assume that for all test functions v in some subspace $S \subset H^2(\Omega)$

$$\|v\|_E \sim \|v\|_{H^2(\Omega)} \tag{6.5}$$

holds, and assume that we find a multiscale basis for S that is strongly stable with respect to the norm $\|\cdot\|_{H^2(\Omega)}$ in the sense of Definition 3.4.1,

then, by (1.12), we find that the stiffness matrix for (6.1) with respect to this multiscale basis has a uniformly bounded condition number.

This chapter is organized as follows. In Section 6.2 we introduce homogeneous and spherical spline spaces as in [2, 3, 4] that will allow us to create bases on the sphere. More specifically, in Section 6.3, we extend the classical result of Powell and Sabin [107]: we derive C^1 continuous piecewise quadratic spline spaces of Powell–Sabin type on the sphere, see our paper [86]. In order to apply the theory above we need suitable basis functions for these spaces that are stable in some sense. In Section 6.4 we present an algorithm to extend bivariate PS B-splines to spherical PS B-splines. Furthermore we prove that properties of the bivariate basis such as partition of unity and stability are inherited by the spherical B-splines. Then, in Section 6.5, we construct a weakly stable hierarchical basis on the sphere, and in Section 6.6 we construct optimal BPX preconditioners for 2nd and 4th order elliptic PDEs on the sphere and we provide some numerical experiments. All these results are published in our papers [86, 92].

6.2 Homogeneous and spherical spline spaces

We begin by introducing homogeneous and spherical spline spaces following [2, 3, 4]. A function f defined on $\mathbb{R}^3$ is *homogeneous of degree d* provided that $f(\alpha v) = \alpha^d f(v)$ for all real α and all $v \in \mathbb{R}^3$. We are interested in the space $\mathbb{H}_d$ of *trivariate polynomials of degree d that are homogeneous of degree d*. The space $\mathbb{H}_d$ is a $\binom{d+2}{2}$ dimensional subspace of the space of trivariate polynomials of degree d. Let $\{v_1, v_2, v_3\}$ be a set of linearly independent unit vectors in $\mathbb{R}^3$. We call

$$\mathcal{T} := \{v \in \mathbb{R}^3 \mid v = b_1(v)v_1 + b_2(v)v_2 + b_3(v)v_3 \quad \text{with} \quad b_i(v) \geq 0\} \tag{6.6}$$

the *trihedron* generated by $\{v_1, v_2, v_3\}$. Each $v \in \mathbb{R}^3$ can be written in the form

$$v = b_1(v)v_1 + b_2(v)v_2 + b_3(v)v_3, \tag{6.7}$$

and we call $b_1(v), b_2(v), b_3(v)$ the *trihedral coordinates of v with respect to $\mathcal{T}$*. Given an integer $d \geq 0$, the *homogeneous Bernstein basis polynomials of degree d on $\mathcal{T}$* are the polynomials

$$B^d_{ijk}(v) := \frac{d!}{i!j!k!} b_1(v)^i b_2(v)^j b_3(v)^k, \qquad i + j + k = d, \tag{6.8}$$

and they form a basis for $\mathbb{H}_d$. We define a *spherical triangle* as the restriction of a trihedron $\mathcal{T}$ to the unit sphere S. The restrictions of the trihedral coordinates (6.7) to a spherical triangle with vertices v_1, v_2 and v_3 are

called *spherical barycentric coordinates*. Any homogeneous polynomial p of degree d and its restriction to a spherical triangle τ has a Bernstein-Bézier representation with respect to τ

$$p(v) := \sum_{i+j+k=d} c_{ijk} B^d_{ijk}(v), \tag{6.9}$$

and the coefficients c_{ijk} are the Bézier ordinates.

Homogeneous polynomials in their Bernstein–Bézier representation can be evaluated efficiently using the classical *de Casteljau algorithm*:

$$p(v) = c^d_{000}(v)$$

with

$$\begin{aligned} c^0_{ijk}(v) &:= c_{ijk}, \\ c^l_{ijk}(v) &:= b_1(v)c^{l-1}_{i+1,j,k} + b_2(v)c^{l-1}_{i,j+1,k} + b_3(v)c^{l-1}_{i,j,k+1}, \\ &\quad l = 1, \ldots, d, \quad i+j+k = d-l. \end{aligned}$$

Also continuity conditions can be expressed analogous to the classical bivariate case. Let $\mathcal{T}$ and $\widetilde{\mathcal{T}}$ be trihedra with vertices $\{v_1, v_2, v_3\}$ and $\{v_4, v_2, v_3\}$. A necessary and sufficient condition for p and $\widetilde{p}$ to be C^r continuous across the common boundary is

$$\widetilde{c}_{ijk} = c^i_{0jk}(v_4), \quad i = 0, 1, \ldots, r, \quad i+j+k = d. \tag{6.10}$$

The directional derivative of a homogeneous Bernstein–Bézier polynomial with respect to direction g is given by

$$D_g p(v) = d \sum_{i+j+k=d-1} c^1_{ijk}(g) B^{d-1}_{ijk}(v). \tag{6.11}$$

We write $\mathbb{H}_d(\Omega)$ for the restriction of $\mathbb{H}_d$ to any subset Ω of the unit sphere S, and refer to $\mathbb{H}_d(\Omega)$ as the *space of spherical polynomials of degree* d. Similarly, we write $\mathbb{H}_d(H)$ for the restriction of $\mathbb{H}_d$ to any hyperplane H in $\mathbb{R}^3$. This is just the well-known space of bivariate polynomials. All these spaces have the same dimension $\binom{d+2}{2}$. Let Δ be a conforming spherical triangulation of $\Omega \subset S$. Then we define the *space of spherical splines of degree* d *and smoothness* r *associated with* Δ to be

$$S^r_d(\Delta) := \{s \in C^r(S) \mid s|_\tau \in \mathbb{H}_d(\tau),\ \tau \in \Delta\}, \tag{6.12}$$

where $s|_\tau$ denotes the restriction of s to the spherical triangle τ. Keeping up continuity conditions (6.10) between neighbouring spherical triangles results in nontrivial relations between their Bézier ordinates. Therefore we will focus on the Powell–Sabin 6-split of a triangulation to overcome this problem.

6.3 Spherical PS splines

The Powell–Sabin 6-split Δ^{PS} of a spherical triangulation Δ is of course very similar to the PS 6-split of a planar triangulation, see Figure 2.3. Each spherical triangle $T_j \in \Delta$ is divided into six smaller triangles with a common vertex as follows:

1. Define the interior point Z_j for each triangle T_j as the incenter of the triangle T_j. If V_1, V_2, V_3 are the vertices of T_j then we define its incenter as the point on S that is obtained by radially projecting the incenter of the planar triangle with vertices V_i, $i = 1, 2, 3$, onto S. Suppose that two triangles T_i and T_j have a common edge (circle segment), then the arc that joins Z_i and Z_j intersects this common edge (circle segment) at a point R_{ij} between its vertices. The arc between two points on S is defined as the circle segment connecting these two points obtained as the intersection of S with a plane passing through the two points and the origin.
2. Join the points Z_j to the vertices of T_j.
3. For each edge (circle segment) of T_j
   - that belongs to the boundary $\partial\Omega$, join Z_j to some point of the edge.
   - that is common to a triangle T_i, join Z_j to R_{ij}.

We restrict our attention to one of the original triangles in Δ with vertices V_1, V_2, V_3 and incenter Z, and the intersection points on the edges are R_{12}, R_{23}, R_{31}. Let g_i and h_i be independent unit vectors lying in the tangent plane of S at V_i, $i = 1, 2, 3$ (see Figure 6.1). The following interpolation problem can be considered for spherical splines. Given any set of values $(\alpha_i, \beta_i, \gamma_i)$, $i = 1, \ldots, N$, find $s(v) \in S_2^1(\Delta^{PS})$ such that

$$\begin{aligned} s(V_i) &= \alpha_i, \\ D_{g_i} s(V_i) &= \beta_i, \\ D_{h_i} s(V_i) &= \gamma_i, \end{aligned} \tag{6.13}$$

for all $i = 1, \ldots, N$. Below we calculate the unique Bézier ordinates of a spherical PS spline satisfying (6.13). This shows that the classical result of Powell and Sabin [107] can be extended to spherical domains, i.e. the dimension of the spherical spline space $S_2^1(\Delta^{PS})$ equals $3N$.

Let the different points in $T(V_1, V_2, V_3) \in \Delta$ have the trihedral coordinates

$$\begin{array}{ccc} V_1 = (1,0,0) & V_2 = (0,1,0) & V_3 = (0,0,1) \\ R_{12} = (\lambda_1, \lambda_2, 0) & R_{23} = (0, \mu_2, \mu_3) & R_{31} = (\nu_1, 0, \nu_3) \end{array} \tag{6.14}$$

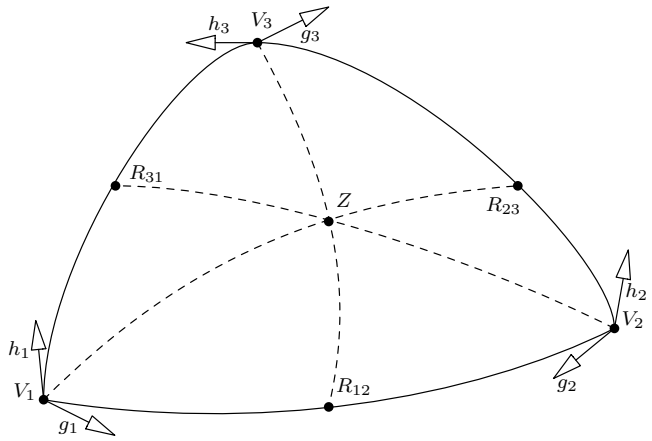

Figure 6.1: The spherical Powell–Sabin macro-element.

and let Z with trihedral coordinates (a, b, c) be the incenter of the triangle. Denote the 19 Bézier ordinates in triangle T by s_i, u_i, v_i, w_i, r_i, θ_i, $i = 1, 2, 3$, and ω, as in the planar case, see Figure 4.4. From (6.11) the following formula is derived:

$$D_g s(V_1) = 2\left[b_1(g)c_{2,0,0} + b_2(g)c_{1,1,0} + b_3(g)c_{1,0,1}\right].$$

If we apply this formula to triangle $\tau_1(V_1, R_{12}, Z)$ we deduce that

$$D_{g_1} s(V_1) = \beta_1 = 2\left[b_1^{\tau_1}(g_1)s_1 + b_2^{\tau_1}(g_1)u_1 + b_3^{\tau_1}(g_1)w_1\right] \tag{6.15}$$

and

$$D_{h_1} s(V_1) = \gamma_1 = 2\left[b_1^{\tau_1}(h_1)s_1 + b_2^{\tau_1}(h_1)u_1 + b_3^{\tau_1}(h_1)w_1\right], \tag{6.16}$$

where $b_1^{\tau_1}, b_2^{\tau_1}, b_3^{\tau_1}$ are the trihedral coordinates with respect to $\tau_1(V_1, R_{12}, Z)$. Similarly for triangle $\tau_2(V_1, R_{31}, Z)$ we find

$$D_{g_1} s(V_1) = \beta_1 = 2\left[b_1^{\tau_2}(g_1)s_1 + b_2^{\tau_2}(g_1)v_1 + b_3^{\tau_2}(g_1)w_1\right] \tag{6.17}$$

and

$$D_{h_1} s(V_1) = \gamma_1 = 2\left[b_1^{\tau_2}(h_1)s_1 + b_2^{\tau_2}(h_1)v_1 + b_3^{\tau_2}(h_1)w_1\right]. \tag{6.18}$$

From the C^1 continuity (6.10) across the edge $[V_1 Z]$ we deduce that

$$v_1 = s_1 b_1^{\tau_1}(R_{31}) + u_1 b_2^{\tau_1}(R_{31}) + w_1 b_3^{\tau_1}(R_{31}). \tag{6.19}$$

From (6.14) we find after some straightforward computations that

$$\begin{aligned} b_1^{\tau_1}(\cdot) &= b_1(\cdot) - \frac{\lambda_1}{\lambda_2} b_2(\cdot) + \frac{\lambda_1 b - \lambda_2 a}{\lambda_2 c} b_3(\cdot), \\ b_2^{\tau_1}(\cdot) &= \frac{1}{\lambda_2} b_2(\cdot) - \frac{b}{\lambda_2 c} b_3(\cdot), \\ b_3^{\tau_1}(\cdot) &= \frac{1}{c} b_3(\cdot), \end{aligned} \tag{6.20}$$

where b_1, b_2, b_3 are the trihedral coordinates with respect to $T(V_1, V_2, V_3)$, and similarly

$$\begin{aligned} b_1^{\tau_2}(\cdot) &= b_1(\cdot) - \frac{\nu_1}{\nu_3} b_3(\cdot) + \frac{\nu_1 c - \nu_3 a}{\nu_3 b} b_2(\cdot), \\ b_2^{\tau_2}(\cdot) &= \frac{1}{\nu_3} b_3(\cdot) - \frac{c}{\nu_3 b} b_2(\cdot), \\ b_3^{\tau_2}(\cdot) &= \frac{1}{b} b_2(\cdot). \end{aligned} \tag{6.21}$$

Equations (6.15)-(6.21) together with $s_1 = \alpha_1$ give the following unique solution for the Bézier ordinates s_1, u_1, v_1, w_1:

$$s_1 = \alpha_1, \tag{6.22}$$

$$u_1 = \frac{\alpha_1 \lambda_1 \begin{vmatrix} b_2(g_1) & b_2(h_1) \\ b_3(g_1) & b_3(h_1) \end{vmatrix} - \frac{\lambda_2}{2} \begin{vmatrix} b_3(g_1) & \beta_1 \\ b_3(h_1) & \gamma_1 \end{vmatrix} - \alpha_1 \lambda_2 \begin{vmatrix} b_1(g_1) & b_1(h_1) \\ b_3(g_1) & b_3(h_1) \end{vmatrix}}{\begin{vmatrix} b_2(g_1) & b_2(h_1) \\ b_3(g_1) & b_3(h_1) \end{vmatrix}}, \tag{6.23}$$

$$v_1 = \frac{\alpha_1 \nu_1 \begin{vmatrix} b_2(g_1) & b_2(h_1) \\ b_3(g_1) & b_3(h_1) \end{vmatrix} + \frac{\nu_3}{2} \begin{vmatrix} b_2(g_1) & \beta_1 \\ b_2(h_1) & \gamma_1 \end{vmatrix} + \alpha_1 \nu_3 \begin{vmatrix} b_1(g_1) & b_1(h_1) \\ b_2(g_1) & b_2(h_1) \end{vmatrix}}{\begin{vmatrix} b_2(g_1) & b_2(h_1) \\ b_3(g_1) & b_3(h_1) \end{vmatrix}}, \tag{6.24}$$

$$w_1 = \left(a - \frac{\lambda_1}{\lambda_2} b - \frac{\nu_1}{\nu_3} c \right) \alpha_1 + \frac{b}{\lambda_2} u_1 + \frac{c}{\nu_3} v_1. \tag{6.25}$$

In a similar way we can compute the Bézier ordinates s_2, u_2, v_2, w_2 and s_3, u_3, v_3, w_3. The remaining Bézier ordinates are obtained from the C^1-

continuity conditions (6.10), i.e.

$$\begin{aligned} r_1 &= \mu_2 u_2 + \mu_3 v_3, \\ \theta_1 &= \mu_2 w_2 + \mu_3 w_3, \\ r_2 &= \nu_3 u_3 + \nu_1 v_1, \\ \theta_2 &= \nu_3 w_3 + \nu_1 w_1, \\ r_3 &= \lambda_1 u_1 + \lambda_2 v_2, \\ \theta_3 &= \lambda_1 w_1 + \lambda_2 w_2, \\ \omega &= a w_1 + b w_2 + c w_3. \end{aligned} \tag{6.26}$$

6.4 A B-spline basis for spherical PS spline spaces

If for each vertex V_i in Δ we choose numbers $(\alpha_{ij}, \beta_{ij}, \gamma_{ij})$, $j = 1, 2, 3$, that form a set of 3 linear independent triplets, then every $s(v) \in S_2^1(\Delta^{PS})$ has a unique representation

$$s(v) = \sum_{i=1}^{N} \sum_{j=1}^{3} c_{ij} B_{ij}(v) \tag{6.27}$$

where the splines $B_{ij}(v)$ are defined as the solution of the interpolation problem (6.13) with

$$(\alpha_k, \beta_k, \gamma_k) = (\delta_{ik}\alpha_{ij}, \delta_{ik}\beta_{ij}, \delta_{ik}\gamma_{ij}), \qquad k = 1, \ldots, N, \tag{6.28}$$

where δ_{ik} represents the Kronecker delta. Such a spline $B_{ij}(v)$ will further be called a spherical PS B-spline. It can easily be shown that the spherical PS B-spline $B_{ij}(v)$ vanishes outside its molecule M_i (i.e. the union of all triangles $T_k \in \Delta$ that contain vertex V_i). So our definition of spherical PS B-spline implies local support.

Let us focus again on triangle $T(V_1, V_2, V_3)$. Assume that V_1 has coordinates $(0, 0, 1)$ in $\mathbb{R}^3$ and that g_1 and h_1 have coordinates $(1, 0, 0)$ resp. $(0, 1, 0)$ in $\mathbb{R}^3$. Let V_2 and V_3 have coordinates (x_2, y_2, z_2) resp. (x_3, y_3, z_3) in $\mathbb{R}^3$. By using Equations (6.22)-(6.26) we find the Bézier ordinates of the B-spline $B_{1j}(v)$ as shown in Figure 6.2 where

$$\begin{aligned} L_{1j} &= \lambda_1 \alpha_{1j} + \tfrac{\lambda_2}{2}(\beta_{1j} x_2 + \gamma_{1j} y_2 + 2\alpha_{1j} z_2) \\ L'_{1j} &= \nu_1 \alpha_{1j} + \tfrac{\nu_3}{2}(\beta_{1j} x_3 + \gamma_{1j} y_3 + 2\alpha_{1j} z_3) \\ \widetilde{L}_{1j} &= a\alpha_{1j} + \tfrac{b}{2}(\beta_{1j} x_2 + \gamma_{1j} y_2 + 2\alpha_{1j} z_2) + \tfrac{c}{2}(\beta_{1j} x_3 + \gamma_{1j} y_3 + 2\alpha_{1j} z_3) \end{aligned} \tag{6.29}$$

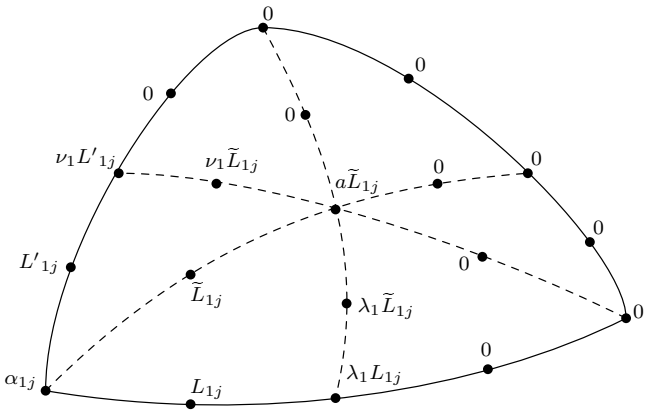

Figure 6.2: Schematic representation of the Bézier ordinates of a spherical B-spline.

We would like these spherical B-splines to have good properties such as the partition of unity property, i.e.

$$B_{ij}(v) \geq 0 \quad \text{for all } v \in \Omega, \tag{6.30}$$

$$\sum_{i=1}^{N} \sum_{j=1}^{3} B_{ij}(v) = 1 \quad \text{for all } v \in \Omega, \tag{6.31}$$

and stability with respect to the max norm, i.e.

$$\|c\|_\infty \sim \| \sum_{i=1}^{N} \sum_{j=1}^{3} c_{ij} B_{ij} \|_{L_\infty(\Omega)} \tag{6.32}$$

for all choices of the coefficient vector c. We prove that these useful properties can be obtained by a good choice of the triplets $(\alpha_{ij}, \beta_{ij}, \gamma_{ij})$. For the remainder of the paper we assume that the directions g_i and h_i are chosen such that the set (V_i, g_i, h_i) forms an orthonormal basis for $\mathbb{R}^3$. This assumption is without loss of generality. We shall make use of known results for bivariate splines, along with a natural radial projection operator that we define here.

Given a subset Ω of S, we define its diameter to be

$$\text{diam}(\Omega) := \sup\{\arccos(u \cdot v),\ u, v \in \Omega\}.$$

By $|\Delta|$ and $|M_i|$ we denote the mesh size of Δ resp. M_i, i.e. the diameter of the largest triangle in Δ resp. M_i. Let T_{M_i} be the tangent plane touching

S at vertex V_i. We define the radial projection from T_{M_i} into S by

$$R_{M_i}\overline{v} := v := \frac{\overline{v}}{|\overline{v}|} \in S, \quad \overline{v} \in T_{M_i}, \tag{6.33}$$

where $|v|$ denotes the Euclidean norm of v. Because R_{M_i} is one-to-one, the inverse $R_{M_i}^{-1}$ is well defined. Let $\overline{M}_i$ be the image of M_i under $R_{M_i}^{-1}$. Then $\overline{M}_i$ is only well defined if we assume that the molecule M_i satisfies $|M_i| < \pi/2$. Since great circles are mapped into straight lines under $R_{M_i}^{-1}$, $\overline{M}_i$ consists of planar neighbouring triangles with one common vertex V_i. In the following we assume that $|M_i| \leq 1$ such that the spherical triangles $T \in M_i$ will have a similar size and shape as their mappings under $R_{M_i}^{-1}$.

Let us consider the planar molecule $\overline{M}_i$. Without loss of generality we may assume that the tangent plane T_{M_i} touching S at V_i is equal to the $z = 1$ plane, and that the directions g_i and h_i coincide with the x resp. y direction. We define bivariate PS B-spline functions $\overline{B}_{ij}(x, y)$, $j = 1, 2, 3$, on the domain $\overline{M}_i$ as solutions to the interpolation problem

$$\overline{B}_{ij}(R_{M_i}^{-1}V_k) = \delta_{ik}\overline{\alpha}_{ij}, \quad D_x\overline{B}_{ij}(R_{M_i}^{-1}V_k) = \delta_{ik}\overline{\beta}_{ij}, \quad D_y\overline{B}_{ij}(R_{M_i}^{-1}V_k) = \delta_{ik}\overline{\gamma}_{ij},$$

for all $V_k \in M_i$. In this way we can identify three bivariate B-spline functions $\overline{B}_{ij}(x, y)$, $j = 1, 2, 3$, with each vertex $V_i \in \Delta$, and each $\overline{B}_{ij}(x, y)$ is completely determined by the triplet $(\overline{\alpha}_{ij}, \overline{\beta}_{ij}, \overline{\gamma}_{ij})$ and the molecule $\overline{M}_i$. The construction of bivariate PS basis functions is well-understood, see e.g. [5, 48, 77, 110] or Chapter 2. These constructions provide an algorithm for calculating the triplets $(\overline{\alpha}_{ij}, \overline{\beta}_{ij}, \overline{\gamma}_{ij})$, and such an algorithm depends at most on the geometry of the molecule $\overline{M}_i$. Not all constructions of bivariate PS basis functions satisfy the properties (6.30), (6.31) and (6.32). In fact, only the basis from [48] satisfies all three properties. However, all constructions can be extended to the sphere by choosing the triplets $(\alpha_{ij}, \beta_{ij}, \gamma_{ij})$ equal to the corresponding triplets $(\overline{\alpha}_{ij}, \overline{\beta}_{ij}, \overline{\gamma}_{ij})$. We prove that the resulting spherical PS B-splines $B_{ij}(v)$ form a partition of unity provided that the bivariate PS B-splines $\overline{B}_{ij}(x, y)$ have this property and that the spherical B-splines are stable given that the bivariate B-splines are stable. Our approach will be to view each spherical B-spline function $B_{ij}(v)$ as a restriction of a trivariate homogeneous function to the unit sphere S. In particular, let f be any function on the sphere and $d \in \mathbb{N}$, then we define $(f)_d$ as its *homogeneous extension of degree d*, i.e.

$$(f)_d(v) := |v|^d f\left(\frac{v}{|v|}\right), \qquad v \in \mathbb{R}^3 \setminus \{0\}. \tag{6.34}$$

Theorem 6.4.1 points out the strong connection between the spherical PS B-splines $B_{ij}(v)$ and the bivariate PS B-splines $\overline{B}_{ij}(x, y)$.

Theorem 6.4.1. *The restriction to the plane T_{M_i} of the homogeneous extension of degree 2 of the spherical B-spline $B_{ij}(v)$ coincides with the bivariate B-spline $\overline{B}_{ij}(x,y)$ associated with vertex V_i and molecule $\overline{M}_i$, or in other words*

$$(B_{ij})_2\big|_{T_{M_i}} = \overline{B}_{ij},$$

where $(B_{ij})_2$ is the homogeneous extension of degree 2 of B_{ij}.

Proof. We will focus on the triangle $T(V_1, V_2, V_3)$. We assume, without loss of generality, that V_1 has coordinates $(0,0,1)$, that T_{M_1} is the $z=1$ plane, and that the directions g_1 and h_1 are given by the vectors $(1,0,0)$ resp. $(0,1,0)$. The PS 6-split divides triangle T into six smaller triangles τ_i, $i=1,\ldots,6$. Equations (6.8) and (6.9) yield

$$B_{11}(v) = \sum_{i+j+k=2} c_{ijk} \frac{2!}{i!j!k!} b_1(v)^i b_2(v)^j b_3(v)^k,$$

with (b_1, b_2, b_3) the trihedral coordinates of v with respect to τ_i, and with $v \in \tau_i$. Define $\mathcal{T}_{\tau_i}$ as the trihedron (6.6) that satisfies $\mathcal{T}_{\tau_i}|_S = \tau_i$. Let w be an arbitrary point in trihedron $\mathcal{T}_{\tau_i}$, then it is easily verified that

$$(B_{11})_2(w) = \sum_{i+j+k=2} c_{ijk} \frac{2!}{i!j!k!} b_1(w)^i b_2(w)^j b_3(w)^k,$$

where $(B_{11})_2$ is the homogeneous extension of degree 2 of B_{11}. Using straightforward calculations it is easy to prove that the values of $(B_{11})_2$ and its partial derivatives at the vertices V_1, $\overline{V}_2$ and $\overline{V}_3$ coincide with the corresponding values of $\overline{B}_1^1$ and its partial derivatives. It are exactly these 9 pieces of data that determine a C^1 piecewise quadratic spline on the PS 6-split of the planar triangle $R_{M_1}^{-1}T$, so this proves that $(B_{11})_2|_{R_{M_1}^{-1}T} = \overline{B}_{11}\big|_{R_{M_1}^{-1}T}$. In general this yields $(B_{ij})_2\big|_{T_{M_i}} = \overline{B}_{ij}$. □

As a consequence of Theorem 6.4.1 we can immediately prove the following useful corollary.

Corollary 6.4.2. *The spherical Powell–Sabin B-splines form a partition of unity (6.30-6.31) whenever the bivariate B-splines $\overline{B}_{ij}(x,y)$ form a partition of unity.*

Proof. Suppose that there exists a $v \in M_i$ such that $B_{ij}(v) < 0$. Let $\overline{v} := R_{M_i}^{-1} v$, then also $(B_{ij})_2(\overline{v}) := |\overline{v}|^2 B_{ij}\left(\frac{\overline{v}}{|\overline{v}|}\right) = |\overline{v}|^2 B_{ij}(v) < 0$. From Theorem 6.4.1 we infer that $\overline{B}_{ij}(\overline{v}) < 0$ but this gives a contradiction with the fact that the bivariate B-splines $\overline{B}_{ij}$ are positive. Thus $B_{ij}(v) \geq 0$ for all $v \in \Omega$.

Because of (6.28) only the B-splines B_{kj}, $j = 1, 2, 3$, are non-zero at vertex V_k. Therefore $\sum_{i=1}^{N} \sum_{j=1}^{3} B_{ij}(V_k) = \alpha_{k1} + \alpha_{k2} + \alpha_{k3}$ and, by construction and the partition of unity property of $\overline{B}_{kj}$, this equals $\overline{\alpha}_{k1} + \overline{\alpha}_{k2} + \overline{\alpha}_{k3} = 1$. Similar arguments show that $D_{g_k} \sum_{i=1}^{N} \sum_{j=1}^{3} B_{ij}(V_k)$ and $D_{h_k} \sum_{i=1}^{N} \sum_{j=1}^{3} B_{ij}(V_k)$ equal zero. From Theorem 7.2 in [2] we know that there exists a unique spherical spline p of degree 2 on each subtriangle $\rho \in \Delta^{PS}$ such that $p(v) = 1$ for all $v \in \rho$. From the uniqueness of the representation (6.27) we find that

$$\sum_{i=1}^{N} \sum_{j=1}^{3} B_{ij}(v) = 1, \quad \text{for all } v \in \Omega.$$

□

Now we prove that the spherical PS B-spline basis is stable with respect to the max norm, given that the corresponding bivariate B-spline basis is stable. The equivalence constants in (6.32) depend at most on the smallest angle in Δ. Because the equivalence constants are allowed to depend on the smallest angle in Δ, we need the following lemma which relates a spherical angle θ to its image under the radial projection $R_{M_i}^{-1}$. A spherical angle is defined as the angle formed at the intersection of the arcs of two great circles.

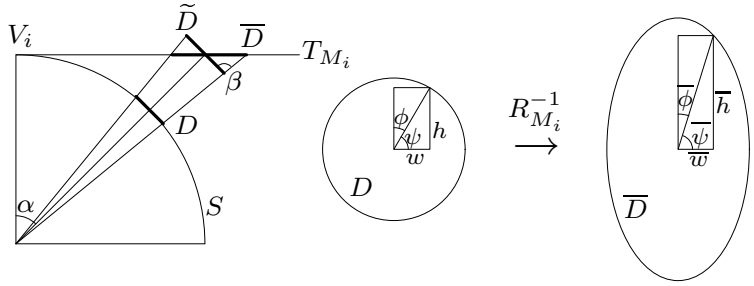

Figure 6.3: Distortion on angles under the radial projection R_{M_i}.

Lemma 6.4.3. *Let θ be an angle in the triangulation of the molecule M_i and let $\overline{\theta}$ be its image under the radial projection $R_{M_i}^{-1}$. Then*

$$\cos|M_i| \tan\theta \leq \tan\overline{\theta} \leq \frac{1}{\cos|M_i|} \tan\theta.$$

Proof. Figure 6.3 displays this proof schematically. Let D be a disk tangent to S with radius R and center v, let $\overline{D}$ be the image of D under the radial

projection $R_{M_i}^{-1}$, and let $\widetilde{D}$ be the disk with radius $\widetilde{R}$ and center $\overline{v}$ that is obtained as the image of D under a central projection from the origin onto the plane through $\overline{v}$ that is parallel to the disk D. Denote α as the angle between the vectors V_i and v. One can easily deduce that

$$\widetilde{R} = \frac{R}{\cos\alpha}.$$

We project $\widetilde{D}$ onto the plane T_{M_i} to obtain $\overline{D}$. It is clear that $\overline{D}$ is no longer a disk but an ellipse and the minor axis of $\overline{D}$ equals $\widetilde{R}$. Consider angle β as in Figure 6.3. If the radius $\widetilde{R}$ is very small compared to the length of vector $\overline{v}$ then β will be close to $\pi/2$ radials. Thus if $\widetilde{R}$ tends to zero then the major axis $\overline{R}$ of $\overline{D}$ tends to $\widetilde{R}/\cos\alpha$, or

$$\overline{R} = \frac{R}{\cos^2\alpha}.$$

Consider the angles ϕ and ψ in the disk D and their projections $\overline{\phi}$ and $\overline{\psi}$ in the ellipse $\overline{D}$ as indicated in Figure 6.3. Then we see that

$$\tan\phi = \frac{w}{h}, \quad \tan\psi = \frac{h}{w}, \quad \tan\overline{\phi} = \frac{\overline{w}}{\overline{h}}, \quad \tan\overline{\psi} = \frac{\overline{h}}{\overline{w}},$$

and

$$\overline{w} = w\frac{\widetilde{R}}{R}, \quad \overline{h} = h\frac{\overline{R}}{R}.$$

This yields

$$\tan\overline{\phi} = \cos\alpha\tan\phi \quad \text{and} \quad \tan\overline{\psi} = \frac{1}{\cos\alpha}\tan\psi.$$

This completes the proof. □

Corollary 6.4.4. *The spherical Powell–Sabin B-splines form a stable basis for the max norm, i.e. for any arbitrary coefficient vector c we have*

$$c_1\|c\|_\infty \le \left\| \sum_{i=1}^{N}\sum_{j=1}^{3} c_{ij}B_{ij} \right\|_{L_\infty(\Omega)} \le c_2\|c\|_\infty$$

with c_1 and c_2 constants that depend at most on the smallest angle in Δ, provided that the corresponding bivariate PS B-splines $\overline{B}_{ij}(x,y)$ form a stable basis with respect to the max norm, and that $|\Delta| \le 1$.

Proof. First we establish the right inequality. There exists a triangle $T \in \Delta$ and a point $v \in T$ such that the following holds

$$\begin{aligned}\left\| \sum_{i=1}^{N} \sum_{j=1}^{3} c_{ij} B_{ij} \right\|_{L_\infty(\Omega)} &= \left| \sum_{i|V_i \in T} \sum_{j=1}^{3} c_{ij} B_{ij}(v) \right| \\ &\leq \|c\|_\infty \sum_{i|V_i \in T} \sum_{j=1}^{3} \|B_{ij}\|_{L_\infty(T)},\end{aligned}$$

and

$$\|B_{ij}\|_{L_\infty(T)} = \max_{v \in T} (B_{ij})_2(v) = \max_{\overline{v} \in R_{M_i}^{-1} T} (B_{ij})_2 \left(\frac{\overline{v}}{|\overline{v}|} \right) = \max_{\overline{v} \in R_{M_i}^{-1} T} \frac{1}{|\overline{v}|^2} \overline{B}_{ij}(\overline{v}).$$

Because $|T| \leq 1$ we have that $1 \leq |\overline{v}| \leq 1/\cos 1$, so

$$\|B_{ij}\|_{L_\infty(T)} \leq \left\|\overline{B}_{ij}\right\|_{L_\infty(R_{M_i}^{-1} T)} \leq K_1$$

where the last inequality follows from the stability of the bivariate basis, so K_1 is a constant depending at most on the smallest angle in $R_{M_i}^{-1} T$. Using Lemma 6.4.3 this establishes the right inequality of the Corollary.

Now we prove the left inequality. Choose an arbitrary molecule $M_i \in \Delta$. It is sufficient to prove that

$$|c_{ij}| \leq K_2 \|s\|_{L_\infty(M_i)}$$

for arbitrary j, where s represents the PS spline surface. Let $\overline{s}$ be the restriction of $(s)_2$ to the plane T_{M_i}, then we have that

$$\|s\|_{L_\infty(M_i)} = \max_{v \in M_i} |(s)_2(v)| = \max_{\overline{v} \in \overline{M}_i} \left| (s)_2 \left(\frac{v}{|v|} \right) \right| = \max_{\overline{v} \in \overline{M}_i} \frac{1}{|\overline{v}|^2} |(s)_2(\overline{v})|,$$

and because $1 \leq |\overline{v}| \leq 1/\cos 1$ we find

$$\cos^2 1 \|\overline{s}\|_{L_\infty(\overline{M}_i)} \leq \|s\|_{L_\infty(M_i)} \leq \|\overline{s}\|_{L_\infty(\overline{M}_i)}. \tag{6.35}$$

On the molecule $\overline{M}_i$ we can define a bivariate PS B-spline basis

$$\left\{ \widehat{B}_{kj} \mid k \text{ such that } V_k \in M_i, j = 1, 2, 3 \right\}$$

with $\widehat{B}_{ij} = \overline{B}_{ij}$, $j = 1, 2, 3$. It is important to see (see also the proof of Theorem 2.5.5) that

$$\overline{s}|_{\overline{M}_i}(u, v) = \sum_{k|V_k \in M_i} \sum_{j=1}^{3} \begin{bmatrix} \widehat{\alpha}_{k1} & \widehat{\alpha}_{k2} & \widehat{\alpha}_{k3} \\ \widehat{\beta}_{k1} & \widehat{\beta}_{k2} & \widehat{\beta}_{k3} \\ \widehat{\gamma}_{k1} & \widehat{\gamma}_{k2} & \widehat{\gamma}_{k3} \end{bmatrix}^{-1} \begin{bmatrix} \overline{s}\left(R_{M_i}^{-1} V_k\right) \\ D_{g_i} \overline{s}\left(R_{M_i}^{-1} V_k\right) \\ D_{h_i} \overline{s}\left(R_{M_i}^{-1} V_k\right) \end{bmatrix} \widehat{B}_{kj}(u, v),$$

and that

$$\alpha_{ij} = \widehat{\alpha}_{ij}, \quad \beta_{ij} = \widehat{\beta}_{ij}, \quad \gamma_{ij} = \widehat{\gamma}_{ij},$$

$$s(V_i) = \overline{s}(R_{M_i}^{-1} V_i), \quad D_{g_i} s(V_i) = D_{g_i} \overline{s}(R_{M_i}^{-1} V_i), \quad D_{h_i} s(V_i) = D_{h_i} \overline{s}(R_{M_i}^{-1} V_i).$$

Because of the stability of the bivariate basis $\left\{ \widehat{B}_{kj} \right\}$ we get

$$|c_{ij}| = \left| \begin{bmatrix} \widehat{\alpha}_{i1} & \widehat{\alpha}_{i2} & \widehat{\alpha}_{i3} \\ \widehat{\beta}_{i1} & \widehat{\beta}_{i2} & \widehat{\beta}_{i3} \\ \widehat{\gamma}_{i1} & \widehat{\gamma}_{i2} & \widehat{\gamma}_{i3} \end{bmatrix}^{-1} \begin{bmatrix} \overline{s}(R_{M_i}^{-1} V_i) \\ D_{g_i} \overline{s}(R_{M_i}^{-1} V_i) \\ D_{h_i} \overline{s}(R_{M_i}^{-1} V_i) \end{bmatrix} \right| \leq K_3 \|\overline{s}\|_{L_\infty(\overline{M}_i)}.$$

Equation (6.35) concludes the proof. □

Let us for instance consider the bivariate B-spline basis developed in [48]. These B-splines form a partition of unity, and from Theorem 2.5.5 we know that they form a stable basis for the max norm. If we extend this basis to a spherical PS B-spline basis, see Figure 6.4, we still have a partition of unity and a stable basis because of Corollaries 6.4.2 and 6.4.4. Furthermore one can define control triangles (2.10) for these bivariate B-splines that are tangent to the surface, which is a nice property from a CAGD point of view. Using Theorem 6.4.1 it is not difficult to define control triangles for the corresponding spherical B-spline basis that are tangent to the spherical surface. This illustrates that several other more specific properties of a bivariate basis are possibly also inherited by the spherical extension. We refer to Section D.2 for more details.

6.5 The hierarchical basis preconditioner

The construction of nested spline spaces of Powell–Sabin type on the sphere is completely analogous to the bivariate case, see Section 3.2. We can use dyadic or triadic refinement, see Figures 3.1 and 3.2, or even a $\sqrt{3}$ refinement, see Figure 3.3. As in the bivariate case, dyadic refinement is not always possible if the initial spherical triangulation Δ_0 is highly irregular. In the following derivation we assume that a triadic refinement scheme is used, and that the sequences (3.2) and (3.3) are regular.

Let S_l be shorthand notation for $S_2^1(\Delta_l^{PS})$. We define the Hermite interpolant $\mathcal{I}_l : C^1(\overline{\Omega}) \to S_l$ similar to the bivariate case, i.e.

$$\mathcal{I}_l s = s, \quad \forall s \in S_l,$$

$$\mathcal{I}_l f(V_i) = f(V_i), \quad \nabla_S \mathcal{I}_l f(V_i) = \nabla_S f(V_i), \quad i = 1, \ldots, N_l,$$

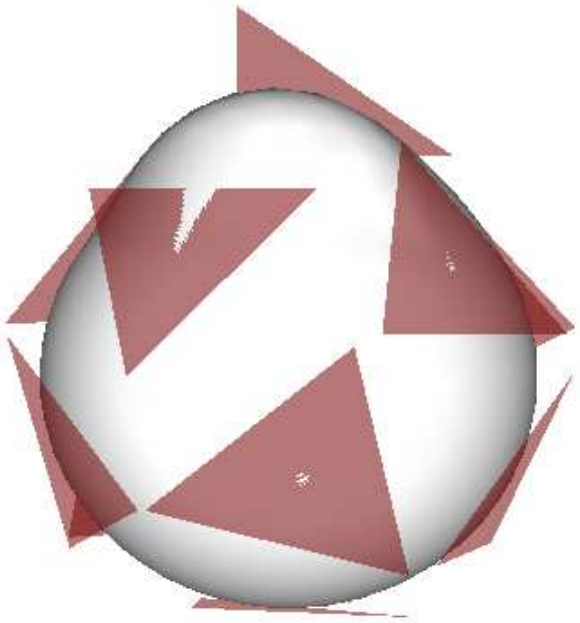

Figure 6.4: Graph of $(B_{ij}(v) + 1)v$ with $v \in S$ and B_{ij} the spherical PS B-spline. The control triangles are tangent to the surface.

for any $f \in C^1(\overline{\Omega})$. Then of course $\mathcal{I}_l \mathcal{I}_{l+1} = \mathcal{I}_l$ also holds. Define the linear functionals $\mu_{ij,l}$ by

$$\mathcal{I}_l f =: \sum_{i=1}^{N_l} \sum_{j=1}^{3} \mu_{ij,l}(f) B_{ij,l},$$

then one can prove that

$$\|s_l\|_{L_p(\Omega)} \sim \left(\sum_{i=1}^{N_l} \sum_{j=1}^{3} |\mu_{ij,l}(s_l)|^p \, 3^{-2l} \right)^{1/p} \tag{6.36}$$

for all $0 < p \leq \infty$, provided that the spherical B-spline basis is stable for the max norm, i.e. Corollary 6.4.4 holds. The proof of (6.36) is similar to the proof of Corollary 2.5.7, but now one has to make use of the Markov inequality for spherical polynomials [98, Prop. 4.3].

We prove that the spherical hierarchical basis is a weakly stable basis (Definition 3.4.1) for $H^2(\Omega)$. We introduce spherical Sobolev spaces $H^m(\Omega)$ as defined in [80, 98], because we use some lemmas from [98] concerning

these Sobolev spaces. Suppose that $\{(\Gamma_j, \phi_j)\}$ is an atlas for Ω, i.e. a finite collection of charts (Γ_j, ϕ_j), where Γ_j are open subsets of Ω, covering Ω, and where ϕ_j are C^∞ mappings $\phi_j : \Gamma_j \to B_j$, B_j an open subset of $\mathbb{R}^2$, whose inverses ϕ_j^{-1} are also C^∞. Let $\{\alpha_j\}$ be a partition of unity on the atlas $\{(\Gamma_j, \phi_j)\}$, i.e. a set of C^∞ functions α_j on Ω vanishing outside the sets Γ_j such that $\sum_j \alpha_j = 1$ on Ω. Then we define the spherical Sobolev spaces $H^m(\Omega)$ as

$$H^m(\Omega) := \left\{ u \mid (\alpha_j u) \circ \phi_j^{-1} \in H^m(B_j), \text{ for all } j \right\}, \tag{6.37}$$

with $H^m(B_j)$ the classical Sobolev space of functions on B_j whose derivatives up to order m belong to $L_2(B_j)$, see Section A.1. With $H^m(\Omega)$ we can associate the norm

$$\|u\|_{H^m(\Omega)} := \sum_j \left\| (\alpha_j u) \circ \phi_j^{-1} \right\|_{H^m(B_j)}. \tag{6.38}$$

This definition does not depend on the choice of the atlas and the partition of unity, i.e. other choices will give rise to the same space with a norm that is equivalent to (6.38). Furthermore the definition (6.37) for the case $m = 2$ is equivalent to the definition (6.2) and the norms (6.38) and (6.3) are also equivalent, see [80, p.37]. We can prove the following theorem.

Theorem 6.5.1. *Let Ω be a subset of the unit sphere S, and suppose $s \in S_n$. Then*

$$n^{-2} \sum_{l=0}^{n} 3^{4l} \|(\mathcal{I}_l - \mathcal{I}_{l-1})s\|_{L_2(\Omega)}^2 \lesssim \|s\|_{H^2(\Omega)}^2 \lesssim \sum_{l=0}^{n} 3^{4l} \|(\mathcal{I}_l - \mathcal{I}_{l-1})s\|_{L_2(\Omega)}^2. \tag{6.39}$$

Proof. Suppose first that $\operatorname{diam}(\Omega) \leq 1$. Similarly to the radial projection R_{M_i} we define

$$R_\Omega \overline{v} := v := \frac{\overline{v}}{|\overline{v}|} \in S, \quad \overline{v} \in T_\Omega,$$

with T_Ω the tangent plane touching S at r_Ω, and r_Ω the center of a spherical cap of smallest possible radius containing Ω. Here a spherical cap is defined as the region of a sphere which lies on one side of a given plane that intersects with the sphere. Let $\overline{\Omega}$ be the image of Ω under R_Ω^{-1}. As before $(s)_2$ is the homogeneous extension of degree 2 of s, and we define $\overline{s}$ as the restriction of $(s)_2$ to $\overline{\Omega}$. The norm equivalence $\|s\|_{H^2(\Omega)} \sim \|\overline{s}\|_{H^2(\overline{\Omega})}$ holds, see Lemma 3.2 in [98]. Furthermore we also have $\|s\|_{L_p(\Omega)} \sim \|\overline{s}\|_{L_p(\overline{\Omega})}$, see Lemma 3.1 in [98]. Now let $s = \sum_{l=0}^n g_l$ with each $g_l \in S_l$. Then it follows that $(s)_2 = \sum_{l=0}^n (g_l)_2$, hence $\overline{s} = \sum_{l=0}^n \overline{g}_l$ with $\overline{g}_l$ the restriction of $(g_l)_2$ to $\overline{\Omega}$.

Furthermore, each $\overline{g}_l$ is a member of the spline space $\overline{S}_l := S_2^1(R_\Omega^{-1}\Delta_l^{PS})$. Proposition 3.4.7 [102] claims that

$$\|\overline{s}\|_{H^2(\overline{\Omega})} \sim \inf \sum_{l=0}^{n} 3^{4l} \|\overline{g}_l\|^2_{L_2(\overline{\Omega})}$$

where the infimum must be taken with respect to all admissible representations $\sum_{l=0}^{n} \overline{g}_l$ of $\overline{s}$. From the norm equivalences above we get

$$\|s\|_{H^2(\Omega)} \sim \inf \sum_{l=0}^{n} 3^{4l} \|g_l\|^2_{L_2(\Omega)} . \tag{6.40}$$

It is now sufficient to prove that

$$n^{-2} \sum_{l=0}^{n} 3^{4l} \|(\mathcal{I}_l - \mathcal{I}_{l-1})s\|^2_{L_2(\Omega)} \lesssim \inf \sum_{l=0}^{n} 3^{4l} \|g_l\|^2_{L_2(\Omega)}$$

and that

$$\inf \sum_{l=0}^{n} 3^{4l} \|g_l\|^2_{L_2(\Omega)} \lesssim \sum_{l=0}^{n} 3^{4l} \|(\mathcal{I}_l - \mathcal{I}_{l-1})s\|^2_{L_2(\Omega)} .$$

To prove these inequalities the same techniques as in the proof of Theorem 3.4.10 can be used.

For general domains Ω, $\operatorname{diam}(\Omega) > 1$, we construct a finite collection of domains Ω_j with $\operatorname{diam}(\Omega_j) \leq 1$, covering Ω. Equation (6.39) is valid for each sub-domain Ω_j. Furthermore we have the equivalences

$$\|(\mathcal{I}_l - \mathcal{I}_{l-1})s\|^2_{L_2(\Omega)} \sim \sum_j \|(\mathcal{I}_l - \mathcal{I}_{l-1})s\|^2_{L_2(\Omega_j)}$$

and

$$\|s\|^2_{H^2(\Omega)} \sim \sum_j \|s\|^2_{H^2(\Omega_j)} .$$

Hence (6.39) is valid for Ω itself. □

From (6.36) we deduce that the set

$$\left\{3^l B_{ij,l} \mid (i,j) \in J_{l-1}\right\}$$

with J_l defined in (3.25) is a uniformly L_2-stable basis for the space $\operatorname{Im}(\mathcal{I}_l - \mathcal{I}_{l-1})$. From Theorem 6.5.1 we therefore conclude that the set

$$\bigcup_{l=0}^{\infty} \left\{3^{-l} B_{ij,l} \mid (i,j) \in J_{l-1}\right\}$$

is a weakly stable basis for $H^2(\Omega)$, i.e.

$$n^{-2}\sum_{l=0}^{n}\sum_{(i,j)\in J_{l-1}} c_{ij,l}^2 \lesssim \left\|\sum_{l=0}^{n} 3^{-l}\sum_{(i,j)\in J_{l-1}} c_{ij,l}B_{ij,l}\right\|_{H^2(\Omega)}^2 \lesssim \sum_{l=0}^{n}\sum_{(i,j)\in J_{l-1}} c_{ij,l}^2.$$

We conclude that the condition number of the stiffness matrix with respect to this hierarchical basis for the problem (6.1) is of the order $\mathcal{O}(|\log h|^2)$ with h the mesh size of the underlying triangulation Δ_n.

6.6 BPX-preconditioners on the sphere

In this section we numerically solve the following two most simple equations

$$-\Delta_S u = f \quad \text{on} \quad S, \tag{6.41}$$

and

$$\Delta_S^2 u = f \quad \text{on} \quad S, \tag{6.42}$$

where Δ_S is the Laplace–Beltrami operator on the two-sphere S. We use C^0 continuous piecewise linear spherical polynomials to discretize the variational problem

$$\int_S \nabla_S u \nabla_S v \; d\omega = \int_S fv \; d\omega \quad \text{for all } v \in H^1(S) \tag{6.43}$$

corresponding to (6.41), and C^1 continuous piecewise quadratic spherical polynomials to discretize the variational problem

$$\int_S \Delta_S u \Delta_S v \; d\omega = \int_S fv \; d\omega \quad \text{for all } v \in H^2(S) \tag{6.44}$$

corresponding to (6.42). For every $f \in L_2(S)$ with $\int_S f \; d\omega = 0$ there exists a weak solution $u \in H^1(S)$ of (6.43) and a weak solution $u \in H^2(S)$ of (6.44). In both cases u is unique up to a constant, see, e.g., [6, 52].

In the previous section we constructed a hierarchical basis on the sphere that yields suboptimal results for problem (6.44). By (6.40) and the techniques shown in Section 3.6 it is easy to prove the following theorem.

Theorem 6.6.1. *The BPX preconditioner given by*

$$\sum_{l=0}^{n}\sum_{i=1}^{N_l}\sum_{j=1}^{3}\langle \cdot, B_{ij,l}\rangle B_{ij,l}$$

yields uniformly bounded condition numbers for the problem (6.44).

Of course, here, the basis functions $B_{ij,l}$ have to be stable in the sense of Definition 2.5.1 for the L_2-norm. If the basis functions are stable with respect to some other L_p-norm, a suitable normalization has to be used. To demonstrate that any L_2-stable basis can be used we will use a spherical variant of the Hermite basis from [110] in our numerical experiment. Consider nested sequences of triangulations (3.2) and (3.3) obtained by ρ-adic refinement. With each vertex $V_i \in \Delta_l$ we associate two directions g_i and h_i such that the set (V_i, g_i, h_i) forms an orthonormal basis for $\mathbb{R}^3$. For instance, suppose that V_i has spherical coordinates $(\cos\theta\sin\phi, \sin\theta\sin\phi, \cos\phi)$, $\theta \in [0, 2\pi]$, $\phi \in [0, \pi]$, then take $g_i = (\cos\theta\cos\phi, \sin\theta\cos\phi, -\sin\phi)$ and $h_i = (-\sin\theta, \cos\theta, 0)$. Let us introduce the functionals

$$\lambda_i^1(f) := f(V_i), \quad \lambda_i^2(f) := \frac{\partial f(V_i)}{\partial g_i}, \quad \lambda_i^3(f) := \frac{\partial f(V_i)}{\partial h_i}, \quad f \in C^1(S).$$

Then we define a nodal basis for $S_2^1(\Delta_l^{PS})$ by the following interpolation problem: find functions $B_{ij,l} \in S_2^1(\Delta_l^{PS})$, $j = 1, 2, 3$, $i = 1, \ldots, N_l$, such that

$$\begin{aligned} \lambda_k^1(B_{ij,l}) &= \rho^{-l}\delta_{j,1}\delta_{i,k}, \\ \lambda_k^2(B_{ij,l}) &= \delta_{j,2}\delta_{i,k}, \\ \lambda_k^3(B_{ij,l}) &= \delta_{j,3}\delta_{i,k}, \end{aligned} \tag{6.45}$$

for all $k = 1, \ldots, N_l$. Then by Corollary 6.4.4 and the work in [110] we find that, under a suitable normalization, this Hermite basis is stable in the sense of Definition 2.5.1 for the L_2-norm and Theorem 6.6.1 holds.

To discretize the second order problem we use C^0 linear elements on the sphere that we derive now. The C^0 continuous piecewise linear spherical polynomials that we describe here are a natural extension of the well-known linear elements introduced by Courant [26]. However, our approach differs significantly from previous constructions (e.g., [8, 52]). We create suitable basis functions for the nested spherical spline spaces

$$S_1^0(\Delta_0) \subset S_1^0(\Delta_1) \subset \cdots \subset S_1^0(\Delta_l) \subset \cdots, \quad l = 0, 1, \ldots,$$

where the triangulations Δ_l are obtained by dyadic refinement. Similar to the connection described in Theorem 6.4.1, we point out a strong connection with the classical Courant elements on the plane.

So let us define a nodal basis for $S_1^0(\Delta_l)$ by solving the following interpolation problem: find functions $\phi_{i,l} \in S_1^0(\Delta_l)$, $i = 1, \ldots, N_l$, such that $\phi_{i,l}(V_k) = \delta_{i,k}$. We can look at each spherical basis functions $\phi_{i,l}$ as the restriction of a trivariate homogeneous function to the sphere S. Clearly we have that $\phi_{i,l} \equiv (\phi_{i,l})_1|_S$. Moreover, if we restrict $(\phi_{i,l})_1$ to the tangent plane touching S at V_i, then we just get a classical Courant element defined

on this tangent plane centered around the vertex V_i. This idea can be exploited to extend several properties of the classical Courant elements to the spherical elements $\phi_{i,l}$. The following theorem is obvious.

Theorem 6.6.2. *The nodal basis functions* $\{\phi_{i,l} \mid i = 1, \ldots, N_l\}$ *satisfy*

$$\|\sum_{i=1}^{N_l} c_{i,l}\phi_{i,l}\|_{L_\infty} \sim \max_i |c_{i,l}|.$$

Proof. There exists a triangle $T \in \Delta_l$ and a point $v \in T$ such that

$$\|\sum_{i=1}^{N_l} c_{i,l}\phi_{i,l}\|_{L_\infty} = \left|\sum_{i=1}^{N_l} c_{i,l}\phi_{i,l}(v)\right| \leq \max_i |c_{i,l}| \sum_{i|V_i \in T} \|\phi_{i,l}\|_{L_\infty} \lesssim \max_i |c_{i,l}|.$$

The other inequality follows from

$$|c_{k,l}| = \left|\sum_{i=1}^{N_l} c_{i,l}\phi_{i,l}(V_k)\right| \leq \|\sum_{i=1}^{N_l} c_{i,l}\phi_{i,l}\|_{L_\infty}.$$

□

The proof of the following theorem is similar to the proof of Theorem 6.6.1.

Theorem 6.6.3. *The BPX preconditioner given by*

$$\sum_{l=0}^{n} 2^{2l} \sum_{i=1}^{N_l} \langle \cdot, \phi_{i,l} \rangle \phi_{i,l}$$

yields uniformly bounded condition numbers for the problem (6.43).

We now provide the results of numerical experiments illustrating the optimality of the BPX preconditioners and we also compare the results of the BPX preconditioners with those obtained using the corresponding hierarchical preconditioners which are suboptimal.

The first problem that we solve is given by

$$-\Delta_S u = 2x \quad \text{on} \quad S, \tag{6.46}$$

and the exact solution u equals x, which can easily be checked since spherical harmonics are eigenfunctions of the Laplace–Beltrami operator on S, see, e.g., [97]. To discretize the problem (6.46) we use the basis functions $\phi_{i,l}$. We start from an almost uniform triangulation Δ_0 by projecting the twelve vertices of the regular icosahedron onto the sphere. These twelve points

define a mesh consisting of twenty equal spherical triangles, cfr. [8]. The finer triangulatons Δ_l are constructed by subdividing the triangles of the previous coarser triangulation into four equal subtriangles. Hence the dimension of the spline space increases like $2+10\cdot 4^n$ with the refinement level n. Inner products of the form $\langle \nabla_S \phi_{i_1,l}, \nabla_S \phi_{i_2,l} \rangle$ will have to be computed. Hereto, we use a 3th order Gaussian quadrature formula on a triangle, see also [4, Prop. 4.1].

The second problem that we solve is given by

$$\Delta_S^2 u = 36xy \quad \text{on} \quad S, \tag{6.47}$$

and the exact solution u equals xy. In order to discretize (6.47) we have to compute inner products of the form $\langle \Delta_S B_{i_1 j_1,l}, \Delta_S B_{i_2 j_2,l} \rangle$. Since the basis functions $B_{ij,l}$ are piecewise quadratic polynomials, we can use the formula

$$\Delta_S B_{ij,l}(v) = \Delta B_{ij,l}(v) - 6B_{ij,l}(v), \quad v \in S,$$

with Δ the usual Laplace operator on $\mathbb{R}^3$, see [97]. Then, to evaluate the inner products, we use again a 3th order Gaussian quadrature formula on a triangle. We show results both for a dyadic and a triadic refinement procedure where we start from the same quasi-uniform triangulation Δ_0 as in the first problem (6.46). For the dyadic resp. triadic refinement procedure the dimension of the spline space increases like $6 + 30 \cdot 4^n$ resp. $6 + 30 \cdot 9^n$ with the refinement level n.

Note that the solution u in (6.46) and (6.47) is only unique up to a constant. From [2, Prop. 7.2] we find that constant functions on the sphere are contained in the spherical Powell–Sabin spline space $S_2^1(\Delta_l^{PS})$ but not in the spherical piecewise linear spline space $S_1^0(\Delta_l)$. Hence, the stiffness matrix corresponding to the nodal basis $\{B_{i,l}^j\}$ will have one zero eigenvalue with an eigenvector corresponding to the constant function. The stiffness matrix corresponding to the nodal basis $\{\phi_{i,l}\}$ will have an eigenvalue of $\mathcal{O}(h^2)$ with an eigenvector that approximates the constant function up to discretization error $\mathcal{O}(h^2)$ w.r.t the L_2 norm. Recall that the condition numbers that we compute are given by $\kappa(\mathcal{C}^{1/2}\mathcal{A}\mathcal{C}^{1/2}) = \lambda_{\max}/\lambda_{\min}$ where $\lambda_{\max}$ denotes the largest eigenvalue of $\mathcal{C}^{1/2}\mathcal{A}\mathcal{C}^{1/2}$ and $\lambda_{\min}$ its smallest nonzero eigenvalue. We also omit the smallest eigenvalue of $\mathcal{O}(h^2)$ for the Poisson equation. Note that, from Theorem 6.4.1 and the theory in Section 3.6, the BPX preconditioner uses all nodal basis functions on all levels. For each redundant basis function we get a zero eigenvalue.

Tables 6.1, 6.2 and 6.3 show the results. We have used a nested iteration conjugate gradient method to solve the problem, see Section 3.6.

Each table has the same setup. The first column contains the resolution level n. Then we distinguish between the results for the BPX preconditioner and the results for the hierarchical basis (HB) preconditioner. For

	BPX			HB		
n	κ	residual	#iter	κ	residual	#iter
1	3.1	2.4897e-05	12	7.6	2.4974e-05	17
2	3.7	1.6766e-05	9	10.7	1.9546e-05	16
3	4.6	4.7350e-06	11	15.2	8.6198e-06	20
4	5.5	4.5474e-06	11	22.2	5.2361e-06	22
5	6.2	1.6705e-06	12	31.9	3.0622e-06	23
6	6.7	1.0193e-06	12	44.9	1.4750e-06	25
7	7.0	6.2720e-07	12	60.9	6.5043e-07	26
8	7.4	1.6451e-07	13	84.2	3.4960e-07	24

Table 6.1: Iteration history for problem (6.46).

	BPX			HB		
n	κ	residual	#iter	κ	residual	#iter
1	52.0	2.2290e-03	0	59.1	2.2222e-03	0
2	66.7	5.1424e-04	2	81.2	3.8158e-04	2
3	78.4	4.2928e-04	1	106.5	6.2316e-04	0
4	87.7	3.1846e-04	3	144.6	2.5778e-04	5
5	95.2	1.6570e-04	3	199.9	1.5944e-04	14
6	100.6	7.9261e-05	5	274.4	6.8452e-05	4
7	105.5	4.0583e-05	4	375.8	4.2450e-05	15

Table 6.2: Iteration history for problem (6.47), dyadic refinement.

each preconditioner we display the spectral condition number κ of the system matrix for the linear system of equations that is solved. Moreover we show the energy norm of the residuals corresponding to the approximate solution, and the number of iterations that are needed on this level to reach discretization error accuracy.

	BPX			HB		
n	κ	residual	#iter	κ	residual	#iter
1	50.5	2.7160e-04	6	76.4	2.9346e-04	11
2	61.0	1.1074e-04	7	114.9	7.5921e-05	7
3	68.6	3.3405e-05	8	170.0	3.5187e-05	21
4	73.7	1.1717e-05	8	241.1	1.1716e-05	25

Table 6.3: Iteration history for problem (6.47), triadic refinement.

Chapter 7

Conclusions

7.1 Overview of contributions

This thesis investigated the construction of optimal multilevel preconditioners for fourth order elliptic equations. Here we would like to give a quick overview of our contributions.

In Section 2.5 we proved that, under a suitable normalization, the class of basis functions for Powell–Sabin spline spaces introduced by Dierckx [48] is a stable basis with respect to all L_p norms with $p > 0$. Furthermore we investigated the case when PS-triangles of minimal area are chosen in more detail. These results are published in [90] and [93]. In Section 2.6 we showed that the Hermite interpolating PS spline approximates a given smooth function f and its derivatives up to optimal approximation order. This result makes use of the Bramble–Hilbert lemma [10], and it is published in [91].

Then, in Chapter 3, we investigated a standard hierarchical basis for a nested sequence of Powell–Sabin spline spaces. We related this hierarchical basis to a fairly general definition of multiresolution analysis and we proved several stability results. Furthermore we derived a priori error bounds for surface compression and we verificated the sharpness of these bounds numerically. All these results are published in the paper [90]. We also introduced a BPX preconditioner and numerically compared this preconditioner with the suboptimal HB preconditioner.

In Chapter 4 we constructed new basis functions for the Powell–Sabin spline space. These new basis functions are not of Hermite type, such as the B-splines from [48], but they are of Lagrange type. This allowed us to define projection operators of Lagrange type that yield a hierarchical basis that is stable for a larger range of Sobolev spaces than the Hermite type

hierarchical basis of the previous chapter. These results are published in [89].

Chapter 5 was devoted to the construction of wavelet Riesz bases. We proposed a construction method for non uniform grids. This construction idea is joint work with colleague Evelyne Vanraes, see [125]. Furthermore we gave a proof of the stability of the one level transform, and we extended results of Lorentz and Oswald [82] to investigate the Riesz stability of shift-invariant wavelet vector spaces in arbitrary dimensions. Piecewise linear and quadratic spline wavelets were constructed in one or two dimensions and we gave a stability analysis based on Fourier techniques. Moreover, we numerically validated these estimates by showing the optimality of these wavelet bases as preconditioner for elliptic PDEs. Furthermore we gave several connections with existing and well-known constructions in the literature. All these results can be found in the papers [85, 88]. On uniform triangulations we constructed a Powell–Sabin spline prewavelet basis. This wavelet basis is stable for all Sobolev spaces $H^s(\Omega)$ with $|s| < 2.5$, see [87].

The results in Chapter 6 are based on the two papers [86, 92]. By using the spherical spline spaces introduced by Alfeld *et al.* in [2, 3, 4] we first extended the classical result of Powell and Sabin from [107] to the surface of the two-sphere. Then we constructed suitable B-spline bases that inherit most properties of the bivariate counterparts. These specific constructions allowed us to prove the suboptimality of the corresponding hierarchical basis preconditioner and the optimality of the corresponding BPX preconditioner for fourth order elliptic problems on the surface of the two-sphere. Furthermore we gave numerical evidence, and we also constructed a BPX preconditioner for second order elliptic problems on the surface of the two-sphere.

7.2 Suggestions for further research

Finally we provide some ideas for further research that are not explored in this thesis. These ideas only indicate that many interesting questions are still open for investigation.

- The *spherical shallow water equations* are a set of equations that describe the inviscid flow of a thin layer of fluid or gas on the two-dimensional surface of the sphere. They have been used for many years by meteorologists, climatologists, and geophysicists because the Earth is approximately spherical, and these equations provide a good first test for numerical methods for solving atmospheric and oceanic problems. Currently most global meteorological applications use spatial discretization schemes that are based on spectral transform methods, which express the variables of interest in terms of the spherical

harmonic basis functions [97] that we have already encountered briefly in Section 6.6. The spectral transform methods yield high-order solutions and give rise to elliptic equations that are computationally inexpensive to solve. The main drawback of the spectral transform methods is their computational complexity, because the spherical harmonics are globally supported. Other approaches camp with the so-called *pole problem*, which refers to a collection of problems related to approximating the solution numerically in spherical geometry. In fact, the spherical coordinate system is discontinuous at the poles.

The spherical shallow water equations are given by [64]

$$\frac{d\widehat{\phi}}{dt} = -(\widehat{\phi} + \overline{\phi})\nabla_S \cdot \vec{v}_S, \tag{7.1}$$

$$\frac{d\vec{v}_S}{dt} = -\nabla_S(\widehat{\phi} + \phi_H) - f\vec{n} \times \vec{v}_S \tag{7.2}$$

with an initial state at time t_0. Here $\frac{d}{dt}$ is the Lagrangian representation

$$\frac{d\widehat{\phi}}{dt} = \frac{\partial\widehat{\phi}}{\partial t} + (\vec{v} \cdot \nabla)\widehat{\phi},$$

$$\frac{d\vec{v}_S}{dt} = \frac{\partial\vec{v}_S}{\partial t} + (\vec{v} \cdot \nabla)\vec{v}_S,$$

where $\vec{v}$ is the velocity and $\vec{v}_S$ is the tangential component on the sphere which is obtained by

$$\vec{v}_S := \vec{v} - \vec{n} \cdot (\vec{n} \cdot \vec{v}),$$

and $\vec{n}$ is the normal to the sphere S. The difference in geopotential of the free surface elevation ϕ_H and the orography (which is constant in time), $\phi - \phi_H$, is split into a basic state geopotential $\overline{\phi} > 0$ that is constant, plus a disturbance $\widehat{\phi}$:

$$\overline{\phi} + \widehat{\phi}(\vec{x}, t) = \phi(\vec{x}, t) - \phi_H(\vec{x}),$$

and f is the Coriolis parameter. By applying the curl and divergence operators to (7.1) and (7.2) one obtains the scalar formulation, see, e.g., [59, 78]. To solve the resulting system one needs to solve elliptic problems of Helmholtz type, and, in certain settings, even fourth order elliptic problems, with each time discretization step.

By our knowledge, up till now, no adaptive wavelet schemes have been developed to solve the shallow water equations on the sphere. The framework described in Chapter 6 easily allows to create wavelets on

the sphere. We have already developed optimal methods for solving second and fourth order elliptic problems. It would be worthwhile to tackle a somewhat larger problem, such as the spherical shallow water equations.

- The construction of multivariate wavelets on arbitrary triangulations is very challenging. Even the case of continuous piecewise linear wavelets construction is unexpectedly complicated. In this dissertation we presented a C^1 continuous L_2-stable wavelet basis that was restricted to uniform triangulations. Up till now there exists no easy to implement C^1 continuous wavelet basis on arbitrary triangulations that is L_2-stable.

- The construction presented in Section 5.6 is a prewavelet basis, which means that wavelets at different resolution levels are orthogonal to each other, but wavelets on the same level are not orthogonal. One could also try to construct an orthogonal wavelet basis for the Powell–Sabin spline space. Inspiration can be found, for instance, in the papers [49, 50].

- The wavelet construction in Section 5.2 gives only one vanishing moment, which might be not enough for some applications. However, on the sphere, more than one vanishing moment does not make sense. In Chapter 6 we proposed how one can elegantly extend Powell–Sabin spline spaces to the surface of the sphere. It would be interesting to construct a wavelet basis on the sphere. Furthermore, uniform triangulations do not exist on the sphere, hence the construction method of Section 5.2 is very useful, and it can be analysed by the theory from Section 5.3. Moreover, since there is no boundary on the complete surface of the sphere, one should use $\sqrt{3}$ subdivision, instead of dyadic or triadic subdivision.

- In this thesis we have seen several constructions that yield optimal multilevel preconditioners for fourth order elliptic equations. We always started from the space of Powell–Sabin splines on the PS 6-split. We also mentioned that there are a lot of other C^1 continuous spline spaces, such as C^1 piecewise quadratics on the PS 12-split, C^1 cubics on Clough–Tocher triangles or on quadrangulations, C^1 quintics, and so on. A lot of the constructions in this thesis can also be applied to those other C^1 spline spaces. What would be interesting is to numerically compare all these methods.

- In our constructions we mostly used the triadic subdivision scheme. From a practical point of view this scheme is not very popular, since the dimension of the spline space increases too fast with the resolution

level. Therefore one should always try to use $\sqrt{3}$ subdivision in the implementations of the PS splines on the PS 6-split. This implies that one might have to consider some special constructions in order to deal with the boundary of the polygonal domain.

- In [114] Speleers proposes a local subdivision scheme based on $\sqrt{3}$-subdivision for PS spline spaces. Adaptive finite element methods for solving elliptic equations often perform better in practical computations than non-adaptive ones. However, usually these methods are not even proven to converge. Only recently ([9, 51, 117]) adaptive methods were constructed for which convergence could be demonstrated. Merging the ideas in these papers will give a theoretically founded optimal adaptive finite element method for solving fourth order elliptic boundary value problems for which the solution has singularities, both in the plane and on the two-sphere.

- In Remark 4.3.4 we gave some critical comments on the construction of the Lagrange-type hierarchical basis from Chapter 4. Lagrange interpolation for smooth spline spaces is rather new, see, e.g., [99]. There might be a way to deal with the comments and to construct an optimal preconditioner for fourth order elliptic PDEs that is comparable to the BPX preconditioner in performance.

Appendix A

Function spaces measuring smoothness

A.1 Sobolev spaces

We recall that *Sobolev spaces* measure the smoothness of a function $f \in L_p(\Omega)$. By $W_p^k(\Omega)$, $k \in \mathbb{N}$, $1 \leq p \leq \infty$, we mean the usual Sobolev space, i.e. the set of all functions in $L_p(\Omega)$ whose distributional derivatives of order less than or equal to k are in $L_p(\Omega)$. We can define the following norm for these Banach spaces

$$\|f\|^p_{W_p^k(\Omega)} = \sum_{\alpha+\beta \leq k} \|D_x^\alpha D_y^\beta f\|^p_{L_p(\Omega)},$$

with α and β positive integers. We also use the semi-norm

$$|f|^p_{W_p^k(\Omega)} = \sum_{\alpha+\beta = k} \|D_x^\alpha D_y^\beta f\|^p_{L_p(\Omega)}.$$

For the special case $p = 2$ we use the notation $H^k(\Omega) \equiv W_2^k(\Omega)$. These spaces $H^k(\Omega)$ are Hilbert spaces with inner product

$$\langle f, g \rangle_{H^k(\Omega)} = \sum_{\alpha+\beta \leq k} \langle D_x^\alpha D_y^\beta f, D_x^\alpha D_y^\beta g \rangle_{L_2(\Omega)}.$$

We also define spaces $W_p^s(\Omega)$ for arbitrary real values of $s \geq 0$ and $1 < p < \infty$. These spaces coincide for integer values of s with the spaces $W_p^k(\Omega)$. If s is not an integer, we write $s = k + \sigma$ where k is an integer and $0 < \sigma < 1$.

Then $W_p^s(\Omega)$ is a Banach space with respect to the norm

$$\|f\|^p_{W_p^s(\Omega)} = \|f\|^p_{W_p^k(\Omega)} + \sum_{\alpha+\beta=k} \int_\Omega \int_\Omega \frac{|D_x^\alpha D_y^\beta f(x) - D_x^\alpha D_y^\beta f(y)|^p}{|x-y|^{2+\sigma p}} dxdy.$$

Again for the special case $p = 2$ we write $H^s(\Omega) \equiv W_2^s(\Omega)$ and the spaces $H^s(\Omega)$ are Hilbert spaces for arbitrary real values of $s \geq 0$. See [1] for a good reference work concerning Sobolev spaces.

A.2 Besov spaces

Strongly related to Sobolev spaces are the function spaces of *Besov* type. Let $f \in L_p(\Omega)$, $0 < p \leq \infty$. We introduce the *difference operator*

$$(\Delta_h^r f)(x) := \sum_{j=0}^{r} \left(\begin{array}{c} r \\ j \end{array} \right) (-1)^{r-j} f(x+jh), \qquad x \in \mathbb{R}^2, \tag{A.1}$$

and define the *r-th order L_p-modulus of smoothness* of $f \in L_p(\Omega)$ (see, e.g., [44])

$$\omega_r(f,t)_p := \sup_{|h| \leq t} \|\Delta_h^r f\|_{L_p(\Omega(rh))}, \tag{A.2}$$

where $|h|$ is the Euclidean length of vector h and $\Omega(rh) := \{x \in \Omega : x + jh \in \Omega,\ j = 0, \ldots, r\}$. The r-th order L_p-modulus of smoothness has the following properties

$$\begin{array}{rcl} \omega_r(f,t)_p & \leq & 2^r \|f\|_{L_p(\Omega)}, \\ \lim\limits_{t \to 0_+} \omega_r(f,t)_p & = & 0, \\ \omega_r(f+g,t) & \leq & \omega_r(f,t)_p + \omega_r(g,t)_p. \end{array} \tag{A.3}$$

If $s, p, q > 0$, we say that f is in the Besov space $B_q^s\left(L_p(\Omega)\right)$ whenever the following is finite:

$$|f|_{B_q^s(L_p(\Omega))} \sim \left\{ \begin{array}{ll} \left(\sum_{l=0}^\infty \left[3^{ls} \omega_r(f, 3^{-l})_p\right]^q\right)^{1/q}, & 0 < q < \infty, \\ \sup_{l \geq 0} 3^{ls} \omega_r(f, 3^{-l})_p\,, & q = \infty. \end{array} \right. \tag{A.4}$$

See [44] for more details concerning Besov spaces.

It is well known that on a domain Ω with Lipschitz boundary the equivalence

$$W_p^s(\Omega) \cong B_p^s\left(L_p(\Omega)\right), \qquad s > 0 \tag{A.5}$$

holds [47].

Appendix B

Jackson and Bernstein estimates for PS splines

In this appendix we prove *Jackson and Bernstein estimates* for PS splines. Our proofs are based on techniques developed in [45], and are published in our paper [90]. More information on these types of estimates can also be found in [17]. It is useful to recall the definitions of Sobolev and Besov spaces, see Appendix A. The setting is the same as in Chapter 3, i.e., we consider nested triangulations (3.2) and (3.3), obtained by regular triadic refinement, and S_l is the PS spline space $S_2^1(\Delta_l^{PS})$.

B.1 The Jackson estimate

Let $f \in L_p(\Omega)$, $0 < p \leq \infty$. We want to show that the *local error of approximation* by PS splines

$$E_l(f,\Omega)_p := \inf_{g \in S_l} \|f - g\|_{L_p(\Omega)}\,, \qquad l \geq 0 \tag{B.1}$$

can be bounded by $E_l(f,\Omega)_p \lesssim \omega_3(f, 3^{-l})_p$, with $\omega_r(\cdot,\cdot)_p$ the r-th order L_p modulus of smoothness (A.2). From Whitney's theorem we know that the estimate

$$E_l(f,\tau)_p \lesssim \omega_3(f, 3^{-l})_p\,, \qquad \tau \in \Delta_l^{PS}$$

holds, since $g|_\tau$ is a quadratic polynomial for all $g \in S_l$. Whitney's theorem is best known for univariate functions and $p \geq 1$ but a proof for multivariate functions and $p > 0$ can be found in the papers [16] and [119].

Denote $\Pi_2(\Delta_l^{PS})$ as the space of all piecewise polynomials of degree ≤ 2 on the triangulation Δ_l^{PS}. Let $\pi \in \Pi_2(\Delta_l^{PS})$. Then $\mathcal{I}_l\pi$ (3.7) is not well

defined because the operator $\mathcal{I}_l$ evaluates the piecewise polynomial π and its partial derivatives at the vertices $V_i \in \Delta_l$ and π may be discontinuous at V_i. Therefore we introduce a new operator $\mathcal{I}_l^\circ$ as follows, let

$$\mathcal{I}_l^\circ f(x,y) := \sum_{i=1}^{N_l} \sum_{j=1}^{3} \mu_{ij,l}^\circ(f) B_{ij,l}(x,y), \tag{B.2}$$

where the $\mu_{ij,l}^\circ$ are linear functionals of the form

$$\mu_{ij,l}^\circ(f) := f^\circ(V_i) + \eta_{ij,l} D_x^\circ f(V_i) + \widetilde{\eta}_{ij,l} D_y^\circ f(V_i), \tag{B.3}$$

with

$$\begin{cases} f^\circ(x) & := & \limsup_{y \to x} f(y) \\ D_r^\circ f(x) & := & \limsup_{y \to x, t \downarrow 0} \frac{f(y+tr)-f(y)}{t|r|} \end{cases} \tag{B.4}$$

Then we still have the property that $\mathcal{I}_l^\circ s_l = s_l$ for each $s_l \in S_l$, but we also have that $\mathcal{I}_l^\circ \pi$ is well defined.

Lemma B.1.1. *If $\pi \in \Pi_2(\Delta_l^{PS})$ and $0 < p \leq \infty$, then for each triangle $\tau \in \Delta_l^{PS}$ we have that*

$$\|\mathcal{I}_l^\circ \pi\|_{L_p(\tau)} \lesssim \|\pi\|_{L_p(M_\tau)} \tag{B.5}$$

and

$$\|\pi - \mathcal{I}_l^\circ \pi\|_{L_p(\tau)} \lesssim \inf_{P \in \mathcal{P}_2} \|\pi - P\|_{L_p(M_\tau)} \tag{B.6}$$

where $\mathcal{P}_2$ is the space of bivariate polynomials of total degree ≤ 2 and $M_\tau \subset \Omega$ satisfies $\tau \subset M_\tau$ and $|\tau| \sim |M_\tau|$.

Proof. Because $\tau \in \Delta_l^{PS}$ there is exactly one vertex $V_i \in \Delta_l$ such that $V_i \in \tau$. Define M_τ as the union of all triangles in Δ_l^{PS} that contain vertex V_i. Then $\tau \subset M_\tau$ and $|\tau| \sim |M_\tau| \sim 3^{-l}$. From Equations (3.9), (B.2)–(B.4) and the Markov inequality for polynomials we find that

$$\begin{aligned} \|\mathcal{I}_l^\circ \pi\|_{L_p(\tau)} &\lesssim \max_{\widetilde{\tau} \subset M_\tau} \|\pi\|_{L_\infty(\widetilde{\tau})} \left\| \sum_{i=1}^{N_l} \sum_{j=1}^{3} B_{ij,l} \right\|_{L_p(\tau)} \\ &\lesssim \max_{\widetilde{\tau} \subset M_\tau} 3^{2l/p} \|\pi\|_{L_p(\widetilde{\tau})} \cdot 3^{-2l/p} \lesssim \|\pi\|_{L_p(M_\tau)} \end{aligned}$$

which is (B.5). Here we have also used that all norms on the finite dimensional space of polynomials are equivalent.

Now define $P \in \mathcal{P}_2$ as the polynomial of best $L_p(M_\tau)$ approximation to π. Since $\mathcal{I}_l^\circ P = P$ we find that

$$\|\pi - \mathcal{I}_l^\circ \pi\|_{L_p(\tau)} \leq \|\pi - P\|_{L_p(\tau)} + \|\mathcal{I}_l^\circ(\pi - P)\|_{L_p(\tau)}$$

and by using (B.5) we find (B.6). □

Let f be in $L_p(\Omega)$ and define for each triangle $\tau \in \Delta_l^{PS}$ the polynomials $P_\tau \in \mathcal{P}_2$ as the best $L_p(\tau)$ approximation to f. Then we define $\pi_l(f) \in \Pi_2(\Delta_l^{PS})$ to be the piecewise polynomial such that $\pi_l(f)|_\tau := P_\tau$ for each triangle $\tau \in \Delta_l^{PS}$.

Theorem B.1.2. *For each $f \in L_p(\Omega)$ we have*

$$\|f - \mathcal{I}_l^\circ \pi_l(f)\|_{L_p(\Omega)} \lesssim \omega_3(f, 3^{-l})_p, \qquad l \geq 0. \tag{B.7}$$

Proof. For each $\tau \in \Delta_l^{PS}$ we have from (B.6) that

$$\begin{aligned} \|f - \mathcal{I}_l^\circ \pi_l(f)\|_{L_p(\tau)} &\leq \|f - \pi_l(f)\|_{L_p(\tau)} + \|\pi_l(f) - \mathcal{I}_l^\circ \pi_l(f)\|_{L_p(\tau)} \\ &\lesssim \|f - P_\tau\|_{L_p(\tau)} + \inf_{P \in \mathcal{P}_2} \|\pi_l(f) - P\|_{L_p(M_\tau)}. \end{aligned}$$

The following equations hold:

$$\begin{aligned} \inf_{P \in \mathcal{P}_2} \|\pi_l(f) - P\|_{L_p(M_\tau)}^p &= \inf_{P \in \mathcal{P}_2} \sum_{\tilde{\tau} \subset M_\tau} \|P_{\tilde{\tau}} - P\|_{L_p(\tilde{\tau})}^p \\ &\lesssim \inf_{P \in \mathcal{P}_2} \sum_{\tilde{\tau} \subset M_\tau} \left(\|P_{\tilde{\tau}} - f\|_{L_p(\tilde{\tau})} + \|f - P\|_{L_p(\tilde{\tau})} \right)^p \\ &\lesssim \inf_{P \in \mathcal{P}_2} \sum_{\tilde{\tau} \subset M_\tau} \|f - P\|_{L_p(\tilde{\tau})}^p \\ &\lesssim \inf_{P \in \mathcal{P}_2} \|f - P\|_{L_p(M_\tau)}^p \ . \end{aligned}$$

So we infer that

$$\|f - \mathcal{I}_l^\circ \pi_l(f)\|_{L_p(\tau)} \lesssim \inf_{P \in \mathcal{P}_2} \|f - P\|_{L_p(M_\tau)} \ . \tag{B.8}$$

Now we make use of the fact that [45]

$$\omega_r(f, t)_p \sim \left(t^{-2} \int_{[-t,t]^2} \|\Delta_h^r f\|_{L_p(\Omega(rh))}^p \, dh \right)^{1/p} .$$

We deduce from (B.8) and Whitney's theorem that

$$\begin{aligned}\|f-\mathcal{I}_l^\circ\pi_l(f)\|_{L_p(\Omega)}^p &= \sum_{\tau\in\Delta_l^{PS}}\|f-\mathcal{I}_l^\circ\pi_l(f)\|_{L_p(\tau)}^p\\ &\lesssim \sum_{\tau\in\Delta_l^{PS}}|M_\tau|^{-2}\int_{[-|M_\tau|,|M_\tau|]^2}\|\Delta_h^r f\|_{L_p(M_\tau(rh))}^p\,dh\\ &\lesssim \max_{\tau\in\Delta_l^{PS}}|M_\tau|^{-2}\int_{[-|M_\tau|,|M_\tau|]^2}\|\Delta_h^r f\|_{L_p(\Omega(rh))}^p\,dh\end{aligned}$$

Equation (B.7) follows from the last inequality because $\max_{\tau\in\Delta_l^{PS}}|M_\tau|\sim 3^{-l}$. □

Theorem B.1.2 immediately implies that the L_p error of approximation by Powell–Sabin splines is bounded by the modulus of smoothness, namely

Corollary B.1.3 (Jackson estimate). *For each $f\in L_p(\Omega)$, $0<p\le\infty$, we have that*

$$E_l(f,\Omega)_p\lesssim\omega_3(f,3^{-l})_p\ . \tag{B.9}$$

B.2 The Bernstein estimate

Now we prove the Bernstein type estimate for Powell–Sabin splines.

Theorem B.2.1 (Bernstein estimate). *For each $l\ge 0$, each $p>0$, and each $r=1,2,3$, we have for $\lambda:=\min(r,r-1+\frac{1}{p})$ the Bernstein inequality*

$$\omega_r(g_l,t)_p\lesssim\left(\min\{1,3^l t\}\right)^\lambda\|g_l\|_{L_p(\Omega)},\qquad g_l\in S_l. \tag{B.10}$$

Proof. For $t\ge 3^{-l}$ this inequality reduces to

$$\omega_r(g_l,t)_p\lesssim\|g_l\|_{L_p(\Omega)}$$

which follows directly from (A.3). We concentrate on $t<3^{-l}$. From the definition of the operator $\mathcal{I}_l$ (3.7) we can write

$$g_l(x,y)=\mathcal{I}_l g_l(x,y)=\sum_{i=1}^{N_l}\sum_{j=1}^{3}\mu_{ij,l}(g_l)B_{ij,l}(x,y),$$

and also

$$(\Delta_h^r g_l)(x,y)=\sum_{i=1}^{N_l}\sum_{j=1}^{3}\mu_{ij,l}(g_l)(\Delta_h^r B_{ij,l})(x,y),$$

with Δ_h^r the difference operator defined in (A.1). For any $(x,y) \in \Omega$ at most 9 B-splines are nonzero at (x,y), hence

$$|(\Delta_h^r g_l)(x,y)|^p \leq 9 \sum_{i=1}^{N_l} \sum_{j=1}^{3} |\mu_{ij,l}(g_l)|^p |(\Delta_h^r B_{ij,l})(x,y)|^p. \tag{B.11}$$

We shall give two estimates for $|(\Delta_h^r B_{ij,l})(x,y)|$. First define $\Gamma_{ij,l}$ as the set of all (x,y) such that (x,y) and $(x,y)+rh$ are in the same triangle $\tau \in \Delta_l^{PS}$ and $B_{ij,l}$ does not vanish identically on τ. Then $B_{ij,l}$ is a polynomial on τ whose r-th order derivatives can be bounded by the Markov inequality for polynomials and we find that

$$|(\Delta_h^r B_{ij,l})(x,y)| \lesssim (3^l|h|)^r, \qquad (x,y) \in \Gamma_{ij,l}. \tag{B.12}$$

The second estimate is for the set $\widetilde{\Gamma}_{ij,l}$ which consists of all (x,y) such that (x,y) and $(x,y)+rh$ are in different triangles from Δ_l^{PS} and $B_{ij,l}$ does not vanish identically on both of these triangles. It is easy to see that $B_{ij,l} \in W_\infty^{r-1}(\Omega)$. Hence $B_{ij,l}$ has $(r-1)$-th order derivatives whose $L_\infty(\Omega)$ norms do not exceed a constant multiple of $3^{l(r-1)}$. We find that

$$|(\Delta_h^r B_{ij,l})(x,y)| \lesssim (3^l|h|)^{r-1}, \qquad (x,y) \in \widetilde{\Gamma}_{ij,l}. \tag{B.13}$$

The set $\Gamma_{ij,l}$ has measure $\lesssim (3^{-l})^2$ because the support of $B_{ij,l}$ has measure $\lesssim (3^{-l})^2$, and a similar argument shows that $\widetilde{\Gamma}_{ij,l}$ has measure $\lesssim |h|3^{-l}$.

If we combine the estimates (B.12) and (B.13) with the estimates for the measures of $\Gamma_{ij,l}$ and $\widetilde{\Gamma}_{ij,l}$ we obtain

$$\begin{aligned} \int_{\Omega(rh)} |(\Delta_h^r B_{ij,l})(x,y)|^p &\lesssim (3^l|h|)^{pr}(3^{-l})^2 + (3^l|h|)^{p(r-1)}|h|3^{-l} \\ &\lesssim |h|^{p\lambda} 3^{pl\lambda} 3^{-2l} \end{aligned} \tag{B.14}$$

where we have used that $|h| \leq t < 3^{-l}$.

We integrate (B.11) and use (B.14) to find

$$\|\Delta_h^r g_l\|_{L_2(\Omega(rh))}^p \lesssim \sum_{i=1}^{N_l} \sum_{j=1}^{3} |\mu_{ij,l}(g_l)|^p |h|^{p\lambda} 3^{pl\lambda} 3^{-2l},$$

and because $\sum_{i=1}^{N_l} \sum_{j=1}^{3} 3^{-2l} |\mu_{ij,l}(g_l)|^p \sim \|g_l\|_{L_p(\Omega)}^2$ (Corollary 2.5.7) we get

$$\|\Delta_h^r g_l\|_{L_p(\Omega(rh))}^p \lesssim (|h|3^l)^{p\lambda} \|g_l\|_{L_p(\Omega)}^p.$$

□

Remark B.2.2. *Jackson and Bernstein estimates are properties of the spline space S_l itself, hence they do not depend on any underlying basis. Therefore, as in Remark 3.3.5, one can show these estimates using any basis for S_l that is stable in the sense of Definition 2.5.1. See for instance [102] where Jackson and Bernstein estimates are derived for Powell–Sabin splines on a 12-split refinement using the Hermite basis [110].*

Appendix C

Mask coefficient matrices

In this appendix we give the 3×3 mask coefficient matrices that are used in (5.22) and (5.23).

$$A_{(-2,-2)} = \frac{1}{9}\begin{bmatrix} 1 & 0 & 2 \\ 0 & 1 & 2 \\ 0 & 0 & 0 \end{bmatrix} \qquad A_{(-1,-2)} = \frac{1}{9}\begin{bmatrix} 1 & 0 & 2 \\ 2 & 0 & 4 \\ 0 & 0 & 0 \end{bmatrix}$$

$$A_{(0,-2)} = \frac{1}{9}\begin{bmatrix} 1 & 0 & 0 \\ 2 & 0 & 2 \\ 0 & 0 & 1 \end{bmatrix} \qquad A_{(-2,-1)} = \frac{1}{9}\begin{bmatrix} 0 & 2 & 4 \\ 0 & 1 & 2 \\ 0 & 0 & 0 \end{bmatrix}$$

$$A_{(-1,-1)} = \frac{1}{9}\begin{bmatrix} 4 & 2 & 4 \\ 2 & 4 & 4 \\ 0 & 0 & 1 \end{bmatrix} \qquad A_{(0,-1)} = \frac{1}{27}\begin{bmatrix} 8 & 2 & 2 \\ 14 & 11 & 14 \\ 2 & 2 & 8 \end{bmatrix}$$

$$A_{(1,-1)} = \frac{1}{9}\begin{bmatrix} 0 & 0 & 0 \\ 4 & 0 & 2 \\ 2 & 0 & 1 \end{bmatrix} \qquad A_{(-2,0)} = \frac{1}{9}\begin{bmatrix} 0 & 2 & 2 \\ 0 & 1 & 0 \\ 0 & 0 & 1 \end{bmatrix}$$

$$A_{(-1,0)} = \frac{1}{27}\begin{bmatrix} 11 & 14 & 11 \\ 2 & 8 & 2 \\ 2 & 2 & 8 \end{bmatrix} \qquad A_{(0,0)} = \frac{1}{9}\begin{bmatrix} 5 & 2 & 2 \\ 2 & 5 & 2 \\ 2 & 2 & 5 \end{bmatrix}$$

$$A_{(1,0)} = \frac{1}{9}\begin{bmatrix} 1 & 0 & 0 \\ 4 & 4 & 2 \\ 4 & 2 & 4 \end{bmatrix} \qquad A_{(2,0)} = \frac{1}{9}\begin{bmatrix} 0 & 0 & 0 \\ 2 & 1 & 0 \\ 2 & 0 & 1 \end{bmatrix}$$

$$A_{(-1,1)} = \frac{1}{9}\begin{bmatrix} 0 & 4 & 2 \\ 0 & 0 & 0 \\ 0 & 2 & 1 \end{bmatrix} \qquad A_{(0,1)} = \frac{1}{9}\begin{bmatrix} 4 & 4 & 2 \\ 0 & 1 & 0 \\ 2 & 4 & 4 \end{bmatrix}$$

$$A_{(1,1)} = \frac{1}{27}\begin{bmatrix} 8 & 2 & 2 \\ 2 & 8 & 2 \\ 14 & 14 & 11 \end{bmatrix} \qquad A_{(2,1)} = \frac{1}{9}\begin{bmatrix} 0 & 0 & 0 \\ 2 & 1 & 0 \\ 4 & 2 & 0 \end{bmatrix}$$

$$A_{(0,2)} = \frac{1}{9}\begin{bmatrix} 1 & 2 & 0 \\ 0 & 0 & 0 \\ 0 & 2 & 1 \end{bmatrix} \qquad A_{(1,2)} = \frac{1}{9}\begin{bmatrix} 1 & 2 & 0 \\ 0 & 0 & 0 \\ 2 & 4 & 0 \end{bmatrix}$$

$$A_{(2,2)} = \frac{1}{9}\begin{bmatrix} 1 & 0 & 0 \\ 0 & 1 & 0 \\ 2 & 2 & 0 \end{bmatrix}$$

$$\tilde{A}_{(0,-3)} = \begin{bmatrix} -2.649638565381197e-02 & -2.514504381498399e-01 & 9.514997716772432e-02 \\ -5.581998732161597e-02 & 1.999268785252507e-01 & 2.180269911861705e-03 \\ 9.760360498942661e-02 & -1.146852652986162e-01 & -6.314130668832016e-02 \end{bmatrix}$$

$$\tilde{A}_{(3,-3)} = \begin{bmatrix} 3.329551186394467e-02 & 1.423407357673028e-01 & -7.066116934061388e-02 \\ 8.901291608157143e-02 & -8.433313451435348e-02 & -2.278582915002053e-03 \\ -2.154174283048086e-01 & -1.700183099895091e-01 & 1.613268088335274e-01 \end{bmatrix}$$

$$\tilde{A}_{(0,-2)} = \begin{bmatrix} -1.027319934536386e-03 & 2.627238299781715e-02 & -2.058238042526939e-02 \\ 6.193084283933032e-04 & -4.141873962772590e-02 & 6.193084283933032e-04 \\ -2.058238042526939e-02 & 2.627238299781715e-02 & -1.027319934536386e-03 \end{bmatrix}$$

$$\tilde{A}_{(1,-2)} = \begin{bmatrix} 5.793682782654931e-03 & 2.507253131582465e-02 & 6.170822938557453e-03 \\ -4.879655861320484e-02 & -8.732934266712920e-02 & -2.009176890381660e-02 \\ 8.003991286758694e-02 & 1.276464109542424e-01 & 2.260542043639538e-02 \end{bmatrix}$$

$$\tilde{A}_{(2,-2)} = \begin{bmatrix} -3.855405958898559e-03 & -2.341046644963156e-02 & 2.033351440574390e-03 \\ -2.341046644963156e-02 & -3.855405958898559e-03 & 2.033351440574390e-03 \\ 2.768642600999824e-02 & 2.768642600999824e-02 & -3.576256757900155e-02 \end{bmatrix}$$

$$\tilde{A}_{(-1,-1)} = \begin{bmatrix} 2.260542043639538e-02 & 8.003991286758694e-02 & 1.276464109542424e-01 \\ 6.170822938557453e-03 & 5.793682782654931e-03 & 2.507253131582465e-02 \\ -2.009176890381660e-02 & -4.879655861320484e-02 & -8.732934266712920e-02 \end{bmatrix}$$

$$\tilde{A}_{(0,-1)} = \begin{bmatrix} 1.661307926654759e-01 & 1.541765874068727e-01 & 1.004418790233459e-01 \\ -1.558821141791788e-01 & -1.655461990047816e-01 & -1.558821141791788e-01 \\ 1.004418790233459e-01 & 1.541765874068727e-01 & 1.661307926654759e-01 \end{bmatrix}$$

$$\tilde{A}_{(1,-1)} = \begin{bmatrix} -2.630104470330473e-02 & -9.198995834543475e-02 & -5.966619549478847e-02 \\ -9.198995834543475e-02 & -2.630104470330473e-02 & -5.966619549478847e-02 \\ 2.503925060912631e-01 & 2.503925060912631e-01 & 2.193174757327797e-01 \end{bmatrix}$$

$$\tilde{A}_{(2,-1)} = \begin{bmatrix} -8.732934266712920e-02 & -2.009176890381660e-02 & -4.879655861320484e-02 \\ 1.276464109542424e-01 & 2.260542043639538e-02 & 8.003991286758694e-02 \\ 2.507253131582465e-02 & 6.170822938557453e-03 & 5.793682782654931e-03 \end{bmatrix}$$

$$\tilde{A}_{(-3,0)} = \begin{bmatrix} 1.810136659133592e-01 & -2.252608568447245e-01 & -2.093920241491727e-01 \\ -2.553721632876749e-02 & 1.073353535802148e-02 & 5.209282974361006e-02 \\ -8.599110138394746e-02 & 1.308691753160441e-01 & 8.309190242353731e-02 \end{bmatrix}$$

$$\tilde{A}_{(-2,0)} = \begin{bmatrix} -3.576256757900155e-02 & 2.768642600999824e-02 & 2.768642600999824e-02 \\ 2.033351440574390e-03 & -3.855405958898559e-03 & -2.341046644963156e-02 \\ 2.033351440574390e-03 & -2.341046644963156e-02 & -3.855405958898559e-03 \end{bmatrix}$$

$$\tilde{A}_{(-1,0)} = \begin{bmatrix} 2.193174757327797e-01 & 2.503925060912631e-01 & 2.503925060912631e-01 \\ -5.966619549478847e-02 & -2.630104470330473e-02 & -9.198995834543475e-02 \\ -5.966619549478847e-02 & -9.198995834543475e-02 & -2.630104470330473e-02 \end{bmatrix}$$

$$\tilde{A}_{(0,0)} = \begin{bmatrix} 4.083426892921084e-01 & -3.188313657255786e-02 & -5.078484494982506e-02 \\ -5.405253872719874e-02 & 5.983297027359225e-01 & -2.567581001370201e-01 \\ -2.861544279518418e-02 & -2.124192958277383e-01 & 6.048650902906697e-01 \end{bmatrix}$$

$$\tilde{A}_{(1,0)} = \begin{bmatrix} -1.655461990047816e-01 & -1.558821141791788e-01 & -1.558821141791788e-01 \\ 1.541765874068727e-01 & 1.661307926654759e-01 & 1.004418790233459e-01 \\ 1.541765874068727e-01 & 1.004418790233459e-01 & 1.661307926654759e-01 \end{bmatrix}$$

$$\tilde{A}_{(2,0)} = \begin{bmatrix} -4.141873962772590e-02 & 6.193084283933032e-04 & 6.193084283933032e-04 \\ 2.627238299781715e-02 & -1.027319934536386e-03 & -2.058238042526939e-02 \\ 2.627238299781715e-02 & -2.058238042526939e-02 & -1.027319934536386e-03 \end{bmatrix}$$

$$\tilde{A}_{(3,0)} = \begin{bmatrix} 2.645028705212706e-01 & -3.010772608614825e-02 & -3.967598932261100e-02 \\ -2.569080244001507e-01 & 7.970072862447103e-03 & 6.204791521404297e-02 \\ -1.360002542897908e-01 & 3.742488523769980e-02 & 2.366160311200287e-03 \end{bmatrix}$$

$$\tilde{A}_{(-2,1)} = \begin{bmatrix} 2.260542043639538e-02 & 8.003991286758694e-02 & 1.276464109542424e-01 \\ 6.170822938557453e-03 & 5.793682782654931e-03 & 2.507253131582465e-02 \\ -2.009176890381660e-02 & -4.879655861320484e-02 & -8.732934266712920e-02 \end{bmatrix}$$

$$\tilde{A}_{(-1,1)} = \begin{bmatrix} 1.661307926654759e-01 & 1.004418790233459e-01 & 1.541765874068727e-01 \\ 1.004418790233459e-01 & 1.661307926654759e-01 & 1.541765874068727e-01 \\ -1.558821141791788e-01 & -1.558821141791788e-01 & -1.655461990047816e-01 \end{bmatrix}$$

$$\tilde{A}_{(0,1)} = \begin{bmatrix} -2.630104470330473e-02 & -5.966619549478847e-02 & -9.198995834543475e-02 \\ 2.503925060912631e-01 & 2.193174757327797e-01 & 2.503925060912631e-01 \\ -9.198995834543475e-02 & -5.966619549478847e-02 & -2.630104470330473e-02 \end{bmatrix}$$

$$\tilde{A}_{(1,1)} = \begin{bmatrix} -8.732934266712920e-02 & -2.009176890381660e-02 & -4.879655861320484e-02 \\ 1.276464109542424e-01 & 2.260542043639538e-02 & 8.003991286758694e-02 \\ 2.507253131582465e-02 & 6.170822938557453e-03 & 5.793682782654931e-03 \end{bmatrix}$$

$$\tilde{A}_{(-2,2)} = \begin{bmatrix} -1.027319934536386e-03 & -2.058238042526939e-02 & 2.627238299781715e-02 \\ -2.058238042526939e-02 & -1.027319934536386e-03 & 2.627238299781715e-02 \\ 6.193084283933032e-04 & 6.193084283933032e-04 & -4.141873962772590e-02 \end{bmatrix}$$

$$\tilde{A}_{(-1,2)} = \begin{bmatrix} 5.793682782654931e-03 & 2.507253131582465e-02 & 6.170822938557453e-03 \\ -4.879655861320484e-02 & -8.732934266712920e-02 & -2.009176890381660e-02 \\ 8.003991286758694e-02 & 1.276464109542424e-01 & 2.260542043639538e-02 \end{bmatrix}$$

$$\tilde{A}_{(0,2)} = \begin{bmatrix} -3.855405958898559e-03 & 2.033351440574390e-03 & -2.341046644963156e-02 \\ 2.768642600999824e-02 & -3.576256757900155e-02 & 2.768642600999824e-02 \\ -2.341046644963156e-02 & 2.033351440574390e-03 & -3.855405958898559e-03 \end{bmatrix}$$

$$\tilde{A}_{(-3,3)} = \begin{bmatrix} -1.171678421738472e-02 & 7.189134375395888e-02 & -2.175343102404871e-01 \\ -7.699067774146577e-03 & 2.492813681712348e-02 & -4.575234826609804e-02 \\ 5.360479238279715e-02 & -8.153224855708370e-02 & 9.707783358337981e-02 \end{bmatrix}$$

$$\tilde{A}_{(0,3)} = \begin{bmatrix} 1.851591042751741e-02 & -5.370310538593751e-02 & 1.147251773170392e-01 \\ -6.716926504763816e-02 & 1.099022863625919e-01 & -1.897051670693409e-01 \\ -6.335735411643897e-02 & 3.218787560125702e-02 & -1.812901060699078e-02 \end{bmatrix}$$

Appendix D

Modeling genus zero surfaces with spherical Powell–Sabin B-splines

This appendix contains some research that we did in the field of Computer Aided Geometric Design (CAGD). Because this topic is somewhat out of the scope of this thesis, we will treat it here separately. This is research in progress and it has not been published yet.

D.1 Introduction

The traditional approach to model a closed manifold surface with tensor product or triangular splines is to decompose the geometric data into a group of charts, and to map each chart into a planar parametric domain. Then a spline surface is fitted to each chart, and finally the different patches are stitched together again to form a closed manifold, see, e.g., [53]. The topology of each chart is restricted: it must be homeomorphic to a disk.

Here we describe a different approach. By using the spherical PS B-splines developed in Chapter 6 we can model genus zero surfaces without decomposing the spherical surface into different charts and mapping each chart to a planar parametric domain. Because the spherical PS splines have C^1 continuity, it is not necessary to keep as many triangles as in the original triangular mesh. The C^1 continuity works as a smoother and a large amount of data in the original mesh becomes superfluous. Therefore the idea is to first reduce the number of triangles in the original mesh. There exist plenty of methods for *mesh decimation*, see, e.g., [58, 73]. Then, the resulting

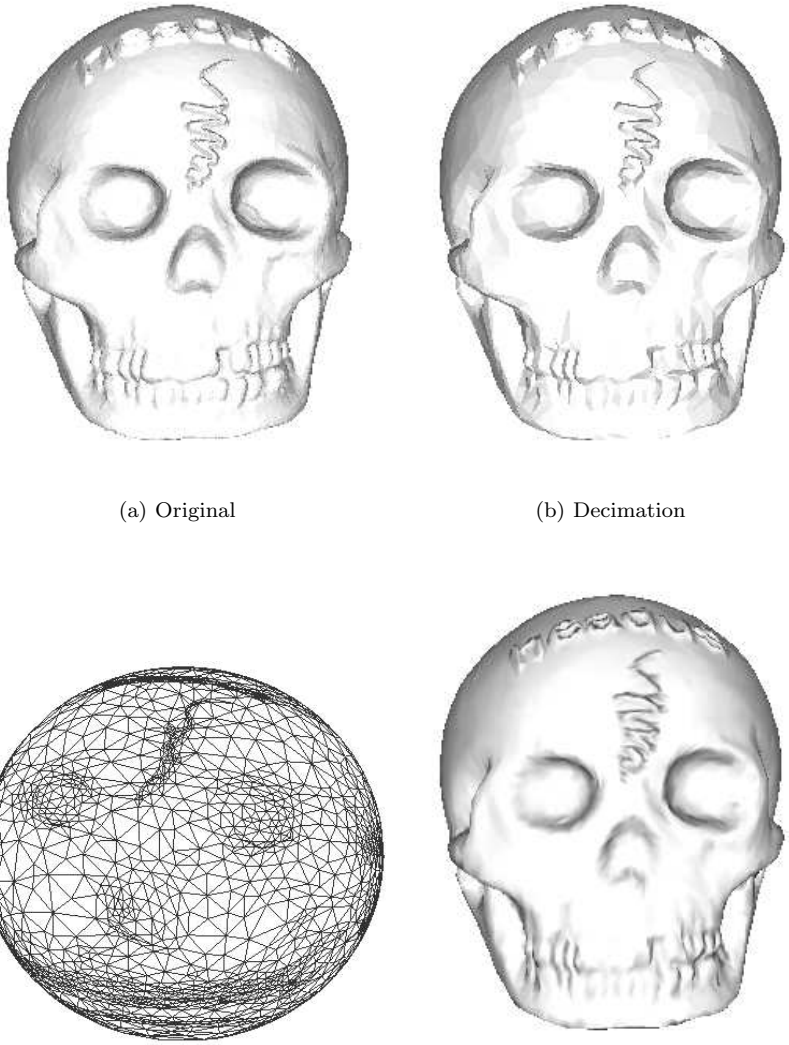

(a) Original

(b) Decimation

(c) Parameterization

(d) Spherical PS Spline

Figure D.1: Modeling a genus zero surface using a single parametric spherical Powell–Sabin spline. (a) The original mesh contains 40000 triangles. (b) The decimated mesh contains 5000 triangles. (c) Parameterization of the decimated mesh. (d) The spherical PS spline.

decimated mesh is mapped onto the surface of the two-sphere. We refer to this process as the *parameterization* of the mesh. Currently there is a lot of active research going on into the area of parameterization of a closed genus zero manifold mesh, see, e.g., [60, 62, 109, 111]. Finally a parametric spherical Powell–Sabin spline is fitted to the data. Figure D.1 shows an example of modeling a genus zero surface with spherical PS splines.

The outline of this appendix is as follows. In Section D.2 we introduce control triangles for spherical PS-triangles. These control triangles will be the key elements in an approximation algorithm that we describe in Section D.3. Finally, in Section D.4, we use the approximation algorithm to compress genus zero meshes.

D.2 Spherical PS B-splines with control triangles

We assume that the reader is familiar with the content of Sections 6.2, 6.3 and 6.4. We mentioned there that it is possible to define control triangles for the spherical B-spline basis that is derived from the bivariate B-spline basis developed in [48], see also Section 2.4. We will explain how control triangles can be defined in more detail here. The principle is illustrated in Figure D.2.

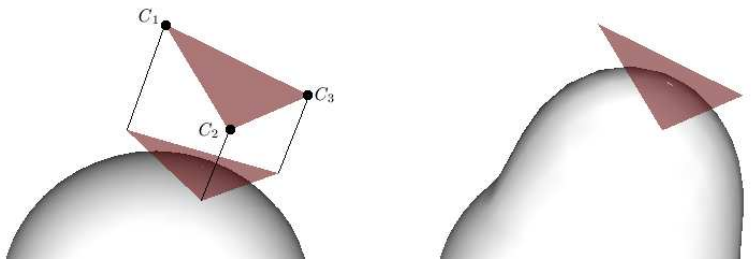

(a) PS-triangle with control triangle (b) Corresponding PS spline surface

Figure D.2: Control triangles as tools for modeling the shape of the spline surface. (a) The triangle tangent to the sphere is the PS-triangle. The control triangle is defined by the 3 control points C_1, C_2, C_3. The orthogonal projection of the 3 control points onto the plane defined by the PS-triangle coincides with the vertices of the PS-triangles. (b) The resulting Powell–Sabin spline surface is tangent to the control triangle.

Let Δ^{PS} be the Powell–Sabin 6-split of a spherical triangulation Δ of the two-sphere S. First we associate with each vertex $V_i \in \Delta$ a PS-triangle t_i. Define M_i as the molecule of vertex V_i (i.e. the union of all triangles $T_k \in \Delta$ that contain vertex V_i) and define T_{M_i} as the tangent plane touching S at vertex V_i. Recall the radial projection R_{M_i} from (6.33). Let $\overline{M}_i$ be the image of M_i under $R_{M_i}^{-1}$. Great circles are mapped into straight lines under $R_{M_i}^{-1}$, hence $\overline{M}_i$ consists of planar neighbouring triangles, centered around the common vertex V_i, and a corresponding 6-split. Suppose that t_i is a valid PS-triangle for vertex V_i in the planar triangulation $\overline{M}_i$. Then t_i is also a valid PS-triangle for vertex V_i in the spherical triangulation Δ, see Figure D.2 (a). We denote the three vertices of PS-triangle t_i by Q_{ij}, $j = 1, 2, 3$, with Cartesian coordinates (U_{ij}, V_{ij}, W_{ij}).

Now, suppose that

$$s(v) = \sum_{i=1}^{N} \sum_{j=1}^{3} c_{ij} B_{ij}(v), \qquad v \in S,$$

is a spherical PS spline. With each vertex Q_{ij} of the PS-triangle t_i we can associate a basis function B_{ij} with corresponding coefficient c_{ij}. The control points of the spherical PS spline $s(v)$ are defined as the points $C_{ij} = Q_{ij} + c_{ij} V_i$. Hence, orthogonal projection of a control point C_{ij} on the tangent plane T_{M_i} gives the PS-triangle vertex Q_{ij}, and the distance between the points Q_{ij} and C_{ij} is given by $|c_{ij}|$. These control points C_{ij} constitute the control triangles $\mathscr{T}_i(C_{i1}, C_{i2}, C_{i3})$. Such a control triangle $\mathscr{T}_i$ is tangent to the surface $(s(v) + 1)v$, $v \in S$, at vertex V_i. Figure D.2 (a) shows three control points C_1, C_2, C_3 and the corresponding control triangle. Figure D.2 (b) shows that the control triangle is tangent to the corresponding spherical PS spline surface.

Remark D.2.1. *Control triangle $\mathscr{T}_i$ is in fact the control triangle in vertex V_i of the bivariate PS-spline*

$$(c_{i1} B_{i1} + c_{i2} B_{i2} + c_{i3} B_{i3})_2|_{T_{M_i}} .$$

Recall the notation $(\cdot)_d$ from (6.34).

From a CAGD point of view those control triangles are very useful, since they mimic the shape of the underlying spline surface. We can get more local control over the spline surface by applying $\sqrt{3}$-subdivision or triadic subdivision (see Section 3.2). Figure D.3 demonstrates this principle. With each subdivision step we refine our underlying spherical triangulation in such a way that the corresponding spherical PS spline spaces are nested. If we increase the dimension of the spline space, we get more control triangles. In this way we can edit the spline surface on a finer level.

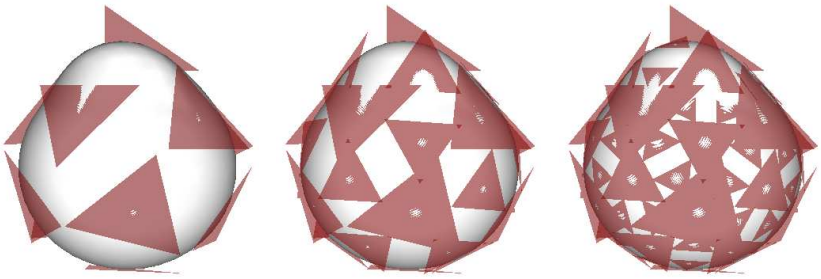

(a) Coarsest level (b) 1 refinement step (c) 2 refinement steps

Figure D.3: $\sqrt{3}$-subdivision for spherical PS splines. Increasing the dimension of the spline space gives more control triangles, and thus more local control.

D.3 Approximating a genus zero mesh

In this section we describe an approximation algorithm that starts from a very simple idea. Suppose that we are given a closed manifold mesh. In the previous section we have shown that control triangles mimic the shape of the underlying PS spline surface. Therefore the idea is to consider the given triangles in the closed manifold mesh as control triangles. Then the underlying PS spline surface will interpolate the original mesh.

If we consider just one PS spline on the sphere then we will never be able to approximate arbitrary genus zero manifolds. In any radial direction the spline surface only has one value, and this is not necessary the case for an arbitrary genus zero mesh. Therefore we will work with a parametric spherical PS spline surface,

$$\Sigma(v) = \begin{bmatrix} s_1(v) \\ s_2(v) \\ s_3(v) \end{bmatrix} \in \mathbb{R}^3, \quad v \in S,$$

where $s_1(v) \in S_2^1(\Delta^{PS})$ defines the x-values, $s_2(v) \in S_2^1(\Delta^{PS})$ defines the y-values and $s_3(v) \in S_2^1(\Delta^{PS})$ defines the z-values.

We also need a suitable triangulation on the sphere. As already mentioned in the introduction there exist plenty of methods for spherical parameterization, see, e.g., [60, 62, 109, 111]. Figure D.1 (c) for instance shows the mesh from Figure D.1 (b) mapped on the sphere. We used the method from [109]. So suppose we are given a mesh. Then we map this mesh on the sphere using some existing parameterization method. We de-

note the resulting triangulation on the sphere by Δ^*. Then each triangle in Δ^* corresponds with a triangle in the mesh. Now we construct a dual triangulation Δ to Δ^*, i.e. for each spherical triangle t_i in Δ^* we take some point V_i inside this spherical triangle t_i. Those newly created points V_i will be the vertices of our new dual triangulation Δ, and the triangles $t_i \in \Delta^*$ will be the corresponding PS-triangles.

With each PS-triangle t_i we have a corresponding triangle $\mathscr{T}_i$ in the closed manifold mesh. We need to define a control triangle for all three splines $s_i(v)$, $i = 1, 2, 3$, in the parametric spline $\Sigma(v)$. Suppose that the three vertices C_{ij}, $j = 1, 2, 3$, of $\mathscr{T}_i$ have Cartesian coordinates (X_{ij}, Y_{ij}, Z_{ij}). Then the control points for $s_1(v)$ are given by the points $Q_{ij} + X_{ij}V_i$, the control points for $s_2(v)$ are given by $Q_{ij} + Y_{ij}V_i$, and the control points for $s_3(v)$ are given by $Q_{ij} + Z_{ij}V_i$. It is easily verified that, by this choice, the triangle $\mathscr{T}_i$ will be tangent to the parametric spline $\Sigma(v)$. Therefore this triangle $\mathscr{T}_i$ will be called the control triangle for the parametric spline $\Sigma(v)$. Figure D.4 shows the different stages of the approximation algorithm.

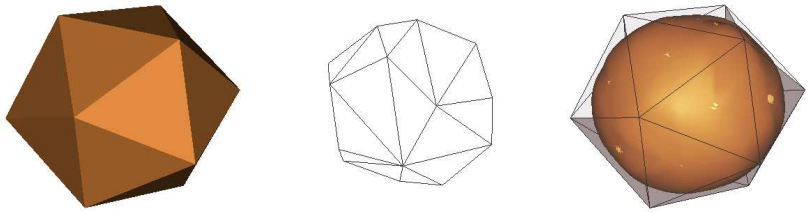

(a) Icosahedron

(b) Spherical triangulation Δ

(c) Parametric spline with control triangles

Figure D.4: The different stages of the approximation algorithm. (a) The original genus zero mesh. (b) The spherical triangulation Δ. (c) The parametric spline $\Sigma(v)$ with control triangles.

D.4 Compression by spline approximation

The parametric spherical PS spline is C^1 continuous. Because C^1 continuity works as a smoother, a large amount of data in the original mesh becomes superfluous. Therefore an important application is compression. First we reduce the number of triangles in the original mesh. This technique is called *mesh decimation* and there exist plenty of methods, see, e.g., [58, 73]. In

Figure D.1 we reduced the number of triangles in the mesh from 40000 to 5000. Then we approximated the decimated mesh with the method explained in the previous section. Figure D.1 (d) shows the result. Hence, one can store the decimated mesh instead of the original mesh. Another example is shown in Figure D.5 where we reduced the number of triangles from 268686 in the original mesh to 10000 in the decimated mesh. Although we have a large compression rate, the resulting spline surface is still very smooth.

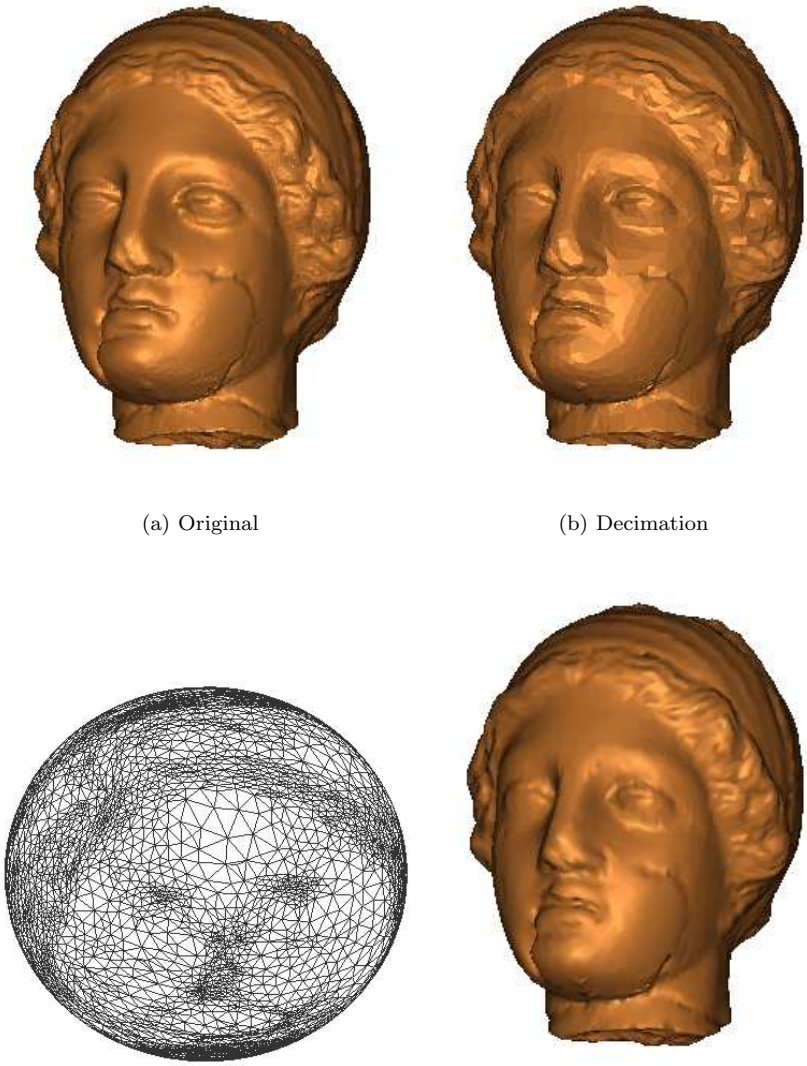

(a) Original (b) Decimation

(c) Parameterization (d) Spherical PS Spline

Figure D.5: Modeling a genus zero surface using a single parametric spherical Powell–Sabin spline. (a) The original mesh contains 268686 triangles. (b) The decimated mesh contains 10000 triangles. (c) Parameterization of the decimated mesh. (d) The spherical PS spline.

Bibliography

[1] R. A. Adams. *Sobolev spaces*. Academic Press, New York, 1975.

[2] P. Alfeld, M. Neamtu, and L. L. Schumaker. Bernstein–Bézier polynomials on spheres and sphere-like surfaces. *Comput. Aided Geom. Design*, 13(4):333–349, 1996.

[3] P. Alfeld, M. Neamtu, and L. L. Schumaker. Dimension and local bases of homogeneous spline spaces. *SIAM J. Math. Anal.*, 27(5):1482–1501, 1996.

[4] P. Alfeld, M. Neamtu, and L. L. Schumaker. Fitting scattered data on sphere-like surfaces using spherical splines. *J. Comput. Appl. Math.*, 73(1-2):5–43, 1996.

[5] P. Alfeld and L. Schumaker. Smooth macro-elements based on Powell–Sabin triangle splits. *Advances in Comp. Math.*, 16:29–46, 2002.

[6] T. Aubin. *Nonlinear Analysis on Manifolds: Monge-Ampère Equations*. Springer-Verlag, New York, 1982.

[7] A. Barinka, T. Barsch, P. Charton, A. Cohen, S. Dahlke, W. Dahmen, and K. Urban. Adaptive wavelet schemes for elliptic problems – Implementation and numerical experiments. *SIAM J. Sci. Comput.*, 23(3):910–939, 2001.

[8] J. R. Baumgardner and P. O. Frederickson. Icosahedral discretization of the two-sphere. *SIAM J. Numer. Anal.*, 22(6):1107–1115, 1985.

[9] P. Binev, W. Dahmen, and R. DeVore. Adaptive finite element methods with convergence rates. *Numer. Math.*, 97(2):219–268, 2004.

[10] J. H. Bramble and S. R. Hilbert. Bounds for a class of linear functionals with applications to Hermite interpolation. *Numer. Math.*, 16:362–369, 1971.

[11] J. H. Bramble, J. E. Pasciak, and J. Xu. Parallel multilevel preconditioners. *Math. Comp.*, 55:1–22, 1990.

[12] M. D. Buhmann, O. Davydov, and T. N. T. Goodman. Cubic spline prewavelets on the four-directional mesh. *Foundations of Computational Mathematics*, 3:113–133, 2003.

[13] C. Burstedde and A. Kunoth. Fast iterative solution of elliptic control problems in wavelet discretizations. 2005. To appear in J. Comput. Appl. Math.

[14] J. M. Carnicer, W. Dahmen, and J. M. Peña. Local decomposition of refinable spaces. *Appl. Comp. Harm. Anal.*, 3:127–153, 1996.

[15] D. Castaño, G. Constantinescu, A. Kunoth, and W. D. Schuh. Approximate continuation of harmonic functions. 2006. Manuscript, in preparation.

[16] Ch. Coatmélec. Approximation et interpolation des fonctions différentiables de plusieurs variables. *Ann. Sci. Ecole Normale Sup.*, 83:271–341, 1966.

[17] A. Cohen. Wavelets in numerical analysis. In P. G. Ciarlet and J. L. Lions, editors, *Handbook of Numerical Analysis, Vol. VII*. North-Holland, Amsterdam, 2000.

[18] A. Cohen, W. Dahmen, and R. A. DeVore. Adaptive wavelet methods for elliptic operator equations – Convergence rates. *Math. Comp.*, 70(233):27–75, 2001.

[19] A. Cohen, W. Dahmen, and R. A. DeVore. Adaptive wavelet methods II – Beyond the elliptic case. *Found. Comput. Math.*, 2(3):203–245, 2002.

[20] A. Cohen, W. Dahmen, and R. A. DeVore. Adaptive wavelet schemes for nonlinear variational problems. *SIAM J. Numer. Anal.*, 41(5):1785–1823, 2003.

[21] A. Cohen, W. Dahmen, and R. A. DeVore. Adaptive wavelet techniques in numerical simulation. *Encyclopedia of Computational Mathematics*, 1:157–197, 2004.

[22] A. Cohen and I. Daubechies. A new technique to estimate the regularity of refinable functions. *Rev. Mat. Iberoamericana*, 12(2):527–591, 1996.

[23] A. Cohen, I. Daubechies, and J.-C. Feauveau. Biorthogonal bases of compactly supported wavelets. *Comm. Pure Appl. Math.*, 45(5):485–560, 1992.

[24] A. Cohen and R. Masson. Wavelet methods for second-order elliptic problems, preconditioning, and adaptivity. *SIAM J. Sci. Comput.*, 21(3):1006–1026, 1999.

[25] A. Cohen and J.-M. Schlenker. Compactly supported bidimensional wavelet bases with hexagonal symmetry. *Constr. Approx.*, 9:209–236, 1993.

[26] R. Courant. Variational methods for the solution of problems of equilibrium and vibrations. *Bull. Amer. Math. Soc.*, 49:1–23, 1943.

[27] S. Dahlke, W. Dahmen, and K. Urban. Adaptive wavelet methods for saddle point problems – Optimal convergence rates. *SIAM J. Numer. Anal.*, 40(4):1230–1262, 2002.

[28] W. Dahmen. Some remarks on multiscale transformations, stability and biorthogonality. In P. J. Laurent, A. Le Méhauté, and L. L. Schumaker, editors, *Curves and surfaces*. Academic Press, 1994.

[29] W. Dahmen. Stability of multiscale transformations. *J. Fourier Anal. Appl.*, 4:341–362, 1996.

[30] W. Dahmen. Wavelet and multiscale methods for operator equations. *Acta Numerica*, 6:55–228, 1997.

[31] W. Dahmen. Multiscale and wavelet methods for operator equations. In C. Canuto, editor, *Multiscale problems and methods in numerical simulation*, pages 31–96. Lecture Notes in Mathematics 1825, Springer-Verlag, 2003.

[32] W. Dahmen, B. Han, R.-Q. Jia, and A. Kunoth. Biorthogonal multiwavelets on the interval: Cubic Hermite splines. *Constr. Approx.*, 16:221–259, 2000.

[33] W. Dahmen and A. Kunoth. Multilevel preconditioning. *Numer. Math.*, 63:315–344, 1992.

[34] W. Dahmen and A. Kunoth. Adaptive wavelet methods for linear-quadratic elliptic control problems: Convergence rates. *SIAM J. Contr. Optim.*, 43(5):1640–1675, 2005.

[35] W. Dahmen, A. Kunoth, and R. Schneider. Wavelet least squares methods for boundary value problems. *SIAM J. Numer. Anal.*, 39:1985–2013, 2002.

[36] W. Dahmen, P. Oswald, and X.-Q. Shi. C^1-hierarchical bases. *J. Comput. Appl. Math.*, 51:37–56, 1994.

[37] W. Dahmen and R. Schneider. Wavelets on manifolds I: Construction and domain decomposition. *SIAM J. Math. Anal.*, 31:184–230, 1999.

[38] W. Dahmen and R. Stevenson. Element-by-element construction of wavelets satisfying stability and moment conditions. *SIAM J. Numer. Anal.*, 37(1):319–352, 2000.

[39] I. Daubechies. *Ten Lectures on Wavelets*. SIAM, Philadelphia, 1992.

[40] I. Daubechies and W. Sweldens. Factoring wavelet transforms into lifting steps. *J. Fourier Anal. Appl.*, 4(3):245–267, 1998.

[41] O. Davydov and R. Stevenson. Hierarchical Riesz bases for $H^s(\Omega)$, $1 < s < 5/2$. *Constr. Approx.*, 22(3):365–394, 2005.

[42] R. A. DeVore. Nonlinear approximation. *Acta Numerica*, 7:1–99, 1998.

[43] R. A. DeVore, B. Jawerth, and B. J. Lucier. Surface compression. *Comput. Aided Geom. Design*, 9:219–239, 1992.

[44] R. A. DeVore and G. G. Lorentz. *Constructive Approximation*. Springer-Verlag, Berlin, 1993.

[45] R. A. DeVore and V. A. Popov. Interpolation of Besov spaces. *Trans. Amer. Math. Soc.*, 305(1):397–414, 1988.

[46] R. A. DeVore and R. C. Sharpley. *Maximal functions measuring smoothness*, volume 293. Mem. Amer. Math. Soc., 1984.

[47] R. A. DeVore and R. C. Sharpley. Besov spaces on domains in $\mathbb{R}^d$. *Trans. Amer. Math. Soc.*, 335:843–864, 1993.

[48] P. Dierckx. On calculating normalized Powell–Sabin B-splines. *Comput. Aided Geom. Design*, 15(1):61–78, 1997.

[49] G. C. Donovan, J. S. Geronimo, and D. P. Hardin. Intertwining multiresolution analysis and the construction of piecewise polynomial wavelets. *SIAM J. Math. Anal.*, 27:1791–1815, 1996.

[50] G. C. Donovan, J. S. Geronimo, and D. P. Hardin. Compactly supported, piecewise affine scaling functions over triangulations. *Constr. Approx.*, 16:201–219, 2000.

[51] W. Dörfler. A convergent adaptive algorithm for Poisson's equation. *SIAM J. Numer. Anal.*, 33(3):1106–1124, 1996.

[52] G. Dziuk. Finite elements for the Beltrami operator on arbitrary surfaces. In S. Hildebrandt and R. Leis, editors, *Partial differential equations and calculus of variations*, pages 142–155. Lecture Notes in Mathematics 1357, Springer, Berlin, 1988.

[53] M. Eck and H. Hoppe. Automatic reconstruction of B-spline surfaces of arbitrary topological type. *Computer Graphics*, 30(Annual Conference Series):325–334, 1996.

[54] G. Faber. Über stetige Funktionen. *Mathematische Annalen*, 66:81–94, 1909.

[55] G. Farin. Triangular Bernstein–Bézier patches. *Comput. Aided Geom. Design*, 3(2):83–128, 1986.

[56] G. Farin. *Curves And Surfaces For Computer Aided Geometric Design: A Practical Guide*. Academic Press, Boston, 4th edition, 1997.

[57] R. Franke. Scattered data interpolation. test of some methods. *Math. Comp.*, 38:181–200, 1982.

[58] Michael Garland and Paul S. Heckbert. Simplifying surfaces with color and texture using quadric error metrics. In David Ebert, Hans Hagen, and Holly Rushmeier, editors, *IEEE Visualization '98*, pages 263–270, 1998.

[59] A. Gelb and J. P. Gleeson. Spectral viscosity for shallow water equations in spherical geometry. *Monthly Weather Review*, 129(9):2346–2360, 2001.

[60] C. Gotsman, X. Gu, and A. Sheffer. Fundamentals of spherical parameterization for 3d meshes. *ACM Trans. Graph.*, 22(3):358–363, 2003.

[61] M. Griebel. Multilevel algorithms considered as iterative methods on semidefinite systems. *SIAM J. Sci. Comput.*, 15(3):547–565, 1994.

[62] X. Gu, Y. Wang, T. F. Chan, P. M. Thompson, and S.-T. Yau. Genus zero surface conformal mapping and its applications to brain surface mapping. In *Proceedings of Infrmation Processing in Medical Imaging*, pages 172–184, 2003.

[63] B. Han and R.-Q. Jia. Multivariate refinement equations and convergence of subdivision schemes. *SIAM J. Math. Anal.*, 29:1177–1199, 1998.

[64] T. Heinze and A. Hense. The shallow water equations on the sphere and their Lagrange-Galerkin-solution. *Meterol. Atmos. Phys.*, 81:129–137, 2002.

[65] S. Jaffard. Wavelet methods for fast resolution of elliptic problems. *SIAM J. Numer. Anal.*, 29(4):965–986, 1992.

[66] R.-Q. Jia. Approximation order from certain spaces of smooth bivariate splines on a three–direction mesh. *Trans. Amer. Math. Soc.*, 295:199–212, 1986.

[67] R.-Q. Jia and Q. Jiang. Spectral analysis of the transition operator and its applications to smoothness analysis of wavelets. *SIAM J. of Matrix Anal. and Appl.*, 24:1071–1109, 2003.

[68] Q. Jiang. Multivariate matrix refinable functions with arbitrary matrix dilation. *Trans. Amer. Math. Soc.*, 351:2407–2438, 1999.

[69] Q. Jiang and P. Oswald. On the analysis of $\sqrt{3}$-subdivision schemes. Preprint, 2003.

[70] Q. Jiang and P. Oswald. Triangular $\sqrt{3}$-subdivision schemes: the regular case. *J. Comput. Appl. Math*, 156:47–75, 2003.

[71] J. Ko, A. J. Kurdila, and P. Oswald. Scaling function and wavelet preconditioners for second order elliptic problems. In W. Dahmen, A. J. Kurdila, and P. Oswald, editors, *Multiscale Wavelet Methods for Partial Differential Equations*, volume 6, pages 413–438. Academic Press, San Diego, 1997.

[72] L. Kobbelt. $\sqrt{3}$-subdivision. In *Computer Graphics Proceedings*, Annual Conference Series. ACM SIGGRAPH, 2000.

[73] L. Kobbelt, S. Campagna, and H.-P. Seidel. A general framework for mesh decimation. In *Graphics Interface '98 Proceedings*, pages 43–50, 1998.

[74] A. Kunoth. *Multilevel Preconditioning.* PhD thesis, Verlag Shaker, Aachen, 1994.

[75] U. Labsik and G. Greiner. Interpolatory $\sqrt{3}$-subdivision. *Comput. Graph. Forum*, 19(3):131–138, 2000.

[76] M. J. Lai and L. L. Schumaker. On the approximation power of bivariate splines. *Advances in Comp. Math.*, 9:251–279, 1998.

[77] M. J. Lai and L. L. Schumaker. Macro–elements and stable local bases for splines on Powell–Sabin splits. *Math. Comp.*, 72:335–354, 2003.

[78] M. Läuter, D. Handorf, K. Dethloff, S. Frickenhaus, N. Rakowsky, and W. Hiller. An adaptive Lagrange-Galerkin shallow-water model on the sphere. In T. Heinze, D. Lanser, and A. T. Layton, editors, *Proceedings of the Workshop "Current Development in Shallow Water Models on the Sphere"*, pages 10–14. Munich University of Technology, Munich, Germany, 2003.

[79] W. Lawton, S. L. Lee, and Z. Shen. Convergence of multidimensional cascade algorithms. *Numer. Math.*, 78:427–438, 1998.

[80] J. L. Lions and E. Magenes. *Non-Homogeneous Boundary Value Problems and Applications, Vol. I.* Springer-Verlag, New York, 1972.

[81] R. Lorentz and P. Oswald. Multilevel finite element Riesz bases in Sobolev spaces. In P. Bjørstad, Magne Espedal, and David Keyes, editors, *Proc. 9th Intern. Conf. on Domain Decomposition Methods in Science and Engineering*. Wiley & Sons, 1996.

[82] R. Lorentz and P. Oswald. Criteria for hierarchical bases in Sobolev spaces. *Appl. Comput. Harm. Anal.*, 8:32–85, 2000.

[83] M. Lounsbery, T. D. DeRose, and J. Warren. Multiresolution analysis for surfaces of arbitrary topological type. *ACM Trans. on Graphics*, 16(1):34–73, 1997.

[84] J. Maes and A. Bultheel. Compactly supported Powell–Sabin spline multiwavelets in Sobolev spaces. TW Report 428, Department of Computer Science, Katholieke Universiteit Leuven, Belgium, May 2005.

[85] J. Maes and A. Bultheel. Easy construction of non-uniform biorthogonal spline wavelets with compact support. In T. E. Simos, G. Psihoyios, and Ch. Tsitouras, editors, *International Conference in Numerical Analysis and Applied Mathematics 2005*, pages 357–360. Wiley-VCH, Weiheim, 2005.

[86] J. Maes and A. Bultheel. A hierarchical basis preconditioner for the biharmonic equation on the sphere. *IMA J. Numer. Anal.*, 2005. Published online.

[87] J. Maes and A. Bultheel. Powell–Sabin spline prewavelets on the hexagonal lattice. In *Wavelet Analysis and Its Applications, University of Macau, Macau, China*. Applied and Numerical Harmonic Series, Springer, 2005. Accepted.

[88] J. Maes and A. Bultheel. Stable lifting construction of non-uniform biorthogonal spline wavelets with compact support. TW Report 437, Department of Computer Science, Katholieke Universiteit Leuven, Belgium, October 2005.

[89] J. Maes and A. Bultheel. C^1 Hierarchical Riesz bases of Lagrange type on Powell–Sabin triangulations. *J. Comput. Appl. Math.*, 2006. In press.

[90] J. Maes and A. Bultheel. Stable multiresolution analysis on triangles for surface compression. *Electr. Trans. Numer. Anal.*, 2006. In press.

[91] J. Maes and A. Bultheel. Surface compression with hierarchical Powell–Sabin B-splines. *Intl. Journal of Wavelets, Multiresolution and Information Processing*, 4(1):177–196, 2006.

[92] J. Maes, A. Kunoth, and A. Bultheel. BPX-type preconditioners for 2nd and 4th order elliptic problems on the sphere. Submitted.

[93] J. Maes, E. Vanraes, P. Dierckx, and A. Bultheel. On the stability of normalized Powell–Sabin B-splines. *J. Comput. Appl. Math.*, 170(1):181–196, 2004.

[94] C. Manni and P. Sablonnière. Quadratic spline quasi-interpolants on Powell–Sabin partitions. To appear in Adv. Comput. Math. (2005).

[95] A. A. Markov. Ob odnom voproce D. I. Mendeleeva. *Zapiski Imperatorskoi Akademii Nauk SP6*, 62:1–24, 1890.

[96] Y. Meyer. *Ondelettes et opérateurs 1–3: Ondelettes*. Hermann, Paris, 1990.

[97] C. Müller. Spherical harmonics. *Springer Lecture Notes in Mathematics, Vol. 17*, 1966.

[98] M. Neamtu and L. L. Schumaker. On the approximation order of splines on spherical triangulations. *Adv. in Comp. Math.*, 21:3–20, 2004.

[99] G. Nürnberger, V. Rayevskaya, L. L. Schumaker, and F. Zeilfelder. Local Lagrange interpolation with bivariate splines of arbitrary smoothness. *Constr. Approx.*, 23(1):33–59, 2005.

[100] G. Nürnberger, L. L. Schumaker, and F. Zeilfelder. Local Lagrange interpolation by bivariate C^1 cubic splines. In *Mathematical Methods for Curves and Surfaces: Oslo 2000*, pages 393–404. Vanderbilt University, 2001.

[101] G. Nürnberger and F. Zeilfelder. Local Lagrange interpolation on Powell–Sabin triangulations and terrain modelling. In W. Haussman et al., editor, *Proceedings Multivariate Approximation*. Birhäuser, Basel, 2001.

[102] P. Oswald. Hierarchical conforming finite element methods for the biharmonic equation. *SIAM J. Numer. Anal.*, 29:1610–1625, 1992.

[103] P. Oswald. On discrete norm estimates related to multilevel preconditioners in the finite element method. In K. G. Ivanov, P. Petrushev, and B. Sendov, editors, *Constructive Theory of Functions*, pages 203–214. Proc. Int. Conf. Varna, 1991, Bulg. Acad. Sci., Sofia, 1992.

[104] P. Oswald. *Multilevel finite element approximation: Theory and applications*. B.G. Teubner, Stuttgart, 1994.

[105] P. Oswald. Multilevel solvers for elliptic boundary value problems on domains. In W. Dahmen, A. J. Kurdila, and P. Oswald, editors, *Multiscale Wavelet Methods for Partial Differential Equations*, volume 6, pages 3–58. Academic Press, San Diego, 1997.

[106] G. Plonka and V. Strela. From wavelets to multiwavelets. In *Mathematical Methods for Curves and Surfaces II*. Vanderbilt University Press, Nashville, TN, 1998.

[107] M. J. D. Powell and M. A. Sabin. Piecewise quadratic approximations on triangles. *ACM Trans. on Math. Software*, 3:316–325, 1977.

[108] A. Ron and Z. Shen. The Sobolev regularity of refinable functions. *J. Approx. Theory*, 106:185–225, 2000.

[109] S. Saba, I. Yavneh, C. Gotsman, and A. Sheffer. Practical spherical embedding of manifold triangle meshes. In *International Conference on Shape Modeling and Applications 2005 (SMI' 05)*, pages 258–267, 2005.

[110] P. Sablonnière. Error bounds for Hermite interpolation by quadratic splines on an α-triangulation. *IMA J. Numer. Anal.*, 7:495–508, 1987.

[111] A. Sheffer, C. Gotsman, and N. Dyn. Robust spherical parameterization of triangular meshes. *Computing*, 72(1-2):185–193, 2004.

[112] Z. Shen. Refinable function vectors. *SIAM J. Math. Anal.*, 29:235–250, 1998.

[113] J. Simoens and S. Vandewalle. A stabilized lifting construction of wavelets on irregular meshes on the interval. *SIAM J. Sci. Comput.*, 24(4):1356–1378, 2002.

[114] H. Speleers, P. Dierckx, and S. Vandewalle. Local subdivision of Powell–Sabin splines. *Comput. Aided Geom. Design.* Accepted.

[115] R. Stevenson. Piecewise linear (pre-)wavelets on non-uniform meshes. In W. Hackbusch and G. Wittum, editors, *Multigrid Methods V*, pages 306–319. Springer-Verlag, Heidelberg, 1996.

[116] R. Stevenson. Locally supported, piecewise polynomial biorthogonal wavelets on non-uniform meshes. *Constr. Approx.*, 19(4):477–508, 2003.

[117] R. Stevenson. An optimal adaptive finite element method. *SIAM J. Numer. Anal.*, 42(5):2188–2217, 2005.

[118] J. Stöckler. Multivariate wavelets. In C. K. Chui, editor, *Wavelets: A Tutorial in Theory and Applications*, pages 325–355. Academic Press, Boston, 1992.

[119] E. A. Storozhenko and P. Oswald. Jackon's theorem in the spaces $L_p(\mathbb{R}^k)$, $0 < p < 1$. *Siberian Math. J.*, 19:630–639, 1978.

[120] G. Strang and G. J. Fix. *An Analysis of the Finite Element Method.* Prentice-Hall, 1973.

[121] W. Sweldens. The lifting scheme: A custom-design construction of biorthogonal wavelets. *Appl. Comput. Harmon. Anal.*, 3(2):186–200, 1996.

[122] W. Sweldens. The lifting scheme: A construction of second generation wavelets. *SIAM J. Math. Anal.*, 29(2):511–546, 1997.

[123] W. Sweldens and P. Schröder. Building your own wavelets at home. In *Wavelets in Computer Graphics*, pages 15–87. ACM SIGGRAPH Course notes, 1996.

[124] H. Triebel. *Interpolation Theory, Function Spaces, Differential Operators.* Deutsche Verlag der Wissenschaften, Berlin, 1978.

[125] E. Vanraes, J. Maes, and A. Bultheel. Powell–Sabin spline wavelets. *Intl. Journal of Wavelets, Multiresolution and Information Processing*, 2(1):23–42, 2004.

[126] E. Vanraes, J. Windmolders, A. Bultheel, and P. Dierckx. Automatic construction of control triangles for subdivided Powell–Sabin splines. *Comput. Aided Geom. Design*, 21(7):671–682, 2004.

[127] J. Windmolders, E. Vanraes, P. Dierckx, and A. Bultheel. Uniform Powell–Sabin spline wavelets. *J. Comput. Appl. Math.*, 154(1):125–142, 2003.

[128] J. Xu. Iterative methods by space decomposition and subspace correction. *SIAM Rev.*, 34(4):581–613, 1992.

[129] H. Yserentant. On the multi-level splitting of finite element spaces. *Numer. Math.*, 49:379–412, 1986.

[130] H. Yserentant. Two preconditioners based on the multi-level splitting of finite element spaces. *Numer. Math.*, 58(2):163–184, 1990.

[131] H. Yserentant. Old and new convergence proofs for multigrid methods. *Acta Numerica*, 2:285–326, 1993.

[132] E. Zeidler. *Applied Functional Analysis : Applications to Mathematical Physics*. Springer-Verlag, New York, 1995.

[133] X. Zhang. Multilevel additive Schwarz methods. *Numer. Math.*, 63(1):521–539, 1992.

Curriculum Vitae

Onderwijs- en onderzoeksloopbaan

- 01/07/2002
  Licentiaat Wiskunde, K.U.Leuven
  geslaagd met grote onderscheiding

- 01/09/2002 - 31/08/2006
  Doctoraatsbursaal K.U.Leuven
  Numerieke Approximatie en Lineaire Algebra Groep
  Departement Computerwetenschappen, K.U.Leuven

Buitenlandse verblijven

- 01/11/2005 - 31/01/2006
  Studieverblijf aan Universität Bonn, Institut für Angewandte Mathematik und Institut für Numerische Simulation, Bonn, Germany

Publicaties

Papers

- J. Maes, A. Kunoth, and A. Bultheel. BPX-type preconditioners for 2nd and 4th order elliptic problems on the sphere. Aangeboden ter publicatie bij SIAM J. Numer. Anal.

- J. Maes and A. Bultheel. Stable lifting construction of non-uniform biorthogonal spline wavelets with compact support. Aangeboden ter publicatie bij J. Four. Anal. Appl.

- J. Maes and A. Bultheel. Powell–Sabin spline prewavelets on the hexagonal lattice. In *Wavelet Analysis and Its Applications, 2005,*

University of Macau, Macau, China, Applied and Numerical Harmonic Analysis Series, Springer, 2006. Ter perse.

- J. Maes and A. Bultheel. A hierarchical basis preconditioner for the biharmonic equation on a sphere. *IMA J. Numer. Anal.*, 2006. Ter perse (online beschikbaar).
- J. Maes and A. Bultheel. C^1 hierarchical Riesz bases of Lagrange type on Powell–Sabin triangulations. *J. Comput. Appl. Math.*, 2006. Ter perse.
- J. Maes and A. Bultheel. Stable multiresolution analysis on triangles for surface compression. *Electr. Trans. Numer. Anal. (ETNA)*, 2006. Ter perse.
- J. Maes and A. Bultheel. Surface compression with hierarchical Powell–Sabin B-splines. *Int. J. Wavelets, Multiresolution and Information*, 4(1):177–196, 2006.
- J. Maes and A. Bultheel. Easy construction of non-uniform biorthogonal spline wavelets with compact support. In T. E. Simos, G. Psihoyios, and Ch. Tsitouras, editors, *International Conference in Numerical Analysis and Applied Mathematics 2005*, pages 357–360. WILEY–VCH, Weinheim, 2005.
- E. Vanraes, J. Maes, and A. Bultheel. Powell–Sabin spline wavelets. *Int. J. Wavelets, Multiresolution and Information*, 2(1):23–42, 2004.
- J. Maes, E. Vanraes, P. Dierckx, and A. Bultheel. On the stability of normalized Powell–Sabin B-splines. *J. Comput. Appl. Math.*, 170(1):181–196, 2004.

Technische rapporten

- J. Maes, and A. Bultheel. Stable lifting construction of non-uniform biorthogonal spline wavelets with compact support. Department of Computer Science, K.U.Leuven, Report TW 437, Leuven, Belgium, October, 2005.
- J. Maes, and A. Bultheel. Compactly supported Powell–Sabin spline multiwavelets in Sobolev spaces. Department of Computer Science, K.U.Leuven, Report TW 428, Leuven, Belgium, May, 2005.
- J. Maes, and A. Bultheel. C^1 hierarchical Riesz bases of Lagrange type on Powell–Sabin triangulations. Department of Computer Science, K.U.Leuven, Report TW 422, Leuven, Belgium, March, 2005.

- J. Maes, and A. Bultheel. On the stability of Powell–Sabin wavelets. Department of Computer Science, K.U.Leuven, Report TW 395, Leuven, Belgium, July, 2004.
- J. Maes, and A. Bultheel. Surface compression with hierarchical Powell–Sabin B-splines. Department of Computer Science, K.U.Leuven, Report TW 391, Leuven, Belgium, May, 2004.
- J. Maes, and A. Bultheel. A genetic approach to detect boundaries for meshless parametrization and surface reconstruction. Department of Computer Science, K.U.Leuven, Report TW 384, Leuven, Belgium, January, 2004.
- E. Vanraes, J. Maes, and A. Bultheel. Powell–Sabin spline wavelets. Department of Computer Science, K.U.Leuven, Report TW 362, Leuven, Belgium, July, 2003.
- J. Maes, E. Vanraes, P. Dierckx, and A. Bultheel. On the stability of normalized Powell–Sabin B-splines. Department of Computer Science, K.U.Leuven, Report TW 359, Leuven, Belgium, May, 2003.
- J. Maes, E. Vanraes, P. Dierckx, and A. Bultheel. Curvature Plots of Powell–Sabin Spline Surfaces. Department of Computer Science, K.U.Leuven, Report TW 358, Leuven, Belgium, May, 2003.